Acknowledgements

I would like to express my gratitude to all those who helped me in different ways for completing this research work. First and foremost, I would like to express my deepest gratitude to my supervisor **Dr. Pankaj Tiwari** for his continuous support and guidance throughout the entire course of my work. His uncompromising approach to complete the experiment part, analysis the data and prepare manuscripts have helped me a lot in completing my research objectives. I am grateful to his useful suggestions and constant encouragement without which it would not be possible to complete this research.

I would also thank my doctoral committee: **Prof. Ramgoapal Uppaluri, Prof. Anugrah Singh** from the Department of Chemical Engineering and **Dr. Ravi Sankar** from the Department of Mechanical Engineering at Indian Institute of Technology Guwahati for their valuable comments and suggestion towards the improvement of my research work.

I am also thankful to all the faculty members, staff members and scientific members in the Department of Chemical Engineering for their cooperation in analytical laboratory and others. I would also like to extend my acknowledgement to the Department of Science and Technology (DST), New Delhi for the financial support.

I am thankful to the Central Instrument Facility (CIF) of Indian Institute of Technology Guwahati for allowing me to carry out NMR, BET and FESEM analyses which has been very important in this research work. In this regard, I would like to acknowledge all the members of CIF for their assistance. I am thankful to the Centre of Excellence for Sustainable Polymers at Indian Institute of Technology Guwahati for providing me the facility to analyse the samples for microscopic image processing and contact angle measurements. I must also

thank Dr. Gooh Pattader Partho Sarathi for allowing me to analyze the samples in his laboratory to measure contact angle.

I thank my fellow Pallab Das, Bhargav Baruah, Imdadul Haque, Nagireddi Srinu, Priyanuj Bhuyan, Arirtra Das, Susma Chokrobarty, Deepsikha Bhagawati, Narendren S, Ritish Malani, Surendra Singh Gaur, Basudhrity Banerjee, Randeep Singh, Gourhari Chakraborty, Rajkumar das, Ch Venkatanarasimha Rao, Naba Kumar Kalita, Kaniska Murmu, Sailesh Ravi Varade, Atanu Pal and Jitendra Singh Rawat for their fruitful discussion, friendly behavior and assistance.

Last but not the least, I would like to express my deepest sense of gratitude to my parents and family members for their continuous support and motivation throughout the journal of my life. Their love, courage, care and sacrifice have made it possible for me to come so far.

Abstract

Crude oil also known as black gold is one of the major source of energy which greatly controls the economy of a country. Based on the demand and supply scenario, the price of crude oil fluctuates in the international market which is controlled by the Organization of the Petroleum Exporting Countries (OPEC). Oil production from reservoirs are usually obtained by the pressure difference beneath the earth surface (primary method). To sustain the oil production water is injected which maintains the reservoir pressure (water flooding). However, more than two-third of the oil remains trapped in the pores of the reservoir which cannot be produced by primary and secondary water flooding due to viscous fingering and require tertiary techniques. Chemical enhanced oil recovery (EOR) is one of the tertiary technique which has been focused in this work for Assam (Indian) reservoirs. The entire work in this thesis has been divided into five different sections as alkali flooding, surfactant flooding, surfactant adsorption, alkali-surfactant flooding and nanoparticle assisted polymer flooding. The detail mechanisms for each chemical EOR process considered in this study have been investigated and the complexities involved were visualized.

The alkali flooding for light to moderate Assam crude oil in sandstone reservoir was examined and the participation of each mechanisms were explored. The mechanisms such as interfacial tension (IFT), emulsification, extent of saponification or neutralization and wettability alteration have been evaluated and their impacts on residual oil recovery were examined. Alkali (NaOH) reduced the IFT value to a minimum of 10^{-2} mN/m at 0.2 wt% NaOH and further increase in NaOH concentration resulted in increase in the IFT (10^{-1} mN/m at 1 wt% NaOH). The extent of W/O (water in oil) emulsification was identified by analysing the effluent oil stream during NaOH sandpack flooding. Alkali flooding increased the

recovery of light to moderate residual oil from 11.3% initial oil in place (IOIP) at 0.2 wt% NaOH to 25.5 % IOIP at 1 wt% NaOH. The increase in oil recovery with increase in alkali concentration was observed due to the enhancement in emulsion quality which results in better sweep efficiency. This behaviour shows the dominant performance of emulsification mechanism over the IFT change in enhancing the residual oil recovery. The effects of slug size and injection pattern on oil recovery were also investigated. The change in the contact angle from 109° to 36.8° resulted in wettability alteration of the system from intermediate wet to favourable water wet.

Alkali and alkali-surfactant synergy actions were investigated to estimate residual oil recovery for sandstone reservoirs using light to moderate Assam crude oil. The IFT value of the system was reduced to 10^{-2} mN/m for both alkali and alkali-surfactants. The emulsification behaviour in addition to IFT reduction was also investigated. Sandpack flooding affirmed that alkali (NaOH) and alkali-surfactant (NaOH-Sodium dodecyl sulfate) flooding were successful in recovering 15.54 % and 24.02 % IOIP respectively. The higher oil recovery with alkali-surfactant flooding system was observed due to the combined mechanisms of IFT reduction and emulsification.

Surfactant used in chemical EOR process shows adsorption characteristics with rock surface which can severely affect the economy of the process. Hence to understand the adsorption phenomena, adsorption of selected surfactant on different reservoir rock surfaces were investigated and discussed in detail. The methodology involves mineralogy and morphology analyses of rock samples, thermal stability examination of surfactant and their adsorption characteristics. The experimental adsorption data were fitted to various isotherm and kinetic models to represent pertinent surfactant adsorption characteristics. The best

model fit was obtained for Langmuir isotherm model and pseudo-second order kinetics. The adsorption studies were also performed at different temperatures and salinity conditions to mimic reservoir conditions. The study inferred that adsorption capacity of surfactant is strongly dependent on the mineral content of the rock in the order of illite > feldspar > montmorillonite > kaolinite.

The alkali-surfactant synergy was further studied for heavy crude oil in carbonate reservoir. Two different alkalis and eight surfactants were considered to obtain optimum chemical slug formulation. The behaviour of interfacial tension (IFT) reduction, emulsification, emulsion stability, wettability alteration and core flooding studies were analysed to estimate percentage of residual oil recovery. An interesting observation during dynamic IFT studies indicated the phenomena of oil-layer break time which enhanced the oil emulsification extent. To imitate reservoir conditions, salinity and temperature of the system were varied from 0-20% and 30 to 80°C respectively. The identified optimum chemical slug formulations were found as 0.6% NaOH (A), 0.05% CTAB (S), 0.05% CTAB + 0.05% TX-100 (S_M) and 0.6% NaOH + 0.05% CTAB + 0.05% TX-100 (AS_M). A maximum residual oil recovery of 24.58% was achieved with optimum surfactant mixture (S_M). For alkali and alkali-surfactant mixture the recovery was not maximum due to emulsification and its stability which greatly control the sweep efficiency.

Nanoparticles has the potential to intensify favourable mobility ratio as well as various other mechanisms such as interfacial tension, wettability alteration and rheology which are responsible for EOR applications. The effect of nanoparticles to recover heavy residual crude oil at higher temperature in sandstone reservoir was evaluated. The stability of silica nanoparticles in the xanthan gum (XG) polymer solution was identified by particle size

analyser and zeta potential method. The behaviour of interfacial tension (IFT), emulsification, creaming index, rheological and wettability alteration characteristics with silica nanoparticles (SNPs) assisted polymer flooding were exposed. The nanoparticles-polymers solution was effective in reducing the contact angle compare to polymer solution indicating wettability alteration behaviour. Finally, SNPs assisted polymer flooding resulted in higher oil recovery of 20.82% at 30°C and 18.44% at 80°C due to the combined effects of IFT reduction, higher viscosity, better emulsion stability and wettability alteration.

This thesis develops understanding of the complexities involved for successful chemical EOR in laboratory scale for Assam (Indian) reservoirs. A successful alkali and alkali-surfactant flooding has been performed in sandstone reservoir for light to moderate crude oil. As surfactant has adsorption characteristics, the adsorption quantity of surfactant on reservoir rock was estimated which was found to be dependent on the rock mineralogy. Several model fittings and thermodynamic analysis of the adsorption process were conducted to achieve detail understanding of the reaction process. In addition to sandstone reservoir, carbonate reservoir was also exposed to alkali and alkali-surfactant flooding for heavy crude oil and based on which optimum chemical slug was obtained. Finally, nanoparticles assisted polymer flooding was performed for heavy crude oil and the potential of nanoparticles in the polymer system to improve residual oil recovery were observed.

List of Tables

Chapter 1

Chapter 2

Chapter 3

Chapter 4

Chapter 5

Chapter 6

Chapter 7

List of Figures

Chapter 1

Chapter 2

Chapter 3

Chapter 4

Chapter 5

Chapter 6

Chapter 7

Acronyms and Nomenclature

AAS	Atomic absorption spectroscopy
AOCS	American oils chemists society
API	American Petroleum Institute
ARE	Average relative error
ASP	Alkali-surfactant-polymer
ASTM	American society for testing and materials
ATR	Attenuated total reflection
AV	Acid value
BET	Brunauer-Emmett-Teller
CMC	Critical micelle concentration
CTAB	Cetyltrimethylammonium bromide
DBS	Dodecylbenzenesulfonate
DLS	Dynamic light scattering
DSF	Dilute surfactant flooding
EDX	Energy dispersive X-ray spectroscopy
EOR	Enhanced oil recovery
FESEM	Field emission scanning electron microscope
FTIR	Fourier transform infrared spectroscopy
FW	Formation water
HPAM	Partially hydrolyzed polyacrylamide
HTAB	Hexadecyltrimethylammonium bromide

IFT	Interfacial tension
INR	Indian rupee
IOIP	Initial oil in place
IUPAC	International union of pure and applied chemistry
JCPDS	Joint committee on powder diffraction standards
LS	Lignosulfonate
NMR	Nuclear magnetic resonance
OIL	Oil India Limited
OIL	Oil in place
OOIP	Original oil in place
PONP	Nonylphenyl polyoxyethylene glycol
ppm	Parts per million
PS20	Polysorbate20
PV	Pore volume
SDBS	Sodium dodecyl benzene sulfonate
SDS	Sodium dodecyl sulfate
SNPs	Silicon dioxide nanoparticles
TDS	Total dissolved solids
TGA	Thermal gravimetric analysis
TX	Triton X
XG	Xanthan gum
XRD	X-ray powder diffraction

Symbols

A	Optimum alkali concentration (0.6 wt% NaOH)
AS_M	Optimum alkali-surfactant mixture (0.6 wt% NaOH + 0.05 wt% CTAB + 0.05 wt% TX-100)
B	Temkin constant
C_e	Equilibrium surfactant concentration (mg/L)
C_o	Initial surfactant concentration (mg/L)
CI	Creaming index (%)
D	Drop width (mm)
k	Effective permeability
K_1	First order constant (min−1)
K_2	Second order constant (g/mg min)
K_F	Freundlich constant
K_H	Linear isothermal model constant (L/m^2)
K_i	Intra particle diffusion constant (mg/g min)
K_L	Langmuir constant (L/mg)
K_T	Temkin constant (L/mg)
k_{ro}	Relative permeability of oil
k_{rw}	Relative permeability of water
L	Length of oil drop (mm)
M	Total mass of Assam reservoir core crushed and used in single reaction (g)
M	Mobility ratio
m	Mass of the reservoir rock (gm)

M_S	Mass of the sample (gm)
N	Normality (N)
n	Freundlich constant
N_C	Capillary number
O/W	Oil in water
Q	total discharge (cm^3/s)
q	Adsorption capacity (mg/g)
q_e	Adsorption at equilibrium time (mg/g)
q^{exp}	Adsorption capacity obtained from experimental run (mg/ g)
q^{model}	Adsorption capacity obtained from isotherm/kinetics models (mg/g)
q_o	Langmuir adsorption capacity (mg/g)
q_t	Adsorption at time t (mg/g)
R	Universal gas constant (8.314 J/ mol. K)
R^2	Correlation coefficient
R_L	Separation factor for langmuir isotherm model
S	Optimum surfactant (0.05 wt% CTAB)
s	Second
S_M	Optimum surfactant mixture (0.05 wt% CTAB + 0.05 wt% TX-100)
S_{oi}	Initial oil saturation (%)
S_{wi}	Initial water/brine saturation (%)
T	Temperature (K)
t	Time (min)
V	Volume of titrant (ml)

v	Volume of surfactant (L)
υ	Darcy velocity (m/s)
V_{ib}	Volume of brine inside core after brine saturation (ml)
V_{irb}	Irreducible brine saturation (ml)
V_o	Oil volume (ml)
V_P	Pore volume (ml)
V_{rb}	Volume of brine removed from core during oil saturation (ml)
V_T	Total volume (ml)
W/O	Water in oil
ΔG	Gibbs free energy change (kJ/mol)
G´	Storage modulus
G´´	Loss modulus
ΔH	Enthalpy change (kJ/mol)
ΔS	Entropy change (kJ/mol)
α	Initial adsorption rate (mg/g min)
β	Elovich constant (mg/g min)
θ	Half of the diffraction angle/Bragg angle
σ	interfacial tension (mN/m)
ρ_H	Density of heavy water phase (g/cm^3)
ρ_L	Density of the oil phase (g/cm^3)
λ_o	Oil mobility (mD/cP)
λ_W	Water mobility (mD/cP)
μ	Viscosity of displacing fluid (cP)

μ_o	oil viscosity (cP)
μ_w	water viscosity (cP)
ω	rotational velocity (rpm)
ω	Angular frequency (rad/s)
Φ	Porosity (%)
$\Delta p/L$	pressure gradient across the length (atm/cm)

Units

%	Percentage
$	Dollar
µl	Microliter
µm	Micrometre
°C	Degree centigrade
cm	Centimetre
cP	Centipoise
g	Gram
Hz	Hertz
hrs	hours
K	Kelvin
kg/m^3	Kilogram per cubic meter
kJ/mol	Kilo joule per mole
km	Kilometre

mPa. s	Millipascal second
mg KOH/g	Milligram of KOH per gram
m^3	Cubic meter
min	Minutes
mV	Millivolt
nm	Nano meter
rad/s	Radian per second
Rs	Rupee
sq	Square
wt%	Weight percentage

Subscript

e	Equilibrium
o	Initial
f	Final
t	Time

Chapter 1

Introduction and Literature Review

This chapter explained in brief the importance of oil production, its consumption and demands in India and worldwide. The scenario of Indian reservoirs, oil production and import rates of the country to meet the energy demands were discussed. The different tertiary oil recovery schemes which enhances oil production rate from reservoirs were elaborated in detail. The focus towards chemical enhanced oil recovery (EOR) techniques to enhance oil production from reservoirs was discussed. The success of different types of chemical EOR which depends on oil and reservoir characteristics were discussed in detail. Also, the mechanisms involved in each chemical process were observed and described in detail. Based on the state of the art for chemical EOR, the scope for the current research were formulated. Finally, considering the literature gaps, specific objectives of the thesis and organization were summarized in this chapter.

1.1 Introduction

As a major contributor to meet world's energy demands, crude oil contributes enormously to the world economy. Existing energy consumption profiles in the world indicate near impossibility to replace crude oil completely with renewable energy. Fig. 1.1a depicts an increase in oil production and consumption profiles on world-wide basis. These profiles are distinct for India (Fig. 1.1b). Being one of the largest importers of crude oil, India's net import is bound to increase in the near future, given that the trend grew from 73% in 2000 to 77% in 2016. Despite enhanced oil production rate from 0.75 (2009) to 1 million barrels

(2016), crude oil import rate in the recent years has increased at a greater rate prior to the year 2010 in India. The crude oil production and consumptions fluctuate every year due to variation in crude oil price. Crude oil price enormously influences several sectors including research and development associated to its economical production using frontier technologies.

Ongoing demand trends for crude oil are ever increasing due to ever increasing energy and commercial product production requirements. There is a greater emphasize upon the economical production of large volumes of crude oil from even matured reservoirs. Considering the available data for Indian crude oil, matured Indian oil reservoirs need to be targeted for enhanced oil production. Fig. 1.2 represent the distribution of crude oil reserves in India. The chart illustrates that 28.3% of oil reserves are in Assam, India. North-East reservoirs (Assam) has the second highest quantity of oil reserves in India, hence crude oil production from such states of India has to be enhanced rigorously to reduce the rate of crude oil import.

Usually, primary and secondary water flooding operations account for 30-40% of the original oil in place (OOIP) [1, 2]. The primary production accounts for the crude oil produced due to natural pressure difference between the underdoing reservoir and surface of the earth. As oil production continues in the primary production, the pressure of the reservoir declines and to maintain the production rate level, water is injected to increase the reservoir pressure. However, even after water flooding operation is conducted, more than two-third of the oil remains trapped in the pores of the reservoir rock [3-5]. Recovery of such oil is difficult with water flooding as the operation after certain production phase exhibits viscous fingering behaviour. To economically extract the trapped residual crude oil, enhanced oil

recovery (EOR) methods (also known as tertiary methods) are deployed. The term enhanced oil recovery is usually suggested to a technique adopted to recover residual oil from matured reservoirs after primary and secondary flooding operations.

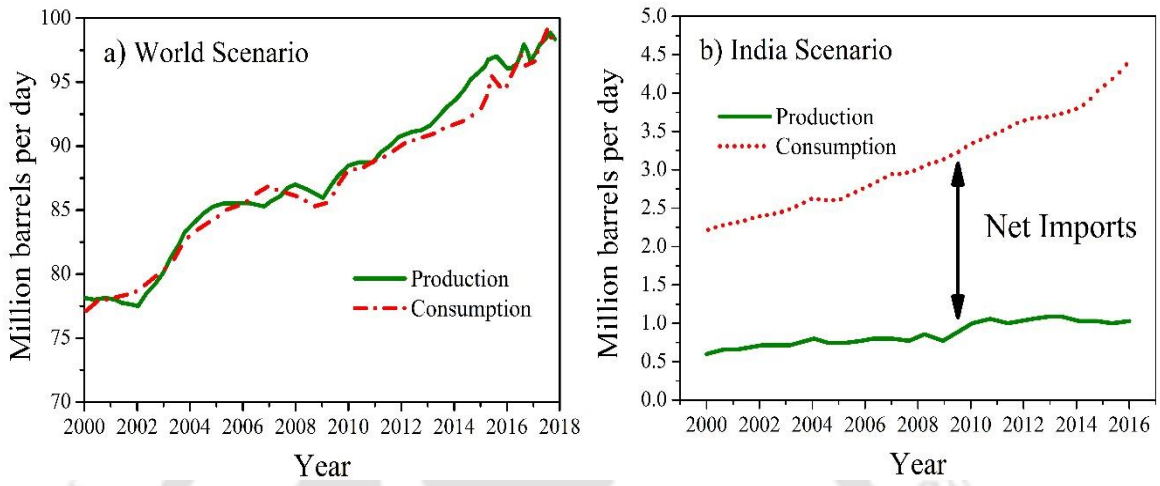

Fig. 1.1: Petroleum liquid production and consumption in a) World-wide and b) India scenario (source - U.S. Energy Information Administration, Short - Term Energy Outlook, May 2016 and January 2017).

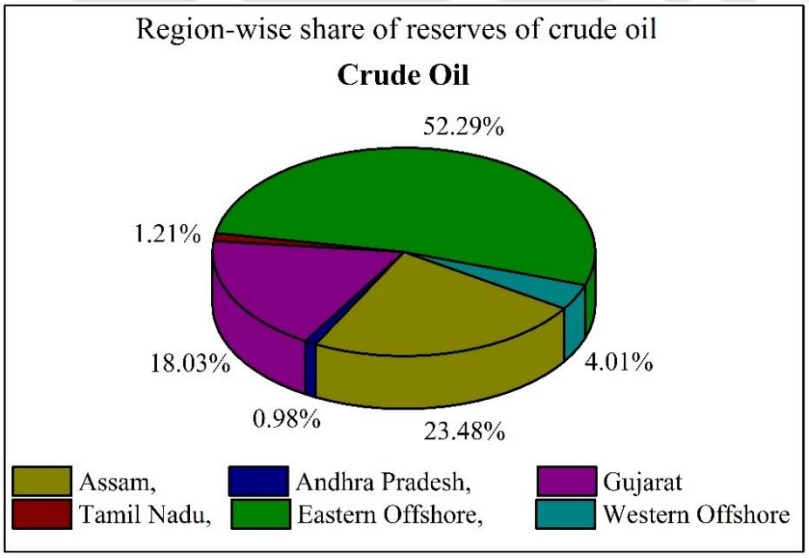

Fig. 1.2: Region-wise reserves of crude oil in India (Source - Indian Petroleum and Gas Statistics FY13, Published on December 2013).

1.2 Enhanced Oil Recovery

Enhanced oil recovery (EOR) schemes can be classified into various categories such as thermal, gas, microbial and chemical (Fig. 1.3). A brief account of these techniques is presented in the following sub-sections.

1.2.1 Thermal Enhanced Oil Recovery

Thermal EOR involves the application of thermal or heat energy to increase the oil temperature which reduce the oil viscosity to thereby foster enhanced oil recovery [6-8]. The most popular thermal recovery methods are continuous steam (or hot water) injection, cyclic steam stimulation (CSS), in-situ combustion and steam assisted gravity drainage (SAGD). Steam based methods involve injection of hot steam in the reservoir through injection wells and oil flows to the surface through production wells. For the case of in-situ combustion, air or oxygen-enriched air is injected into the reservoir to burn a portion of oil for generating heat. Eventually, oil recovery is enhanced through the generated heat and combustion gases. Thermal recovery methods are applicable for reservoirs with highly viscous oil at a lower depth and API [9]. Thermal recovery methods constitute the risk of safety issues during larger production schemes and can severely damage the underground oil well structure. This is regarded to be very serious limitation of the thermal EOR technique in oil reservoirs [10].

1.2.2 Gas Enhanced Oil Recovery

Gas injection method is one of the oldest EOR techniques which involves injection of miscible and immiscible gas. The injected gas dissolves into the oil phase which reduces oil viscosity and interfacial tension between oil and water. Such behaviour improves the sweep efficiency to thereby enhance the oil production. The most popular gas injection schemes such as nitrogen and flue-gas injection, hydrocarbon injection, CO_2 flooding, etc. [9] have

precise screening criteria for field applications. For nitrogen and flue gas flooding, the parameters correspond to a depth of > 6000 ft and API gravity of 35-48°. For hydrocarbon injection, the screening criteria refer to a depth of >4000 ft and API gravity of 23-41°. For CO_2 flooding method, the suggested depth is more than 2400 ft and recommended API gravity is about 22 – 36°. CO_2 flooding method is also applicable at higher depths and higher API gravity. Further, additional specific reservoir condition for the flooding scheme is dependent on the expansion of injected gas for driving the crude oil [10].

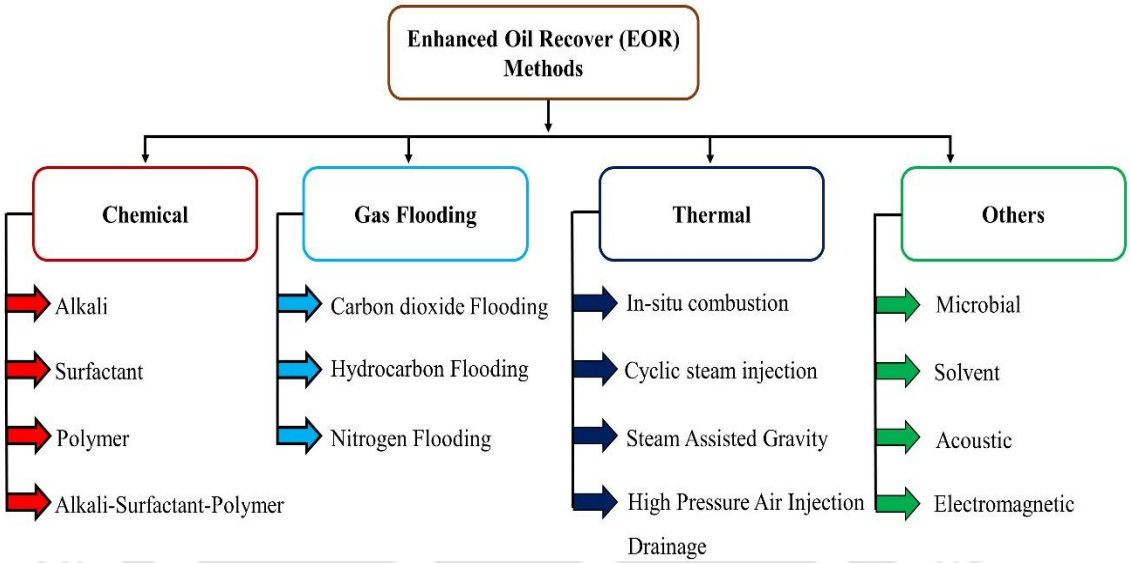

Fig. 1.3: Schematic diagram of various enhanced oil recovery methods.

1.2.3 Chemical Enhanced Oil Recovery

Among various enhanced oil recovery (EOR) methods, chemical flooding technique is an important theme to produce residual oil prevalent in the crude oil reservoir after conducting secondary water flooding operation. Chemical EOR is usually targeted with alkali, surfactant and polymer or their combinations to increase capillary number, reduce interfacial tension,

emulsify the crude oil, improve overall oil displacement efficiency, facilitate mobility control, and alter wettability [9, 11-20].

1.2.3.1 Capillary Number

After conducting water flooding operation, significant amount of oil still remains in the reservoir. Such oil are trapped by capillary forces at the pore scale level due to low capillary number. The capillary number (Nc) is defined as a dimensionless ratio of viscous to capillary forces and is expressed as [21]

$$Nc = \frac{\mu v}{\sigma} = \frac{k\Delta p}{\sigma L} \qquad 1.1$$

Where μ, v, σ, k and $\frac{\Delta p}{L}$ are the displacing fluid viscosity, Darcy velocity, interfacial tension (IFT) between displaced and displacing fluid, effective permeability to the displaced fluid and pressure gradient across the length respectively.

Therefore, enhancement in oil mobility requires enhancing capillary number and this is primarily achieved by decreasing the IFT value of the oil-water system and increasing viscosity of the displacing fluid. The capillary number can also be enhanced by reducing the oil viscosity or increasing pressure gradient. Thus, the residual oil can be mobilized and recovered with an increased capillary number through chemical flooding operations. Fig. 1.4 depicts the variation of normalized residual saturation with capillary number. As depicted, the residual saturation reduced with increase in the capillary number.

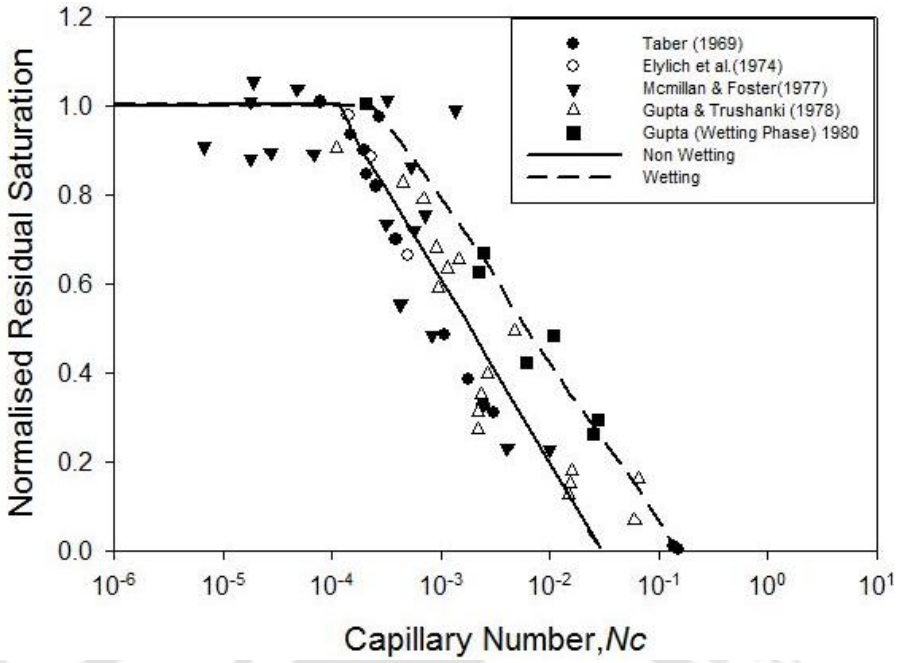

Fig. 1.4: Capillary desaturation curves for sandstone cores [11].

1.2.3.2 Interfacial Tension (IFT)

Interfacial tension is defined as the force per unit length parallel to the surface, i.e., perpendicular to the local density or concentration gradient. The IFT behaviour is dependent on the interaction between the crude oil and chemical phase at the interface. The reduction in IFT value helps releasing the trapped residual oil to enhance oil recovery. IFT is dependent on the temperature and salinity of the system.

1.2.3.3 Displacement Efficiency

In crude oil reservoir fields, two types of displacement efficiencies namely microscopic efficiency and macroscopic efficiency exist. Microscopic displacement efficiency indicates the displacement or mobilization of oil at the pore scale level. It measures the effectiveness of the displacing fluid in moving the oil at the pores of the rock due to the contact of the displacing fluid with the crude oil. Macroscopic or volumetric sweep efficiency indicates the

effectiveness with which the displacing fluid sweeps out the volume of a reservoir (both areally and vertically) and the effectiveness of the displacing fluid in moving out the displaced oil toward production wells.

1.2.3.4 Mobility Ratio

Mobility ratio is defined as the ratio of the mobility of the displacing fluid (i.e. aqueous phase) to the mobility of the displacing fluid (i.e. oil phase).The mobility ratio, M, for a water flood is expressed as:

$$M = \frac{Mobilitywater}{Mobilityoil} = \frac{\lambda_w}{\lambda_o} = \frac{k_{rw}/\mu_w}{k_{ro}/\mu_o} = \frac{k_{rw}\mu_o}{k_{ro}\mu_w} \qquad 1.2$$

Where λ_w and λ_o are water and oil mobilities, respectively, in mD/ cp; k_{rw} and k_{ro} are relative permeabilities of water and oil, respectively; μ_o and μ_w are oil and water viscosities, respectively. The value of M indicates various interesting scenarios. For the case in which M is greater than 1, the invading fluid will tend to bypass the displaced fluid. This is unfavorable and under such condition the oil recovery cannot be maximized due to poor sweep efficiency. For maximum displacement efficiency and higher oil recovery, M should be less than or equal to 1. In such case, the viscosity of the displacing fluid (i.e aqueous phase) increases and viscosity of the displaced fluid (i.e oil phase) decreases.

1.2.3.5 Wettability Alteration

Wettability is the preference of one fluid to spread on or adhere to a solid surface in presence of other immiscible fluids. Wettability alteration can cause the trapped oil in the pore space to get replaced with water and allows oil to flow to the production platform. Wettability depends on the mineral ingredients of the core rock, composition of the oil/water, initial water saturation and temperature. Oil-wet reservoirs are well known to not imbibe

water in the rock matrix during flooding operations and thereby result in low oil recovery. For such case, wettability alteration from oil-wet to water-wet using surfactants can improve oil recovery. Hence, wettability alteration is an important mechanism of chemical EOR and cannot be ignored.

1.3 State of the Art of Chemical Based Enhanced Oil Recovery

Chemical EOR can be categorized into different schemes such as alkali, surfactant, polymer and combined alkali-surfactant-polymer flooding. The most relevant work from literature has been summarized in this section. The available state of the art in various major themes are presented in the following sub-sections.

1.3.1 Alkali Flooding Based Enhanced Oil Recovery

Considering the cost competence, alkali flooding received considerable attention in many countries such as USA, Canada, China and Saudi Arabia [13, 14, 22-25]. Apart from several mechanisms such as interfacial tension (IFT) reduction, emulsification, wettability alteration and improved sweep efficiency, the success of alkali flooding to achieve higher oil recovery is largely dependent on the acid number/content of the crude oil [23, 26-29].

1.3.1.1 Influence of Acid Number and Mechanisms Involved in Alkali Flooding

The early research investigation of Atkinson (1927) deliberated upon the role of IFT reduction in enhancing oil recovery based on alkali flooding process [30]. The pertinent mechanism of alkali flooding is depicted in Fig. 1.5. As shown, alkali reacts with the natural organic acids (naphthenic acid group) prevalent in the crude oil and facilitates the formation of an in-situ surfactant at oil–water interface that reduces the interfacial tension (IFT) [29-33]. Further, IFT reduces to an ultra-low value for a scenario that involves simultaneous

adsorption of both ionized and unionized acids at the system (oil–water) interface due to mixed micelles formation [34].

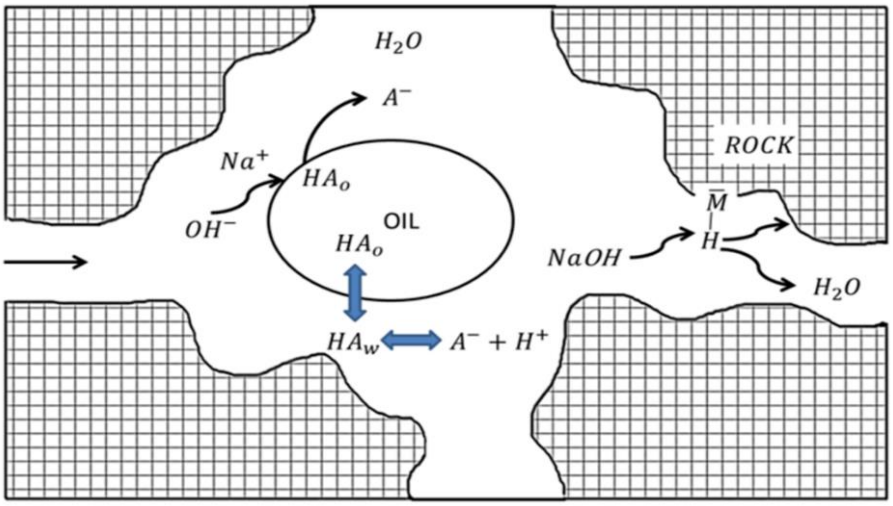

Fig. 1.5: Schematic representation of crude oil - alkali reaction mechanism [33].

Invariably, researchers have attempted to correlate acid value of crude oil with optimality of IFT reduction and residual oil recovery during alkali flooding. Cooke et al. [14] observed that the acid value of 1.5 and above favours alkali flooding through oil emulsion bank formation. The authors conveyed that both IFT reduction and emulsification are responsible for higher oil recovery. The concentration of polyvalent ions such as calcium and magnesium salt in the alkaline water must be kept low to avoid adverse effect which avoids to accomplish lower IFT and better emulsification. Salinity and pH of the flood water controls the residual oil saturation percentage. The micro-model analysis during alkaline flooding infers that the wettability alteration of the matrix material takes place from strongly water wet to preferentially oil-wet. This alteration in wettability of the system was due to the adsorption of formed soap molecules on the solid surface.

Ge et al. [35] investigated the role of acid value on residual oil recovery by performing alkali flooding tests with sandpack systems. Crude oil from four different reservoirs (Zhuangxi 106, Chenzhuang, Binnan and Xia-8) with different acid values (1.846, 2.018, 3.852 and 4.660 mg of KOH/g of sample respectively) were investigated. The data confirmed that with an increase in acid value from 1.846 to 4.660 mg of KOH/g of sample, the oil recovery factor increased from 12.4 to 20.4%. The crude oil with higher acid value possesses higher organic acid content and facilities higher enrichment in terms of in-situ surfactants. The presence of in-situ surfactants at the oil-water interface favours instantaneous IFT reduction and improves penetration of alkali solution in oil phase to form water in oil (W/O) emulsions. Such dispersion enhances viscosity of the displacing fluid and thereby promotes sweep efficiency by reducing viscous fingering. The carried out investigations infer that IFT reduction is not the only criteria for successful alkali flooding as emulsion mechanism also contributes significantly to the oil recovery factor. Similar views have also been reported by other researchers to confirm that emulsification mechanism contributes significantly towards oil recovery factor [22, 24, 36].

Pie et al. [36] studied IFT behaviour of crude oil-alkali solution system in the alkali concentration range of 0.1 – 1 wt%. A minimum IFT value of 10^{-2} mN/m was obtained at 0.2 wt%. However, corresponding tertiary oil recovery was only 10.63%. As the concentration of alkali was increased, the IFT of the system increased due to pH effect of the solution. On the other hand, oil recovery factor increased significantly to 20.9%. The increase in residual oil recovery was due to the formulation of W/O emulsion produced due to the penetration of alkali solution in the oil phase. For a variation in alkali solution concentration from 0.1 to 1

wt%, the average droplet size of water droplets created in the W/O emulsion increased from 1.012 to 2.785 µm, thereby affirming better emulsion quality at higher alkali concentration. The viscosity of the emulsion increase with emulsion quality, which strongly controls the sweep efficiency. Micromodel analysis revealed viscous nature of W/O emulsion. Due to this, water mobility gets reduced and sweep efficiency gets improved. This is due to the diversion of alkali solution into unswept regions of the system to promote higher oil recovery. The authors further optimized alkali flooding process parameters and concluded that an alkali slug of 0.5 PV with an injection rate of 0.25 mL/min through continuous injection pattern provided the highest oil recovery. Similar synergy of IFT reduction and emulsification mechanism has been reported by other researchers [23, 37, 38].

Gong et al. [26] investigated the influence of alkali (NaOH and Na_2CO_3) solution on wettability alteration. The authors found that wettability alteration improved displacement efficiency and increased residual oil recovery by about 10%. The micromodel experiments conducted using alkali solution clearly indicates the variation in the wettability of the pore wall from water wet to favourable oil wet. Quartz substrate in brine solution and variant alkali solution concentration was subjected to contact angle measurements to evaluate the pertinent variations in the system wettability. Below 0.2 wt% Na_2CO_3 solution concentration, contact angle value was lower than 90 ^{o} and affirms that the system is water wet. However, above 0.2 wt %, the contact angle reached values greater than 90^o and confirmed wettability variation from water wet to oil wet. Also, compared to Na_2CO_3, NaOH provided better wettability behaviour. For 0.1 wt% NaOH solution concentration, the system wettability varied from water wet to oil wet. However, there are no direct relationships between acid

value, equilibrium IFT, emulsification and residual oil recovery to affirm a successful chemical EOR process [18, 39]. Recent studies revealed that the displacement of oil from pores of reservoir rocks involves the phenomena to occur at oil–water interface (IFT reduction) and oil–solid (rock) interface (wettability) [40, 41]. In other investigation, higher oil recovery of residual crude oil has been inferred to occur due to wettability alteration of reservoirs from water-wet to intermediate or oil-wet condition [26]. Numerous studies that conveyed successful alkali flooding and explaining the mechanisms responsible for higher residual oil recovery have been summarized in Table 1.1.

Table 1.1: Literature data on residual oil recovery by alkali flooding.

Sr. No	Author	Mechanisms	Materials	Parameters	Key results
1	Cook et al.[14]	Interfacial Tension and emulsification	Crude oil (Natural), kerosene and Tetradecane Acid Value - 1.95 to 7.36 mg KOH/g-oil	pH - 8.2 to 99.2 Acid Value - 1.5 above mg KOH/g-oil Salinity - 25%	• Low calcium and magnesium quantity to avoid formation of less active surface soap. • Salinity and pH affects the quantity of residual oil saturation percentage.
2	Ge et al. [35]	Interfacial Tension, emulsification and displacement efficiency	Heavy crude Zhuangxi 106, Chenzhuang, Binnan, and Xia-8 (China) Acid Value - 1.85 to 4.66 mg KOH/g-oil Viscosity @50°C - 390 to 3950 mPa. s	Best crude - Xia-8 NaOH - 0.5 wt% Salinity - 0.5 wt%	• Oil recovery increases with increase in acid value and maximum recovery of 20.4% was obtained. • NaOH showed better oil recovery compare to Na_2CO_3 • Lower temperature investigation resulted in better displacement efficiency and lowest IFT (10^{-2} mN/m)
3	Pie et al. [36]	Interfacial tension, emulsification and displacement efficiency	Binnan Heavy crude (Shengli, China) Acid value - 2.69 mg KOH/g-oil Viscosity @ 55°C- 2000 mPa. s Sandpack, Porosity - 42.2 - 44.5% Chemical - NaOH	IFT - 10^{-2} NaOH - 1 wt% Slug Size - 0.5 PV Injection rate - 0.25 ml/min	• Alkali penetration improves sweep efficiency by forming W/O emulsion which diverts the water in the unswept region • Emulsion droplet number and sizes increases with alkali concentration • Cyclic injection pattern with optimum injection rate resulted in an oil recovery of 20.9 %
4	Gong et al. [26]	Wettability alteration and displacement efficiency	Heavy crude (Alberta, Canada) Acid value - 1.07 mg KOH/g-oil Viscosity @ 22°C- 1202 mPa. s Brine TDS @ 22°C - 28020 mg/L Sandpack, Porosity - 34.5 - 36.5% Chemical - NaOH	NaOH - 0.7 wt%	• Wettability alteration was achieved by change in contact angle values from 24° to 165° • Oil recovery of 14% was achieved

1.3.2 Surfactant Flooding Based Enhanced Oil Recovery

Numerous studies have been conducted on surfactant flooding to validate its efficacy on recovering residual oil from reservoirs [42-45]. The injection of surfactants into oil reservoirs to enhance oil recovery was initiated as early as 1960 [46]. Surfactants enhance sweep efficiency due to higher capillary number and thereby facilitate IFT reduction, wettability alteration and emulsion formation to improve oil recovery [45, 47-50]. Due to the inclusive role of above mentioned mechanisms, surfactant flooding has considered to be an effective and successful method for recovering residual oil from reservoirs. Numerous works addressed surfactant flooding as an EOR method with various combinations such as alkali-surfactant flooding [28], surfactant-polymer schemes, alkali-surfactant-polymer flooding [51], dilute surfactant flooding (DSF) [52], smart DSF [53], silica nanoparticles-surfactant [54] and silica nanoparticles-surfactant-polymer flooding [55]. Various surfactants deployed for the residual oil recovery investigations include anionic (alkyl ether sulfates [45], sodium lauryl sulfate [56], Sodium dodecyl benzene sulfonate [51] etc), cationic (hexadecyltrimethylammonium bromide [HTAB] [56], Cetyltrimethylammonium bromide [CTAB] [49] etc), non-ionic (Tergitol [56], etc), and natural surfactants [57].

1.3.2.1 Mechanisms Involved in Surfactant Flooding

Yuan et al. [19] targeted the effect of interfacial tension and emulsification mechanism on oil recovery by performing surfactant flooding experiments for high temperature and high salinity reservoirs. Twelve surfactants from five different categories were screened by the authors along with the variation in temperature from 90 - 120°C at fixed choice of salinity as 20 x 10^4 mg/L. Upon aging at 90-120°C and at 20 x 10^4 mg/L salinity for a period of 125 days, two surfactant formulations exhibited stable ultra-low IFT value of $\leq 10^{-3}$ mN/m. The

oil recovery increased with a reduction in initial and dynamic IFT reduction. An additional oil recovery of about 7% was obtained for a reduction in the IFT system from 10^{-1} to 10^{-3} mN/m. However, the IFT reduction and oil recovery correlation was not valid below an IFT level of 10^{-4} mN/m. Under such conditions, the emulsification became dominant to facilitate a maximum oil recovery of 36.65% for a surfactant concentration enhancement from 0.2 to 0.5 wt%. The emulsification became much significant for a variation in surfactant concentration from 1 to 3 wt%. Due to this, the displacement process has been severely affected and oil recovery reduced despite obtaining ultra-low IFT values for chosen surfactant concentration.

By conducting dilute surfactant flooding experiments, Pu et al. [52] investigated the role of interfacial tension and emulsification on displacement efficiency. The investigations involved fixed surfactant concentration (0.2 wt%) and salinity variation to obtain solution system at different IFT level (10^{-1} to 10^{-5} mN/m). Such formulation was considered to eliminate the effect of surfactant concentration on the displacement efficiency behaviour. The five distinct surfactant formulations with IFT levels from 10^{-1} to 10^{-5} mN/m exhibited increasing displacement efficiency from 12.44 to 21.45% respectively. In other words, IFT reduction has a significant role in controlling displacement efficiency. However, the impact of emulsification is on the contrary i.e., the displacement efficiency reduced with increasing emulsification and this was facilitated for the system with lower IFT.

Kumar et al. [58] analysed the interfacial interaction and wettability alteration of four cationic surfactants from trimethylammonium bromide (C_nTAB) family (i.e. $C_{10}TAB$, $C_{15}TAB$, $C_{16}TAB$ and $C_{19}TAB$). Among these, the authors observed that $C_{15}TAB$ and

C_{16}TAB surfactants exhibited lower surface and interfacial tension. The authors also found that with increasing carbon atom number in the surfactants, their CMC (critical micelle concentration) decreased significantly. The identified two surfactants have also been successful to facilitate early reduction in contact angle and also alteration in the wettability of oil wet carbonate rock to water wet. Further, the system contact angle reduced with increase in salinity upto a certain limit and eventually increases.

Jarrahian et al.[50] carried out a mechanistic study on wettability alteration (through contact angle measurement) using cationic (C_{12}TAB), anionic (SDS) and non-ionic (Triton X-100) surfactants and carbonate rock (dolomite). Among the chosen surfactants, C_{12}TAB was highly efficient to facilitate the alteration in wettability (to more water wet) as the surfactant irreversibly desorbed stearic acid from the carbonate surface via ionic interaction. Triton X-100 adsorption on dolomite surface occurs due to polarization of π electrons and ion exchange. The adsorption of released stearic acid on the new layer on the surface through hydrophobic interaction facilitates variation in the wettability of the system to weak water wet. SDS indicated neutral wet condition for the chosen system as adsorption of SDS on the dolomite surface occurs due to hydrophobic interaction between adsorbed acid and tail of surfactant.

1.3.2.2 Stability of Surfactant for Enhanced Oil Recovery Applications

Surfactant screening is required in the context of negligible degradation in high temperature saline crude oil reservoirs. Targeting the application of surfactants in such extreme reservoir conditions, Kamal et al. [59] studied the effect of thermal aging on two different surfactants. The thermally aged surfactants were subjected to various analytical

techniques (FTIR, NMR, TGA) to detect variations in the prevalent functional groups before and after thermal aging. The aged and non-aged samples were also evaluated for their IFT reduction behaviour. Thermo-gravimetric Analysis (TGA) that infers upon short term thermal behaviour of the considered material indicated no sign of degradation for surfactants A (carboxybetaine based amphoteric surfactant) and B (anionic surfactant Alfoterra L167-4s). After aging both samples at 90°C for 10 days, based on FTIR and NMR spectra, surfactant B indicated degradation characteristics. The IFT behaviour of amphoteric surfactant remained the same and did not vary even after aging. However, for the anionic surfactant, the IFT value increased by two orders of magnitude after aging. The stable amphoteric surfactant was further investigated to variations in temperature and system salinity. For such case, it was analysed that the system IFT increased with increased temperature, but decreased with increase in salinity.

1.3.2.3 Adsorption Characteristics of Surfactant on Reservoir Rock

The adsorption characteristics of surfactants are dependent on rock characteristics. Hence, appropriate analysis is required prior to injecting surfactants into crude oil reservoirs for EOR applications. Park et al. [60] carried out fundamental investigations with respect to the determination of interfacial properties and adsorption characteristics of four different surfactants (two anionic - DBS and LS; and two non-ionic - PS20 and PONP) on kaolinite samples. Langmuir and Freundlich isotherm model have been evaluated to fit well with measured equilibrium adsorption data. However, the former model provided better fitness. The adsorption of various surfactants is in the following order: LS > PS20 > DBS > PONP (with adsorption capacities of 5.28, 3.45, 3.26, 3.06 mg/g respectively). The interfacial tension between model oil and 1 wt% surfactant solution was in the order of DBS > PONOP

> PS20 > LS. Based on IFT reduction behaviour and financial loss incurred due to surfactant loss, the authors concluded that among all four considered surfactants, DBS is the best surfactant.

Amirianshoja et al. [61] carried out detailed investigations with respect to the effect of rock mineralogy on surfactant adsorption using anionic (SDS) and non-ionic (Triton X-100) surfactants and CMC method. Mineralogical investigations referred to mixing of quartz, kaolinite, feldspar, illite and montmorillonite in various proportions to evaluate the adsorption characteristics. For Triton X -100, the adsorption was highest with montmorillonite and the adsorption quantity increased from 1.5 to 28.5 mg/g for an increase in montmorillonite concentration from 5 to 20%. The adsorbed quantity was negligible with anionic surfactant due to the charge nature between the minerals and surfactant. Therefore based on adsorption characteristics, the authors inferred that the mineralogical order for non-ionic surfactant is as per the following order: montmorillonite > illite > kaolinite.

Researchers also used natural surfactants for EOR application and further investigated upon their adsorption characteristics. Zendehboudi et al. [57] studied adsorption behaviour of a non-ionic natural surfactant (Zizyphus Spina Christi) on carbonate rock surface. The CMC of the surfactant was obtained at 3.65 wt%. Adsorption behaviour was investigated in the operating temperature range of 28 to 75°C. An exothermic adsorptive behaviour was apparent for the system that affirmed reduction in adsorptive quantity of surfactant with increasing temperature. The consideration of natural surfactant reduced the system IFT by 69%. The measured adsorption data fit well with Freundlich adsorption isotherm and pseudo-second order kinetics (R^2 value of above 0.99 for both cases). The natural surfactant increased imbibition and thereby enhances oil recovery factor from 47 to 77%.

Using conductivity technique, Ahmadi et al. [62] examined the adsorption characteristics of a novel surfactant Glycyrrhiza Glabra on crushed carbonate reservoir rock. The CMC of the novel surfactant was evaluated to be 3.5 wt%. The adsorption behaviour of the surfactant on carbonate rock exhibited exothermic nature were adsorption capacity reduces with increase in the temperature. The authors inferred that compared to other two surfactants (alkyl poly glycosides and alkyl sulfates surfactants), the natural surfactant has greater potential in reducing IFT. Measured equilibrium and kinetics of surfactant adsorption have been evaluated to fit well with Langmuir and pseudo second order models.

Table 1.2: Literature data on residual oil recovery by surfactant flooding.

Sr. No	Author	Mechanisms	Materials	Parameters	Key results
1	Yuan et al. [19]	Interfacial tension and emulsification	Heavy crude (Tarim Basin, China) Viscosity - 2.88 mPa. s Reservoir rock Porosity - 32 to 34.8%	IFT - 10^{-4} mN/m	• Linear fit between IFT reduction and oil recovery was observed. • Surfactant concentration of 0.5% resulted in maximum oil recovery of 36.65% with IFT 10^{-4} mN/m. • Higher surfactant concentration above 0.5 % reduces oil recovery due to formation of too strong emulsion which reduces sweep efficiency
2	Pu et al. [52]	Interfacial tension and emulsification	Surfactant - ethoxylated fatty alcohol carboxylate (AEC) Light crude (Tarim Basin, China) API gravity crude - 42.33°, viscosity of crude - 42.0 mPa. s @ 30°C Salinity - NaCl and $CaCl_2$	Surfactant - 17(NaCl) + 2.8($CaCl_2$)] x 10^4 mg/L + 0.2 wt% AEC IFT - 10^{-4} mN/m Emulsification rate - 1.44 mL/min	• Five IFT level from 10^{-1} to 10^{-5} mN/m was formulated with variation in salinity and surfactant of 0.2 wt% was fixed. • Displacement efficiency increases with reduction in IFT values but decreases with increase in emulsification. • Highest oil recovery of 21.45% was acquired by dilute surfactant flooding at lowest IFT of 10^{-4} mN/m and eliminates the effect of emulsification mechanism.

3	Kumar et al. [58]	Interfacial tension and wettability alteration	Surfactant - C_{10}TAB, C_{15}TAB, C_{16}TAB and C_{19}TAB	IFT - 0.23 mN/m Salinity - 6 wt%	• C_{15}TAB and C_{19}TAB showed lowest surface and interfacial tension • As number of carbon increases, CMC decreases significantly. • C_{15}TAB and C_{19}TAB facilitate early reduction in contact angle and alters wettability from oil wet to water wet. • Contact angle reduces with increase in salinity
4	Jarrahian et al. [50]	Wettability alteration	Crystalline dolomite as carbonate rock Model oil (Stearic acid dissolved in n-heptane) Surfactant - C_{12}TAB, Triton X-100 and Sodium dodecyl sulfate (SDS)	Contact angle C_{12}TAB - 22° Triton X 100 - 65° SDS - 76°	• C_{12}TAB was more dominant in changing the wettability of the system to favourable strong water wet. • Triton X 100 reduces the wettability to weak water wet whereas SDS to neutral wet.
5	Kamal et al. [59]	Interfacial tension reduction and thermal stability	Light crude (Arabian oil field) Viscosity - 13.1 mPa. s Surfactant - Carboxybetaine based amphoteric surfactant (Surfactant A) and propoxylated anionic surfactant (Surfactant B) Salinity - 57,643 ppm	Temperature - 30° C Salinity - 58000 ppm	• TGA analysis indicated that both surfactants (A and B) were stable up to 90°C (short term thermal exposure) • Long term thermal aging of surfactants at 90° C for 10 days and its analytical measurement by FTIR and NMR showed unstable nature of surfactant A whereas surfactant B was still stable. • IFT of system increases with temperature but for salinity opposite trend was observed.

6	Park et al. [60]	Interfacial tension and adsorption	Non-ionic surfactant - polysorbate20 (PS20) and nonylphenyl polyoxyethylene Glycol (PONP) Anionic surfactant - dodecylbenzenesulfonate (DBS) and lignosulfonate (LS) Adsorbent - kaolinite	Minimum adsorption - 3.06 mg/g adsorbent by PONP surfactant Langmuir model	• Surfactant adsorption (mg/g adsorbent) on kaolinite surface followed the order as LS > PS20 > DBS > PONP. • IFT reduction by surfactant at 1 wt% occurred as DBS > PONOP > PS20 > LS
7	Amirianshoja et al. [61]	Adsorption	Surfactant - Sodium dodecyl sulfate (SDS), Triton X 100 Minerology- Quartz, mont-morillonite, illite and kaolinite	Non-ionic surfactant adsorption 1.5, 1.5-4.5 and 1.5-28.5 g/kg for kaolinite, illite and montmorillonite respectively	• More adsorption with non-ionic surfactant compare to anionic surfactant due to rock minerology • Adsorption of non-ionic surfactant follow the order as montmorillonite > illite > kaolinite

8	Zendehboudi et al. [57]	Interfacial tension reduction and adsorption	Sarvack reservoir Viscosity - 1.6 mPa. s Natural surfactant - Zyziphus Spina Christi Carbonate rock - Azadegan oilfield (Northern Persian Gulf) Porosity - 12% Adsorption - Isotherm and kinetics	Freundlich Model, Pseudo-second order kinetics CMC - 3.65%	• Increased oil recovery from 47% to 77% and reduces IFT by 69 %. • CMC of the surfactant was detected at 3.65% • Adsorption data showed Freundlich Isotherm and pseudo-seconder as best model fit. • Natural surfactant was found economical viable for flooding and is environmental friendly.
9	Ahmadi et al. [62]	Interfacial tension and adsorption	Natural surfactant - Glycyrrhiza Glabra Carbonate rock cores (Azadegan oilfield, Persian Gulf) Porosity - 12% Permeability - 1 to 10 mD	CMC - 3.5 wt% Langmuir adsorption isotherm and Pseudo second order kinetics Exothermic reaction	• Adsorption of surfactant on carbonate rock increases with increase in surfactant concentration till saturation point. • Experimental data was best fitted with Langmuir isotherm model (R^2 - 0.9964) and pseudo second order kinetics. • The reaction is exothermic in nature and adsorption decreases with increase in temperature. • The natural surfactant is eco-friendly, easily available and cheap.

1.3.3 Polymer Flooding Based Enhanced Oil Recovery

Due to viscous fingering effect, secondary recovery of crude oil using water flooding is well known to exhibit poor sweep efficiency and recovery factors. To circumvent the problem, polymer flood has been proposed as early as 1950 [16, 63]. Through thickening effect, polymer modifies aqueous system rheology and thereby promotes oil recovery through minimization of water channelling and enhancement of sweep efficiency. Further, polymer addition facilitates surface active transformations and stable oil water emulsions may get produced [64-67]. Till date, several successful laboratory, pilot plant and field application of polymer flooding have been reported for mature oil fields and associated systems [17, 20, 68-70].

1.3.3.1 Polymer Flooding in Fields and Laboratories

Standnes and Skjevrak [71] collected relevant critical information on polymer flooding and reported 72 polymer flooding field cases that were undertaken since 1964 (66 onshore and 6 offshore projects). Majority of these projects were implemented in the USA (64%) followed by Canada (8%) and China (5.6%). Six out of seventy two investigated cases indicated discouraging outcomes due to too low average permeability (~7 mD), low injected polymer concentration (213 ppm), higher viscosity reduction, high resistance factor, high permeability contrast and higher polymer retention. Polymer used in such studies refer to 92% HPAM (partially hydrolyzed polyacrylamide) and 8% biopolymer.

Jooybari et al. [70] reviewed the scenario of polymer flooding for heavy crude oil in laboratory scale, pilot test and field applications that were undertaken from 1960. Polymer flooding increased oil recovery from 2.2 to 44% of OOIP for laboratory investigation but such high recoveries cannot be achieved for field application due to many technical

parameters. Based on the analytical data and influence of parameters, the authors developed a screening criteria for heavy crude oil. According to the analysis of the authors, the screened data for field application of polymer assisted flooding of heavy crude oil are as follows: depth < 5250 ft; temperature < 149° F; permeability > 1000 mD; porosity > 21%; oil gravity > 11° API; oil viscosity < 5400 cP; oil saturation > 50% and formation water < 46,0000 ppm.

The performance characteristics of polymer flooding operations vary significantly due to variations in reservoir conditions and crude oil parameters. Few studies carried out till date affirm that variations in temperature and salinity (moderate to extreme) do strongly influence polymer flooding performance characteristics [72-75]. This is possibly due to viscosity reduction of the aqueous system that has been brought forward by in situ chemical degradation. Other studies conveyed that polymer degradation is due to amide groups existent in few polymers that interact with ions existent in the reservoir formation water and undergo hydrolysis to form carboxylic groups [76, 77]. Thereby, aqueous system viscosity gets reduced and precipitation also occurs. Further, thermal stability of oil water emulsions also controls oil recovery factor and higher operating temperatures detrimentally influences emulsion stability due to rate of enhancement in the coalescence of oil droplets [78, 79].

1.3.3.2 Nanoparticle Assisted Polymer Flooding

Sharma et al. [55] investigated the potential of silica nanoparticles (~15 nm) assisted polymer flooding for enhanced oil recovery application. Experimental investigations targeted formulation, stability, rheology, IFT reduction and flooding methodologies to evaluate cumulative oil recovery. The stability of nanoparticles in polymer solution was evaluated by varying the nanoparticle concentration from 0.5 to 2 wt%. The visual observation depict that

sedimentation occurred and the phenomena was stable for around one month with 0.5 wt% SiO_2. This value was reduced to 27, 22 and 19 days for 1, 1.5 and 2 wt% respectively. Nanoparticles in polymer solution underwent agglomeration and formed clusters. The average size of these clusters increased with increased in nanoparticle concentration. Zeta potential value for all considered nanoparticle concentration was above -30 mV and this inferred stability of nanoparticles in polymer solution. The viscosity of aqueous chemical solutions improved by about 3 times by considering nanoparticles. The effect of temperature on viscosity variation is not significant with the presence of nanoparticles in the polymer solution. The IFT of the system was monitored for 27 days and similar IFT reduction behaviour was observed for the nanoparticle-polymer systems. The IFT reduction continued even at elevated temperature and thereby inferred upon the potential of nanoparticles at higher temperature. The observed pressure drop during nanoparticle assisted polymer flooding was 0.318 MPa at 30°C, which reduced by 10% at 90°C. The cumulative oil recovery with polymer was 58.17% and this increased to 62.22% for 1.0 wt% SiO_2 nanoparticle - polymer containing system. However, at higher temperature of 90°C, the oil recovery reduced negligibly from 62.22% to 61.67%. In summary, oil recovery determined from flooding experiments affirmed efficacy of nanoparticles for high temperature reservoirs. The relative permeability curve further converged with the variations in the wettability of the system from intermediate wet to water wet.

Bayat et al. [80] targeted TiO_2, Al_2O_3 and SiO_2 nanoparticles for EOR application on limestone samples at operating temperatures of 26, 40, 50, and 60°C. Compared to brine, the IFT using Al_2O_3, TiO_2, and SiO_2 was reduced by 33, 37 and 42% respectively. The displacement test indicated an oil recovery of 51.9, 50.8, and 48.7% for Al_2O_3, TiO_2, and

SiO_2 respectively at 26°C. With increase in temperature, the oil recovery factor increased and maximum oil recovery was obtained at 60°C. The oil recovery obtained was 65.7% for Al_2O_3, 61.9% for TiO_2 and 57.7% with SiO_2. The nanofluids behaved as a Newtonian fluid in the entire temperature range and was comparably more viscous (1.28 to 1.65 cP) with respect to brine (0.94 cP). The contact angle was lowest for SiO_2 and this value reduced from 26° to 18° for an increase in temperature from 26 to 60°C. Similarly, for TiO_2 and Al_2O_3, the contact angle reduced from 57 to 46° and 71 to 61° respectively for a similar increase in temperature. The study was confined to nanoparticles in aqueous system and did not target investigations with polymer-nanoparticle systems.

Table 1.3: Literature data on residual oil recovery by polymer flooding.

Sr. No	Author	Mechanisms	Materials	Parameters	Key results
1.	Standnes and Skjevrak [71]	Mobility and viscosity	HPAM and biopolymer	Average permeability 563 mD and polymer injection in secondary mode.	• Compiled data of polymer flooding in fields or pilot plants in last 50 years. • 72 projects (66 onshore and 6 offshore) were examined out of which 64 % was in USA, 8% in Canada and P.R. China, 4% in Germany (5.6 %), etc. • 92% project was conducted with HPAM and remaining with biopolymer.
2	Jooybari et al. [70]	Mobility and viscosity	HPAM	Average oil mobility 0.31 md/cp and oil/polymer viscosity ratio 279	• Detailed review investigation on the advances and technology of polymer flooding in laboratory, pilot plant and oil field for heavy oil reservoirs since 1960s. • Oil recovery with polymer flooding varied from 2.2 to 44 %. • Screening criteria produced based on the data are : temperature < 149 °F, formation water < 46000 ppm, depth < 5250 ft, porosity > 21 %; permeability > 1000 md; oil gravity > 11 °API, oil viscosity <5400 cp; oil saturation > 50%.

4	Sharma et al. [55]	Interfacial tension, Rheology and wettability alteration	Silica nanoparticles - 0.5 to 2 wt%, Polyacrylamide - 1000 ppm, Sodium dodecyl sulfate - 0.14 wt% Flooding - Sandpack, Porosity - 29.77% ± 1.34%, Permeability - 1006 mD ± 86.50 mD.	Nanoparticles - 1 wt%, Slug Size - 0.5 PV	• Nanoparticles significantly reduces the IFT and reveal better stability at higher temperature. • Tertiary recovery of 24.68 was obtained with 1 wt% SiO_2 nanoparticles. • Nanoparticles improves viscosity and changes the wettability of the system from intermediate wet to strongly water wet. • Tertiary oil recovery of 24.68% was obtained with 1 wt% of SiO_2 nanoparticles
5	Bayat et al.[80]	IFT, viscosity, wettability alteration and Adsorption	Nanoparticles - Al_2O_3, TiO_2, and SiO_2; Temperature -26, 40, 50 and 60°C;vPorous media - Limestone, Porosity - 43%, permeability - 3.12 D; Crude - Malaysian crude oil - density 0.863 g/cm3 and viscosity - 21.7 ± 0.02 cP @ 26°C	Nanoparticles Concentration - 0.005 wt% (50 mg/L), Temperature - 60°C, Slug Size - 2 PV	• Lowest adsorption of 8.2% was observed with Al_2O_3, 27.8% with TiO_2 and 43.4% with SiO_2. • Nanoparticles showed better performance at higher temperature with tertiary oil recovery in the order Al_2O_3 (9.9%) > TiO_2 (6.6%) > SiO_2 (2.9%). • For contact angle and IFT reduction the behaviour was opposite with best performance achieved by SiO_2 followed by TiO_2 and Al_2O_3.

1.3.4 Combined Alkali-Surfactant-Polymer Flooding

Chemical based enhanced oil recovery (EOR) is promising to recover residual crude oil on an economic basis from the oil reservoirs subjected to primary and secondary recovery operations. Typically, alkali, surfactant, polymer, alkali–surfactant, surfactant–polymer and alkali–surfactant–polymer injection formulations are induced to recover the residual oil [19, 51, 56, 57, 70, 81-84]. Chemical injection in heavy oil reservoirs after water flooding needs to ensure that the flooding process facilitates contacting with the oil rich area and thereafter should enhance sweep efficiency to ensure higher oil recovery [85, 86]. Combined alkali-surfactant-polymer (ASP) flooding due to its synergy has the advantage of improved displacement efficiency, favourable mobility and lower interfacial tension, all of which enhance oil recovery [87, 88]. Hence, combined ASP flooding has been found to be efficient for higher oil recovery for heavy oil reservoirs [89]. The incremental production in oil recovered through alkali-surfactant-polymer flooding has also been suggested to be cost competitive [88].

Pie et al. [20] investigated the synergy of alkali (NaOH) - polymer (HPAM) interaction to enhance crude oil recovery. Sandpack flooding data conveyed an increase in tertiary oil recovery factor from 4.55 to 16.09 % for a variation in HPAM concentration from 250 to 2000 ppm. The incremental oil recovery factor was higher for an enhancement in polymer concentration from 250 to 1000 ppm (4.55 to 13.87%) and beyond 1000 ppm the incremental recovery factor became smaller (16.09%). The oil recovery factor is greatly controlled by the viscosity factor i.e., viscosity of the polymer solution. The case corresponding to polymer only flooding was not effective to enhance oil recovery due to viscous fingering effect brought forward by the significantly lower viscosity of polymer (30 mPa. s) in comparison

with that of the heavy oil (3950 mPa. s). Compared to polymer flooding alone, alkali flooding resulted in better oil recovery of 30.31% at 1 wt% NaOH. Alkali flooding penetrates into the aqueous solution in the oil phase and assists in the formation of water in oil emulsion. This emulsion diverts the aqueous solution to unswept regions and facilitates enhancement in sweep efficiency. Therefore, highest oil recovery of 43.38% was achieved for 1 wt% NaOH and 1000 ppm HPAM formulation. This is due to synergy of the alkali and polymer constituents during flooding. Micromodel test revealed synergy of the water in oil emulsion formation and viscosity modification based mobility.

In the presence of various alkalis and salts, Kumar and Mandal [5] investigated the role of both ionic and non-ionic surfactants on IFT, wettability alteration and emulsification mechanisms. Among the chosen surfactants, the ionic surfactant performed better in terms of IFT reduction due to its ability to form charged monolayer at the interface. The presence of salt in the solution further reduced IFT due to the enhancement of the accumulation of surfactant molecules at the interface. The addition of alkali to surfactant-salt solution further reduced the IFT to ultra-low value (10^{-4} mN/m). This was due to the ability of alkali to produce suitable hydroxyl ions at the interface that react with the acid groups of the crude oil to form in-situ surfactant. The emulsion formed with crude oil in the presence of alkali-surfactant was stable for more than two months. An optimum concentration was obtained based on the IFT, wettability and phase behaviour studies. FTIR analysis indicated that carboxylic acid group is prevalent in the crude oil and disappearance of such group to form in-situ surfactant at oil-water interface.

Pie et al. [28] performed sandpack and micromodel flooding experiments to determine residual oil recovery of alkali and alkali-surfactant flooding processes. The authors found that the alkali reduced IFT to 10^{-2} mN/m. However, for the alkali-surfactant system, the IFT reduced to an ultra-low value of 10^{-4} mN/m. The sandpack flooding confirmed maximum oil recovery of 19.96% with 1 wt% NaOH alkali but not with alkali-surfactant flooding (18.63%). The micromodel experiments conveyed that the alkali solution penetrates in the oil phase and enables the formation of W/O (water in oil) emulsion that contributes to sweep efficiency enhancement. Compared to the alkali flooding, the sweep efficiency was reduced for the alkali-surfactant system. This was due to the formation of O/W (oil in water) emulsion as confirmed during microscopic flooding tests.

Fu et al. [51] performed organic alkali-surfactant-polymer flooding in Shengli oilfield that were characterized with higher content of divalent ions (Ca^{2+} and Mg^{2+}). An ultra-low IFT value of 10^{-3} mN/m was obtained with the synergistic effect of surfactant (Shengli petroleum sulfonate) and organic alkali (ethanolamine) with the Shengli crude oil. Flooding experiments indicated oil recovery of only 4% for surfactant, 10.7% using polymer, 13.7% using surfactant-polymer combination and maximum oil recovery of 21.7% using organic alkali-surfactant-polymer (ASP). Combination with additional increase in the concentration of organic alkali, the oil recovery further increased to 23.4%. Microscopic displacement tests were carried out to converge upon the involved mechanisms for various combinations of chemicals. The authors conveyed that alkali reacts with the acidic group of crude oil to form W/O (water in oil) emulsion. The emulsion diverts the flooding fluid to unswept region and promotes sweep efficiency. Together, the surfactant and in-situ formed surfactant reduce the

IFT to ultra-low values and activate dispersion of crude oil to form O/W (oil in water) emulsion and thereby promote displacement efficiency. Without any precipitation of salt, higher oil recovery with organic ASP flooding was obtained due to the combined effect of improved sweep efficiency and better displacement efficiency.

Table 1.4: Literature on combined alkali-surfactant-polymer flooding.

Sr. No	Author	Mechanisms	Materials	Parameters	Key results
1	Pei et al. [20]	Displacement efficiency	Heavy crude (Shengli, China) Acid value - 4.66 mg KOH/g-oil Viscosity - 3950 mPa. s Brine TDS - 5000 mg/L Sandpack Porosity - 41.38 - 43.64% Permeability - 2016 -2194 Chemical - NaOH	NaOH - 1 wt% and 0.1 wt% NaOH + 1000 ppm HPAM, Slug Size - 0.5 PV	• Highest oil recovery of 30.31% and 43.38% was achieved using alkali and alkali-polymer flooding respectively. • Alkali-polymer synergy showed better emulsification and displacement efficiency compared to alkali or polymer alone flooding.
2	Kumar and Mandal [5]	IFT, Emulsification and Wettability Alteration	Surfactant - cetyltrimethylammonium bromide (CTAB), sodium dodecyl sulfate (SDS) and polysorbate 80 (Tween 80) Alkalis - sodium hydroxide (NaOH), sodium carbonate (Na2CO3), ammonium hydroxide (NH4OH), sodium metaborate (SMB) and diethanolamine (DEA) Ankleswar oil field, India, Acid value - 0.32 mg KOH/g, API gravity of 37.72°and viscosity of 12.2 mPa. s @ 30°C.	Salinity - 6 wt% Alkali - 0.2 wt% (except SMB - 0.5 wt%) Surfactant - CTAB - 1.17 mM/l, SDS - 10.7 mM/l and Tween 80 - 0.0136mM/l	• Ionic surfactant showed better IFT reduction compare to non-ionic and alkali-surfactant-salt synergy reduces IFT to ultra-low value of 10^{-3} mN/m. • Ionic surfactant (CTAB and SDS) changes rock wettability more effectively compare to Tween 80. • More tight and stable emulsion (up to two months) was attained with alkali-surfactant due to generated interfacial components.

3	Pie et al.[28]	IFT, Displacement efficiency and emulsification	Binnan heavy crude (Shengli, China), Acid value - 2.69 mg of KOH/g, Viscosity - 2000 mPa. s @55°C, TDS - 5000 mg/L, NaOH 0.1 to 1 wt%, SLPS - 0.03 to 0.1 wt%, ORS - 0.1wt%, SLPS and ORS - surfactants from oil field Sandpack Porosity - 42 to 45% Permeability - 1950 to 2300 mD	Slug Size - 0.5 PV Alkali- 1.0 wt% NaOH, Alkali-surfactant - 1.0 wt% NaOH + 0.1 wt% SLPS	• Alkali-surfactant (AS) results in lower oil recovery than alkali alone even though ultra-low IFT was detected by AS. • Alkali flooding micromodel test showed better penetration of alkali in the oil phase to form W/O emulsion which increases the sweep efficiency as compare to alkali-surfactant test.
4	Fu et al [51]	IFT and displacement efficiency	Zhuangxi heavy oil (Shengli, China), Acid value - 2.14 mg KOH/g, viscosity 1550 mPa. s at 50°C Alkali- Ethanolamine Surfactant - Shengli petroleum sulfonate (SLPS), Anqing petroleum sulfonate, Xinjiang petroleum sulfonate, Heavy alkyl benzene sulfonate, α-olefin sulfonate and Sodium dodecyl benzene sulfonate Polymer - Hydrolyzed polyacrylamide Sandpack Porosity - 37.5 to 39% Permeability - 1350 to 1450 mD	Slug size - 0.5 PV Polymer - 0.1 wt% Surfactant - 0.1 wt% Alkali - 0.75 wt%	• Organic alkali-surfactant-polymer (ASP) flooding was performed to eliminate the effect of precipitation from calcium and magnesium evolved during inorganic ASP system. • Ultra-low IFT was accomplished with alkali-surfactant synergy. • Alkali-surfactant-polymer forms W/O emulsion which improves the sweep efficiency and maximizes oil recovery to 23.4 %. The recovery increases with increase in alkali concentration. • Oil recovery achieved with surfactant was 4%, polymer 10.7%, surfactant-polymer 13.7% and alkali-surfactant-polymer was 23.4%.

1.4 Prominent Issues in the Literature and Scope for Further Research

1.4.1 Alkali Flooding

Till date, several successful alkali flooding experiments have been conducted to determine residual oil recovery. The available literature reported active participation of several mechanisms such as IFT reduction [14, 29, 31], emulsification of crude oil [14, 29, 36] and sweep efficiency [36, 90] towards higher residual oil recovery. The crude oil with higher acid value is promising due to the ease of formation of in-situ surfactant at the oil-water interface and facilitate significant IFT value reduction, higher emulsification, improved sweep efficiency and higher oil residual oil recovery [35]. Few studies also conveyed the dominancy of one of these mechanisms as controlling mechanism for the residual oil recovery factor [28, 90].

Despite indicating the potential of alternate mechanisms or their combination for various crude oil-reservoir systems, the literature findings cannot be generalized for any crude oil-reservoir system. Hence, alkali flooding characteristics need to be investigated on a case to case basis, given the fact that the EOR characteristics and pertinent mechanisms are significantly dependent on the crude oil, rock and formation water characteristics. Available state of the art elaborates upon the acid value and residual oil recovery but the quantification of naphthenic acid in crude oil (which varies from reservoir to reservoir) was not considered in the context of in-situ soap formation extent. Further, step wise neutralization and saponification of acid groups with alkali was not assessed with which simultaneous IFT reduction and emulsification aided with alkali penetration into the oil phase can be visualized. Such studies can provide a deeper understanding of the complexities involved during alkali flooding. The contribution of individual or synergistic mechanisms towards oil

recovery depends on the crude oil and other formation properties. Hence, it is important to consider each such system as a distinct system to infer upon the possible mechanisms that contribute towards residual oil recovery. These include the dominance of either or more of the following phenomena: IFT reduction, emulsification, wettability alteration, naphthenic acid content and its role in saponification and neutralization.

1.4.2 Synergy of Alkali-Surfactant Flooding

The interactions of chemical(s) with crude oil (IFT and emulsification mechanisms) have profound impact on residual oil recovery. Typically, minimum IFT is indicated to maximize emulsification of crude oil [91]. A linear relationship between IFT reduction and additional oil recovery invariably conveys the stronger role of IFT reduction mechanism in influencing EOR characteristics [19]. However, other studies conveyed that while IFT reduction is necessary, it need not be regarded as a primary mechanism to contribute towards higher residual oil recovery, given the fact that residual oil recovery could be higher at intermediately lower IFT values at which better emulsification can be achieved [36, 43, 92]. Similarly, while ultra-low IFT value obtained due to synergetic action of alkali-surfactant is effective for oil recovery [45], the alteration in the displacement efficiency due to emulsification as dominant mechanism is also held responsible for higher oil recovery [28].

Considering the complexities involved in IFT reduction and emulsification mechanism, a critical observation of the available literature for higher oil recovery is inconclusive. Advanced studies with surfactant systems affirmed ultra-low IFT [93] but it cannot be generalized as alkali-surfactant combination can also reduce IFT to ultra-low value [15]. The mechanism responsible for better oil recovery with alkali-surfactant flooding depends on the reservoir and crude oil properties. Hence each crude oil has to be analysed distinctly to

investigate the role of various mechanisms and system properties in influencing EOR characteristics. The synergy of alkali-surfactant with Assam crude oil has not been investigated till date to converge upon the efficacy of alkali-surfactant flooding for Assam (Indian) reservoirs. Also, the available literature for the on field application of surfactant flooding systems in carbonates reservoirs is limited [94]. In summary, carbonate reservoirs and Assam crude oil systems have to be addressed and optimal alkali-surfactant slug formulation needs to be identified for the said system.

1.4.3 Surfactant Flooding

An important limitation of surfactant flooding to achieve higher residual oil production is its adsorption with the rock surface [19, 57, 95-97]. Therefore, the adsorption behaviour needs to be evaluated and incorporated in order to decide more appropriate surfactants and its concentration range for successful chemical EOR schemes. On the contrary, surfactant adsorption is detrimental for its effectiveness and technical/economic competitiveness. With enhanced surfactant adsorption, the cost of the process is bound to enhance due to existent surfactant loss and marginal variations in desired IFT reduction. Thereby, surfactant adsorption characteristics are highly significant. Apart from desired characteristics such as minimal adsorption capacity, surfactant stability and thermal aging are relevant parameters to investigate upon [59].

Several available literature on surfactant adsorption characteristics addresses non-realistic assumptions and scenarios for carried out surfactant adsorption characteristics. These include utilization of synthetic but not real cores, room temperature investigations, aqueous but not saline media and fixed choice of rock properties such as mineral content and surface area, etc. Further, surfactant stability, thermal aging and loss characteristics are potentially

dependent on the reservoir conditions and these parameters were also not investigated by researchers. Also, as far as reservoir rock samples of North-East India are concerned (which is the targeted field of study in this work), adsorption of Na-lignosulphonate (surfactant extracted from Black liquor effluent from paper mill) was investigated for rock sample of Oil India Limited (OIL), Duliajan, India. In this literature as well, rock mineralogy has not been considered for its critical influence on surfactant adsorption characteristics [98].

1.4.4 Nanoparticles - Polymer Flooding

Polymer flooding has the ability to recover heavy residual oil from reservoirs by maintaining favourable mobility ratio. Polymer when injected in the oil reservoir, improves the viscosity of the displacing fluid which reduces viscous fingering and pushes the oil to the production unit. Recent investigations targeted nanoparticle assisted polymer flooding and indicated that such technology has significant impact to enhance residual oil recovery factor [99-102]. Compared to conventional polymer flooding, nanoparticles have unique ability to improve system rheology, reduce IFT and alters wettability due to which additional oil recovery can be achieved.

A critical insight into the available prior art conveys that both polymer flooding and nanoparticle assisted polymer flooding received little attention with respect to integrated studies associated to IFT reduction, wettability alteration, emulsion stability, rheology and tertiary oil recovery. Few literatures report emulsification and emulsion stability during polymer flooding studies [64, 65, 67]. However, the synergy of the crude oil-polymer-nanoparticle system has not been evaluated in the context of emulsification and system stability. Also, the effect of temperature and salinity of such processes has been studied to a limited extent. The associated tradeoffs to nanoparticle inclusive polymer flooding systems

need to be critically examined, given the fact that higher nanoparticle concentrations could clog the porous structure of the oil reservoirs and detriment oil recovery.

1.5 Objectives

Considering the significant limitation of enhanced oil recovery studies for Assam crude oil and Indian reservoir systems, the primary objective of the thesis is to investigate chemical EOR characteristics for the specified system. It is well known that the success of chemical EOR depends on crude oil, reservoir rock characteristics that demand case specific investigations. The chemical EOR based higher residual oil recovery is strongly influenced with various mechanisms and hence a detail examination of all potential mechanisms is important to understand the system characteristics thoroughly. The interaction of chemicals with crude oil and other process parameters are often very complex and require distinct observation for precise combinations of crude, rock and formation water systems. The following objectives have been chosen for the carried out work reported in the PhD thesis:

1.5.1 Characterization of Assam Crude Oil and Rock

Crude oil, formation water and reservoir rock collected from Assam oil fields, India are to be characterized in detail to evaluate their characterization parameters and categories. The investigations confine to two different crude oils, formation water collected from reservoir source and reservoir rock samples obtained from various oil fields of Assam.

1.5.2 Synergy of different Mechanisms and Optimum Alkali Flooding

The potential of alkali flooding to recover residual crude oil (light to moderate Assam crude) has to be addressed. Alternate mechanisms that contribute to residual oil recovery such as IFT, emulsification quality, role of naphthenic acid, wettability alteration and sweep

efficiency will be explored. Eventually, optimal flooding process parameters (slug volume and injection pattern) will be determined.

1.5.3 Alkali-Surfactant Flooding in Sandstone and Carbonate Reservoirs

By targeting a systematic methodology for the determination of optimal chemical slug, the ability of alkali-surfactant flooding system to recover residual Assam crude oil from sandstone and carbonate reservoirs needs to be evaluated. The systematic methodology could initially screen alkalis (NaOH and Na_2CO_3) based on IFT reduction. Thereafter, various surfactants could be screened for their potential towards IFT reduction and emulsification extent of Assam crude oil. The optimality of alkali and surfactant mixture concentrations can be explored from optimal concentration perspective in terms of desired synergy such as ultra-low IFT value, extent of emulsification and wettability alteration. Finally, lab scale core flooding experiments need to be conducted to determine role of IFT reduction, emulsification, wettability alteration and displacement efficiency mechanisms.

1.5.4 Role of Rock Minerology on Surfactant Adsorption Capacity

The major emphasis of this work is to investigate upon surfactant adsorption characteristics for Assam reservoir rocks (India) with an emphasis upon summarized research gaps. The experimental investigations need to target temperature variations (30–70°C), synthetic formation water and reservoir rock samples. Rock mineralogy related characterization parameters (obtained from XRD analysis) have to be correlated with surfactant adsorption characteristics and compared with those obtained for the synthetic reservoir cores. Methodology adopted for the surfactant adsorption characteristics needs to consider thermal aging based surfactant stability, dynamic IFT evaluation and fitness of isotherm, kinetic and thermodynamic models.

1.5.5 Silica Nanoparticle-Polymer Flooding

The role of silica nanoparticles (SNPs) on polymer flooding of Assam crude oil (India) needs to be examined. The stability behaviour of nanoparticles in polymer solution and improvement in emulsion quality (average droplet size), stability period, creaming index, IFT reduction, rheology and wettability alteration are to be targeted. Finally, Berea core based flooding experiments are to be considered to evaluate the effect of polymer and SNPs-polymer systems on additional oil recovery.

1.6 Organization of the Thesis

Along with a brief introduction to enhanced oil recovery, **Chapter 1** of the thesis is devoted to various mechanisms that contribute to higher crude oil recovery for alkali, alkali-surfactant and nanoparticles induced flooding systems. Following this, the state of the art was summarized along with prominent issues and scope for further research. Finally, the objectives and organization of the thesis content has been presented.

Chapter 2 summarizes the materials and methods adopted in the work. These include physicochemical characterization of Assam crude oil, ionic composition of formation water, thermal stability of chemicals and core flooding experiments to estimate residual oil recovery.

The experimental findings associated to the synergy of interfacial tension, emulsification, wettability alteration and neutralization and saponification extent during alkali flooding for light to moderate Assam crude oil have been presented in **Chapter 3**. Considering residual oil recovery, alkali concentration, slug size and injection pattern were optimized.

Chapter 4 presents the research findings associated to investigations that targeted the synergy between alkali and surfactants for sandstone reservoirs and Assam crude oil system.

The IFT and emulsification behaviour with different alkalis and surfactants were evaluated. Subsequently, the best alkali-surfactant was subjected for oil recovery studies using sandpack flooding experiments.

The thermal stability of various surfactants and their adsorption characteristics for various rock samples have been presented in **Chapter 5**. The effect of variant mineralogical parameters of the rock have been examined along with temperature and system salinity to influence adsorption characteristics.

Chapter 6 addresses the development of optimal formulation of alkali, surfactant and its combination for higher residual oil recovery in carbonate reservoirs. For the chosen surfactants, a correlation was developed between IFT reduction and emulsification. Among the chosen surfactants, best surfactant was chosen to evaluate residual oil recovery characteristics of Assam crude oil.

Chapter 7 presents the application of silica nanoparticles for potential enhancement in the oil recovery factor at variant temperature. Potential mechanisms that contribute towards silica nanoparticle integrated polymer flooding based enhanced recovery have been examined. These include IFT reduction, emulsification, mobility and wettability alteration.

Chapter 8 summarizes conclusions of the carried out research work and possibilities to extend the research work in the future.

Chapter 2

Materials and Methods

In this chapter, the materials and experimental methods used to evaluate oil properties, formation water composition, rock characterization, thermal stability of surfactants, adsorption of surfactants, stability of nanoparticles and sandpack/core chemical flooding were described. The physiochemical properties of Assam crude oil such as acid value, API gravity, naphthenic acid content and viscosity were evaluated in this chapter. Similarly, the compositional analysis of Assam reservoir formation water using AAS and detail characterization of Assam reservoir rock using XRD, BET and EDX were obtained. Thermal stability of the surfactant were identified by FTIR, NMR and TGA analyses. The adsorption behaviour of surfactant on rock surface were identified by ultraviolet - visible spectroscopy and different isotherm and kinetic models were explored. The stability of nanoparticles in aqueous chemical phase were achieved by particle size analyser. The mechanisms investigation for different chemical EOR schemes were identified by evaluating surface/interfacial tension, emulsification and its creaming rate, contact angle measurement and finally chemical flooding experiments.

2.1 Materials

Crude oil and reservoir formation water samples were collected from Assam oil field, India. Natural reservoir rocks were collected from Hapjan and Jorajan oil field, Assam, India whereas synthetic Berea cores (Carbon Tan, Idaho Gray, Gray Berea and Silurian dolomite) were purchased from Kocurek Industries, Inc. Caldwell, USA. Sand particle were procured

from construction sites at Indian Institute of Technology Guwahati. Sodium hydroxide (NaOH), Sodium chloride (NaCl), Sodium carbonate (Na_2CO_3), Potassium chloride (KCl), Sodium dodecyl sulfate (SDS), Titriplex III, Magnesium sulfate heptahydrate ($MgSO_4 \cdot 7H_2O$) and Calcium chloride dihydrate ($CaCl_2.2H_2O$) were procured from Merck specialities Pvt. Ltd., India. Sodium bicarbonate ($NaHCO_3$), Sodium dodecyl benzene sulfonate (SDBS), Span 80, Tween 80, Brij 30 and Xanthan gum were purchased from Sigma-Aldrich chemicals Pvt. Ltd., India. Cetyl trimethylammonium bromide (CTAB), Trition X-100 (TX-100) and Hydrophilic Silicon dioxide nanoparticle (SNPs) with average particle size of 15 nm were procured from Sisco Research Laboratories, India. Sodium lignosulphonate was purchased from National Chemicals, India. The materials and different chemical EOR schemes used in this work is tabulated in appendix A Table A1.1.

2.2 Methods

The physiochemical properties of two different Assam crude oil samples such as density, American Petroleum Institute (API) gravity and acid value were evaluated by ASTM standards. Naphthenic acid quantification of the crude oil was estimated using extraction and back extraction method. Identification of functional groups present in the crude oil was performed by Fourier Transform Infrared (FTIR) analysis. Atomic Absorption Spectroscopy (AAS), Ion Chromatography and Alkalinity Test quantify the presence of various ions present in reservoir formation water. The viscosity of the samples were measured using rheometer, whereas surface tension and interface tension were measured using auto tensiometer. The interfacial tension between two liquid phases in the range of 10^{-1} to 10^{-3} mN/m was detected using spinning drop tensiometer. Thermal stability analyses of selected surfactant samples were carried out by Nuclear Magnetic Resonance (NMR) spectroscopy,

FTIR spectroscopy and Thermogravimetric Analysis (TGA) techniques. The characterization of rock samples and sand particles used in flooding experiments were accomplished using X-ray Powder Diffraction (XRD), Field Emission Scanning Electron Microscope (FESEM), Energy Dispersive X-ray (EDX) and Brunauer–Emmett–Teller (BET). The adsorption of surfactant on rock surface were quantified by obtaining the initial and final concentrations of surfactant before and after adsorption experiments using ultraviolet -visible spectrophotometer. Different adsorption isotherm and kinetic models were studied and the best models were identified. Thermodynamics parameters were evaluated to specify the feasibility, spontaneity and exothermic nature of the adsorption process. Emulsification of the crude oil was investigated by carrying out emulsification test and its stability were observed by creaming index. The stability of nanoparticles in the aqueous phase were identified by particle size analyser. Wettability alteration for chemical enhanced oil recovery systems were identified through contact angle measurement. Flooding experiments were conducted to quantify the percentage of cumulative oil recovery for different chemical enhanced oil recovery schemes.

2.2.1 Density and American Petroleum Institute (API) Gravity

The density of the crude oil were measured using specific gravity bottle by ASTM D4025 method. Specific gravity (density relative to water) which is defined as the ratio of density of crude oil to density of water was used to calculate the API gravity. API gravity was evaluated using the equation as given below

$$API\ gravity = \frac{141.5}{Specific\ gravity} - 131.5 \qquad 2.1$$

2.2.2 Acid Value, Naphthenic Acid Extraction and Saponification

Acid value is defined as the amount of KOH in milligram required to neutralize one gram of sample. Acid value of the crude oil was evaluated using the American oils chemists society (AOCS) official methods (Te TA-64, 1997). The expression used to calculate the acid value is as follows

$$AV = \frac{N \times V \times 56.1}{M_S} \qquad 2.2$$

Where AV, N, V and M_s are the acid value (mg KOH / gm sample), normality of NaOH (N), volume of titrant (ml) and mass of the sample (gm), respectively.

Naphthenic acid from the crude oil was extracted with alkali solution and was subsequently back extracted again from alkali solution using HCl solution [103, 104]. Assam crude oil (20 g) was mixed with 20 ml of hexane and the mixture was extracted (three times) with a sample of 10 ml of 1 M NaOH for each cycle (prepared with 50% ethanol and 50% H2O). Subsequently, the alkali layer was collected and extracted in three cycles (with 10 ml hexane for each cycle) to remove traces of dissolved crude oil. Eventually, the alkali solution pH was reduced to 2 by adding HCl. The acidified solution was first contacted with dichloromethane in three cycles (10 ml for each cycle) and then was dried with sodium sulfate in N_2 environment to reach a final solution volume of 3 ml. An aliquot of 10 µl from this sample was measured for its weight using a microbalance after stabilizing the same (allowing solvent losses) for 30 min. The measured weight corresponds to the naphthenic acid content in the crude oil. The experiments were repeated and the values with standard deviation are reported. Also, saponification and neutralization extent of crude oil during

alkali flooding was evaluated by measuring the total acid value of crude oil before and after alkali flooding experiments [18]. In this regard, it is important to note that the acid value reduction does not refer to saponification alone, as part of alkali would be consumed for acid neutralization which does not form soap. Hence, the acid value measurement procedure corresponds to the extent of saponification and neutralization.

2.2.3 Fourier Transform Infrared (FTIR) Spectroscopy

FTIR spectra of crude oil and surfactants were conducted to detect the presence of various functional groups present in the samples. IR spectrometer (Shimandzu - IR Affinity) using ATR (attenuated total reflection) and KBr pellet methods were used to perform the analysis. The infrared spectra were recorded between 600 and 4000 cm^{-1} at room temperature. FTIR characterization of thermally aged surfactants were executed to observe any change or degradation in functional groups for validating thermal stability of the surfactants.

2.2.4 Atomic Absorption Spectroscopy (AAS), Ion Chromatography and Alkalinity

Cationic ions present in the reservoir formation water were characterized using atomic absorption spectrophotometer (Varian - AA240). Standard samples of known concentration (5 to 50 ppm) were prepared based on metal ions and calibration curves (concentration vs adsorption) were produced. Based on the calibration curve the unknown concentrations of cations in the formation water were identified. Quantification of chloride ions were performed using ion chromatography (Metrohm - Basic IC 792). The bicarbonate ions present in the sample were evaluated by alkalinity test using titration method [105].

2.2.5 Viscosity

Viscosity of crude oil, chemical solutions with nanoparticles (aqueous phase) and emulsion were analysed using rheometer (Anton Paar - MCR 301). The rheometer was fitted with thermostatic water bath to control the temperature to a set value within ± 0.1°C. For non-Newtonian fluid, the viscosity of the samples were measured by varying the shear rate from 1 to 1000 s^{-1} and for simplicity, viscosity at 1 s^{-1} shear rate (near zero shear viscosity) is reported. All the data was stored and extracted by Rheoplus V 3.1 software. The viscosity measurement experiments were repeated four times for each sample to attain reproducibility and the data with standard deviation was reported. Frequency sweep (oscillation) measurements were carried out to observe the behaviour of G´ (storage modulus) and G´´ (loss modulus) [106]. The angular frequency omega was set from 0.1 to 10 (rad/s). Storage modulus (G´) indicates gel/solid like behaviour and loss modulus (G´´) resembles viscous/liquid like behaviour.

2.2.6 Surface Tension and Interfacial Tension

The surface tension values of the surfactant samples were measured using tensiometer (Kruss - Tensiometer K9) by platinum plate method to identify the critical micelle concentration (CMC). Initially, the plate was burned to red hot for removable of impurities present in the surface of the plate. The aqueous phase was poured in the glass vessel and was then placed in the measuring position of the apparatus. The movement of the glass vessel was adjusted to a position such that the plate remains close to the solution surface. After adjusting the glass vessel movement, the system was calibrated by setting the initial reading to zero. The measurement button on the instrument was then pressed which automatically dip the plate in the solution and then pulls the plate out of the surface. The maximum reading

displayed on the instrument denotes the surface tension value. The interfacial tension for crude oil and polymer-nanoparticle solution were measured in the similar manner using auto tensiometer (Kwoya - DY300) by Wilhelmy plate method. However, in this case, dense phase (aqueous media) was poured in the glass vessel and on top of which light phase (oil media) was poured without disturbing the surface. The plate was dipped in the sample up to the interface and then the IFT reading was obtained. The system was connected with water bath which can regulate the temperature up to 70°C.

The interfacial tension between two liquid (crude oil and aqueous chemical solution) in the lower range of 10^{-1} to 10^{-3} mN/m were measured using Spinning drop tensiometer (Kruss - Site100). The heavier phase (aqueous) was poured in the cylinder connected to the capillary tube and then the lighter phase (crude oil) was injected by micro syringe in the capillary tube. The capillary rotation speed was maintained at sufficient rpm such that the length to diameter ratio was always found to be ≥ 4. Subsequently, the interface image was utilized to calculate the IFT value using the following expression

$$\sigma = \frac{r^3\omega^2(\rho_H - \rho_L)}{4}; \frac{L}{D} \geq 4 \qquad 2.3$$

Where σ is the interfacial tension (mN/m), ρ_H is the density of heavy water phase (g/cm3), ρ_L is the density of the oil phase (g/cm3), ω is the rotational velocity (rpm), D (=2r) is the measured drop width (mm) and L is the length of the oil drop (mm). The IFT analysis at moderate to extreme reservoir conditions were performed by thermostatting the temperature of measuring cell from 30-70°C.

2.2.7 Thermal Stability Analysis

The thermal stability of surfactants were determined using TGA (NETZSCH - 209 F1 TG) within the temperature range of 30–900°C. The study was conducted using nitrogen gas with a flow rate of 40 ml/min at a heating rate of 10°C/min. For long term stability, the surfactants were aged at 90°C for 10 days. FTIR and NMR spectroscopy of the aged samples were analysed. For FTIR, moisture removed KBr (Potassium bromide) and aged samples were used to prepare a pellet by pressurizing the mixture at high pressure. Pure KBr was used as background and the pellets of different samples were analysed to identify the prevalent functional groups. NMR spectral analysis of the aged samples were conducted using 600 MHz NMR spectrometer (Make: Bruke) with 5 mm diameter NMR tube and D_2O solvent as reference peak.

2.2.8 X-ray Powder Diffraction (XRD)

Rock samples from Assam reservoir field and Berea cores purchased from USA were grinded and screened to 100–120 mesh. The sieved rock samples were washed with millipore water for three times and dried in an oven at 100°C for 24 hrs. Finally, the dried samples were cooled at room temperature and then subjected for characterizations. For X-ray diffractogram (Bruker - D8-Advance), the samples were crushed into fine powder and analysed to determine its mineral compositions in the Bragg angle (2θ) range of 10–90°. Match software was used to determine the percentage of different minerals.

2.2.9 Field Emission Scanning Electron Microscope (FESEM) and Energy Dispersive X-ray (EDX)

Field emission scanning electron microscope (FESEM) analysis (Zesis - Sizma) was performed by placing the sample in carbon tape which was attached to the sample holder

(stub) and was coated with gold to reduce charging. The images was then captured and analysed to spot the adsorption of nanoparticles in oil and rock surfaces. Electron dispersive X-ray (EDX) analysis of the rock samples were performed using Field emission scanning electron microscope in which EDX detector was attached to determine the elemental composition of reservoir rock.

2.2.10 Brunauer–Emmett–Teller (BET)

The pore volume, pore size, pore size distribution and total surface area of the rock samples were calculated by BET analyser (Quantachrome, Autosorb-IQ MP) using liquid N_2 and degassing temperature of 150°C. BET method was used to calculate the pore volume, actual pore size and total surface area. The pore size distribution was determined by BJH (Barrett-Joyner-Halenda) method.

$$D_p = \frac{6 \times 10^3}{\rho \times S_A} \qquad 2.4$$

Where ρ and S_A are the density of sample and BET surface area (m^2/g) respectively.

2.2.11 Ultraviolet -Visible Spectrophotometer

Surfactant samples were prepared in the concentration range of 100–5000 ppm and were diluted to 100–600 ppm to obtain calibration curve for supplementing adsorption studies. The calibration curve was obtained using ultraviolet - visible spectrophotometer (Shimadzu - UV 2600) at a wavelength of 277 nm (λ_{max}) which is incidentally the peak for all calibrated samples. The obtained calibration curves of surfactant using formation water and millipore water along with its CMC value is presented in appendix C (Fig C5.1).

2.2.12 Adsorption Experiment Procedure

The rock samples were mixed with surfactant solutions in the gravimetric ratio of 1:5 with surfactant concentration varying from 100–5000 mg/L. The mixture was subjected to rigorous agitation by placing it in an orbital shaker (Lab Companion - SIF-6000R) at 120 rpm and 30°C for 24 h. After agitation, the sample was centrifuged at 10,000 rpm in a centrifuge (Sigma - 2–16 P) to separate the mixture. The liquid sample after centrifugation was subjected to ultraviolet - visible spectroscopy to obtain the equilibrium concentration. Based on initial and final surfactant solution concentration, the adsorption amount q (mg/g), was evaluated using the expression:

$$q = (C_o - C_f)\frac{v}{m} \qquad 2.5$$

Where C_o is the initial concentration (mg/L), C_f is the final equilibrium concentration (mg/L), v is the surfactant volume (L) used in the reaction and m is the mass (g) of the reservoir rock used for adsorption. To further evaluate the thermodynamic parameters of adsorption process, the temperature of the system was varied from 30 to 70°C.

2.2.13 Adsorption Isotherms and Kinetic Models

In order to determine the adsorption capacity of Triton X-100 on Assam reservoir rock at constant temperature, four different adsorption isothermal models were applied. To obtain a deeper insight into the inefficiency of the EOR process, kinetics studies was also performed with four different kinetic models. The mathematical expression and the significance of these models are summarized in Table 2.1.

The average relative error (ARE) for adsorption isotherm model and adsorption kinetics were calculated using the equation [107]

$$ARE = \frac{100}{n}\sum_{i=1}^{n}\left|\frac{q^{model} - q^{exp}}{q^{exp}}\right| \quad 2.6$$

Where q^{model} and q^{exp} are the adsorption values (mg/g) obtained from models (isotherm/kinetics) and experimental data. ARE method was selected for error calculation as it reduces the distribution of fractional error within the entire concentration range and can under or overestimate the experimental data [108].

2.2.14 Evaluation of Thermodynamic Parameters

The fundamental thermodynamic parameters such as enthalpy, entropy and Gibbs free energy can be calculated using Langmuir isotherm constant whose value depends on the temperature of the system. Gibbs free energy chance was evaluated using the expression:

$$\Delta G = -RT \ln K_L \quad 2.7$$

Where R is the universal gas constant (8.314 Jmol/K), T is the temperature (K) and K_L Langmuir constant (L/g). Also, other thermodynamic parameters such as enthalpy and entropy can be calculated using the expression:

$$\ln K_L = \frac{\Delta S}{R} - \frac{\Delta H}{RT} \quad 2.8$$

Using a plot of 1/T vs ln KL, ΔH and ΔS values can be determined from the slope and intercept respectively.

Table 2.1: Adsorption isotherm and kinetic models.

		Equation	Comments	References
Isothermal Models	Linear Isotherm	$q_e = K_H C_e$	It assumes that adsorption of adsorbate on adsorbent surface is a linearity function in which the variation of dependent and independent variable are linear.	[59, 109]
	Langmuir	$q_e = \frac{q_o K_L C_e}{1 + K_L C_e}$	Empirical formula which assumes monolayer adsorption with adsorption on finite number of localized sites and no interaction between the adsorbed molecules.	[107]
	• Separation Factor (R_L)	$R_L = \frac{1}{1 + K_L C_o}$	It is a non-dimensional constant describing the adsorption nature, favourable adsorption ($0 < R_L < 1$); unfavourable adsorption ($R_L > 1$); linear adsorption ($R_L = 1$) and irreversible adsorption ($R_L = 0$)	[108]

	Freundlich	$q_e = K_F C_e^{1/n}$	It shows the non-ideal and reversible adsorption process with multiple layer adsorptions and surface heterogeneity.	[109]
	Temkin	$q_e = B \ln K_T + B \ln C_e$	The model assumes that in a layer during adsorption covering, the heat of adsorption decrease linearly and is not a function of logarithmic.	[110, 111]
Kinetic Models	Pseudo-first order	$\ln(q_e - q_t) = \ln q_e - K_1 t$	It is a truly second order reaction treating it is first order reaction in which one reactant is in large excess compare to other reactant.	[112]
	Pseudo-second order	$\frac{t}{q_t} = \frac{1}{K_2 q_e^2} + \frac{t}{q_e}$	The model assumes that the adsorption capacity depends on the active sites on the adsorbent surface.	[113, 114]
	Intra particle diffusion	$q_t = K_i \, x \, t^{1/2}$	It helps in understanding the adsorption process by taking into account of diffusion mechanism.	[115]
	Elovich's	$q_t = \frac{1}{\beta} \ln(\alpha\beta) + \frac{1}{\beta} \ln(t)$	It does not predict any diffusion mechanism and assumes heterogeneous surfaces of adsorbent.	[116]

2.2.15 Emulsification Test

Emulsification test was conducted to observe the amount of emulsion formed between crude oil and different chemical solutions. Crude oil and chemical solutions were mixed in the ratio of 3:7 in graduated glass tube and the samples were shaken rigorously in a shaker for 30 minutes. These emulsions were collected in a slit and were exposed to microscope (Nikon - Eclipse LV100N POL) to evaluate the drop diameter and droplet size distribution using ImageJ software. The oil–water emulsions produced in the effluent collected during alkali flooding experiments were analysed using microscope (Olympus - CX-31). Stability of the emulsion were identified by visually observing the emulsion tube kept at stationary position without disturbance for hrs or days.

2.2.16 Contact Angle Measurements

The contact angle between oil saturated sand surface and drop of chemical solution was measured using drop shape analyser DSA 25 (Kruss - Germany) with inbuilt software version Kruss Advance 1.1.0.2. Polished powdered sand was compressed to form a pellet in pelletizer and saturated with crude oil in an oven at 80°C for 7 days. The oil saturated sand surface was then placed in the chamber to achieve ambient temperature and the chemical solution (10 ml) was dropped on it by a needle of 0.5 mm OD. The variation in the contact angle with time was then noted to observe the change in wettability of the quartz surface. To observe the behaviour in contact angle with nanoparticles the method used was little different. Berea core was cut into pieces, polished and saturated with oil for 3 days at 80°C. Oil saturated Berea pieces were then further saturated with polymer-nanoparticles (nanofluid) solutions for another 24 hrs and then washed with deionized water. The samples were then dried in an oven at 40°C for 24 hrs. The rock samples were then submerged in a water container and an

oil droplet was placed carefully on the top surface of the rock by a needle. Drop shape analyser (Holmarc - HO-IAD-CAM-01B) with inbuilt software version 8.1.0.0 was used to measure the contact angle.

2.2.17 Particle Size Analyser and Zeta Potential

The average size of the cluster nanoparticles in the aqueous polymer solutions and its zeta potential were measured by dynamic light scattering (DLS) using particle size analyser (Beckman Coulter - Delsa Nano C) at 25°C. The sample was poured in the cuvette and then placed inside the chamber of the instrument. A laser beam was illuminated and the fluctuation in laser beam due to the Brownian motion were detected to calculate the particle size and zeta potential.

2.2.18 Creaming Index

Creaming index behaviour was performed to evaluate the role of silica nanoparticles on emulsion stability. The emulsion formed was kept in the vials in an undisturbed position for days and were visualized. The stability was monitored after 10 days by measuring the height of lower serum and the height of total emulsion. The equation used to calculate the percentage of creaming index is as follows:

$$CI = \frac{H_{serum}}{H_{emulsion}} \times 100\% \qquad 2.9$$

Where, CI is the creaming index in percentage, H_{serum} is the height of the lower serum and $H_{emulsion}$ is the height of total emulsion.

2.2.19 Sandpack/Core Flooding Experiments

A schematic diagram of the core flooding experimental system is illustrated in Fig. 2.1. The setup consists of three hydraulic pumps to deliver chemical, oil and water to the core reactor. An additional pump was attached to the core reactor for supplying overburden pressure. The core reactor was facilitated with pressure transducers at the inlet and outlet of the core holder through which pressures across the core can be measured. The delivery end of the core sample holder was connected to a backpressure regulator to control the pressure differential across the core sample at desire value.

To prepare sandpack column of reactor size 3.9 cm diameter and 11 cm length, local sand (collected from construction sites) was screened in a sieve shaker to desired mesh size. The sand was then washed several times with millipore water and dried in an oven for 24 hrs. Subsequently, the core holder with sieve mesh was held vertically connecting to a pneumatic vibrator and filled with formation water up to a certain level by closing the bottom end. The sand was poured in several steps and the level of synthetic formation water inside the core holder was always maintained above the sand surface to avoid trapping of air bubbles. The core holder was shaken in each step to enable air tight arrangement, and at the end the core holder was left to vibrate for 1 h to confirm tight sandpacking [20, 26, 36, 51]. For core flooding experiments, purchased Berea cores with dimension (3.9 cm diameter and 11 cm length) were used. The flooding experiments were then conducted by injecting reservoir formation water to evaluate the permeability of brine using Darcy's Law.

$$Q = \frac{-kA\Delta P}{\mu L} \qquad 2.10$$

Where Q = Total discharge in cm^3/sec, A = Cross sectional flow area in cm^2, Δp = Pressure drop between inlet and outlet of the core reactor in atm, μ = Viscosity of brine in cP, L = Length of core in cm.

Oil saturation was then executed by injecting oil in the core at 800 psi until brine cut reaches to less than 1% and was left at pressurized condition for 24 hrs to attain uniformity. After achieving reservoir condition, the original oil in place (OOIP), irreducible brine saturation/initial oil saturation and porosity of the core were measured through material balance equations as

$$\phi = [V_p/V_t] \times 100 \quad (2.11)$$

$$Vp = V_{irb} + V_o \quad (2.12)$$

$$V_{irb} = (V_{ib}) - (V_{rb}) \quad (2.13)$$

$$S_{wi} = V_{irb} / V_p \quad (2.14)$$

$$S_{oi} = V_o/V_p \quad (2.15)$$

$$S_{oi} + S_{wi} = 1 \quad (2.16)$$

Where ϕ = Porosity (%), Vp = Pore volume of Berea core (ml), V_t = Total volume of Bera core (ml), V_{irb} = Irreducible brine saturation (ml), V_o = Oil volume occupied in Berea core during oil saturation (ml), V_{ib} = Volume of brine inside Berea core after brine saturation (ml), V_{rb} = Volume of brine removed from Berea core during oil saturation (ml), S_{wi} = Initial water/brine saturation (%), S_{oi} = Initial oil saturation (%).

Water is then injected to measure the percentage of oil recovered by water flooding until oil cut in the effluent reaches to less than 1%. Chemical slug of 0.5 PV (pore volume) followed by chase water were then accomplished to calculate the percentage of oil recovery by chemical flooding. A schematic diagram explaining flooding procedure is represented in appendix B Fig. B 2.1.

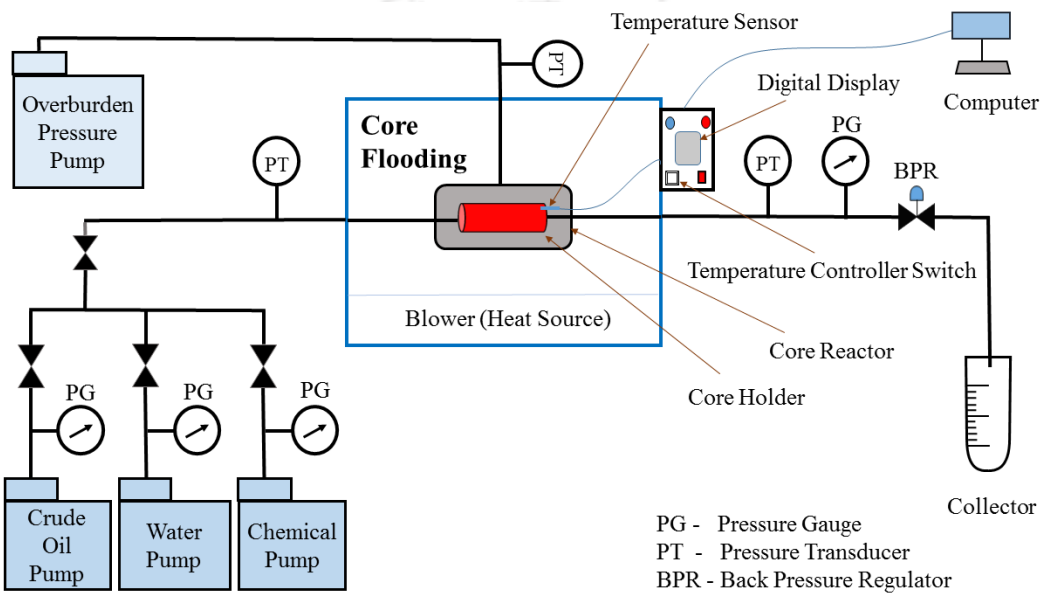

Fig. 2.1: Schematic diagram of core flooding apparatus.

2.2.20 Chemical Flooding Schemes

Various chemical flooding schemes in this work has been investigated to evaluate the potential of different chemical combination in enhancing the residual oil recovery for Assam reservoirs.

- Alkali flooding - Alkali flooding experiments were conducted with Assam crude oil (light to moderate crude oil) to observe the efficacy of alkali in terms of residual oil

recovery. The efficiency of alkali to recover residual oil is estimated in laboratory scale and the role of different mechanisms were evaluated (Chapter 3).

- Alkali-surfactant flooding - The ability of alkali, surfactant and alkali-surfactant combination flooding to recover residual oil was identified for sandstone reservoir (Chapter 4) and carbonate reservoir (Chapter 6). For sandstone reservoir light to moderate crude oil was used and for carbonate reservoir, heavy crude oil was considered.
- Polymer-nanoparticles flooding - In this section (Chapter 7), silica assisted polymer-nanoparticle flooding was explored. The effect of nanoparticles on various mechanism which are held responsible for higher oil recovery were examined.

Chapter 3

Alkali Flooding in Sandstone Reservoir for Light to Moderate Crude Oil

This chapter examines the synergy of different mechanisms such as interfacial tension, emulsification, wettability alteration and extent of saponification during alkali flooding for light to moderate Assam crude oil. The interfacial interaction between alkali NaOH and Assam crude oil were investigated. The oil recovered in the effluent stream during alkali (NaOH) flooding was analysed to identify the quality of water in oil (W/O) emulsion produced and the extent of saponification. Sandpack flooding experiments were conducted to quantify the percentage of residual oil recovered. The effects of slug volume and injection pattern during NaOH flooding experiments were also investigated. Further, change in the contact angle values indicates the wettability alteration of the system from intermediate wet to favourable water wet.

3.1 Characterization of Crude Oil and Reservoir Rock

This section describes the characterization of crude oil, formation water and sand particle used for flooding experiments. Assam crude oil used in this study has density of 892.4 kg/m^3, API gravity of 27.06 °, acid number of 2.94 mg of KOH/gm sample and viscosity of 33.4 mPa. s at 25°C (13.8 mPa. s at 30°C). The surface tension of the crude oil was found to be 27.3 mN/m. The composition of the formation water collected from Assam reservoir consist of Na^+ = 1308 ppm, Ca^{2+} = 18 ppm, K^+ = 65 ppm, Mg^{2+} = 12 ppm, Cl^- = 876 ppm. Fig. 3.1 revealed the elemental compositional anlaysis of the sand particles used for sandpack

flooding experiments with existence of oxygen and silica as major elements in the sand along with traces of Al, Fe and Na.

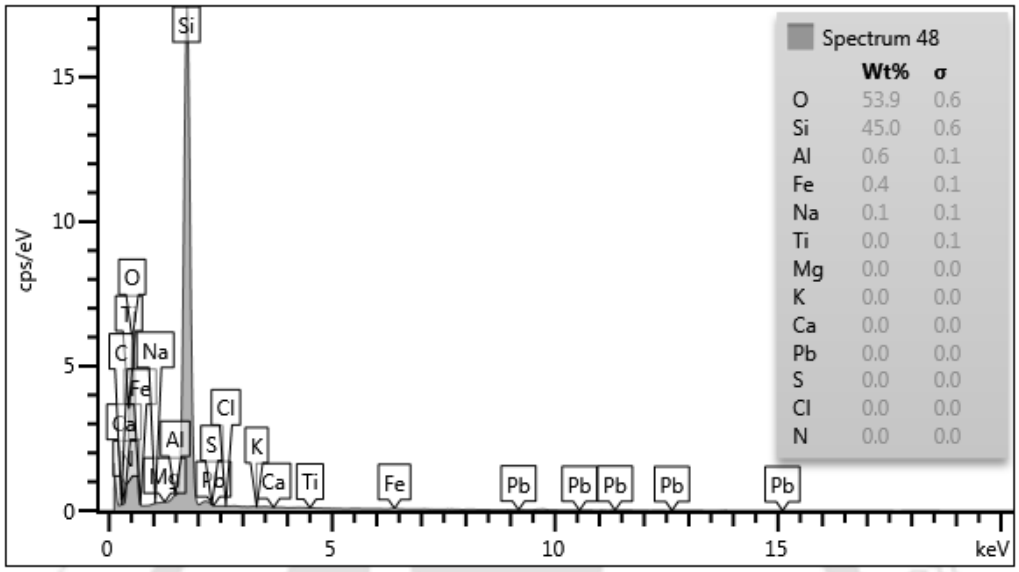

Fig. 3.1: Elemental compositions of sand particles used for flooding experiments.

3.2 Fourier Transform Infrared (FTIR) Analysis

FTIR spectral analysis of Assam crude oil (Fig. 3.2) confirms the existence of various functional groups. Peaks observed at 2953, 2923 and 2853 cm^{-1} denote the C-H stretching of saturates whereas peak at 1455 cm^{-1} indicates the C-H bend of saturated aliphatic hydrocarbons. Peak in the range of 3700-3100 cm^{-1} indicates O-H stretch of phenolic functionalities and peak in the range of 1600 – 1720 cm^{-1} shows C=O stretch of the carboxylic acid [117, 118]. Also, the peak observed in the range of 700 – 1000 cm^{-1} could be analysed to correlate the out of the plane bending of =C-H aromatic ring. This confirms that there are alkyl substituents in the crude oil sample [118, 119]. The FTIR spectra obtained for the aqueous effluent sample from 1 wt% NaOH flooding confirmed the existence of characteristic peak at 1642 cm^{-1} that refers to the -C=C- stretch of petroleum soap or in-situ

surfactant during flooding experiments [118]. Similarly, the peak observed within 3250 – 3500 cm^{-1} affirms O-H stretching of the phenolic group.

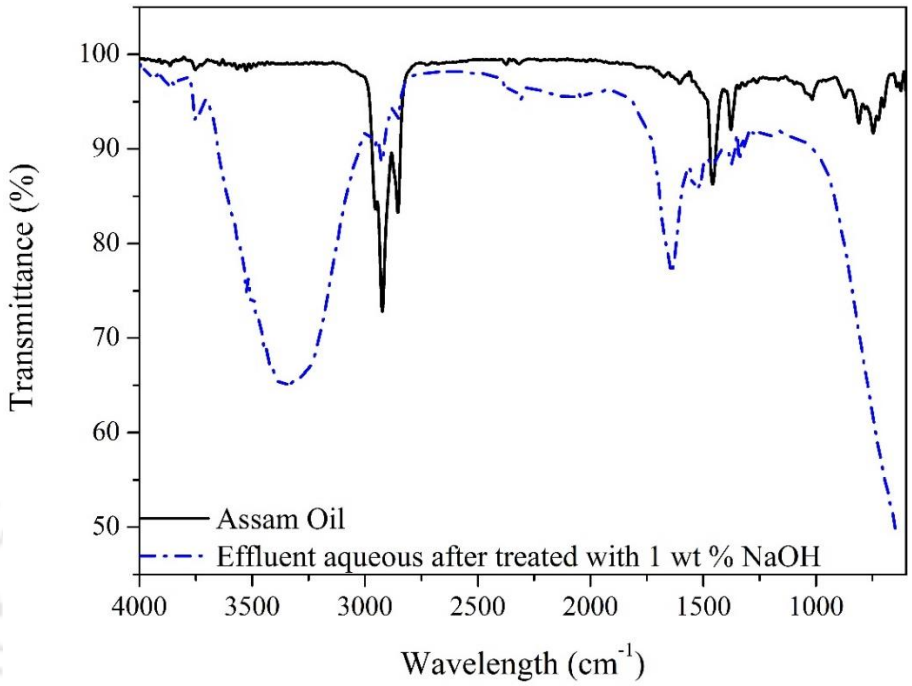

Fig. 3.2: FTIR spectra of Assam crude oil and effluent collected from 1 wt% NaOH flooding.

3.3 IFT Behaviour of Crude with Alkaline Solution

The variation in interfacial tension for crude oil and alkali system at different concentration of NaOH (0.2–1 wt%) is depicted in Fig. 3.3. The dynamic IFT at different alkali concentration was observed and it took almost 40-50 min for the system to achieve equilibrium IFT as shown in Fig. 3.3a. The variation in dynamic IFT involved different pattern, initially IFT decreased with time and then it starts increasing and finally flattens off indicating achievement of equilibrium. The main reason for such complex response was due to the adsorption and desorption of active surfactant species at the oil-alkali interface [15, 36, 120]. The initial decrease in IFT is due to higher adsorption and lower desorption of in-

situ surfactant at the oil water interface. This cause higher accumulation of in-situ surfactant at the interface which reduces the IFT. After certain duration as the accumulation increases, higher concentration gradient develops which increases the desorption rate. The increase in desorption rate causes reduction of active species at the oil-water interface and hence the IFT increases. Finally, an equilibrium IFT was achieved when both the adsorption and desorption rates are equal and the IFT remains constant which does not change further.

The equilibrium IFT of the chosen system varied from 0.06-0.42 mN/m as shown in Fig. 3.3b. The equilibrium IFT decreased with increase in NaOH concentration and minimal equilibrium IFT value of 0.071 mN/m was obtained at 0.2 wt% NaOH. Further increase in NaOH concentration resulted in shooting up the IFT. The enhancement of IFT profiles with increasing alkali concentration could be because of pH effect. At lower alkali concentration, the solution pH is low which enables higher concentration of unionized acids and subsequent reduction of critical micelle concentration (CMC) of the ionized acids. Due to this reason, lower interfacial coverage occurs which results in a higher IFT. On the other hand, higher alkali solution concentration enhances pH of the aqueous phase and thereby reduces concentration of unionized acids and enhances interfacial coverage to reduce IFT at an optimal pH of the solution. Till optimum pH, the decrease in IFT is mainly due to increase in ionized acid until CMC is reached. A further increase in the solution pH enables complete ionization of acid groups and significant reduction of unionized acids to enhance the IFT of the alkali-oil system [34, 36, 121].

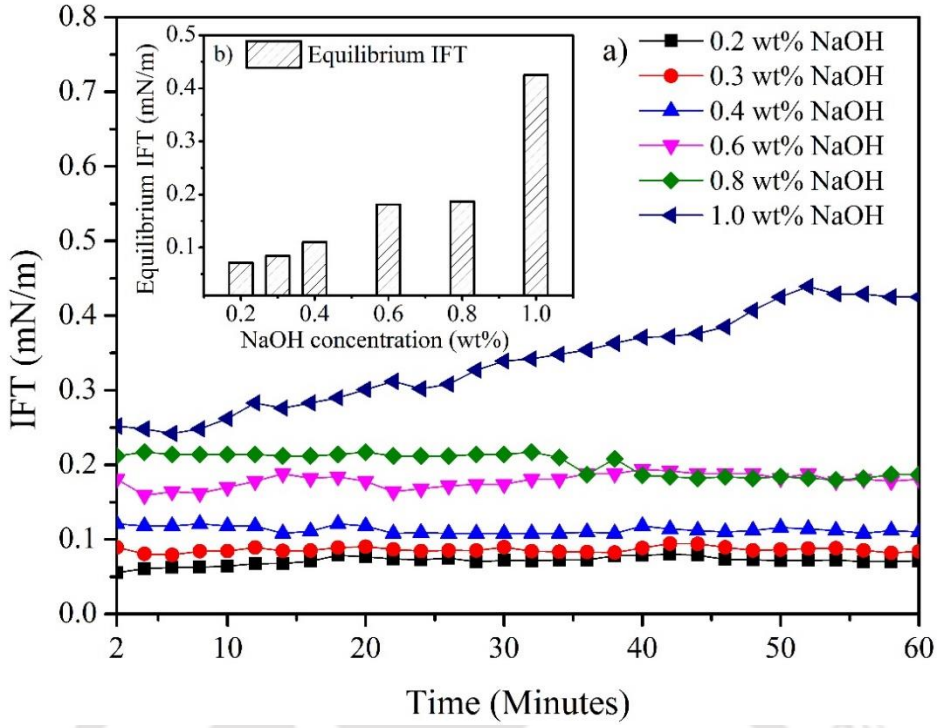

Fig. 3.3: IFT behaviour of Assam crude oil at different NaOH concentrations a) Dynamic IFT and b) Equilibrium IFT.

3.4 Sandpack Flooding

The effectiveness of alkali (NaOH) flooding was evaluated by conducting twelve sandpack flooding experiments. Sandpack permeability and oil saturation varied from 1900 - 2100 mD and 79 - 84% respectively. Table 3.1 summarizes the core flooding experiments with residual recovery of crude oil for various sets of operating parameters such as alkali concentration, slug size and injection pattern.

Table 3.1 Detail of sandpack flooding experiments performed with alkali (NaOH).

Flooding expt. no.	Porosity (%)	Permeability (mD)	Initial oil saturation (%)	Water flooding recovery (IOIP %)	Chemical NaOH (wt%)	Slug size (PV)	Tertiary recovery (IOIP %)	Total oil recovery (IOIP %)
1	34.61	2090	83.7	33.36	0.2	0.5	11.29	44.65
2	33.65	2010	80.7	34.20	0.4	0.5	14.29	48.49
3	34.46	1987	80.8	34.72	0.5	0.5	18.59	53.31
4	32.85	1987	82.7	35.02	0.6	0.5	21.85	56.87
5	34.69	1914	81.1	33.55	0.8	0.5	24.62	58.17
6	35.47	1907	80.0	32.99	1	0.5	25.48	58.47
7	34.42	1951	80.6	34.27	1	0.25	20.70	54.97
8	34.98	2059	82.5	32.19	1	0.75	24.41	56.60
9	31.92	2047	79.3	35.19	1	1	23.46	58.65
10	34.16	2069	81.0	35.49	1	1.5	21.46	56.95
11	34.86	2032	80.1	33.83	1	2	18.55	52.38
12	33.91	2099	82.5	35.31	1	0.25+0.25	18.64	53.95

3.4.1 Effect of Alkali Concentration on Residual Oil Recovery

To investigate the role of alkali (NaOH) on residual oil recovery, flooding experiments with NaOH solution varying from 0.2 - 1 wt% were conducted (Table 3.1). Fig. 3.4 illustrates the cumulative crude oil recovery profiles. The increment in oil recovery was found to be significant with increase in NaOH concentration. The recovery factor reaches more than double as the concentration of NaOH increases from 0.2 wt% to 0.8 wt% as shown in Fig. 3.4a. The increase in oil recovery with increase in alkali concentration was due to the effect of pH and penetration of aqueous alkali solution into the oil phase to enable better water in oil (W/O) emulsion (more explanation in section 3.4.2 "Emulsion formation and droplet distribution"). The oil recovery approaches a stagnant point at 0.8 wt% beyond which the recovery factor becomes negligible. The reason for reaching such stagnant point during oil recovery was controlled by the quality of W/O emulsion produced and its corresponding sweep efficiency (more explanation in section 3.4.3 "Effect of slug volume). The W/O emulsion produced with 1 wt% NaOH was found better compared to 0.8 wt% NaOH (Fig. 3.5), but the sweep efficiency remains more or less the same and could not be triggered further due to which oil recovery flats off (Fig. 3.4b). However, maximum residual oil recovery, 25.48% of initial oil in place (IOIP) was obtained with 1 wt% NaOH. The maximum oil recovered can be further explained by the pressure drop curve as provided in appendix C Fig. C3.1 and C3.2. Higher pressure drop results in penetration of alkali solution in the oil phase resulting in high viscous W/O emulsion which reduces the mobility of aqueous phase and thereby improves the sweep efficiency ultimately resulting in higher oil recovery[36]. The obtained data affirms that cumulative oil recovery increased with increasing alkali concentration, which is in good agreement with the data reported in literature [22, 36, 118, 122]. Flooding experiments beyond 1 wt% NaOH are not suitable due

to greater emulsion formation (higher saponification) which severely reduce the sweep efficiency (see section 3.4.3 "Effect of slug volume") Samanta et al. [118] reported that this trend may be due to the mechanism of IFT reduction, emulsion formation, improved vertical and areal sweep efficiency. Similarly, Almalik et al. [24] reported that for Safaniya oil (Saudi Arabia) at 1wt% NaOH, higher pH accounted for IFT reduction and higher cumulative oil recovery (86.73% IOIP) was achieved. Saponification (section 3.5 "Effect of alkali concentration on neutralization and saponification process") and wettability alteration (section 3.6 "Wettability alteration with alkali") are the other two mechanisms responsible for higher oil recovery.

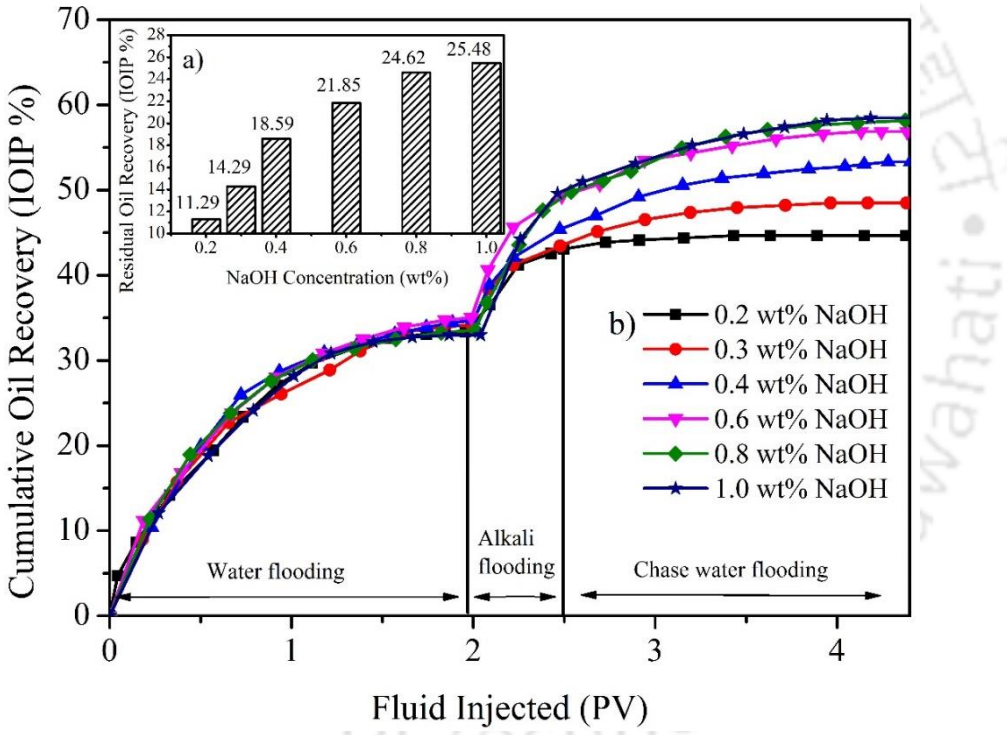

Fig. 3.4: Oil recovery at various NaOH concentrations a) Cumulative oil recovery and b) Residual (Tertiary) oil recovery.

3.4.2 Emulsion Formation and Droplet Distribution

The emulsification mechanism was studied by analysing the extent of emulsion formation. This phenomenon was observed by evaluating the droplet size distributions using microscope images obtained for various NaOH concentrations (Fig. 3.5). Pertinent droplet size distributions of the emulsions formed are presented in Fig. 3.5. It can be analysed that the droplet average diameter was found low for 0.2 wt% NaOH case and subsequently increased with increasing alkali concentration. The emulsion size distribution varied from 0 – 7 μm (small) for 0.2 wt% NaOH case (Fig. 3.6a) to 0 – 15 μm (large) for 1 wt% NaOH (Fig. 3.6f). The average emulsion droplet size were evaluated to be 2.85, 3.59, 4.03, 4.45, 4.95 and 5.63 μm for 0.2, 0.3, 0.4,, 0.6, 0.8 and 1 wt% NaOH respectively. From emulsion study, it is conformed that with increasing alkali concentration, the extent of emulsification increases and thereby enhances average emulsion droplet size that facilitates the release of trapped oil and hence higher residual oil recovery [23, 36-38].

Previous studies investigated the effect of viscous behaviour of W/O emulsion in porous media and developed correlations between emulsion quality and viscosity behaviour. They observed that the viscosity of emulsion increases with increase in emulsion quality [23, 123]. An increase in emulsion viscosity blocks water channelling which diverts the injected water towards the un-swept region accessing more reservoir area both aerially and vertically thereby increasing displacement efficiency [28, 37, 124].

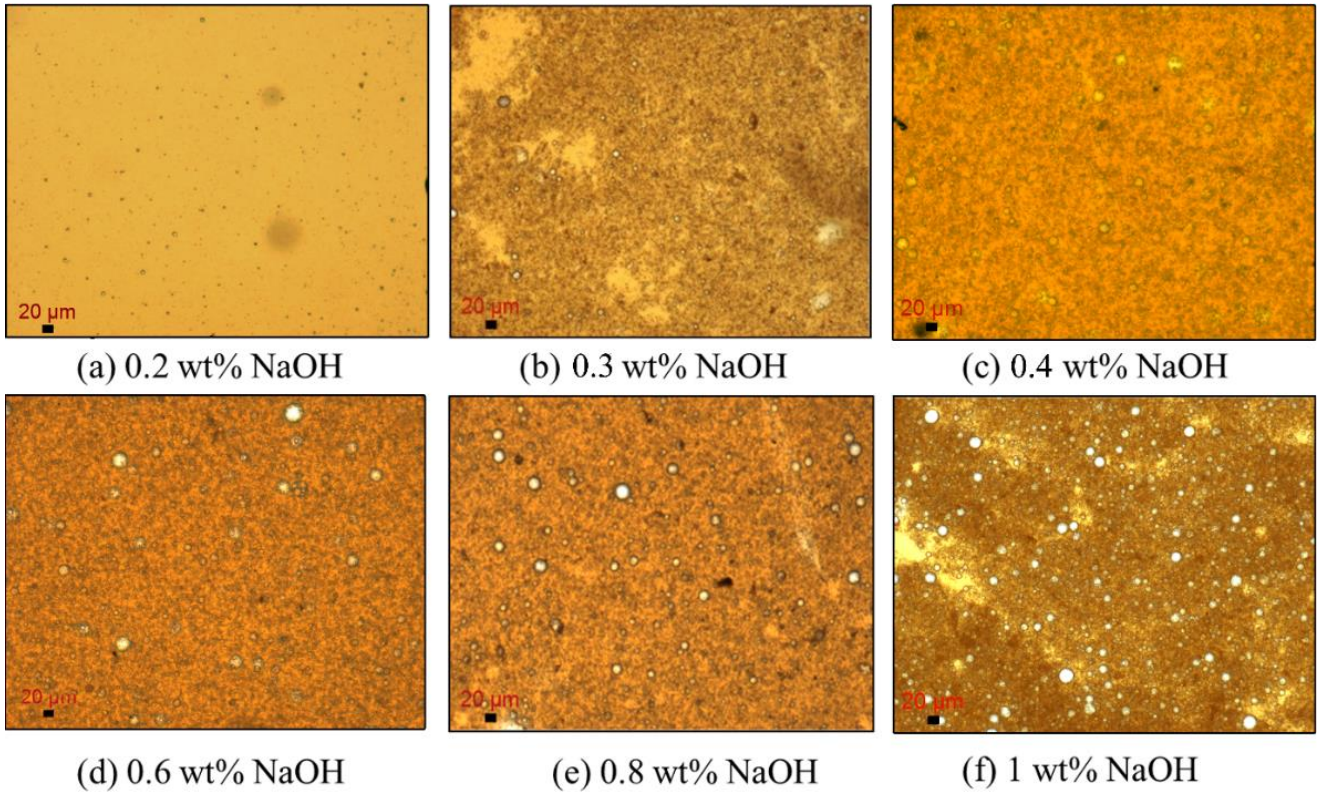

Fig. 3.5: Microscopic images of emulsions formed in the recovered oil samples during alkali flooding (0.2 to 1 wt% NaOH).

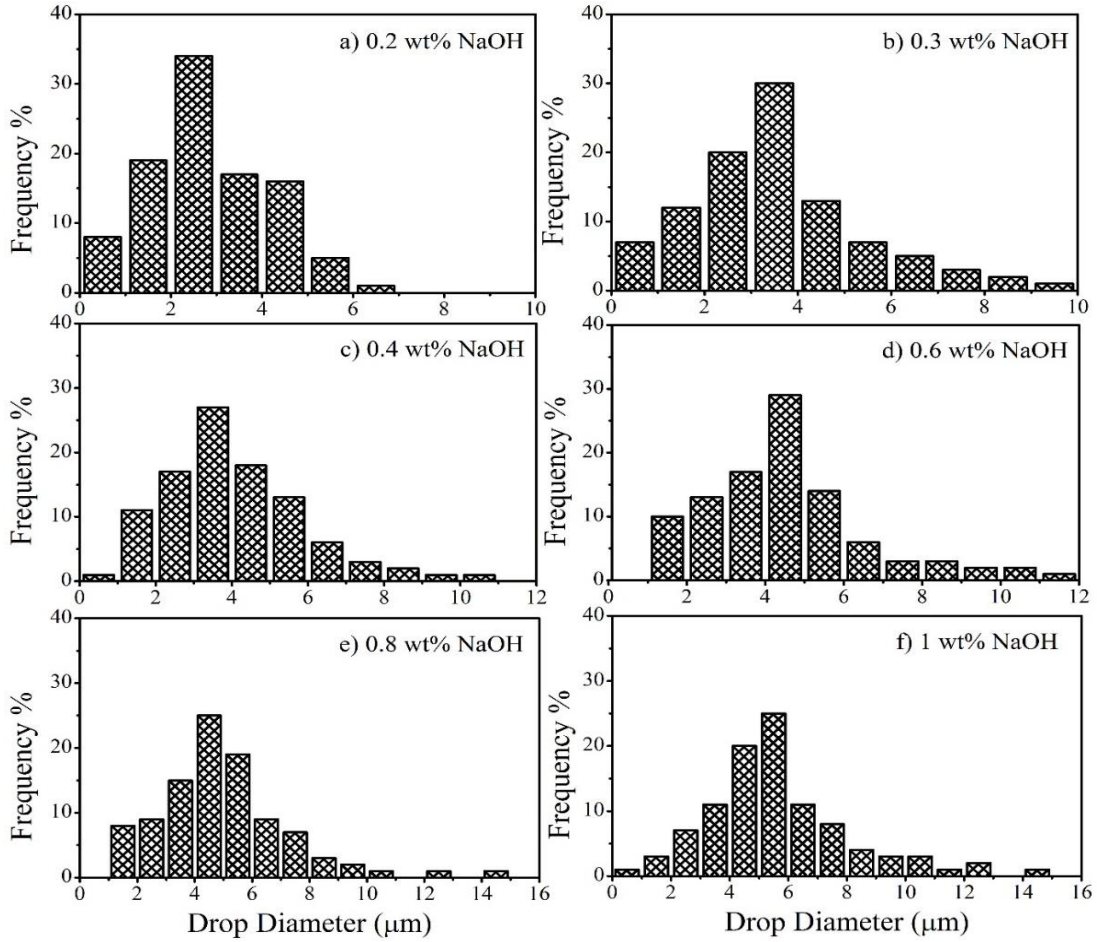

Fig. 3.6: The distribution of droplet diameter in the emulsion formed during sandpack alkali flooding.

3.4.3 Effect of Slug Volume

For optimal process economics, a low slug volume which is sufficient to recover maximum residual crude oil is desirable. Fig. 3.7 depicts the variation of residual oil recovery with slug volume prepared using alkali (1 wt% NaOH). Initially oil recovery of 20.9% IOIP was obtained at 0.25 PV and then additional oil up to 25.48% IOIP was recovered at 0.5 PV. Further increase in slug volume (up to 2 PV) resulted in less residual oil recovery till 18.55% IOIP. Initially with increase in slug size from 0.25 to 0.5 PV the W/O emulsions formed has the potential to block water channelling which reduces viscous fingering. This phenomena causes the aqueous phase to reach in more oil area region thereby increasing sweep efficiency. The decrease in residual oil recovery above 0.5 PV was due to the negative effect of the formed emulsions. At higher slug size more W/O emulsion formed which is highly viscous and difficult to displace due to poor mobility. Therefore, an optimal slug volume exists during which the W/O emulsion formed has the characteristic ability to block water channelling and thereby maintains optimum mobility to increase sweep efficiency and hence higher oil recovery [36].

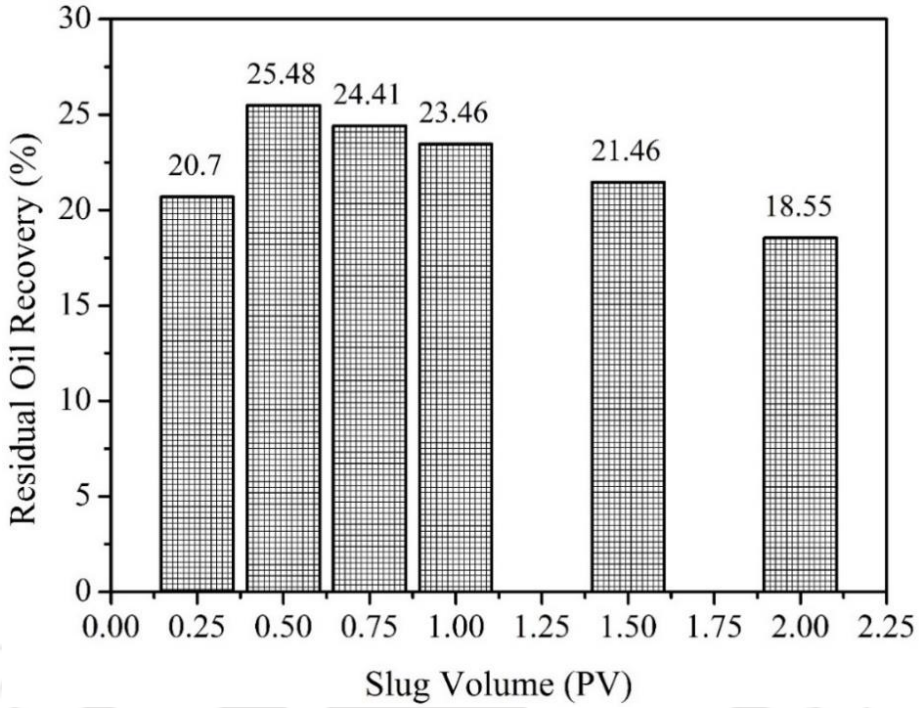

Fig. 3.7: Effect of slug size on residual oil recovery at 1% wt% NaOH.

3.4.4 Effect of Injection Pattern

In order to compare the effect of injection pattern on residual oil recovery, two flooding experiments were carried out for a fixed alkali concentration of 1 wt% NaOH. The first experiment corresponds to a cyclic injection pattern in which 0.25 PV slug volume was provided in two time slots to a total slug volume of 0.5 PV. In the second case, continuous injection pattern of 0.5 PV was considered. For both the cases, extended chase water flooding was followed. For cyclic injection case, the total overall oil recovery decreases from 58.47 % IOIP to 53.95 % IOIP despite maintaining same total slug volume of 0.5 PV (Fig. 3.8). This is due to the fact that during cyclic injection, the W/O emulsion bank gets easily broken down and thereby reduces the plugging effect. Fig. 3.9 shows the droplet size distribution of the emulsion collected during cyclic flooding experiments. It can be observed that the droplets formed are not uniform and varies in droplet sizes from 3.99 - 4.85 μm. This is

possibly due to the cyclic injection pattern that encourages the breakdown of emulsions. The lower oil recovery during cyclic injection may also be due to the dilution of alkali solution which produces less W/O emulsion [36]. Therefore, among cyclic and continuous injection patterns, continuous injection pattern was found to be effective for alkali flooding to achieve maximum crude oil recovery.

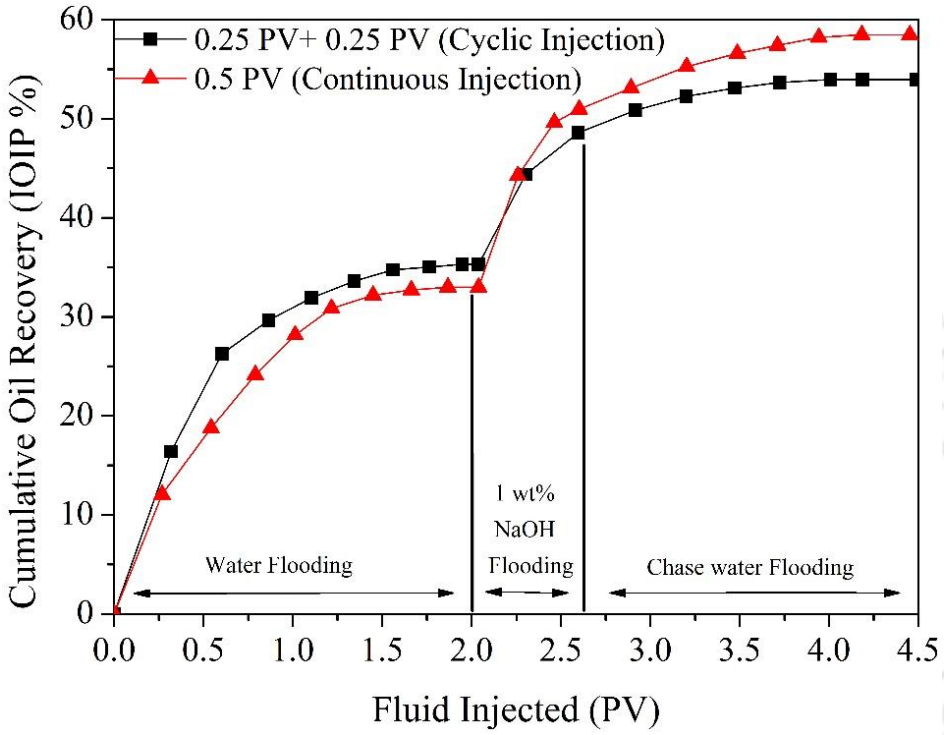

Fig. 3.8: Effect of injection pattern on cumulative oil recovery (1 wt% NaOH).

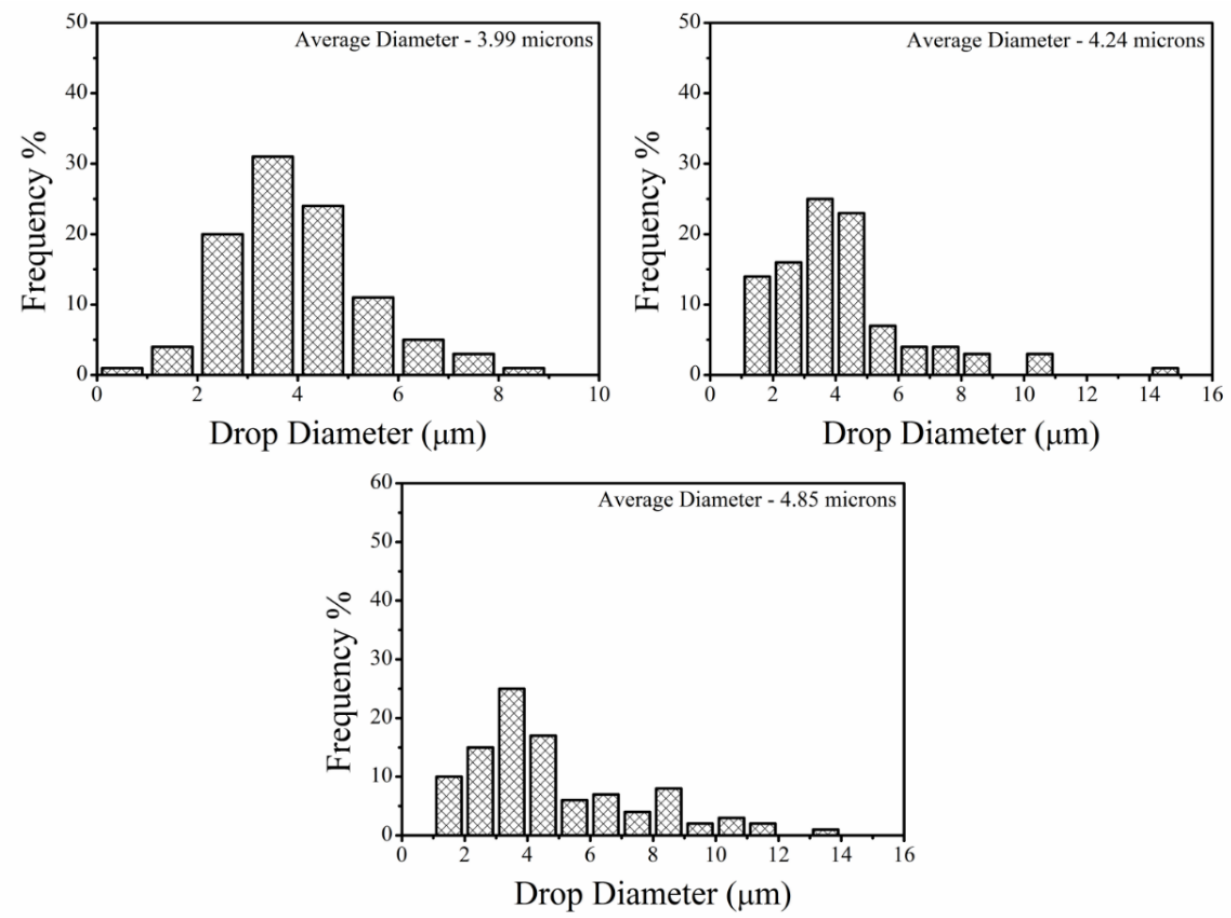

Fig. 3.9: Droplets size distribution of emulsion formed during cyclic injection pattern flooding (1 wt% NaOH).

3.5 Effect of Alkali Concentration on Neutralization and Saponification Process

An average naphthenic acid content of 0.35 mg of KOH/gm which corresponds to 12% of total acid present in the crude oil was confirmed during experimental investigations. Fig. 3.10 shows the extent of neutralization and saponification of crude oil at different NaOH concentration. At 0.2 wt% NaOH concentration, only 14.6% of the acid group participated for neutralization and saponification reactions whereas remaining 85.4% of the acid fractions remained unconverted and are available for further soap formation reaction. On further increasing the concentration (up to 1 wt%), the extent of neutralization and saponification increased up to 34.5% which is due to the increase in Na^+ ions and almost two-third of the acid group remained unconverted. The mechanism of alkali reaction with the acidic groups of crude oil to generate an in-situ surfactant at the interface is already shown in Fig. 1.5 [33]. As illustrated, the oil-alkali interaction can be analysed to be the partition of organic acid between oleic and aqueous phase followed with further hydrolysis of the acid (HAo) and alkali (NaOH) to produce in-situ surfactant or petroleum soap (NaA) at the oil-water interface to reduce the IFT. Also, the interaction between hydrogen bonding of the ionized acid and neutral acid enables the formation of complex acid soap [18, 33]. From the extent of neutralization and saponification reaction it was observed that not all the acids react and almost 65.5% of the acid group remains unconverted.

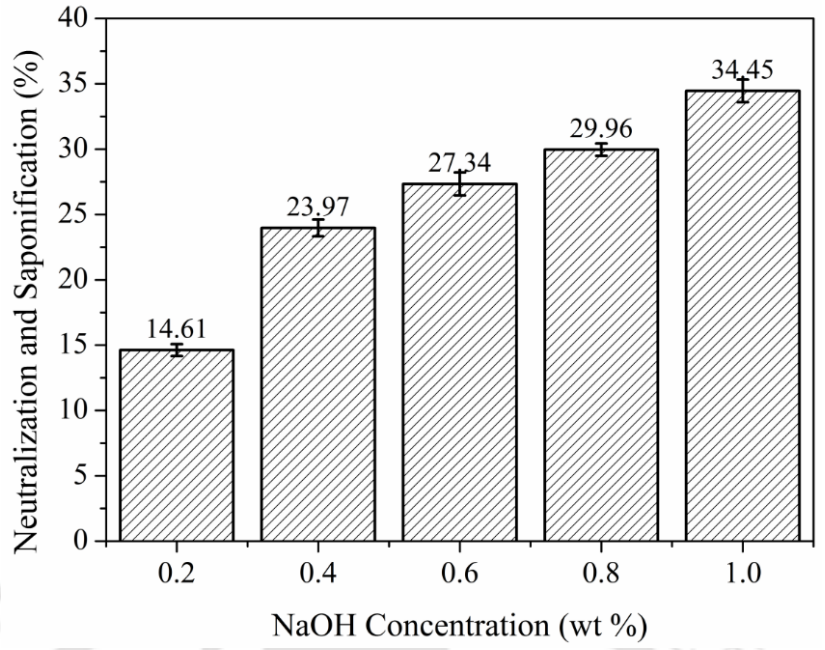

Fig. 3.10: Extent of neutralization and saponification of Assam crude oil recovered from alkali flooding at different NaOH concentrations.

3.6 Wettability Alteration with Alkali

The effect of alkali concentration on wettability alteration (at ambient temperature) was observed by measuring the contact angle between oil saturated sand surface and alkali (NaOH) solution at different concentration (Fig. 3.11). The change in contact angle with formation water (0% NaOH) varies from 109^o to 75.2^o and after 15 min no further change in contact angle were observed as shown in Fig 3.11a. The final angle measured at 0.2 wt%, 0.4 wt%, 0.60 wt%, 0.8 wt% and 1 wt% NaOH were found to be 53.9^o, 41.5^o, 38.9^o, 37.3^o and 36.8^o respectively (Fig. 3.11b). The spreading of oil on the quartz surface increased with increase in NaOH concentration indicating the change in wettability of the system from intermediate wet to water wet [5]. The change in wettability/contact angle occurs due to the adsorption of in-situ surfactant on the mineral surface [26]. Increase in NaOH concentration favours in-situ surfactant formation at the oil-water interface due to the interaction of alkali

and naphthenic acid group of the crude oil. The in-situ surfactant then diffuses in the aqueous phase which develops the hydrophilicity. This results in adsorption of in-situ surfactant on the quartz surface which displaces the oil from the pores of the rock. Hence the study reveal active participation of wettability alteration in addition to IFT reduction and emulsification mechanism which enhances oil recovery.

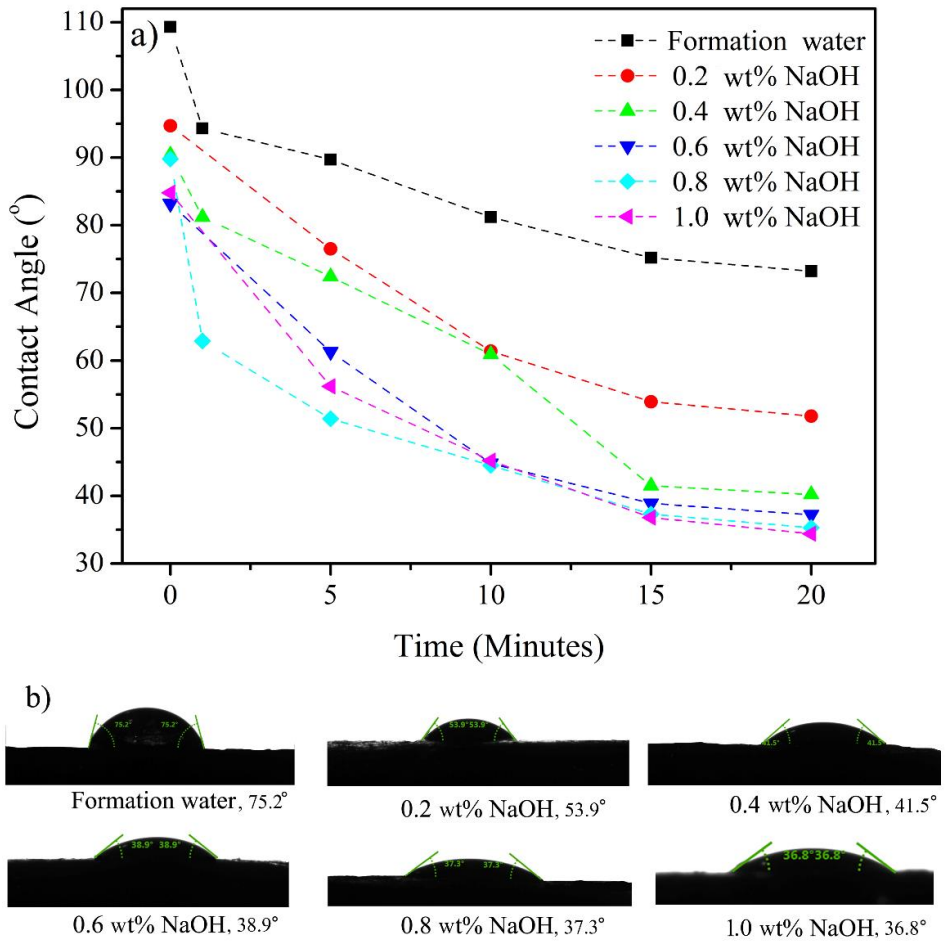

Fig. 3.11: Change in contact angle between oil saturated sand surface and NaOH/Formation water a) Variation in contact angle with time and b) Final value of contact angle at equilibrium state.

3.7 Effect of Alkali on Various Factors

The effect of alkali concentration on key important properties such as equilibrium IFT, emulsification, wettability alteration and extent of saponification/neutralization on residual oil recovery were investigated as summarized in Fig. 3.12. For variation in NaOH concentration from 0.2 to 1 wt%, the equilibrium IFT, average emulsion droplet size, contact angle, extent of neutralization and saponification and residual oil recovery varied from 0.0714 mN/m to 0.425 mN/m, 2.85 μm to 5.63 μm, 54^o to 37^o, 14.61% to 34.45% and 11.29% to 25.48% of IOIP, respectively. Thus, it is apparent that with increasing alkali concentration, more naphthenic acid is consumed and thereby contributes to the enhancement in average emulsion droplet size. At 1 wt% NaOH flooding, 34.5% neutralization and saponification occurred to facilitate the average emulsion droplet size reaching 5.63 μm with higher residual oil recovery of 25.48% IOIP. Incidentally, minimum equilibrium IFT was obtained at 0.2 wt% NaOH (0.0714 mN/m) whereas the residual oil recovery was not maximum (11.29% IOIP). This shows that IFT reduction is necessary for emulsion formation but minimum IFT does not assure maximum oil recovery due to the contribution of other mechanisms. The change in contact angle of the reservoir from initial 109^o (formation water) to final 36.8^o (1 wt% NaOH) altered the wettability of the system from intermediate wet to water wet. Therefore, it is apparent that emulsification, saponification and wettability alteration have a greater role in influencing residual oil recovery and IFT reduction alone does not contribute towards the same [26, 28, 36, 39]. In this study, the effect of saponification was observed to be more dominant as it regulates the extent of emulsion and droplet distribution which increases with increase in alkali concentration. The alteration in the wettability furthers contributes towards oil recovery. However, the mechanism of IFT reduction is necessary to form emulsion.

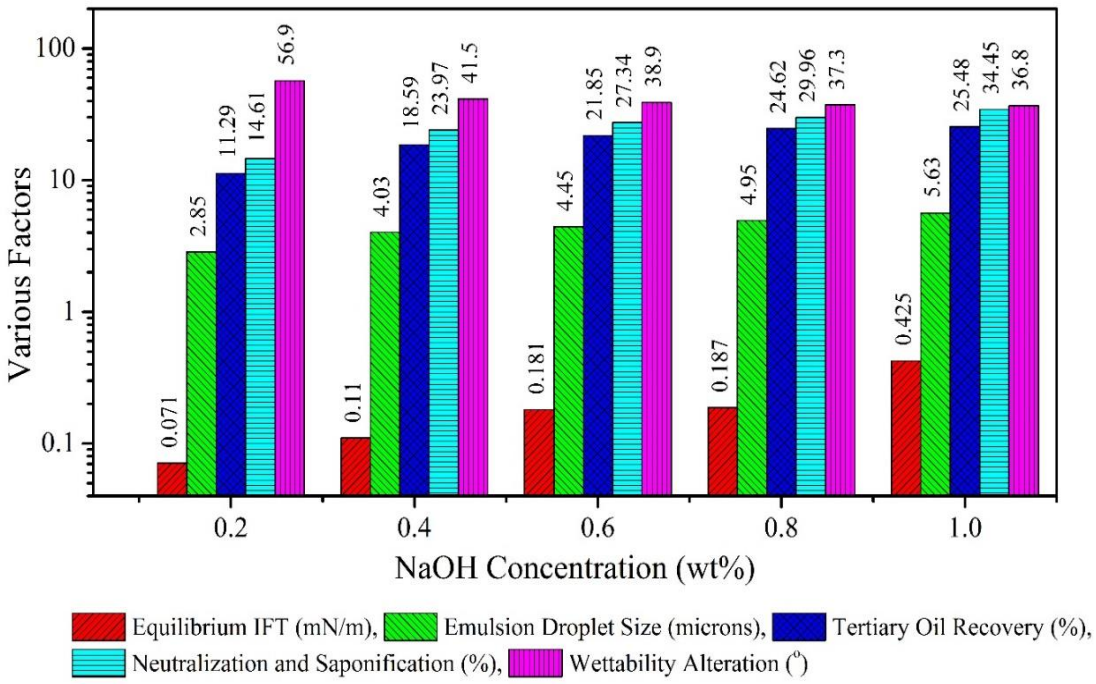

Fig. 3.12: Effect of alkali concentration (NaOH) on equilibrium IFT, emulsion droplet size, oil recovery and neutralization and saponification.

Table 3.2 summarizes a comparative assessment of alkali flooding based residual oil recovery for various crude oil systems. It can be observed that light to moderate crude oils, from Louisiana and Texas-Frlo fields had shown significant difference in the oil recovery; higher recovery for Texas-Frlo (26%) compared to of Louisiana (21%). This might be due to the higher naphthenic acid content of Texas Frlo which had not been addressed in the carried out investigations. On the other hand, for lighter crude oil of Louisiana field higher residual recovery of 28% was obtained while no IFT reduction occurred (as no droplets formed). For heavy crude oil of Xia China field), the higher recovery of 30.3% could be possible due to IFT reduction, emulsion formation and wettability alteration phenomena. Also, for one case, Sheng [18, 125] and Li [126] reported that IFT reduction was possible for crude oil collected from Daqing reservoir having zero acid number. For such cases, the IFT

reduction increases with increasing alkali concentration [126]. Hence, it is apparent that generalized rules of thumb could not be presented to indicate upon direct relationships between acid value of crude IFT reduction and residual oil recovery [18]. A case to case investigation is required to affirm upon the competence of microscopic mechanisms during alkali flooding of crude oil systems.

Table 3.2: Comparison of residual oil recovery of various crudes using alkali flooding.

Author	Oil field	Density (g/cm^3)	μ (mPa. s)	Acid value (mg of KOH/gm)	Alkali conc. (wt%)	IFT reduction (mN/m)	Drop size (μm)	Rock types	Tertiary oil recovery (%)
Tang et al. [22]	Xia 8 heavy oil	0.9712	3950	4.66	1 wt% $NaBO_2$	0.1	3.55-4.23	Sand pack	27.1
Wang et al. [23]	Alberta heavy oil	0.9665	1360	1.07	0.3 wt% NaOH + 0.3 wt% Na_2CO_3	0.1	0.5-5	Sand pack	14.9
Pei et al. [36]	Binnam heavy oil	0.9742	2000	2.69	1 wt% NaOH	0.1	2.785	Sand pack	19.9
Ehrlich et al. [39]	Louisiana light to moderate crude	0.8871	19.2	0.61	0.1 wt% NaOH	0.03	-	Berea core	21
Ehrlich et al. [39]	Texas-Frlo light to moderate crude	0.9218	44.2	1.39	0.1 wt% NaOH	0.09	-	Berea core	26
Ehrlich et al. [39]	Louisiana light crude	0.8761	29.1	1.02	0.1 wt% NaOH	No drops formed for measuring IFT	-	Berea core	28
Pei et al. [20]	Xia Heavy oil	0.9816	3950	4.66	1 wt% NaOH	-	-	Sand pack	30.3
Current Work	Assam light to moderate crude	0.8926	33.4	2.87	1 wt% NaOH	0.42	5.63	Sand pack	25.5

3.8 Conclusions

The effect of IFT behaviour, emulsification, wettability alteration, saponification mechanism and their subsequent effects on residual oil recovery for Assam crude using NaOH were addressed. Minimum IFT value (0.071 mN/m) could be achieved at 0.2 wt% NaOH. However, the flooding data affirmed that further enhancement in alkali concentration improves residual oil recovery and maximum oil recovery of 25.48% (IOIP) could be obtained at 1 wt% NaOH. Assam crude oil has been characterized to constitute high acid value but lower naphthenic acid (12% of the acid value). Despite possessing such lower naphthenic acid content, saponification was found significant to enable soap formation, IFT reduction and emulsification. The extent of neutralization and saponification was found to be 34.5% at 1 wt% NaOH and thereby conveys the possible dominance of neutralization in fostering the physicochemical changes associate to emulsification and IFT reduction. Further, an optimal slug size of 0.5 PV and continuous injection pattern was found to be optimal process parameter to achieve maximum oil recovery. The change in contact angle from 109^{o} (formation water) to 36.8^{o} (1 wt% NaOH) indicates the change in wettability of the current system from intermediate wet to water wet which contributes in enhancing the residual oil recovery.

Chapter 4

Alkali-Surfactant Flooding in Sandstone Reservoir for Light to Moderate Crude Oil

This chapter addresses the interfacial tension (IFT) behaviour between alkalis (NaOH and Na_2CO_3), surfactants (cetyltrimethylammonium bromide and sodium dodecyl sulphate), combinations of alkalis and surfactants with light to moderate Assam crude oil. Based on the IFT studies, an optimum alkalis concentration were obtained. The synergism between alkalis and surfactants to reduce IFT and emulsify the crude oil were also investigated. Finally, sandpack flooding experiments were performed to estimate the residual oil recovery with alkali and alkali-surfactant combinations.

4.1 Interfacial Tension between Crude Oil and Chemical Solution System

The IFT variation with concentration of alkalis, surfactants and alkali surfactant combinations for the chosen crude oil-aqueous phase system is depicted in Fig 4.1. The IFT reduction behaviour of alkali-surfactant system usually depends upon the surfactant critical micelle concentration (CMC). CMC is the concentration at which the surfactant monomers at the oil-water interface get saturated and confirms lowest IFT achievement. A further enhancement in surfactant concentration does not assist in IFT reduction due to enhancement in micelles formation [127]. For alkalis, the IFT reduction is primarily controlled by the formation of mixed micelle of unionized and ionized acids [34, 121].

Table 4.1 summarizes minimum IFT obtained for various alkalis, surfactants and alkali-surfactant combinations. The IFT value for crude oil-millipore water was found to be 24.3

mN/m. The IFT reduced significantly to a lower value with an increase in the alkali concentration. However, IFT value increases marginally and remains constant upon further enhancement in alkali concentration (Fig. 4.1a). Based on the obtained IFT trends, the optimal values of alkali concentration were found to be 0.1 wt% and 0.25 wt% for NaOH (5.15×10^{-2} mN/m) and Na_2CO_3 (4×10^{-1} mN/m) respectively. The IFT behaviour is also influenced with pH variation, as pH variation influences ionization extent of the acid groups. This effect on both ionized and unionized acid groups at the oil-water interface contributes in reducing the IFT and minimum IFT can be achieved at an optimum pH due to enhancement of ionized acid content up to the CMC [36]. Early reduction in IFT with alkali is due to an increase in pH which results in enhanced anions (A^-) concentration of the acidic components (HA) of the crude oil. Due to this, IFT reduces to a minimal value (unionized acid content decreases with increasing CMC). A further increase in the alkali concentration enables a shift in the equilibrium to form undissociated soap (NaA/KA) and thereby reduces A^- ion concentration at the interface and hence enhances IFT (due to enhanced ionized acid content). A further increase in alkali concentration does not vary IFT significantly (with flat profile), as most of the unionized content in the crude oil has been consumed [34, 36, 121].

Fig. 4.1b shows the IFT behaviour of crude oil and surfactants (CTAB and SDS) systems. Initially, with an increase in concentration of both surfactants, IFT reduced due to the adsorption of surfactant molecules at the oil-water interface [19]. For SDS surfactant case, the IFT reduced to 2.3 mN/m at 0.1 wt% SDS. Beyond this concentration, IFT reduction was insignificant. On the other hand, for CTAB surfactant, minimum IFT (1.84×10^{-1} mN/m) was achieved at 0.04 wt% of CTAB. However, beyond 0.06 wt% of CTAB, no changes in the IFT values were observed. This is due to saturation level of surfactant adsorption at the oil-water interface [19]. The variation in IFT values for crude oil with alkali-surfactant solutions

are presented in Fig. 4.1c (with 0.1wt % NaOH) and Fig. 4.1d (with 0.25 wt% Na_2CO_3). The synergy between NaOH (0.1 wt%) and CTAB/SDS (Fig. 4.1c) resulted in an optimum IFT value of 10^{-2} mN/m (1.1×10^{-2} mN/m with 0.04 wt% CTAB and 4.1×10^{-2} mN/m with 0.1 wt% SDS).

Similarly, due to the synergy of Na_2CO_3 (at 0.25 wt%) with CTAB/SDS, IFT reduced to 4.82×10^{-2} mN/m for 0.04 wt% CTAB and 2.26×10^{-1} mN/m for 0.01 wt% SDS (Fig. 4.1d). For both alkalis, NaOH and Na_2CO_3, minimal IFT value with CTAB was obtained at its CMC value while for SDS the optimum/minimum IFT was observed at much lower concentration (less than half of its CMC value). For better cost effectiveness, IFT studies were further conducted with 0.1 wt% Na_2CO_3 (Fig. 4.1d). A similar trend was observed for the interaction of Na_2CO_3 with both the surfactants i.e., IFT value first decreases and then increases and finally get stabilized with increasing surfactant concentrations. The minimum IFT values obtained were 1.5 x 10-2 mN/m for 0.04 wt% CTAB and 3.88×10^{-1} mN/m for 0.05 wt% SDS. Considering both alkalis, the reduction in IFT was found better for both NaOH and NaOH-surfactant systems. The observed results also affirm that along with a surfactant, 0.1 wt% Na_2CO_3 can be as effective as 0.1 wt% NaOH. This confirms upon the complexity of the synergy between alkali and surfactant for the chosen Assam crude oil. At higher surfactant concentration, the distribution of surfactant molecules at the oil-water interface contributes to IFT increment [19, 128]. The IFT enhancement with surfactant concentration was due to micelle formation in both oil and aqueous phases. The solubilisation of these micelles results in reduction of adsorption of in-situ surfactant at the interface and thus enhances IFT [129]. The concentrations of Na_2CO_3 and NaOH were not increased beyond their optimum values of 0.25 wt% and 0.1 wt% respectively, as for such cases the IFT reduction was not found to be insignificant and would also enhance the costs of chemical

EOR process. In summary, the carried out investigations confirmed that synergistic interaction of alkalis and surfactants is required to optimize the performance of tertiary flooding process [43, 90].

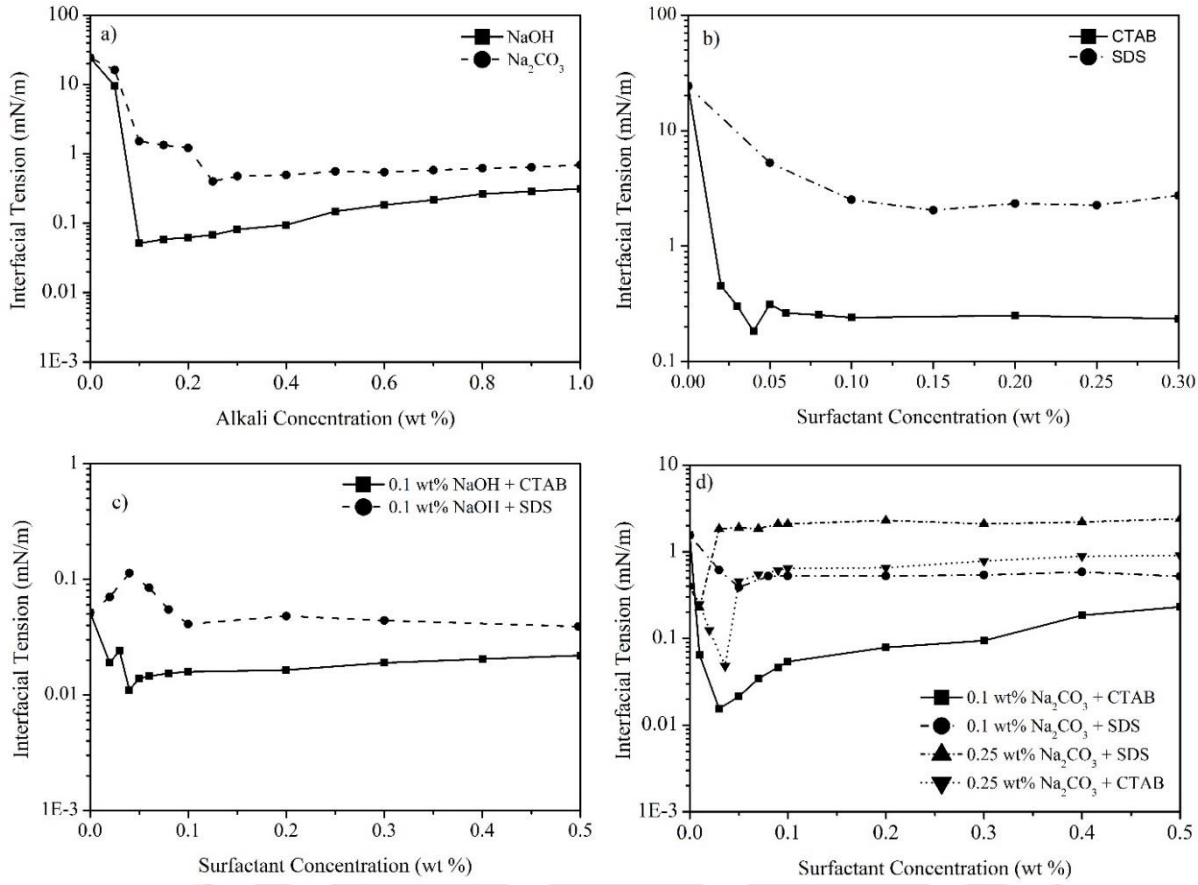

Fig. 4.1: Effect of alkali, surfactant and alkali-surfactant solution on IFT for light to moderate Assam crude oil.

4.2 Emulsification and Sandpack Flooding

To account for the actual cause of tertiary oil recovery, emulsification tests and sandpack flooding experiments were further investigated in detail. SDS was selected for flooding experiments due to anionic nature of sandpack. The volume of each phase (oil/emulsion/water) observed in emulsification test (after 30 minutes) and cumulative oil recovery obtained using sandpack flooding experiments are presented in Fig. 4.2. Flooding

experiments were conducted at optimum concentration of chemical slug followed by chase water flooding as shown in Fig. 4.2a. For optimum concentration of 0.1 wt% NaOH alkali solution, a total oil recovery of 51.46% IOIP (Initial oil in place) was obtained which corresponds to 24.25% of ROIP (Residual oil in place) and is almost equal to that of literature [130] (Table 4.2). The sandpack flooding with 0.25 wt% Na_2CO_3 exhibited lower oil recovery (11.85% IOIP) in comparison with 0.1 wt% NaOH (15.54% IOIP). This is due to higher IFT and lesser emulsification of crude in comparison with NaOH. The oil recovery increases further for the combined alkali-surfactant flooding in comparison with alkali alone. For the chemical slug of SDS (0.1 wt%) and NaOH, tertiary recovery value of 24.02% IOIP (38.79 % of ROIP) was achieved. However, for Na_2CO_3 and SDS, the combined alkali-surfactant flooding could recover only 33% of ROIP. This fluctuation in oil recovery is mainly due to the emulsification process. Emulsification capacity increases in the order of NaOH-SDS (alkali-surfactant) > NaOH > Na_2CO_3. Higher emulsification of 12 % was observed with alkali-surfactant solution but not with alkali alone case (4 to 8 %). This is due to better interfacial tension reduction. Therefore, from emulsification and flooding experiments, alkali-surfactant flooding provided more oil recovery than alkali flooding alone.

Table 4.2 summarizes the tertiary recovery obtained at a laboratory scale for various oil fields. Water flooding recovery data obtained with Assam crude oil was found to be similar to that reported for Shengli (China) and Saskatchewan (Canada) heavy crude oil but was lower than that reported for Ahmedabad crude (India). For alkali (NaOH) flooding, the oil recovery data obtained in the present study are more or less similar to that reported in literature. The values of residual oil recovered by alkali-surfactant flooding are similar to Saskatchewan (Canada) oil field which conveys the potential of chemical EOR for the chosen

crude oil-water system. Further, comparison of obtained data with other relevant literatures (Table 4.2) conveyed that it is extremely difficult to generalize and correlate crude oil and core/rock parameters for chemical flooding scheme. However, it can be analysed that the trends of enhanced oil recovery for heavy crude are similar to that obtained with light crudes and the magnitude of the tertiary recovery is influenced by the acid value of the crude oil (Table 4.2). Further, it is also important to note that the optimal chemical slug (composition and PV) is significantly different for variant cases while rock-porosity and initial oil saturation parameters are more or less similar.

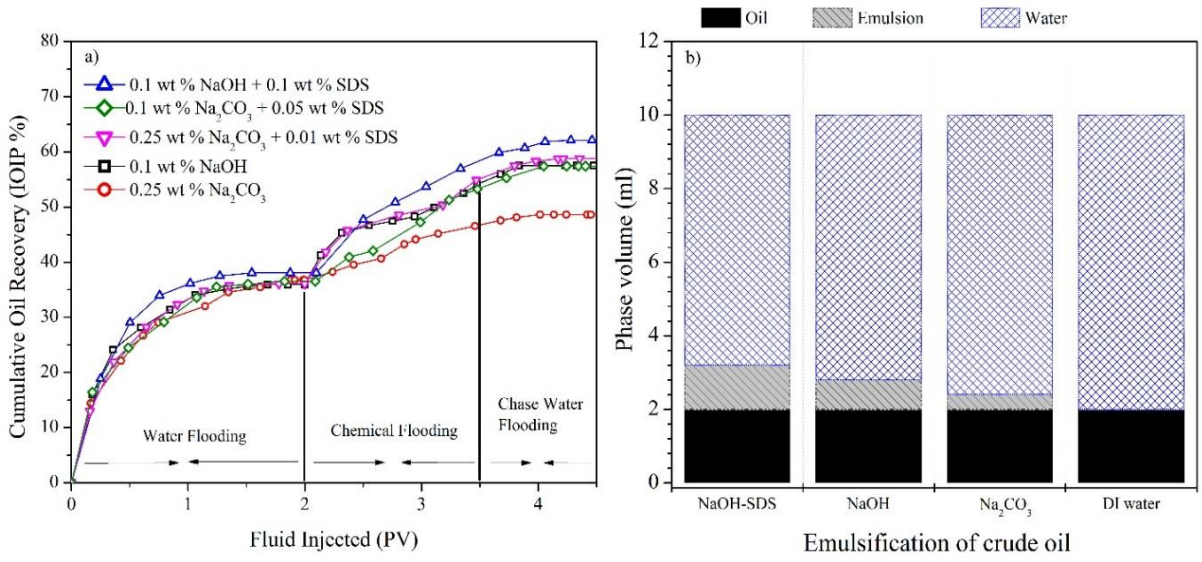

Fig. 4.2: Data obtained for a) Cumulative oil recovery using sandpack flooding and b) Emulsification after 30 minutes.

Table 4.1: Summary of optimal IFT data for various alkali and alkali-surfactant systems.

Sr No.	Alkalis	Concentration (wt%)	Surfactants	Concentration (wt%)	Minimum IFT (mN/m)
1	NaOH	0.1	-	-	5.15×10^{-2}
2	Na_2CO_3	0.25	-	-	4×10^{-1}
3	-	-	SDS	0.1	2.3
4	-	-	CTAB	0.04	1.84×10^{-1}
5	NaOH	0.1	CTAB	0.04	1.1×10^{-2}
6	NaOH	0.1	SDS	0.1	4.1×10^{-2}
7	Na_2CO_3	0.25	CTAB	0.04	4.82×10^{-2}
8	Na_2CO_3	0.25	SDS	0.01	2.26×10^{-1}
9	Na_2CO_3	0.1	CTAB	0.04	1.5×10^{-2}
10	Na_2CO_3	0.1	SDS	0.05	3.88×10^{-1}

Table 4.2: Summary of chemical EOR data for alkali-surfactant systems investigated in this work and literature.

Properties	**Acid value**	**Oil types**	**Origin**	**Density**	**Viscosity**	**Porosity**	**Permeabi-lity**	**Chemical slug**	**Initial oil saturation**	**Water flooding**	**Chemical flooding**	
Unit	mg KOH/ g of Oil		Oil field	g /cm^3	mPa. s	%	mD		%	%	IOIP* %	ROIP** %
Present Work	3.15	Light to moderate	Assam (India)	0.892	33.4	38.3	2054	0.1 wt% NaOH	74.1	35.92	15.54	24.25
						35.8	2104	0.25 wt% Na_2CO_3	78.5	36.79	11.85	18.75
						34.66	2097	0.1 wt% NaOH + 0.1 wt% SDS	80.1	38.08	24.02	38.79
						36.4	2087	0.25 wt% Na_2CO_3 + 0.01 wt% SDS	79.5	36.08	20.68	32.35
						37.5	2024	0.1wt% Na_2CO_3 + 0.05 wt% SDS	78.9	36.53	20.89	32.91
Samanta et al. **[118]**	0.038	Light	Ahmedabad (India)	0.830	119	38.66-39.59	4449-4837	0.5-1 wt% NaOH	79.1-80.9	50.7-51.6	13.9-15.2	28.2-31.6
Samanta et al. **[130]**	-	Light	Ahmedabad (India)	-	-	38.66-39.58	1233-1235	0.1-0.3 wt% SDS	80.2-82.1	51.6-52.5	17.9-21.5	37.1-45.4

Liu et al. [45]	1.32	Heavy	Saskatchewan (Canada)	0.964	1800	35.4	2500	0.3 wt% Na_2CO_3 + 0.3 wt% NaOH + 300 ppm surfactant	87	34	23.4	33.4
Chen et al. [43]	2.71	Heavy	Shengli (China)	0.946	1306	-	1417	0.5 wt% Na_2CO_3 + 0.2 wt% ABS	88.5	29.8	16.5	23.5
Tang et al. [22]	4.66	Heavy	Shengli (China)	0.971	3950	40.2	1273	0.5 wt% $NaBO_2$ + 0.1 wt% SBET-12	89.1	29.1	17.7	24.9
Pie et al. [28]	2.69	Heavy	Shengli (China)	0.947	2000	43.85	2015	0.1 wt% NaOH	90.14	31.76	19.96	29.25
Pie et al. [28]	2.69	Heavy	Shengli (China)	0.947	2000	44.21	2016	0.1 wt% NaOH + 0.1 wt% SLPS	90.05	34.33	18.63	28.37

4.3 Conclusions

Two alkalis (NaOH and Na_2CO_3) were used to examine IFT reduction behaviour for light to moderate Assam crude oil. NaOH was found more effective for Assam crude as it reduces the IFT to a minimum value of 5.15 $x10^{-2}$ mN/m. The data obtained from IFT analyses, emulsification test and flooding experiments confirmed that NaOH was better as compared to Na_2CO_3 for Assam crude oil (oil recovery 24.25% of ROIP). The synergistic action of alkali and surfactant in reducing the IFT indicated that CTAB is a better surfactant as compared to SDS for Assam crude. However, both reduce IFT to a value of 10^{-2} mN/m. Alkali-surfactant combination (0.1 wt% NaOH+0.1 wt% SDS) has been evaluated to be the best to achieve a residual oil recovery of 38.79 % of ROIP.

Chapter 5

Surfactant Adsorption Characteristics on Reservoir Rock

The adsorption characteristics of surfactant on reservoir rocks emphasising upon the mineralogy content of the rock were addressed. The mineralogy/morphology analysis of rock samples and thermal aging based surfactant stability analysis were adopted. Surfactant was chosen based on the interfacial tension reduction behaviour with light to moderate Assam crude oil. Different adsorption isothermal and kinetics models were fitted with the experimental data to represent pertinent surfactant adsorption characteristics. The adsorption behaviour at different salinity and temperature were investigated to mimic reservoir condition. The carried out research indicates that the adsorption capacity of surfactant is strongly dependent on the mineral content of the rock in the order of illite > feldspar > montmorillonite > kaolinite. These findings provide newer insights into real time surfactant adsorption characteristics, which are often ignored in conventional approaches and methodologies.

5.1 Rock Characterization

Detailed characterizations of reservoir rock were performed to evaluate its charge nature, minerals content, surface properties and pore shapes. Fig. 5.1a presents the EDX elemental peaks of Assam reservoir rock which shows that oxygen and silica are the major constituents with traces of Aluminium, Iron, Magnesium, Calcium, Potassium and Sodium. Fig. 5.1b depicts the XRD diffraction pattern which represents the existence of two major peaks and several other minor peaks. Using this peak information and available database (JCPDS), the compositional analysis showed quartz 61.1%, kaolinite 8.2%, feldspar 7.7%, illite 14.5%,

montmorillonite 2.5% and dolomite 6%. Therefore, both XRD and EDX analyses confirm that Assam reservoir rock is anionic in nature. Based on BET analysis, the data shows a specific surface area of 4.97 m^2/g with an average pore radius of 6.99 nm and total pore volume of 0.017 cc/g. Fig. 5.1c depicts the N_2 adsorption and desorption isotherms with a hysteresis loop at a value of 0.42 for P/P_o. The isotherms indicate type II (H3) classification based on IUPAC and confirm upon the existence of slit shaped pores [110, 111] and abundance of micro, meso and macro pores [112].

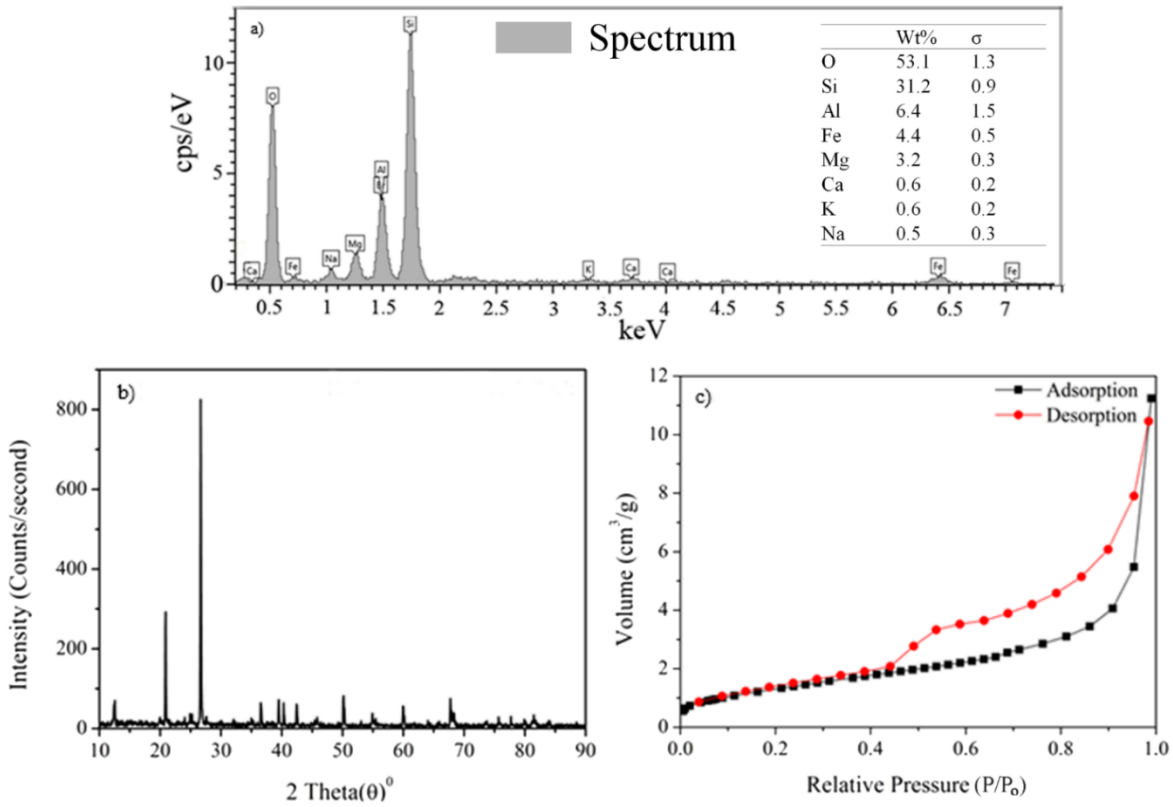

Fig. 5.1: Characterization of Hapjan (Assam) reservoir rock (a) EDX (b) XRD of powder reservoir rock and c) BET adsorption and desorption curve for N_2.

5.2 Interfacial Tension

5.2.1 Surfactant Selection Based on IFT

Initial selection of surfactants was purely based on the charge nature of reservoir rock and its interaction with Assam crude oil. As EDX and XRD analyses confirmed anionic nature of rock, the evaluation of cationic surfactants not considered due to opposite charge nature which ultimately results in higher adsorption. Therefore, two anionic and five non-ionic surfactants were subjected for the estimation of their IFT values (Table 5.1). It was observed that Triton X-100 has greater potential in IFT reduction compared to other six surfactants, therefore, Triton X-100 was further evaluated for adsorption process.

The dissimilarity between oil side and water side molecules at the interface was reduced when surfactant was adsorbed at the interface which reduces the IFT [113]. IFT depends on the interaction of hydrophilic group between water and surfactant molecules and hydrophobic group of oil and surfactant molecules which results in ultra-low IFT and can be achieved with special surfactant structures [113, 114]. Another possible reason for better IFT reduction with Triton X-100 could be due to high interfacial activity, large interaction energy at the interface, higher adsorption of surfactant molecules at oil-water interface and their adsorption strength, unionized acid species, packing of surfactant molecules at the interface, surface elasticity, surface viscosity and charge at the surface [51, 113, 115, 116].

Table 5.1: IFT values of various anionic and non-ionic surfactants with Assam crude oil at 0.025 wt% surfactant concentration.

Surfactant (Name)	SDS	Sodium lignosulphonate	Triton X-100	Span 80	Tween 80	Brij 30	Titriplex III
IFT (mN/m)	0.78	2.14	0.22	0.98	2.82	3.12	No droplet

5.2.2 Effect of Formation Water on IFT

The synthetic formation water constitutes NaCl which contributes to IFT variation with salinity effect. The effect of salinity on IFT reduction was studied by several researchers [5, 15, 131]. The equilibrium IFT variation of crude oil –surfactant solution system is depicted in Fig. 5.2 for both millipore water and synthetic formation water. It can be seen that when synthetic formation water was used, the IFT of the system reduced from 16.3 mN/m (without surfactant) to 0.22 mN/m at 0.02 wt% surfactant concentration. Corresponding variation in the system IFT for millipore water is from 24.3 to 2.29 mN/m. Further, beyond 0.02 wt%, the IFT reduction was not significant and fairly remains constant. The reduction in IFT with surfactant solution occurs due to accumulation of surfactant molecules at the oil-water interface [132, 133]. However, with formation water, the amount of in-situ surfactant at the interface develops which further reduces the IFT to a minimum value. Therefore, synergy effect was observed between the salt present in formation water and surfactant molecules [56]. The salt and surfactant together impact the double electrode layer, developing a thin layer with the arrangement of surfactant and formed in situ surfactant molecules at the interface to detect lowest IFT value [134-136]. The partition mechanism of surfactant

molecules at the oil-water interface can be enhanced with salt which further decreases the IFT [137].

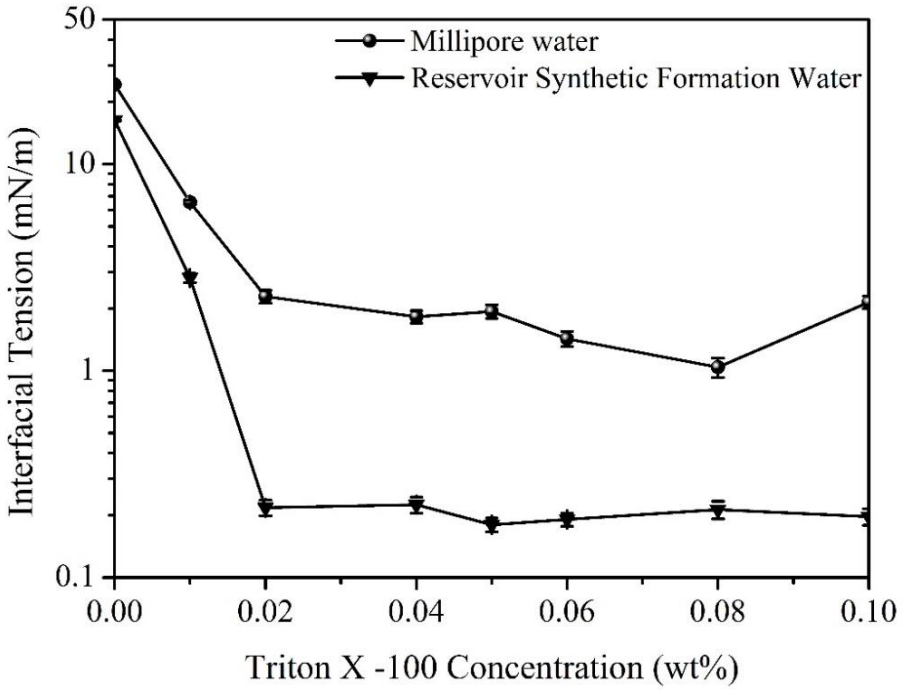

Fig. 5.2: IFT variation with millipore water and synthetic reservoir formation water using Triton X-100.

5.3 Surfactant Stability

The stability of Triton X-100 was evaluated using TGA, FTIR, NMR and IFT analysis. Fig. 5.3a illustrates the variation of weight loss with temperature using which the minimal temperature at which degradation occurs can be determined. From the TGA graph, it can be observed that the surfactant is thermally stable up to 305^{o}C. Therefore, it is expected that at the reservoir operating condition of 70-90^{o}C, the surfactant degradation does not occur as it is thermally stable without any weight loss. To further ensure upon the surfactant stability at reservoir temperature, the surfactant was thermally aged by keeping at 90^{o}C in an oven for 10 days. After aging, the surfactant was characterized with FTIR, NMR and IFT studies. Fig. 5.3b and Fig. 5.3c represent the FTIR and NMR spectra of Triton X-100 before and after

thermal aging respectively. From FTIR spectra, it was observed that the functional groups present do not change at all and thereby indicates the stability of surfactant from chemical analysis perspective. Similar inference can be also drawn from the NMR spectra of Triton X-100 [59].

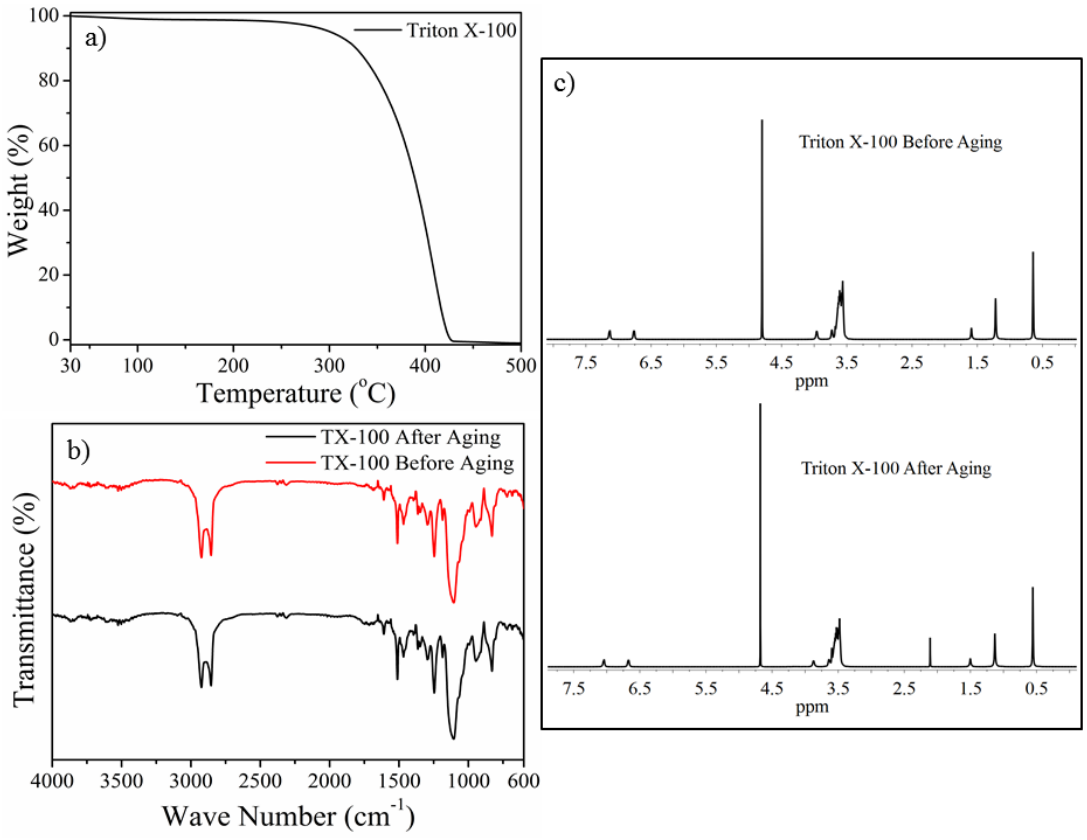

Fig. 5.3: Surfactant stability analysis of Triton X-100 using (a) TGA showing degradation or weight loss, (b) FTIR indicating functional group before and after aging and (c) ^{1}H NMR showing negligible change in proton.

5.3.1 Crude oil – Surfactant IFT Before and After Aging

Fig. 5.4a shows the variation in dynamic IFT between Assam crude and Triton X-100 using formation water as aqueous medium. It was observed that after 40 minutes equilibrium IFT was reached and beyond which no further changes was observed for 0.02 wt% Triton X-100. The dynamic IFT behaviour arises due to simultaneous adsorption of surfactant

molecules, ionized and unionized acid group at the interface [138]. The equilibrium IFT between Assam crude oil and Triton X-100 solution at various concentration with aged and non-aged sample is depicted in Fig. 5.4b. It was observed that the IFT value reduced to 10^{-1} mN/m at 0.02 wt% surfactant concentration. Further, at 0.05 wt%, the equilibrium IFT is 0.16 mN/m and 0.138 mN/m for aged and fresh surfactant respectively. The study reveals the stability of the surfactant in terms of IFT behaviour in addition to other analytical analyses. The related reduction in IFT with increasing surfactant concentration is due to an increase in the surfactant molecules at the oil-water interphase. The IFT reduction with surfactant solution concentration is limited to a specific concentration at which the interfacial film formation is facilitated by adsorbed surfactant molecules and any further enhancement in surfactant solution concentration does not enhance the sorptive capacity of the film due to adsorption saturation in the interfacial film [139]. Therefore, IFT remains constant despite further enhancing surfactant concentration.

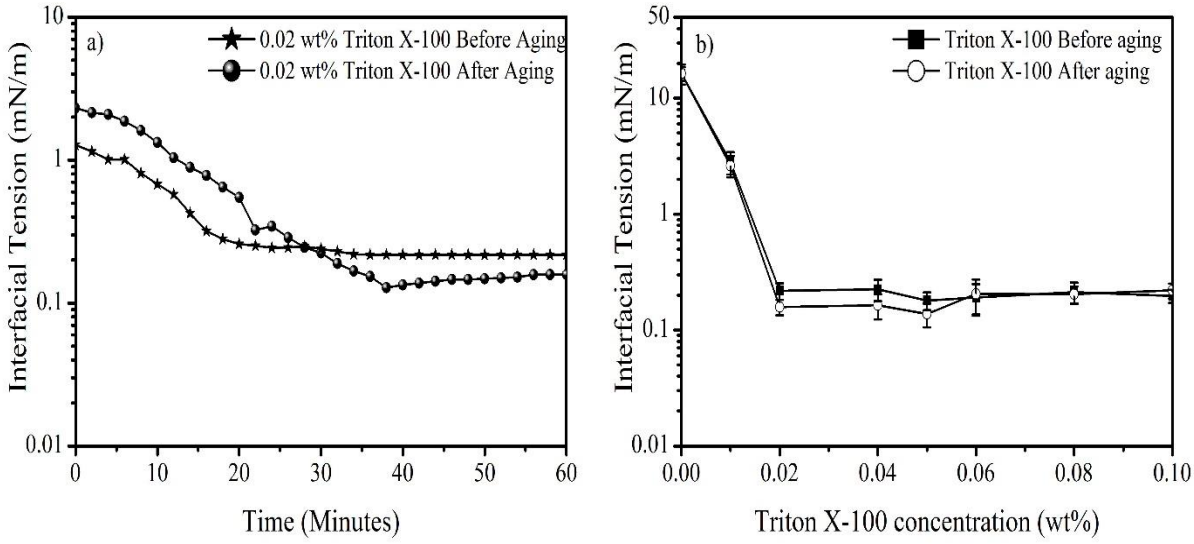

Fig. 5.4: Interfacial tension behaviour of Assam crude oil showing (a) Dynamic IFT variation with time at 0.02 wt% Triton X-100 for both aged and non-aged samples b) IFT behaviour with different Triton X-100 concentrations (wt%) for both aged and non-aged surfactants.

5.4 Adsorption Isotherms

The fitness plots of the measured adsorption equilibrium data are depicted in Fig. 5.5(a-d) for Linear, Langmuir, Freundlich and Temkin models. Corresponding summary of correlations, regression coefficient (R^2) and average relative error for all equilibrium adsorption isotherms have been presented in Table 5.2. It can be analysed that among all models, Langmuir model fitness plot provides maximum regression coefficient of 0.99 and minimal average relative error of 2.58%. From the Langmuir isotherm fitness plot, equilibrium constant K_L and maximum monolayer coverage capacity q_o were evaluated and presented in Table 5.2. The non-dimensional separation factor R_L was also evaluated which varies between 0.809 - 0.974 and thereby affirms the favourability of the adsorption process. Further, it can be noted that the fitness of Freundlich isotherm model was not significant (R^2 = 0.81 as indicated in Fig. 5.5c) but was comparatively better than that obtained for the linear model. Further, its average relative error for the isotherm case was 3.50% which is second lowest. Considering these observations, it is inferred that the Langmuir isotherm model is the best fit model to represent pertinent batch equilibrium of crude oil on the surfactant surface with an R^2, relative error, q_o (mg/g) and K_L (L/mg) values of 0.99, 2.58%, 16.89 and 0.0025 respectively. The results revealed that the surface of the adsorbent is homogeneous with monolayer adsorption and no interaction between the adsorbed molecules. Similar behaviour was observed by Ahmadi et al. [62] and Barati et al. [140] while investigating the adsorption behaviour of natural non-ionic surfactants on carbonate minerals.

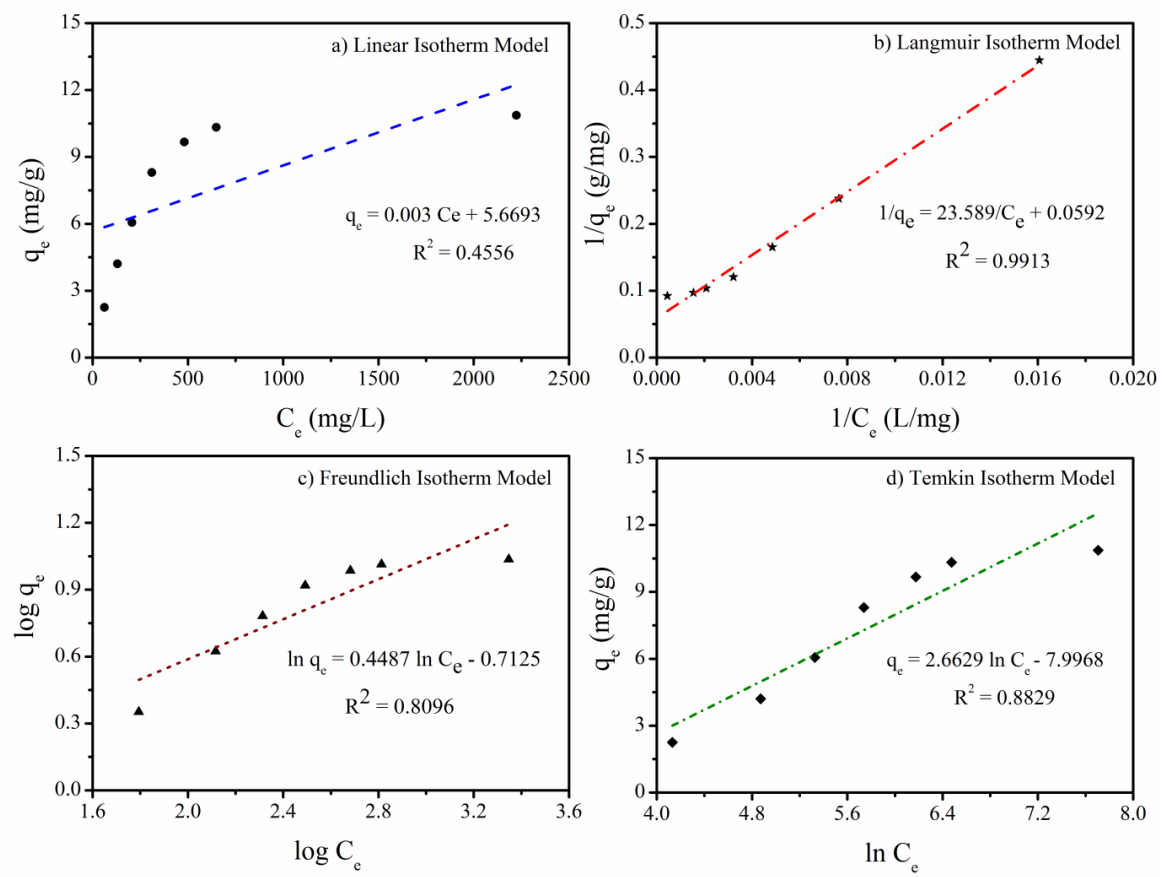

Fig. 5.5: Adsorption Isothermal model fitting of Triton X-100 on Hapjan (Assam) reservoir rock (a) Linear isotherm model (b) Langmuir isotherm model (c) Freundlich isotherm model and (d) Temkin isotherm model.

Table 5.2: Parameters of various adsorption isotherm models fitting.

Isothermal models	**Correlations**	**Parameters**		**R^2**	**Average relative error (%)**
Linear	$q_e = 0.003C_e + 5.6693$	K_H	C	0.456	22.01
		0.003	5.669		
Langmuir	$1/q_e = 23.589/C_e + 0.0592$	q_o	K_L	0.99	2.58
		16.89	0.002		
Freundlich	$\log q_e = 0.4487 \log C_e - 0.3094$	n	K_F	0.81	3.50
		2.22	0.733		
Temkin	$q_e = 2.6629 \ln C_e - 7.9968$	K_T	B	0.88	5.55
		0.049	2.662		

5.4.1 Adsorption Kinetic Models

The measured adsorption kinetic data were subjected to Lagergren's psuedo-first order rate, pseudo second order rate, intra-particle diffusion and Elovich models. The obtained fitness plots for these cases are depicted in Fig. 5.6(a - d) respectively. Corresponding R^2 and average relative error for pseudo-first order model are 0.95 and 9.65% respectively (Table 5.3). However, for pseudo-second order model, these values are the best (0.99 and 3.64% respectively as presented in Table 5.4). On the other hand, intra-particle diffusion model and Elovich model fitness parameters are significantly poor (0.76 and 34.67% error for intra-particle diffusion model as indicated in Table 5.5 and 0.84 and 10.32% error for Elovich model as conveyed in Table 5.6). Hence, among all models, it can be concluded that the pseudo-second order model fits well to represent the measured adsorption kinetics data. Therefore from the kinetics analysis we can suitably predict the adsorption of Triton X-100 on Hapjan (Assam) reservoir rock over entire experimental concentration range and time periods [62, 141].

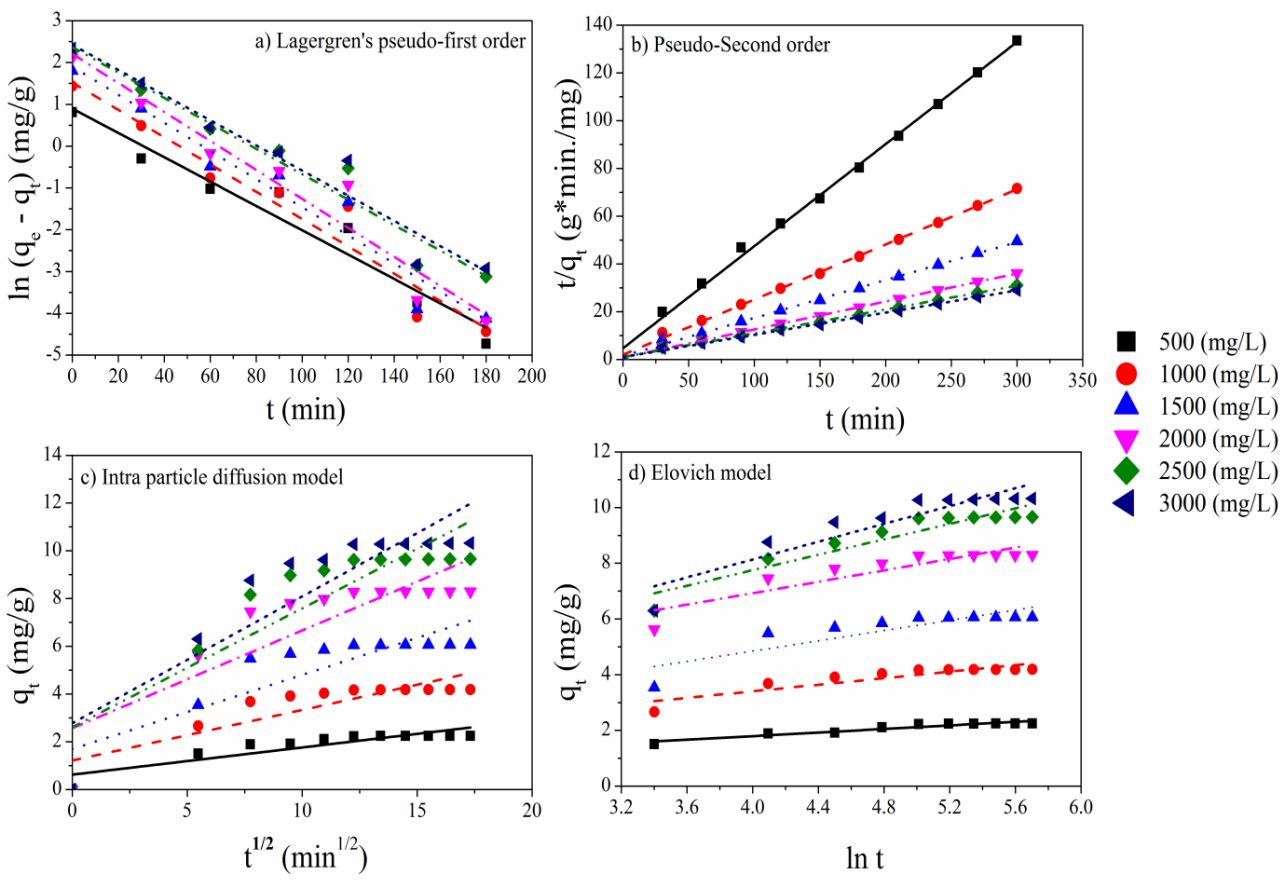

Fig. 5.6: Adsorption Kinetics of Triton X-100 on Hapjan (Assam) reservoir rock (a) Lagergren's pseudo-first order (b) Pseudo-second order (c) Intra particle diffusion model and (d) Elovich model.

Table 5.3: Lagergren's pseudo-first order kinetics correlation developed at different Triton X-100 concentrations.

Surfactant concentration (mg/L)	Correlation	R^2	q_{model} (mg/g)	q_{exp} (mg/g)	Average relative error (%)
500	$\ln(q_e - q_t) = -0.0291t + 0.8984$	0.95	2.45	2.24	9.14
1000	$\ln(q_e - q_t) = -0.0327t + 1.5219$	0.94	4.58	4.18	9.35
1500	$\ln(q_e - q_t) = -0.0336t + 1.9025$	0.95	6.70	6.06	10.58
2000	$\ln(q_e - q_t) = -0.0347t + 2.2031$	0.95	9.05	8.30	9.06
2500	$\ln(q_e - q_t) = -0.0304t + 2.3673$	0.95	10.66	9.67	10.31
3000	$\ln(q_e - q_t) = -0.0301t + 2.425$	0.94	11.30	10.32	9.44
	Average	0.94			9.65

Table 5.4: Pseudo-second order kinetics correlation developed at different Triton X-100 concentrations.

Surfactant concentration (mg/L)	Correlation	R^2	Q_{model} (mg/g)	Q_{exp} (mg/g)	Average relative error
500	$t/q_t = 0.4276t + 4.71$	0.997	2.33	2.24	3.94
1000	$t/q_t = 0.2308t + 2.0116$	0.998	4.33	4.18	3.43
1500	$t/q_t = 0.159t + 1.4916$	0.997	6.28	6.06	3.76
2000	$t/q_t = 0.1172t + 0.8597$	0.998	8.53	8.30	2.79
2500	$t/q_t = 0.0995x + 1.0409$	0.997	10.05	9.67	3.92
3000	$t/q_t = 0.0931x + 1.0081$	0.997	10.74	10.32	4.01
	Average	0.997			3.64

Table 5.5: Intra particle diffusion model kinetics correlation developed at different Triton X-100 concentrations.

Surfactant concentration (mg/L)	**Correlation**	**R^2**	**q_{model} (mg/g)**	**Q_{exp} (mg/g)**	**Average relative error (%)**
500	$q_t = 0.1139(t)^{0.5} + 0.6235$	0.79	2.95	2.24	31.46
1000	$q_t = 0.2114(t)^{0.5} + 1.2159$	0.75	5.54	4.18	32.44
1500	$q_t = 0.3104(t)^{0.5} + 1.6964$	0.75	8.05	6.06	32.94
2000	$q_t = 0.409(t)^{0.5} + 2.5687$	0.73	11.34	8.30	36.62
2500	$q_t = 0.489(t)^{0.5} + 2.6082$	0.78	13.28	9.67	37.41
3000	$q_t = 0.5308(t)^{0.5} + 2.7809$	0.78	14.16	10.32	37.16
	Average	0.77			34.67

Table 5.6: Elovich model kinetics correlation developed at different Triton X-100 concentrations.

Surfactant concentration (mg/L)	**Correlation**	**R^2**	**q_{model} (mg/g)**	**q_{exp} (mg/g)**	**Average relative error (%)**
500	$q_t = 0.3213 \ln(t) + 0.5096$	0.91	2.45	2.24	8.90
1000	$q_t = 0.5879 \ln(t) + 1.0511$	0.81	4.60	4.18	9.86
1500	$q_t = 0.9216 \ln(t) + 1.1597$	0.74	6.72	6.06	10.97
2000	$q_t = 1.0234 \ln(t) + 2.8326$	0.80	9.10	8.30	9.71
2500	$q_t = 1.3876 \ln(t) + 2.1996$	0.88	10.70	9.67	10.71
3000	$q_t = 1.6004 \ln(t) + 1.7307$	0.85	11.54	10.32	11.77
	Average	0.84			10.32

5.5 Effect of Temperature and Formation Water on Adsorption Characteristics

The temperature dependency of adsorption characteristics on Assam rock surface is depicted in Fig. 5.7a. The plot also presents the effect of formation water and millipore water in terms of adsorption capacity. The figure indicates an adsorption of 10.87 mg/g at 30^{o}C which reduces to 6.23 mg/g at 70^{o}C using synthetic formation water as aqueous medium. The reduction in adsorption with variation in temperature was observed to be around 42.68%. This is due to the fact that at higher temperature, the adsorption rate of adsorbate within the surface and interior pores of adsorbent decreases due to reduction in viscosity [141]. Further variation of adsorption with temperature can be explained with the help of thermodynamic parameters as Gibbs free energy, enthalpy and entropy.

The role of formation water and millipore water (salinity effect) during adsorption was found to be as significant as that of temperature effect as shown in Fig. 5.7b. As the aqueous medium is changed from formation water to millipore water, the adsorption reduces from 10.87 mg/g to 7.53 mg/g at 30^{o}C. The adsorption capacity decreases by 30.7 % when the aqueous medium is bereft of salinity condition. The increase in adsorption capacity with increasing salinity (NaCl concentration) is due to the unequal charge distribution at the interface that allows compression of electric double layer formed at the adsorbent surface. This results in higher adsorption capacity due to a reduction in the electrostatic repulsion between the adsorbate and the adsorbent surfaces [141, 142]. At higher temperature 70^{o}C, the adsorption capacity decreases from 6.23 mg/g to 4.86 mg/g as the synthetic formation water aqueous phase is replaced by millipore water. Therefore a significant difference in adsorption behaviour with millipore water was observed at higher temperature with a

reduction in adsorption capacity of 22%. These observations are useful to convey the realistic behaviour of the surfactant adsorption with reservoir rock at reservoir operating conditions and thereby facilitate a better understanding of variations in the laboratory and pilot/real reservoir conditions. Thereby, the methodology adopted in this work can be used for the extrapolation of laboratory measured experimental trends to predict the surfactant adsorption characteristics in real reservoir scenario or pilot plant studies.

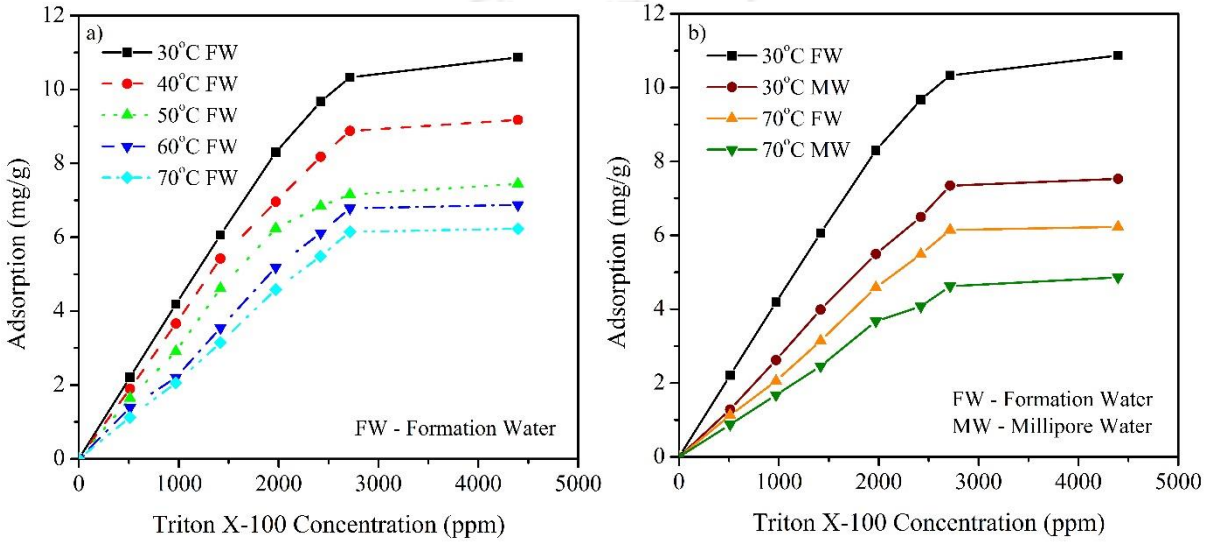

Fig. 5.7: Effect of a) temperature and b) formation water (salinity) on adsorption capacity.

5.6 Thermodynamic Parameters of Adsorption

Fig. 5.8 depicts the plot for the evaluation of thermodynamic parameters and Table 5.7 summarizes the associated parameters. It can be noted that the Gibbs free energy change is -2.318 kJ/mol at 30°C which conveys the spontaneity and feasibility of adsorption process. Negative enthalpy ΔH = -15.846 kJ/mol conveys that adsorption process is exothermic in nature and hence higher adsorption capacity exists at lower system temperature. Further, negative value of entropy ΔS = -0.045 kJ/mol k expresses the reduction in randomness of

molecules at interface and hence reduction in adsorption capacity at higher temperature [141].

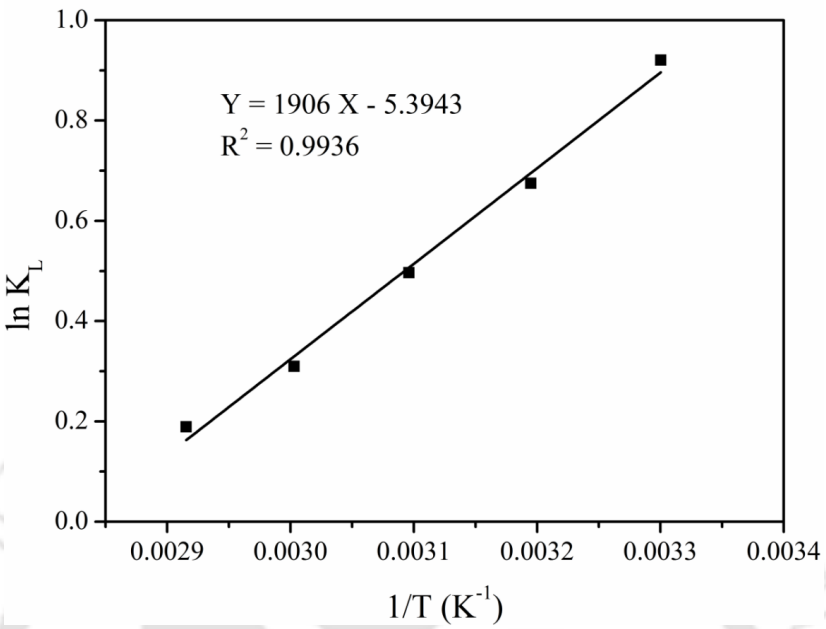

Fig. 5.8: Langmuir constant and temperature plot to obtain thermodynamics parameters.

Table 5.7: Values of thermodynamics parameters.

Temperature	K_L	ΔG	ΔH	ΔS (kJ/mol
303	2.51	-2.318		
313	1.964	-1.757	-15.846	-0.045
323	1.643	-1.333		
333	1.363	-0.857		
343	1.208	-0.538		

5.7 Effect of Different Minerals on Adsorption Capacity for Field and Synthetic Cores

Table 5.8 summarizes the adsorption capacity of different synthetic and natural anionic reservoir cores at 70°C with formation water as the aqueous phase. For comparison purpose the results of Muherei et al. [143] obtained at 25°C are also included. The variation in the

adsorption capacity is attributed to the variations in the mineral compositions and surface area of the rock samples. The mineral compositions of all natural and synthetic cores deduced from XRD analysis are shown in Table 5.9. The XRD spectrum analysed with MATCH software to determine the percentage of minerals composition are provide in appendix C (Fig C5.2 to C5.6). The relationship between mineral composition (%) and adsorption quantity (mg/g) showing the linearity (R^2) was plotted (Fig. 5.9) and the obtained data are summarized in Table 5.10. Higher illite content resulted in higher adsorption capacity, showing linearity with R^2 value of 0.95. Similarly, the R^2 value for feldspar, montmorillonite and kaolinite were found to be 0.92, 0.91 and 0.81 respectively. For quartz and dolomite large deviation in linearity was observed with R^2 value of 0.47 and 0.18 respectively whereas with combination of the major four minerals (illite, feldspar, montmorillonite and kaolinite) highest linearity dependency with R^2 value of 0.98 was obtained. The correlation so developed indicates the contribution of each minerals in the order of illite > feldspar > montmorillonite > kaolinite. Another possible reason for higher adsorption can be the surface area of reservoir rocks. For instance, Assam natural cores has a higher surface area of 4.97 m^2/g in comparison with standard Berea core (2.1 m^2/g) used in present study. The surface area of standard Berea sample as reported in literature is in between 0.82-1.23 m^2/g [144, 145]. Thus from above discussion it can be conclude that the effect of mineral content and its types along with the surface area can seriously affect the adsorption quantity. However, the exact role of surface area was not investigated in detail due to the variation in the quantity of different minerals on synthetic and natural rock.

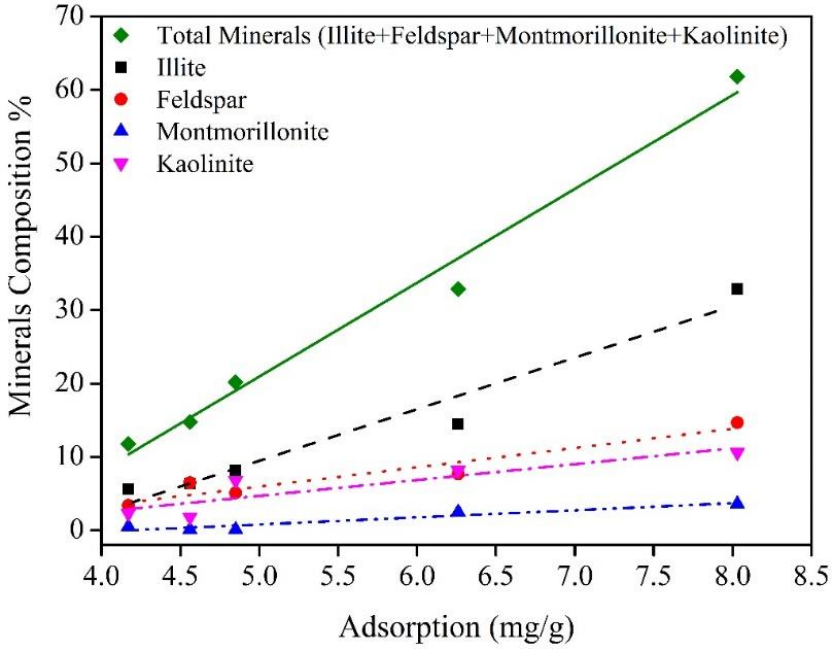

Fig. 5.9: Linear model fitting of each minerals that affects the adsorption process.

Further, from economic perspective, financial loss due to surfactant adsorption was evaluated for various adsorbents and is summarized in Table 5.8 along with relevant data. The total volume of Assam reservoir rock was considered as 3×10^9 m^3. The porosity and density of individual rock were used for the calculation (Table 5.8). The financial loss incurred during EOR process with Triton-X 100 surfactant has been evaluated as 0.48 billion $, which is higher with the literature value reported for DBS surfactant–kaolinite adsorbent system [60]. The difference in cost analysis is because of the volume of reservoir rock considered. In the current study, we assume actual average reservoir volume (area 30 sq. km and 100 m depth) and not one acre by 3m depth as considered for the above literature.

Table 5.8: Adsorption capacities and cost analysis of natural and synthetic cores at 70°C using synthetic formation water (4445 ppm salinity).

S. No	Cores	Core types	Gas permeability (mD)	Brine permeability (mD)	Porosity (%)	Density (Kg/m^3)	Adsorption (mg/g)	Triton X-100 cost (Rs/Kg)	Adsorption loss (Crores Rs)	Adsorption loss (billion $[1])	Reference
1	Hapjan (Assam)	Natural	20.2	-	20.2	2.45	6.23	3454	3,194	0.48	This work
2	Jorajan (Assam)	Natural	2	-	10.4	2.32	8.03	3454	2,007	0.30	This work
3	Carbon Tan	Synthetic	42	10-12	12.2-17.7	2.19	4.56	3454	1,262-1,832	0.19-0.27	This work
4	Idaho Gray	Synthetic	7187-7956	2150-2400	29	1.82	5.07	3454	2,772	0.42	This work
5.	Gray Berea	Synthetic	200-315	60-100	19-20	2.11	4.17	3454	1,732-1,824	0.26-0.27	This work
6	Sandstone	Synthetic	-	-	-	-	1.5	3454	-	-	Muherei et al. [49]

1$= 66.85 INR

Table 5.9: XRD of all core samples showing the mineral compositions.

Cores	Mineral composition					
	quartz	**kaolinite**	**feldspar**	**illite**	**montmorillonite**	**dolomite**
Hapjan (Assam)	61.1	8.2	7.7	14.5	2.5	6
Jorajan (Assam)	35.6	10.6	14.7	32.9	3.6	2.6
Carbon Tan	79.2	2.3	3.4	5.6	0.5	9.0
Idaho Gray	45.5	1.8	6.5	6.4	0.1	39.7
Gray Berea	78.6	6.8	5.1	8.2	0.1	1.2

Table 5.10: Linear model fitting of the four major mineral compositions which affect the adsorption process.

Mineral types	Correlation	R^2
illite	Y = 0.136X + 3.7359	0.9554
feldspar	Y = 0.349X + 2.9638	0.9164
montmorillonite	Y = 0.9461X + 4.2873	0.9135
kaolinite	Y = 0.3741X + 3.3517	0.809
Total Mineral content (illite + feldspar + montmorillonite + kaolinite)	Y = 0.077X + 3.3939	0.9847

5.8 Conclusions

The screening of a desired surfactant for Assam reservoirs based on IFT analysis and reservoir rock charge nature was addressed. Further this study conveys the relevance of correlating rock characteristics with adsorption capacity. EDX, XRD and BET results conveyed the anionic nature of the Assam rock sample with different mineral composition and surface area. Triton X-100 was chosen due to its potential to reduce IFT even at low concentration (0.02 wt %) compared to other six surfactants signifying the effectiveness of the chosen surfactant for chemical EOR application. TGA, NMR and FTIR studies conveyed that the surfactant is stable at reservoir conditions with negligible effect of thermal aging. The salinity effect was confirmed during millipore water based IFT studies and conveyed that the IFT was significantly higher (> 1 mN/m) with millipore. Among alternate equilibrium isotherm models and kinetic models, the best fit models correspond to Langmuir model (R^2 = 0.99 and 2.58% error) and pseudo-second order model (R^2 = 0.99 and 3.64% error). Thermodynamic adsorption parameters specify the feasibility, spontaneity and exothermic nature of the adsorption process. The study also demonstrates the adsorption quantity of Triton X-100 on Assam rock surface i.e. 6.23 mg/g at reservoir temperature of 70^{o}C using reservoir formation water as aqueous medium. The linear correlation developed shows the dependency of the mineral content on the adsorption quantity in the order of illite > feldspar > montmorillonite > kaolinite with R^2 value of 0.95, 0.92, 0.91 and 0.81 respectively.

Chapter 6

Alkali-Surfactant Flooding in Carbonate Reservoir for Heavy Crude Oil

This chapter focused on the experimental investigations targeting optimum chemical slug formulation for tertiary enhance oil recovery (EOR) of heavy Assam crude oil in carbonate reservoir. Two alkalis and eight surfactants were screened based on interfacial tension (IFT), emulsification, wettability alteration and core flooding studies. The salinity and temperature of the system were varied from 0-20% and 30 to 80°C respectively to imitate reservoir condition. The residual oil recovery achieved by performing carbonate Berea core (Silurian dolomite) flooding experiments for alkali, surfactants and their combinations were estimated and the mechanisms responsible for each system were discussed in detail.

6.1 Identification of Competent Alkali

6.1.1 IFT Studies of Alkali-Crude Oil System

Heavy crude oil which has density of 926.6 kg/m^3, acid number of 2.72 mg KOH/g sample, API gravity of 21.2° and viscosity of 20.1 mPa·s (at 30°C) was chosen. The variation in the IFT values between alkali (NaOH/Na_2CO_3) and crude oil system was conducted by varying alkali concentration in the range of 0.1 – 2 wt%. While similar IFT reduction trend exist for both alkalis, the reduction was significant for NaOH (Fig. 6.1a). For NaOH solution, the minimal IFT value of 5.3 x 10^{-1} mN/m was obtained at 0.6 wt%. On the other hand, minimal IFT value for Na_2CO_3 was obtained at 0.8 wt% concentration (1.16 mN/m). The IFT reduction at higher concentrations was due to the solution pH. As alkali concentration increases, higher pH favours ionization of acid groups prevalent in the crude oil and hence IFT decreases. At optimal pH, minimal IFT can be achieved due to adsorption of both ionized

and un-ionized acids at the interface, with un-ionized acid concentration being too low to influence the critical micelle concentration (CMC). A further enhancement in alkali concentration minimizes un-ionized ions at the interface and hence enhances IFT value. Thereby, IFT values reach saturation and become constant at higher alkali concentration due to ionization of all non-ionized acids [34, 36, 121].

The dynamic IFT values of the selected alkali (NaOH) varied from 4 x 10^{-2} to 2.6 mN/m (Fig. 6.1b). Dynamic IFT profile involved a steady increase and saturation at maturity of time frame, with transient behaviour in the range of 10 – 20 min. This is due to the formation of in-situ surfactant at the oil-water interface and its accumulation by adsorption and desorption rate. The initial IFT reduction occurs due to the accumulation of active species at the oil-water interface with lower desorption rate. However as time proceeds, a higher concentration gradient develops at the interface which enhance desorption rate reducing concentration of active species at the interface to counter effect the IFT reduction phenomena [15].

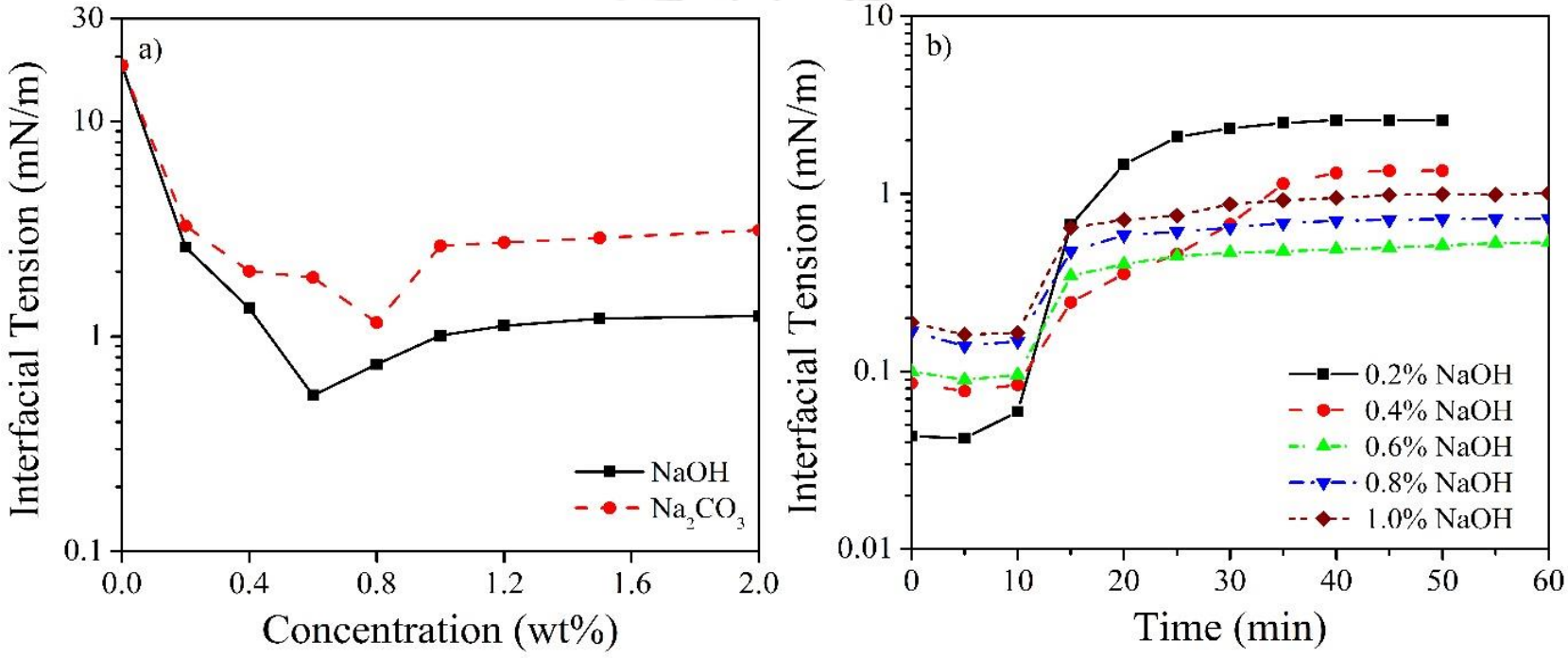

Fig. 6.1: Interfacial tension between crude oil and alkali solutions using formation water as aqueous medium at temperature of 30°C a) different concentrations of NaOH and Na_2CO_3 and b) Dynamic interfacial tension of NaOH at different concentrations (wt%).

6.1.2 Effect of Salinity and Temperature on IFT for Alkali-Crude Oil system

The IFT behaviour of NaOH (at 0.6 wt%) - crude oil system at reservoir conditions of salinity and temperature was analysed (Fig. 6.2). The IFT varied from 2.4 x 10^{-1} mN/m at higher salinity (20 wt%) to 5.84 x 10^{-1} mN/m at no salinity (0 wt%) which showed no significant changes in IFT value even after enhancing the salinity (Fig. 6.2a). The minor variation in IFT occurred primarily due to pushing of in-situ surfactant at the oil-water interface by the ionic solution which increases adsorption quantity of in-situ surfactant at the interface [146, 147]. Fig. 6.2b depicts the increase in IFT value from 5.3 x10^{-1} mN/m to 2.2 mN/m as temperature changed from 30 to 80^{o}C respectively. At lower temperature, a stable rigid film gets formed at the interface due to accumulation of cations to obtain a lower IFT. At higher temperature, IFT enhances due to the destabilization of this film [148, 149].

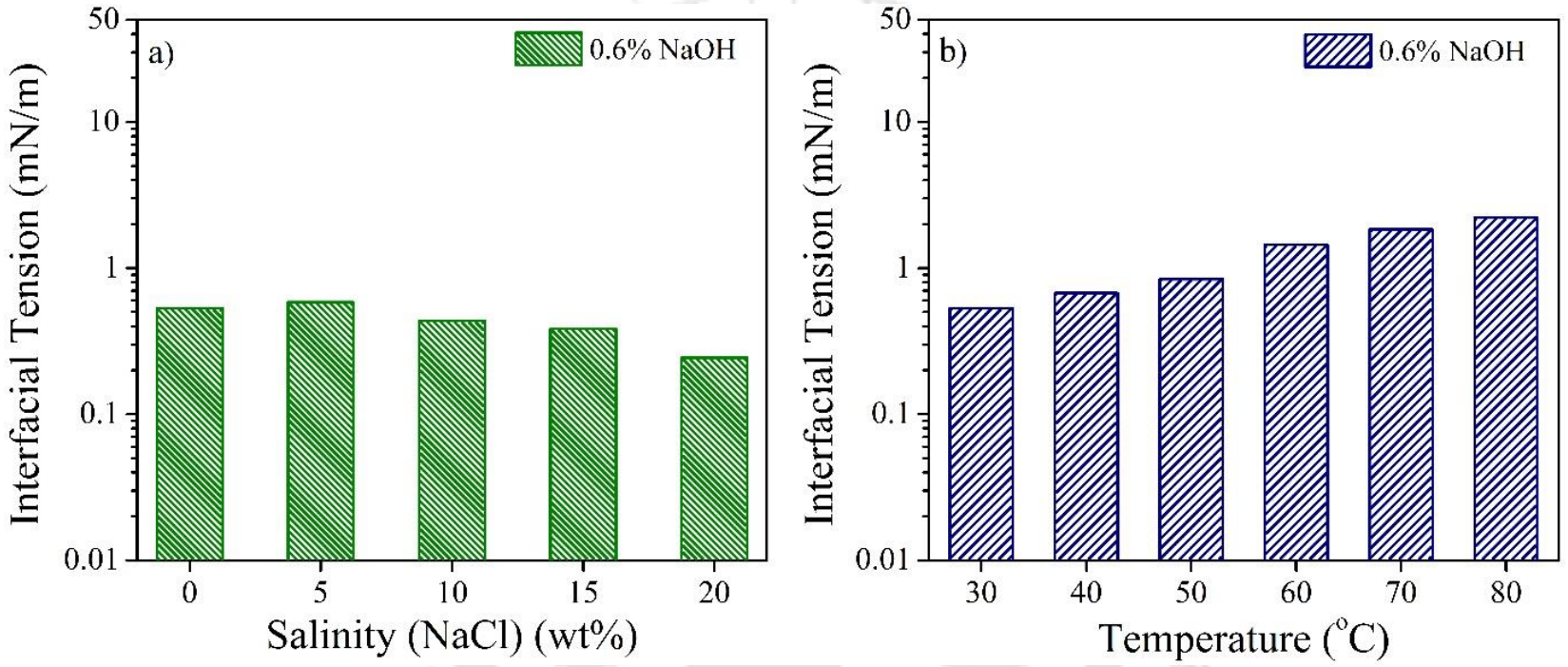

Fig. 6.2: Interfacial tension of NaOH (0.6 wt%) - crude oil system with variation in a) salinity from 0 to 20 wt% at 30°C and b) temperature from 30 to 80°C using formation water.

6.2 Identification of Competent Surfactants

6.2.1 IFT Behaviour of Surfactant-Crude System

Based on the minimal equilibrium IFT values achieved for the chosen heavy crude oil, eight surfactants belonging to the categories of cationic (one), anionic (two) and non-ionic (five) were evaluated (Fig. 6.3). The concentration of each surfactant was varied from 0.01 to 0.3 wt% (Fig. 6.3a). CTAB and TX-100 surfactants were able to reduce the IFT to a lowest value of 10^{-2} mN/m approximately. Also, it needs to be mentioned that drop formation was not possible for Triplex III surfactant and hence IFT measurements could not be carried out. An important observation of the carried out investigations is that, except for Brij 30 (minimal IFT was achieved at 0.15 wt%), a small portion of surfactant (0.025 wt%) is enough for substantial IFT reduction and negligible changes in IFT reduction occurred at higher surfactant concentrations. Initially, with increasing surfactant concentration, the enhancement of adsorption capacity of the surfactant molecules at the oil-water interface facilitates IFT reduction. Further increase in surfactant concentration enables saturation of adsorption to yield a constant IFT profile. In few cases, marginal or negligible IFT enhancement with higher surfactant concentration is due to variation in distribution of surfactant molecules at the oil-water interface [128].

The dynamic IFT curves for CTAB and TX-100 surfactants at 0.025 wt% concentration are shown in Fig. 6.3b. The minimum transient IFT values, 6.2×10^{-3} mN/m and 3.1×10^{-2} mN/m were obtained for CTAB and TX-100 respectively. However, the equilibrium IFT values for CTAB and TX-100 were found as 7.5×10^{-2} and 1.16×10^{-1} mN/m respectively. CTAB and TX-100 showed lower IFT values compare to other surfactants because of the hydrophilic and hydrophobic group interaction between water, surfactant and oil molecules

at the interface [113]. Higher adsorption of surfactant molecules at interface, packing of surfactant molecules, large interfacial area, surface viscosity and charge at the surface also contributes to achieve ultra-low IFT values [51, 113, 115, 116]. The ultra-low value of IFT can also be achieved with surfactant retaining special structure [113, 114]. While investigating dynamic IFT for CTAB, it was observed that the oil layer formed in the capillary tube gets elongated and after certain time breaks down, though the IFT values remains unaffected with $L/D \geq 4$. This phenomenon was observed with CTAB only and not for other surfactants. CTAB might undergo better emulsification due to excellent time dependent behaviour of oil break time in the test sample.

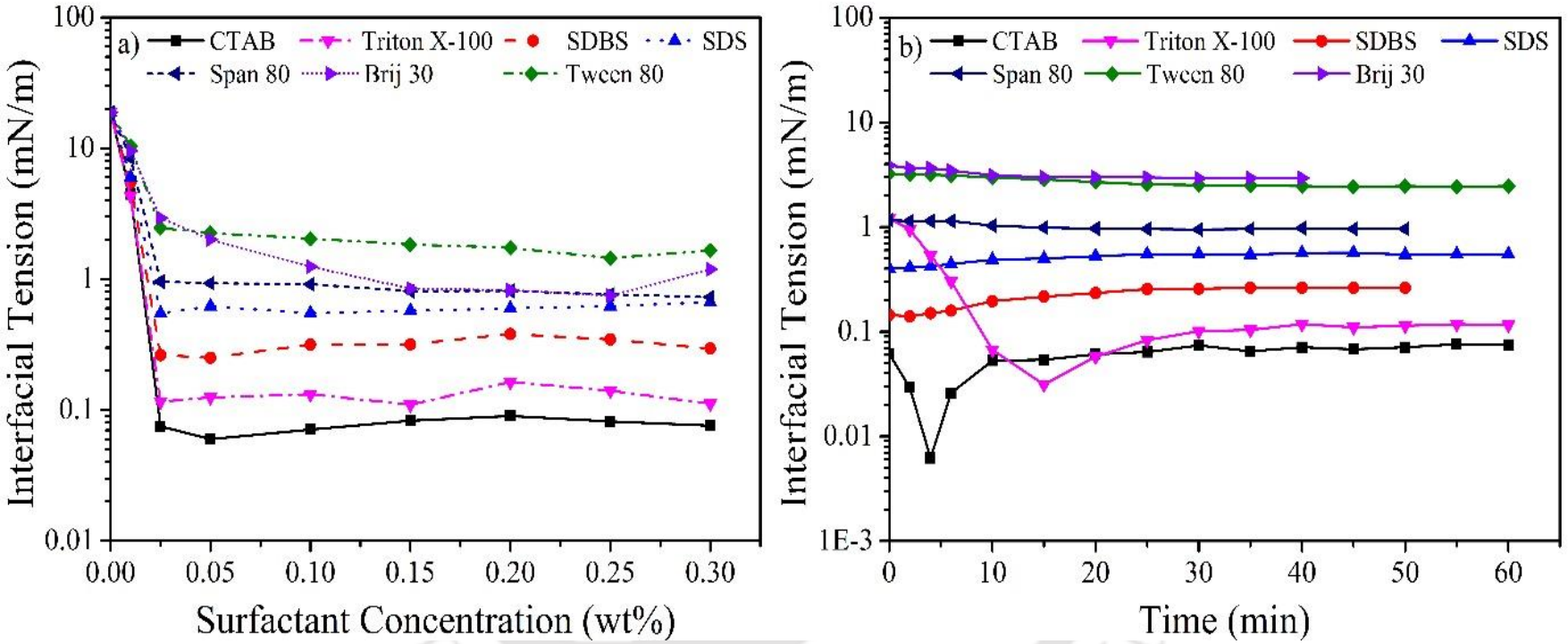

Fig. 6.3: Interfacial tension between crude oil and surfactants with a) concentration and b) dynamic interfacial tension for different surfactants at 0.025 wt%.

6.2.2 Emulsification Behaviour and Correlation with IFT Value

To determine the potential of the surfactants to form emulsion with crude oil, emulsion tests were carried out at higher concentration (0.3 wt%) of surfactants. For all eight surfactants, Fig. 6.4 illustrates the obtained phase behaviour during emulsification process. As can be seen, strong and dark emulsion (similar to that of oil) was formed in the top section of the tubes and light emulsion (being light in colour) changes at the bottom section of the tubes to thereby indicate colour variation of the aqueous phase. Fig. 6.4a, demonstrate that CTAB cationic surfactant was able to completely emulsify oil and water in the measuring tube and hence confirms 100% emulsification. The second best emulsification was achieved with Triton X-100 non-ionic surfactant, while other non-ionic surfactants indicated very low or negligible emulsification. Overall, emulsification extent for various surfactants is in the following order: CTAB> TX-100> SDBS> SDS> Span 80> Brij 30> Titriplex III> Tween 80. Except for CTAB case, the emulsions formed with surfactants disappeared within few minutes. Emulsions formed with CTAB was stable even after 30 days (Fig. 6.4b). The emulsion stability period achieved with different surfactants depends on the electrostatic repulsion and steric hindrance at the oil-water interface which controls the coalescence rate of oil droplets [19].

A plot of IFT values and emulsification extent for various surfactants confirmed a linear relationship with an R^2 value of 0.96 (Fig. 6.4c and Table 6.1). Two anionic surfactants, Titriplex III and Tween 80 were not considered in the figure. Titriplex III did not form droplet thus IFT cannot be measured whereas Tween 80 showed no sign of emulsions. The dark colour of the tube containing Titriplex III solution (Fig. 6.4a) indicated sticky nature of oil in the outer periphery of the tube and deeper visualization confirmed no emulsification. Overall, it was inferred that CTAB has greater potential for IFT reduction and complete

emulsification of oil-water system with better stability. This could be due to strong steric hindrance phenomena that occurs with enhanced surfactant concentration [150].

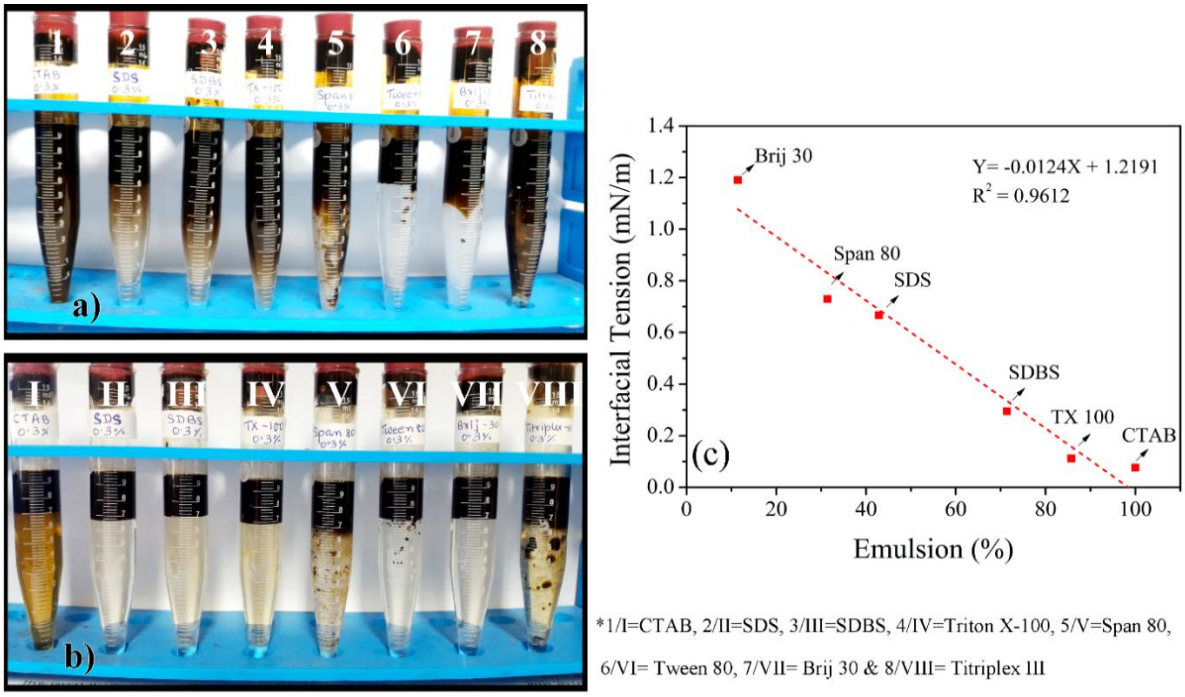

Fig. 6.4: Emulsification of crude oil - water system using different surfactants at concentration of 0.3 wt% a) after instant shaking and b) after settling for 30 days and c) a linear relationship observed between IFT and emulsion for different surfactants (at 0.3 wt% concentration).

Table 6.1: Results of the emulsion test for different surfactants at 0.3 wt% concentration.

Surfactants	Types	Emulsion volume			Emulsion (%)	IFT (mN/m)	Minimum IFT (mN/m)
		Strong (ml)	Light (ml)	Total (ml)			
CTAB	Cationic	7	0	7	100	7.6×10^{-2}	6.0×10^{-2}
SDBS	Anionic	3.5	1.5	5	71.42	2.9×10^{-1}	2.5×10^{-1}
SDS	Anionic	1	2	3	42.85	6.6×10^{-1}	5.5×10^{-1}
TX-100	Non-Ionic	5	1	6	85.71	1.1×10^{-1}	1.1×10^{-1}
Span 80	Non-Ionic	1.2	1	2.2	31.42	7.2×10^{-1}	7.2×10^{-1}
Brij 30	Non-Ionic	0.4	0.4	0.8	11.4	1.2	7.4×10^{-1}
Tween 80	Non-Ionic	0	0	0	0	1.6	1.4
Titriplex III	Non-Ionic	0.5	0	0.5	7.14	No drop	No drop

6.2.3 Surfactant Thermal Stability Analysis

Successful EOR application requires thermal stability of the chosen surfactants. TGA (Thermogravimetric Analysis) and FTIR (Fourier Transform Infrared Spectroscopy) analyses were carried out to evaluate stability of CTAB and TX-100 Fig. 6.5). TGA curves (Fig. 6.5a) revealed that CTAB and TX-100 are thermally stable up to 210^{o}C and 280^{o}C, respectively. To evaluate the thermal stability of the surfactants at reservoir prevalent temperature, the samples were aged at 90^{o}C in an oven for 10 days. FTIR spectra of both aged and non-aged (original) samples (Fig. 6.5b) indicated no significant change in the functional groups due to aging. A comparison of IFT data obtained for aged and non-aged samples (Table 6.2) confirms no significant variation in the IFT values and hence indicates stability of the screened surfactants.

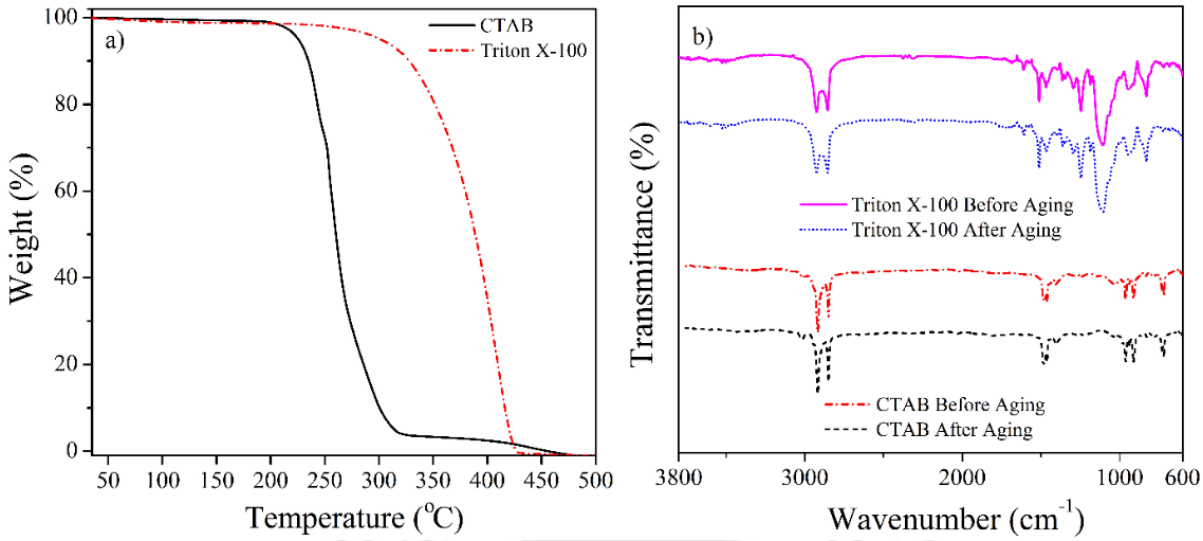

Fig. 6.5: Characterization of surfactants, CTAB and TX-100 a) TGA analysis and b) FTIR spectra.

Table 6.2: Stability of surfactant: Interfacial tension values for original and aged (aging at 90°C for 10 days) surfactants (CTAB and TX-100).

Surfactant concentration	Interfacial tension (mN/m)			
	CTAB original	CTAB aged	TX-100 original	TX-100 aged
0.01	4.45	6.02	4.32	4.87
0.025	7.5×10^{-2}	9.4×10^{-2}	1.16×10^{-1}	1.28×10^{-1}
0.05	6.1×10^{-2}	8.1×10^{-2}	1.25×10^{-1}	1.08×10^{-1}
0.1	7.1×10^{-2}	7.4×10^{-2}	1.32×10^{-1}	1.84×10^{-1}
0.15	8.3×10^{-2}	9.2×10^{-2}	1.1×10^{-1}	2.12×10^{-1}
0.2	9.1×10^{-2}	8.7×10^{-2}	1.64×10^{-1}	2.04×10^{-1}
0.25	8.2×10^{-2}	8.4×10^{-2}	1.41×10^{-1}	2.14×10^{-1}
0.3	7.6×10^{-2}	8.1×10^{-2}	1.12×10^{-1}	2.32×10^{-1}

6.3 Identification of Optimal Surfactant Mixture

6.3.1 Dynamic IFT of Surfactant Mixture

CTAB (cationic) and TX-100 (non-ionic) were mixed to prepare chemical slug and the IFT behaviour of surfactant mixture was evaluated (Fig. 6.6). As observed that 0.025 wt% surfactant concentration is enough for IFT reduction (Fig. 6.3), concentration of 0.01 - 0.05 wt% was extrapolated for the surfactants to determine the lowest IFT. Lower transient IFT values (~10^{-3} mN/m) were obtained for 0.06 wt% surfactant mixture (0.05% CTAB + 0.01% TX-100) and 0.1wt% (0.05% + 0.05% TX-100) concentrations. Among these, since minimal transient IFT value was achieved in 3 min, 0.1 wt% mixture was chosen as the optimal composition. The time bias for optimal mixture composition identification is due to the fact that injected surfactant system has limited time for interaction with porous media and hence early reduction in dynamic IFT facilitates mobilization of residual oil prior to surfactant losing its effectiveness with dilution or adsorption [19]. CTAB (cationic) and TX-100 (non-ionic) mixture yielded a lower equilibrium IFT of 3.7 x 10^{-2} mN/m, which is due to the synergistic bond interaction of TX-100 and CTAB (cationic-non-ionic) molecules at the oil-water interface [12].

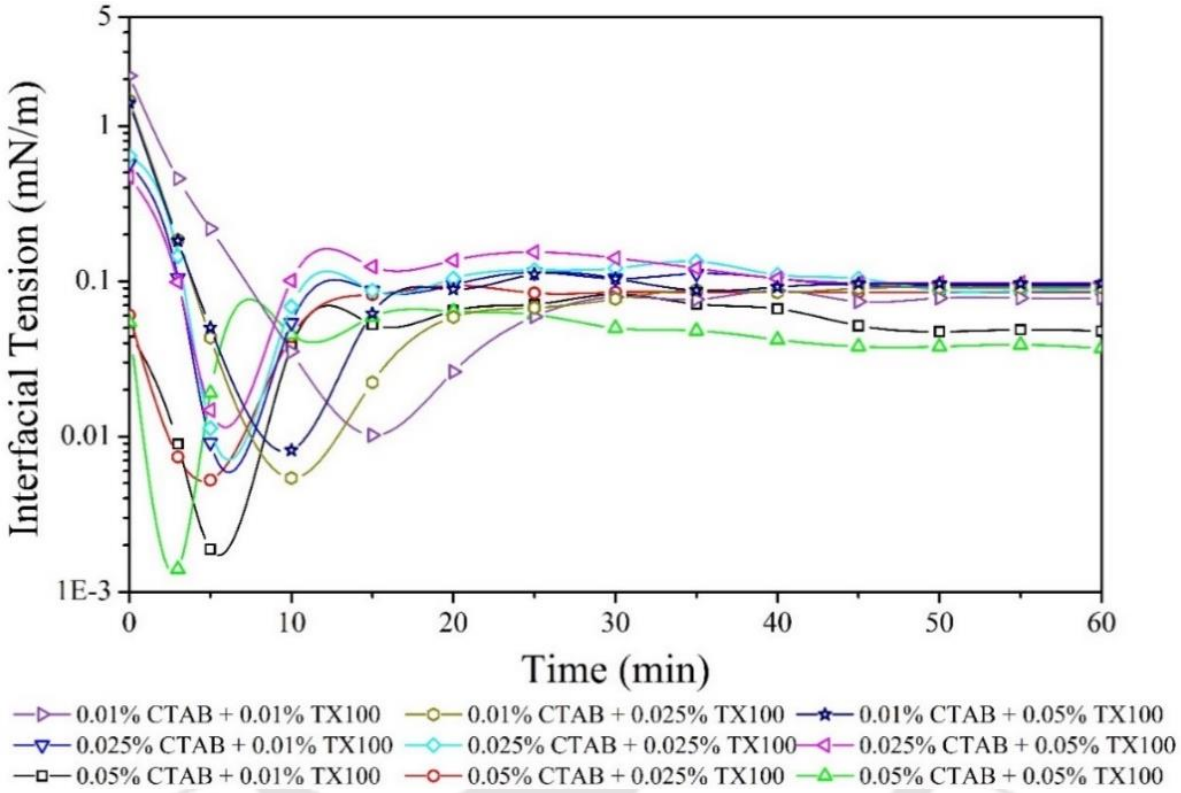

Fig. 6.6: Dynamic interfacial tension behaviour of surfactants mixture at various concentration combinations (all samples were prepared on wt% basis).

6.3.2 Effect of Temperature on Optimum Surfactant Mixture Formulation

The IFT variation with temperature and salinity for optimum surfactant mixture (S_M) of 0.1 wt% is shown in Fig. 6.7. The obtained trends were found similar to that for alkali-crude oil system (Fig. 6.2). A minimal IFT of 3.7 x 10^{-2} mN/m was achieved at 30°C, which increased to 2.14 x10^{-1} mN/m at 80°C. At lower temperature, surfactant molecules diffuse either in oil or water phase and form a stabilized film at the interface to reduce the IFT. However, at higher temperature, destabilization of the interface film facilitates higher IFT values [148, 149]. Also, adsorption is an exothermic process and higher system temperature hinders diffusion of surfactant molecules at the interface to destabilize the film and enhance IFT values.

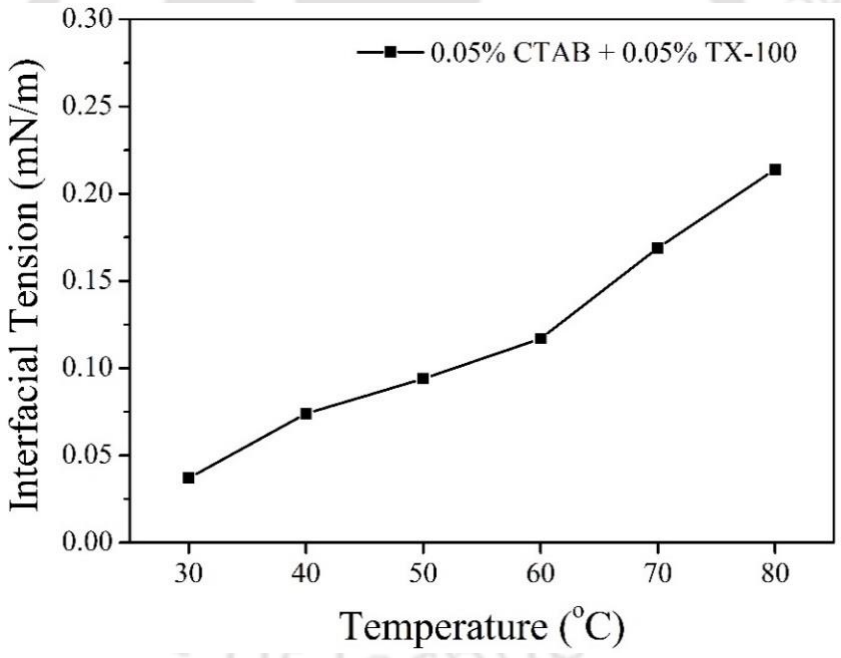

Fig. 6.7: Effect of temperature on interfacial tension at optimum surfactant mixture (S_M) concentration (0.1 wt%).

6.3.3 Effect of Salinity on Optimum Surfactant Mixture (S_M) System

The effect of salinity (0 - 20 wt%) on dynamic IFT behaviour and emulsification for optimum surfactant mixture (S_M) was investigated (Fig. 6.8). The dynamic IFT curves (Fig. 6.8a) illustrate minimum transient IFT (~10^{-2} mN/m) at lower salinity (0 - 10 wt%). However, the lowest IFT of 3.2 x 10^{-3} mN/m was obtained at 20 wt% salinity. The minimum value of transient dynamic IFT is mainly controlled by the adsorption and desorption of in-situ surfactants at the interface [15]. Due to the enhanced adsorption of in-situ surfactant at the interface, IFT reduces for higher salinity systems [56, 146, 147]. The in-situ surfactant further participates in the dissolution activity at the oil-water interface and facilitates better bond interactions at the interface to minimize IFT [151]. An interesting observation in the current investigation is with respect to the effect of oil drop layer break time on emulsification during dynamic IFT investigation. During IFT measurements, it was observed that the injected oil drop elongates with time and after certain duration (at oil layer break time) it breaks to two drops with each drop maintaining L/D ratio ≥ 4. The emulsion formed was found to be maximum for the case of no salinity condition [152] and the break time observed was in between 8-9 min (Fig. 6.8b). The oil layer break time increased with increasing salinity concentration. For 5 wt% and 10 wt% salinity, the break times were recorded as 18-19 min and 29-30 min respectively. At higher salinity (15 wt% and 20 wt%), the oil layer did not break at all and the emulsion so formed reduced greatly. The solubility ratio of oil and water varies widely with salinity and is responsible for the variations in the emulsion formation and oil break time [153]. At low salinity, due to more number of surfactant molecules at the oil-water interface, oil drop/layer break early and form better emulsion (cationic interface charge). With increasing salintiy, the formation of in-situ surfactant (Na^+ ions) replaces large amount of surfactant molecules at the interface and

reduces emulsification extent. The structural arrangement of CTAB surfactant molecules, balances associated to hydrophilic and lipophilic group and their interactions with the crude may also control the emulsion mechanism [154]. Hence from the emulsification behaviour, optimum salinity was evaluated to be at no salinity (0 % NaCl) which correspond for formation water composition (4445 ppm).

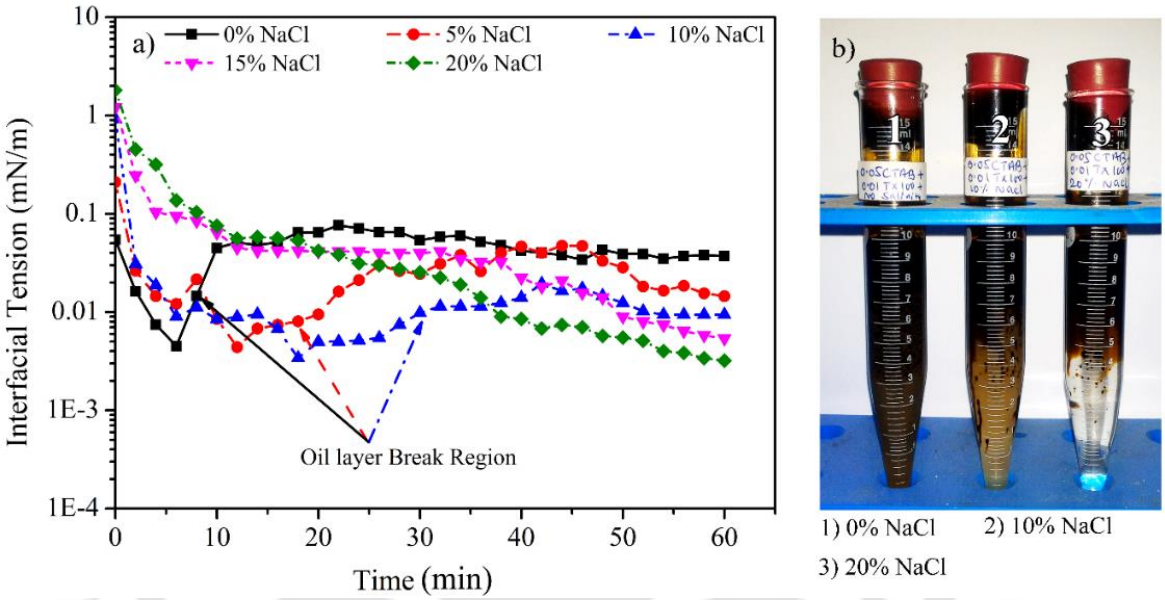

Fig. 6.8: Effect of salinity on (a) dynamic interfacial tension and (b) emulsification at optimum surfactant mixture (S_M) 0.1 wt%.

6.3.4 Adsorption of Optimum Surfactant Mixture on Carbonate Berea Rock

The adsorption of non-ionic surfactant (TX-100) at optimum concentration of 0.05wt% was found to be 0.35 mg/g. The lower adsorption of non-ionic surfactant in Berea core was due to ionic charge nature of the rock and steric hindrance facilitated by the adsorbed surfactant molecules at the surface interface [62, 155]. As cationic surfactant, CTAB cannot be detected by ultraviolet - visible spectrophotometer, its adsorption is expected to be less than TX-100 as both CTAB and Berea rock are positive charged and repulsion forces dominate at the surface interface. Even though considering similar adsorption of both

cationic and non-ionic surfactants on Berea core, the maximum amount of surfactant mixture that can be adsorbed has been estimated to be 0.7 mg/g. However, in real scenario, depending upon the charge nature of reservoir rock, the adsorption at optimum surfactant mixture (S_M) concentration (0.05% CTAB + 0.05% TX-100) is expected to vary from 0.35 to 0.7 mg/g.

6.4 Alkali-Surfactant Interfacial Tension Behaviour

The optimal concentrations of individual alkali and surfactant systems showed synergy for their mixture (AS_M - 0.6% NaOH + 0.05% CTAB + 0.05% TX-100). The optimal alkali-surfactant slug formulation exhibited an ultra-low IFT of 6.72 $x10^{-3}$ mN/m and its dynamic behaviour conveyed that the system requires 40 min to reach steady state (Fig. 6.9a). Emulsion images for optimal alkali, surfactant, surfactant mixture and alkali-surfactant mixture samples are depicted in Fig. 6.9b and Fig. 6.9c. For alkali system (at 0.6% NaOH), negligible emulsion activity can be seen. However for the alkali-surfactant mixture (AS_M) system, emulsification occurred but not as significant as that corresponding to individual surfactant (CTAB) and surfactant mixture (S_M) systems. These observations are in accord with emulsification trends observed for surfactant mixture with salinity (Section 6.3.3). The emulsification reduced due to the replacement of surfactant molecules with in-situ surfactants that get formed by ionization of acidic constituents of the crude oil at the interface. Thereby, in-situ surfactants disturb the solubility ratio of surfactants and contribute towards poorer emulsification. Despite obtaining synergy with alkali-surfactants mixture (AS_M), the oil layer break time (during dynamic IFT measurement) could not be observed. This indicates significant reduction in the surfactant system potential to enable emulsion formation.

The emulsions formed with different chemical combinations were assessed towards their stability (Fig. 6.9b and 9c). Upon enhancing CTAB concentration from 0.05 to 0.2%, more stable and strong emulsions could be observed after 24 h. The emulsion formed with AS_M formulation was found to be stable for 180 min. To validate the efficacy of emulsification and obtain a better sweep efficiency for higher oil recovery, core flooding experiments were conducted (Section 6.6).

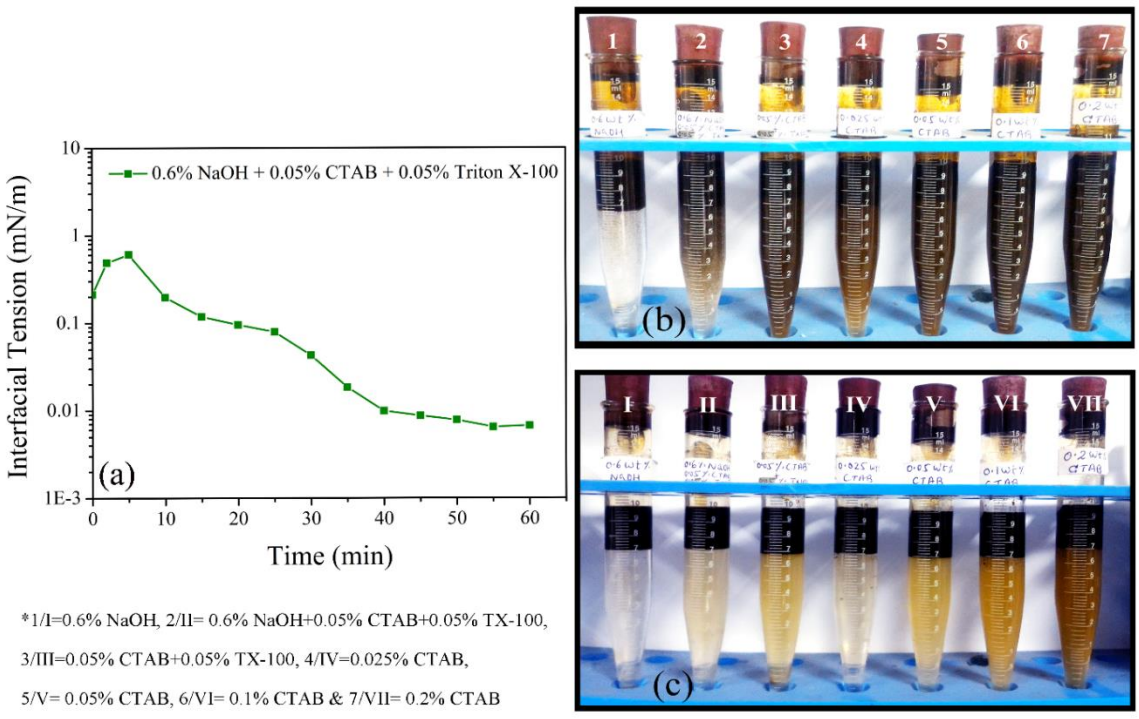

Fig. 6.9: Dynamic interfacial tension and emulsification behaviour of crude oil-aqueous system a) dynamic IFT at optimum alkali-surfactant mixture (AS_M) concentration, b) extent of emulsification achieved with alkali, surfactant, surfactant mixture and alkali-surfactant mixture after instant shaking (t = 0) and (c) after settling for 24 hrs.

6.5 Effect of Chemical Solution on Wettability Alteration

Favourable wettability alteration in reservoirs increases oil production by introducing a huge interface movement of the trapped residual oil [5, 156-158]. To visualize the effect of wettability alteration, contact angle measurements were conducted with optimum chemical combinations such as 0.6 wt% NaOH (A), 0.05 wt% CTAB (S), 0.05 wt% CTAB + 0.05 wt% TX-100 (S_M) and 0.6 wt% NaOH + 0.05 wt% CTAB + 0.05 wt% TX-100 (AS_M). The variation in the initial contact angle (time t = 0) for different chemical combinations is depicted in Fig. 6.10a. Time dependent variation of the contact angle is illustrated in Fig. 6.10b. The initial contact angle with formation water (FW) was found as 79.6^o which reduced to 51.3^o in 600 sec and then remained constant which specify that the saturated rock surface was intermediate wet [5]. For alkali, surfactant, surfactant mixture and alkali-surfactant mixture combinations, initial contact angle values were found to be 46.6^o, 28.6 ^{o}, 31.9^o and 47.5^o respectively. The contact angle decreased with time for all chemical solutions and for alkali-surfactant mixture the reduction was more drastic. This signify that all chemical solution at their optimum concentration were effective in changing the wettability of the system from intermediate wet to water-wet. Alkali reacts with the acid group of the crude to ionize the acid component which develops the hydrophilicity and enhances its capacity through partitioning in the water phase. Also, additional Na^+ ions prevalent in the formation water react with the acid group and alter wettability through ion-binding mechanism [159]. For the surfactant system, the reduction in contact angle was due to electrostatic forces that allow cationic monomers to interact with the negative carboxylic groups of crude oil and form ion pairs. These ion pairs dissolve in the oil phase and to some extent into the micelles to thereby assist water penetration into the rock surface pores changing the wettability of the system [49].

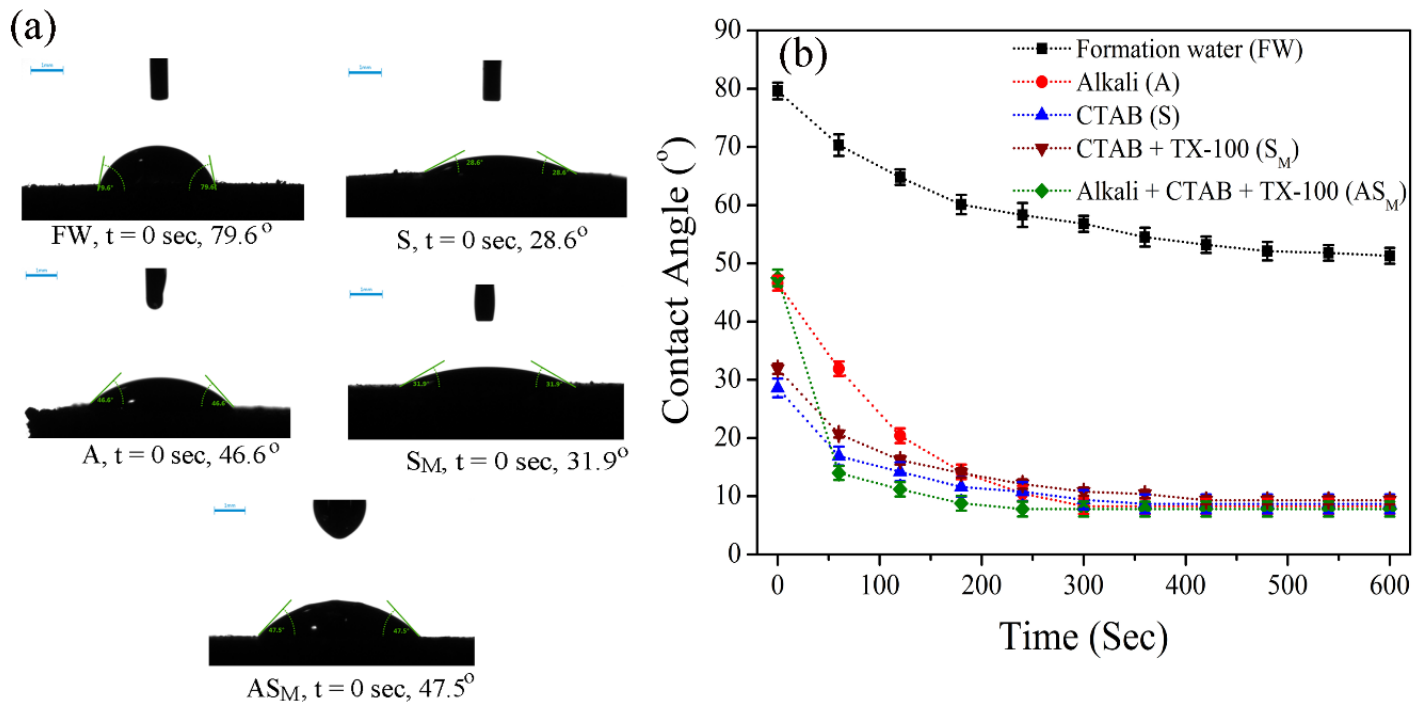

*FW = Formation water, t = time, A = 0.6% NaOH alkali, S = 0.05% CTAB surfactant, S_M = 0.05% CTAB + 0.05% TX-100 surfactant mixture, AS_M = 0.6% NaOH + 0.05% CTAB + 0.05% TX-100 alkali-surfactant mixture

Fig. 6.10: The change in the contact angle of oil saturated Berea carbonate rock surface with different chemical solutions a) initial contact angle at time zero and b) change in contact angle with time.

6.6 Core Flooding to Estimate Residual Oil Recovery

Laboratory scale core flooding experiments were conducted by injection of various chemical combinations such as alkali (A), surfactant (S), surfactant mixture (S_M) and alkali-surfactant mixture (AS_M) at their optimum concentrations. The obtained cumulative residual oil recovery are presented in Fig. 6.11 and Table 6.3. Alkali flooding produced additional oil recovery of 12.79% IOIP due to the combined effects of wettability alteration and IFT reduction (in the range of 10^{-1} mN/m). Due to negligible emulsification mechanism, recovery could not be enhanced. The chosen surfactant at optimum concentration (0.05 wt% CTAB) provided an oil recovery of 22.58% IOIP which further improved to 24.58% IOIP by using optimum surfactant mixture (0.05 wt% CTAB + 0.05 wt% TX-100). Optimum surfactant mixture exhibited 2% more oil recovery due to the fastest reduction in dynamic IFT value (3 minutes) (section 6.3.1 (Fig. 6.6)). Similar behaviour was observed by Yuan et al. [19] while performing surfactant core flooding experiments. Recovery factor was improved for surfactant case due to additional effects of emulsion formation. Emulsion facilitates diversion of water by preferentially blocking the path of the water seepage reducing viscous fingering and increases sweep efficiency. However, increasing surfactant (CTAB) concentration beyond 0.1 wt% reduced oil recovery. This is due to the formation of strong and stable emulsions (which increase number of dispersions of emulsion droplets rapidly) at the oil-water interface that strengthen interface film and hence reduced sweep efficiency [160].

The experimental schemes considered for AS_M flooding and the obtained oil recovery trends are depicted in Fig. 6.11b. Using optimum AS_M chemical slug, 14.46% additional oil recovery was obtained. This value is in between the values obtained for alkali and, surfactant flooding schemes. Alkali with surfactant mixture (AS_M) reduces emulsion capacity of the

system (Section 6.4) and thus lower oil recovery was obtained. To verify the effect of emulsion mechanism on oil recovery, a dual injection scheme was considered with additional 0.5 PV of optimum surfactant mixture (S_M) after 0.5 PV AS_M flooding. For the case, an enhancement in additional oil recovery from 14.46 to 18.65% IOIP affirmed dominant emulsification mechanism due to additional surfactant.

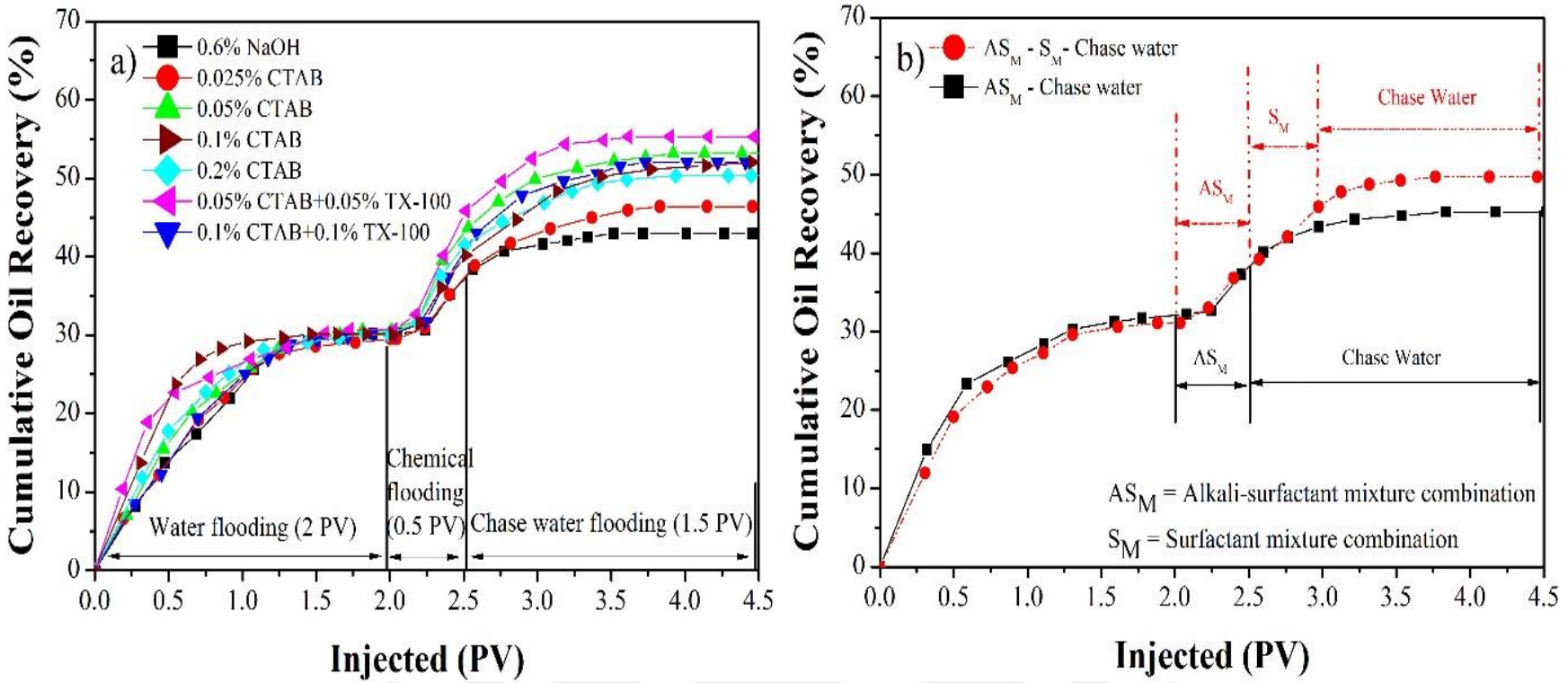

Fig. 6.11: Cumulative residual oil recovery obtained by a) injection of various chemical compositions and combinations and b) alkali-surfactant mixture (AS_M) and dual injection scheme, alkali-surfactant mixture followed by surfactant mixture (AS_M - S_M).

As strong emulsion played a major role in lowering the oil recovery factor due to poor sweep efficiency, a slug of 5000 ppm xanthan gum polymer was mixed in the optimum alkali-surfactant mixture formulation (AS_M - 0.6 % NaOH (A) + 0.05% CTAB + 0.05% TX-100 S_M). Xanthan gum has the efficacy to form emulsion and improve rheology properties whose detail investigation is reported in next chapter (chapter 7). The main objective to introduce polymer is to improve the sweep efficiency for higher residual oil recovery and achieve a comparison with different chemical EOR formulation. Fig. 6.12 depicts the percentage of cumulative oil recovered for alkali, surfactant mixture, alkali-surfactant mixture and alkali-surfactant mixture-polymer combinations. The cumulative oil recovery was lowest for alkali (42.95%) followed by alkali-surfactant mixture (45.24%) and surfactant mixture (55.30%). However, the oil recovery was enhanced and maximum recovery of 55.77% was obtained with AS_M + 5000 ppm xanthan gum (Table 6.3). This showed that a combination of alkali-surfactant mixture-polymer (AS_MP) could result in highest oil recovery for the current crude oil system. However, since this study was focused for only alkali and alkali-surfactant combination to achieve higher oil recovery at lower cost, the application of polymer was neglected. The effect of different types of polymer, their concentration and cost analysis can be performed in future studies.

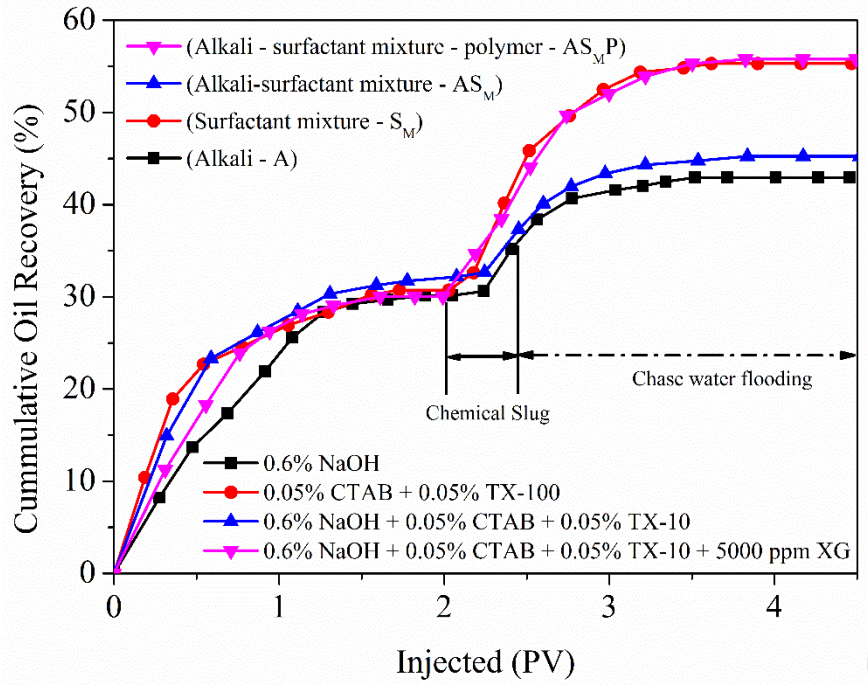

Fig. 6.12: Comparison of different chemical EOR schemes in terms of cumulative oil recovery.

Table 6.4 presents a comparative summary of residual oil recovered obtained for various crude oils in carbonate reservoirs. Maximum oil recovery of 56.51% was achieved by Ge and Wang [161] using heavy crude oil from Tahe, China oil field. However, the study did not reported the role of emulsification and its variation with salinity which can determine the sweep efficiency factor for higher oil recovery. Similarly, Lu et al.[162] attempted to validate their results through simulation with UTCHEM simulator and concluded upon possible mechanisms for oil recovery. Nevertheless, in such studies, the role of emulsification and its interaction was not considered. Ghosh and Obassi [163] data revealed lowest oil recovery of 15% for middle east crude oil and such studies were conducted for high salinity and temperature conditions. Despite conveying the potential of chemical EOR for high temperature reservoirs, the authors neglected behaviour of interfacial tension (IFT) and its correlation with the acid value of crude oil. Saha et al.[164] performed such investigations

to correlate the effect of acid content on IFT reduction and residual oil recovery. Research conducted by Al-Amodi et al. [2] was successful in recovering 42% of oil but no explanation was provided with respect to the effect of IFT and wettability alteration mechanism. On the other hand, Mahmoud and Abdelgawad [165] deeply neglected the effect of emulsification on oil recovery factor. The tertiary oil recovery achieved in the present work (24.58%) exists in between the recovery values reported by Al-Amodi et al. [2] and Mahmoud and Abdelgawad [165]. Also, the effect of various parameters and mechanisms responsible for higher oil recovery were explored in detail to minimize literature gaps.

Table 6.3: The details of the core flooding experiments performed: Residual oil recovery obtained from carbonate Berea cores (at 30°C) using various chemical combinations and compositions.

Porosity (%)	Brine permeability (mD)	Initial oil saturation (%)	Chemical formulation (wt%)	Water flooding recovery (%)	Chemical recovery (IOIP %)	Total oil recovery (%)	Residual oil recovery (ROIP %)
20.8	90.3	80.1	0.6% NaOH (A)	30.16	12.79	42.95	18.31
20.3	92.9	79.9	0.025% CTAB (S)	29.52	16.87	46.39	23.94
19.6	71.9	82.5	0.05% CTAB	30.57	22.58	53.15	32.52
20.9	74.1	79.9	0.1% CTAB	30.13	21.91	52.04	31.36
19.4	66.7	79.4	0.2% CTAB	30.11	20.24	50.35	28.96
20.3	49.2	79.1	0.05% CTAB + 0.05% TX-100 (S_M)	30.72	24.58	55.30	35.48
20.2	82.6	79.6	0.1% CTAB + 0.1% TX-100	30.26	21.75	52.01	31.87
20.3	84.3	80.3	0.6% NaOH + 0.05% CTAB + 0.05% TX-100 (AS_M)	30.78	14.46	45.24	20.89
19.9*	68.4	80.1	0.6% NaOH + 0.05% CTAB + 0.05% TX-100 (AS_M); 0.05% CTAB + 0.05% TX-100 (S_M)	31.07	18.65	49.72	27.06
20.1	77.0	80.8	0.6% NaOH + 0.05% CTAB + 0.05% TX-100 + 5000 ppm XG (AS_MP)	29.99	25.78	55.77	36.82

* Dual slug injected - First chemical slug of 0.5 PV followed by second chemical slug of 0.5 PV and then 1 PV chase water flooding.

Table 6.4: Literature comparison of oil recovery in carbonate reservoirs.

Author	Oil Field	Crude category	Density (kg/m^3)	μ (mPa. s)	Acid value (mg KOH/gm sample)	Chemical composition	IFT reduction (mN/m)	Wettability alteration	Emuls-ification	Oil recovery experiment	Rock nature	Tertiary oil recovery (%)
Ge and Wang [161]	Tahe (China)	Heavy	923.55	420	0.43	AEC-6 + NPC-7	10^{-1}	No	-	Imbibition	Tahe Core	56.51
Lu et al. [162]	Surrogate oil	Heavy	920	2.1	0.15	Carboxylate surfactant	10^{-3}	Negligible	-	Imbibition	-	33.3
Ghosh and Obassi [163]	Middle Eastern oil field	Light	-	2.4	-	Alkyl polyglycos-ides	-	Yes	Yes	Core Flooding	Middle Eastern oil field core	15
Mahmoud and Abdelga-wad [165]	-	Medium	870	13.1	-	EDTA	Yes	Yes	-	Core Flooding	Indiana limestone core (Berea)	20.16
Al-Amodi et al. [2]	Arabian crude (Saudi Arabia)	Light	875.7	13.1	-	Capstone FS-50 + HPAM	10^{-3}	-	-	Core Flooding	Indiana limestone core (Berea)	42
Current work	Assam (India)	Heavy	926.6	20.1	2.72	CTAB + TX-100	10^{-2}	Yes	Yes	Core flooding	Silurian dolomite (Berea)	24.58

AEC - Ethoxylated fatty alcohol carboxylate; NPC - Phenol ether carboxylate; EDTA - Ethylenediaminetetraacetic acid; HPAM- Partially hydrolyzed polyacrylamide, CTAB - Cetyltrimethylammonium bromide, Tx-100 - Triton X -100.

6.7 Conclusions

The role of all major mechanisms (equilibrium IFT reduction, dynamic IFT reduction with break time phenomena, extent of emulsification and wettability alteration) in influencing flooding characteristics of heavy crude oil-carbonate rock-formation water system were investigated. The identified optimal chemical slug formulations refer to 0.6% NaOH (A), 0.05% CTAB (S), 0.05% CTAB + 0.05% TX-100 (S_M) and 0.6% NaOH + 0.05% CTAB + 0.05% TX-100 (AS_M). Alkali-surfactant synergy action resulted in ultra-low IFT of 10^{-3} mN/m (6.72×10^{-3} mN/m), but reduces the emulsification capacity and stability period. Highest oil recovery of 24.58% was observed for optimum surfactant mixture (S_M) of 0.1wt% (0.05% CTAB + 0.05% TX-100) due to the contribution of IFT reduction, emulsification, optimum stability, better sweep efficiency and wettability alteration mechanism. Oil recovery decreases with further increase in surfactant concentration due to the formation of strong emulsion which affects the sweep efficiency. Addition of 5000 ppm polymer (xanthan gum) to the alkali-surfactant mixture (AS_MP slug) resulted in additional 1.2% chemical tertiary oil recovery. In summary, residual recovery of heavy crude oil from carbonate rock-formation water systems has been evaluated to be dependent on IFT reduction, emulsification extent, emulsion stability, sweep efficiency and wettability alteration.

Chapter 7

Nanoparticle-Polymer Flooding in Sandstone Reservoir for Heavy Crude Oil

The potential of silica nanoparticles (SNPs) towards emulsification, rheological properties and wettability alteration characteristics in nanoparticles assisted polymer (Xanthan gum - XG) flooding were inspected in this chapter. The stability of nanoparticles in xanthan gum solution was evaluated by particle size analyser and zeta potential method. The rheological behaviour of the xanthan gum-SNPs system in addition to interfacial tension and emulsification mechanism at variant temperatures were also investigated. Wettability alteration studies involved change in the contact angle measurements for oil drops with respect to nanoparticles saturated rock surface. Finally, nanoparticles assisted polymer flooding were conducted using Berea Core (Idaho Gray) at different temperatures to estimate the residual oil recovery factor.

7.1 Stability Evaluation of SNPs by Particle Size and Zeta Potential Measurements

The stability of the XG-SNP solution and formation water−SNP systems were examined by visualizing the time-dependent transparency of sample in the vial. An XG concentration of 5000 ppm was selected based on the emulsification studies (Section 7.4) and SNPs of 0.3 wt % considering emulsification and IFT behaviour (Section 7.3). Fig. 7.1a and 7.1b depict images of samples samples prepared for XG−SNP aqueous system and formation water−SNP, respectively (kept for 1 and 10 days). Fig. 7.1a indicates the better stability of

XG−SNP systems due to the absence of sedimentation phenomena. Fig. 7.1b shows contrasting stability behaviour for formation water−SNP system, with rigorous sedimentation of 70% nanoparticles in first 24 h and settling of almost all nanoparticles after 10 days indicating a transparent and clear aqueous phase. Similar inferences were deduced for formation water−SNP systems prepared with 0.1 and 0.5 wt % SNPs. The results suggested that SNPs can be helpful in polymer flooding not in water flooding.

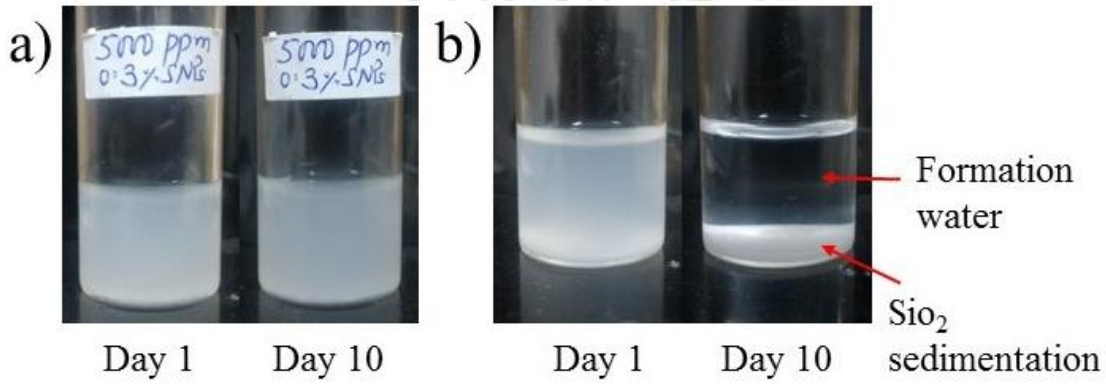

Fig. 7.1: Images of nanoparticles in aqueous phase at 30°C (a) 5000 ppm xanthan gum and 0.3 wt% SNPs and (b) reservoir formation water and 0.3 wt% SNPs.

To further validate the negligible effect of sedimentation phenomena of XG-SNPs solution system, particle size distribution and zeta potential were evaluated using dynamic light scattering (DLS). Fig. 7.2 presents the average nanoparticle cluster sizes with variation in the concentration of SNPs (0.1, 0.3 and 0.5 wt %). The nanoparticles underwent clustering due to agglomeration, because of which the cluster size increased to about 3.73 to 4.46 microns. Agglomeration rate and cluster size can be enhanced with an increase in the polymer solution concentration [55]. However, Fig. 7.2 suggests that the agglomeration has no impact on the system stability. After 10 days, the average particle size of the agglomerated nanoparticles marginally varied from 3.95 to 3.73 microns for 0.1 wt% SNPs and 4.64 to

4.03 microns for 0.5 wt% SNPs. The reduction in average particle size with time is due to the fact that large agglomerated nanoparticles in the solution settle at the bottom and smaller cluster agglomerated nanoparticles are retained in the supernatant system. Hence, a marginal reduction in the average particle size is indicative of a stable aqueous polymer-SNPs system [55]. Similar phenomena were reported by Sharma et al. [55] where the average nanoparticle cluster size increased from 3.54 to 4.54 microns with an enhancement in SiO_2 nanoparticle concentration from 0.5 to 2 wt% in 1000 ppm polyacrylamide concentration.

Table 7.1 summarizes the zeta potential values of the XG-SNPs solutions. For 5000 ppm XG solution with SNPs concentration of 0.1, 0.3 and 0.5 wt%, the zeta potential values were evaluated to be -21.87, -25.77 and -26.52 mV respectively with a standard deviation of < ±2%. Negligible variation in the values of zeta potential (~2 to 4 %) was observed after 10 days, and hence XG-SNPs solution system can be considered as partially stable as no rapid coagulation or flocculation was observed. The reason for not achieving a value of ± 30 mV (stable system) could be due to the effect of synthetic formation water/salinity/different ions composition in the formation water in addition to the pH of the system. Study carried out by Farooq et al. [166] clearly explained the characteristic role of divalent and monovalent ions in altering the zeta potential values at different pH.

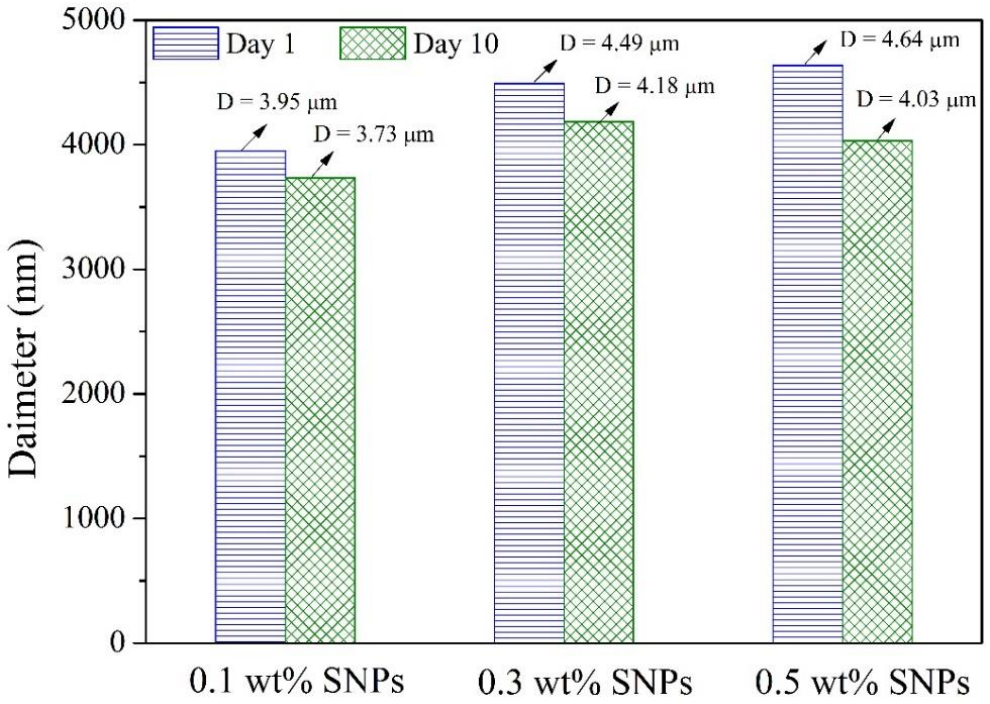

Fig. 7.2: Particle size distributions for XG-SNPs solution systems (0.1, 0.3 and 0.5 wt% SNPs in 5000 ppm XG) at 30°C.

Table 7.1: Zeta potential data for variant SNPs concentrations at 5000 ppm xanthan gum and 30°C.

Silica nanoparticles (wt%)	Zeta potential (mV) day 1	Zeta potential (mV) day 10
0.1	-21.87	-21.35
0.3	-25.77	-24.36
0.5	-26.52	-25.64

7.2 Rheological (Viscosity) Evaluation of Xanthan Gum-SNPs Systems

The variation in the viscosity values with shear rate for XG-SNPs system is depicted in Fig.7.3a (30°C) and 7.3b (80°C). Viscosity of the system varied from 2460-2970 mPa. s to almost 50 mPa. s when shear rate changed from 1 to 200 s^{-1}. The viscosity was found higher at low shear rate of 1 s^{-1} and reduced drastically to a smaller constant value at higher shear rate (~200 s^{-1}). Similar trend was also observed by Son et al. [167] using SiO_2 nanoparticles. Fig. 7.3c describes the variation in viscosity of the system with temperature for XG and XG-SNPs systems at shear rate of 1 s^{-1}. The initial viscosity observed with XG at 30°C was 2460 mPa. s (0 wt% SNPs) which enhanced to 2970 mPa. s when 0.5 wt% SNPs was introduced. Similar behaviour was observed at elevated temperature (80°C); viscosity increased from 593 mPa. s (0 wt% SNPs) to 771 mPa. s (0.5 wt% SNPs). The viscosity of the system with SNPs was improved even at higher temperature and reservoir formation water conditions which is probably due to the formation of complex three-dimensional macromolecular structures [168]. The viscosity enhancement with SNPs in the polymer solution is due to adsorption of polymer on the nano-silica particle surface that is driven by a hydrogen bonding based interaction. At higher temperature, the adsorption of polymer on silica surface reduces and thus weakens the hydrogen bonding between polymer and silica and deteriorates the three-dimensional network structure [168, 169].

To understand the viscoelastic behaviour of the nanofluid, storage modulus and loss modulus experiments were performed. Fig. 7.4 presents the storage modulus (G´) and loss modulus (G´´) behaviour of the samples. The obtained values revealed that at a lower initial frequency of 0.01 Hz, G´ is much higher than G´´ for all the concentrations of SNPs. As frequency increased from 0.01 to 0.1 Hz, the storage and loss modulus reduced drastically

and the difference between G´ and G´´ becomes constant. However, as frequency increased further, the rate of enhancement of storage modulus was fasters than that of the loss modulus and thereby confirms viscoelastic properties of the system [106]. No crossover point existed between G´ and G´ which indicates solution behaviour as a gel in a bulk phase [170, 171]. Similar observations and behaviour have been reported by Kennedy et al. [172]. The authors indicated viscosity enhancement with viscoelastic moduli. The storage and loss modulus trends infer that SNPs are favourable for EOR at higher temperatures.

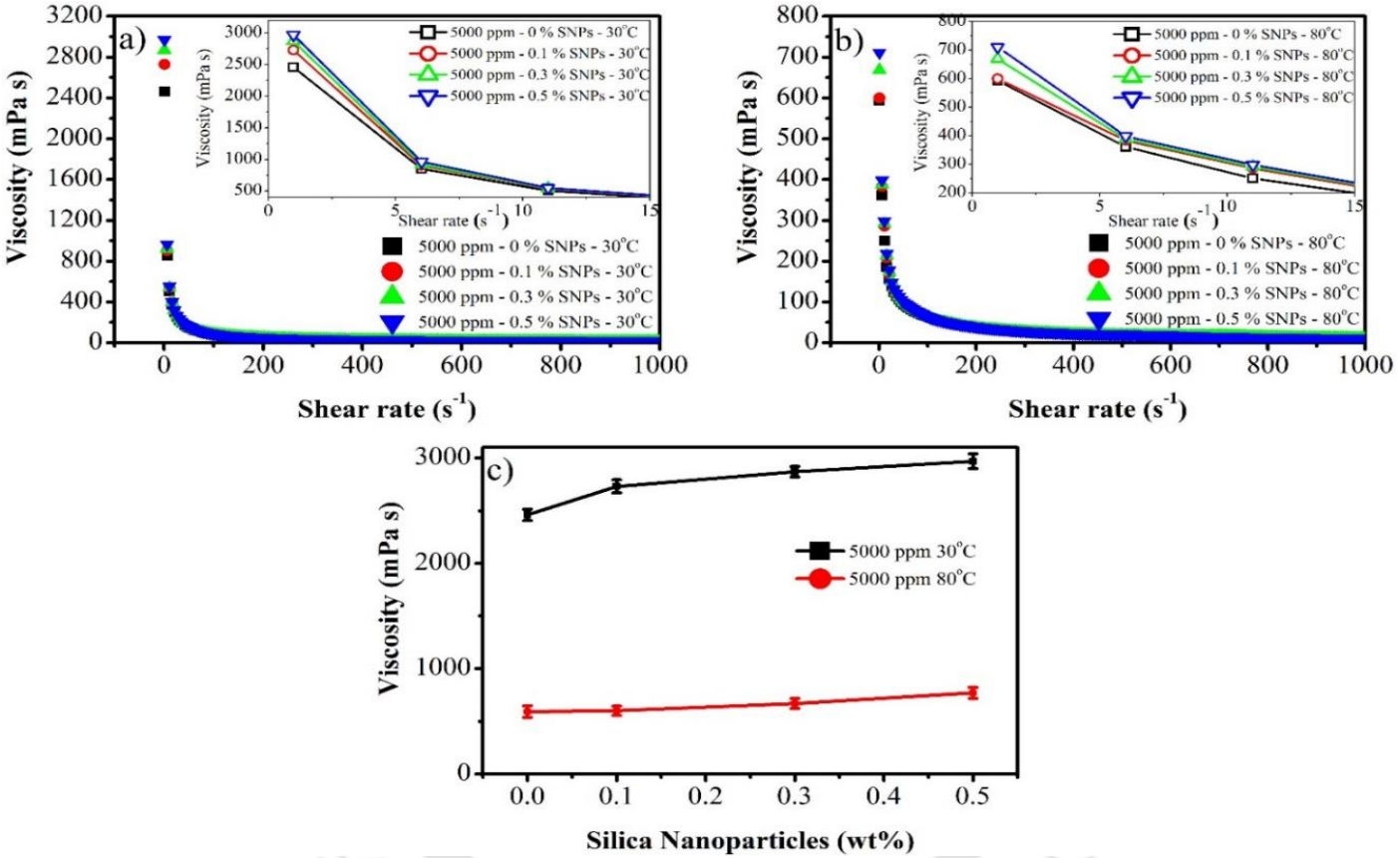

Fig. 7.3: Viscosity and rheological behavior of XG (5000 ppm) -SNPs system (a) at 30°C (b) 80°C and (c) at shear rate of $1s^{-1}$.

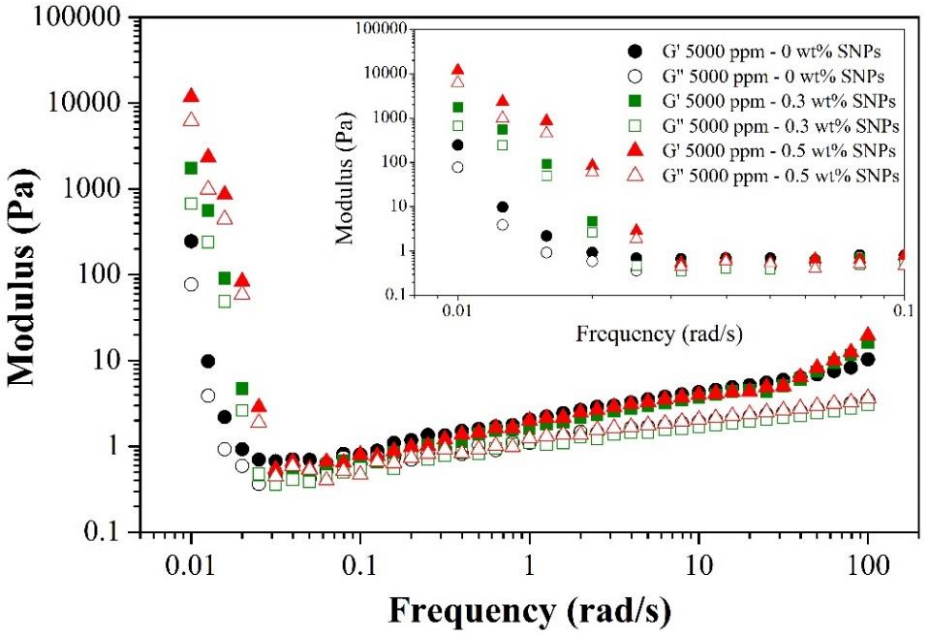

Fig. 7.4: Storage modulus (G´) and loss modulus (G´´) behaviour of the samples at different SNPs concentrations.

7.3 Effect of SNPs on Interfacial Tension of Crude Oil-Aqueous Polymer Systems

The interfacial tension between crude oil and XG (5000 ppm)-SNPs solutions were measured at lower (30 ± 2°C) and higher (70 ± 2°C) temperature (Fig. 7.5). In the absence of SNPs, the IFT value of crude oil-XG solution system was found to be 17.8 mN/m at 30°C. After incorporation of SNPs, the IFT value of the system reduced to 10.75, 8.67 and 8.54 mN/m as SNPs concentration increased to 0.1, 0.3 and 0.5 wt% respectively. Similar trends exist at higher temperature (70°C), where the IFT of the system reduced from 14.64 mN/m (without SNPs) to 8.54, 6.46 and 6.86 mN/m for 0.1, 0.3 and 0.5wt% of SNPs concentration respectively. Several factors such as large surface to volume ratio, higher adsorption, suspension stability and hydrophilic-hydrophobic interaction at the oil-water interface have contributed towards IFT reduction at higher SNPs concentrations [173, 174]. Also, the figure (Fig 7.5) confirms that IFT remains constant after 0.3 wt% of SNPs for both lower and higher

temperature cases. Hence, 0.3 wt% SNPs was regarded to be optimum for core flooding experiments. The inability to further lower IFT value with higher SNPs concentration (>0.3 wt%) could be due to the saturation of SNPs at oil-polymer solution interface at their optimal concentration [55, 174]. The reduction in IFT was better at an elevated temperature for Assam crude oil and this is in agreement with the trends presented in the literature [55]. The reduction in IFT value with implementation of nanoparticles causes easy flow of trapped residual oil, as the work required to deform the oil reduces which moves the oil droplet in the pore throat and improves oil recovery [130, 175].

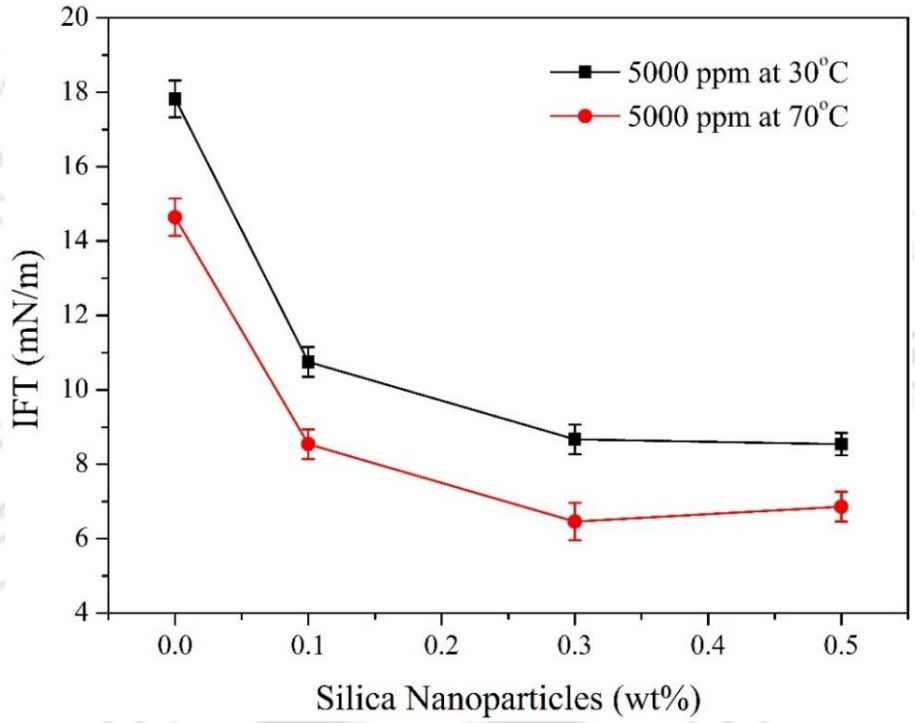

Fig. 7.5: Effect of SNPs concentration and temperature on the IFT of crude oil-polymer-SNPs solution system at 5000 ppm xanthan gum.

7.4 Effect of SNPs on Stability of Emulsions

Emulsification stability studies were conducted for crude oil – XG polymer system in the concentration range of 1000 – 5000 ppm. Fig.7.6 (a-d) shows that while emulsification existed for the entire concentration range, its stability varied. At a lower polymer concentration, due to poor coverage of polymer on the oil droplet, the oil droplets undergo extremely fast coalescence to form bigger droplets and thereby emulsion stability gets reduced [176, 177]. With increasing polymer concentration, emulsion stability enhances due to greater adsorption of polymer on the oil droplet, bridging between two oil droplets occurs and facilitates flocculation [178]. The emulsion formed at 1000 ppm XG disappeared very quickly (within 30 min). However, the emulsion stability for this case enhanced to 5-6 h due to the addition of SNPs (Fig. 7.6b). Similar trends were found at 3000 and 5000 ppm XG where emulsion stability enhanced to 18 and more than 25 days respectively (Fig. 7.6c and 7.6d). Therefore, as 5000 ppm XG showed higher emulsification and better stability period (Fig. 7.6a), the effect of SNPs (0.1-0.5 wt%) at 5000 ppm polymer concentration was evaluated. For more than 0.3 wt% SNPs concentration, the emulsion stability reached a stagnant point and could not be improved further (Fig.7.6d). SNPs get adsorbed at the oil-water interface and facilitate IFT reduction and contribute towards emulsion stability [106]. At 0.3 wt%, SNPs adsorption at the oil-water interface attained a saturation phase due to which the stability could not be increased significantly. Therefore considering the cost of polymer and SNPs and the emulsion stability of the polymer-SNPs solution, 5000 ppm XG and 0.3 wt% SNPs can be inferred to be the optimal values.

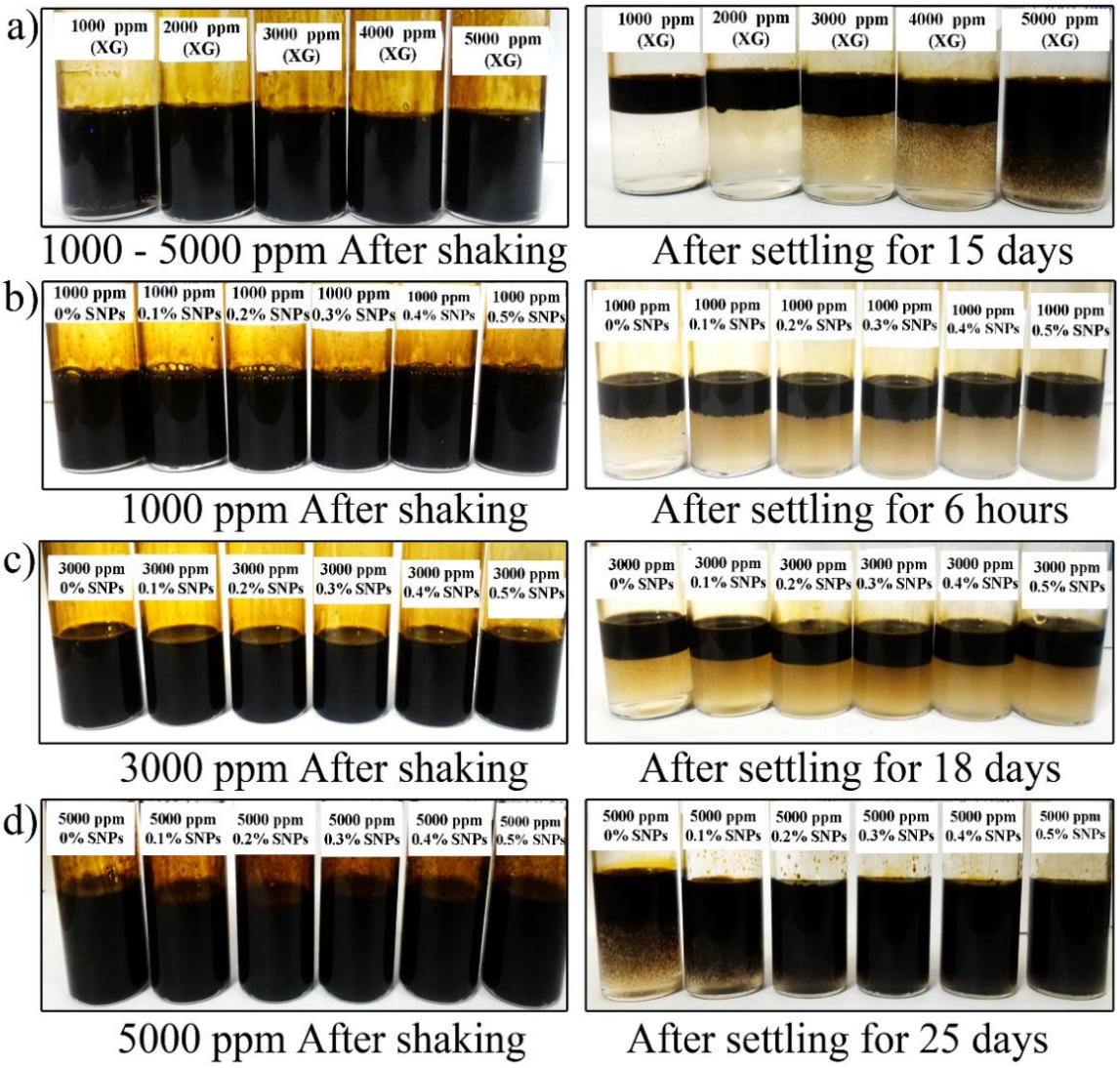

Fig. 7.6: Emulsification images of crude oil-xanthan gum-SNPs systems at 30°C (a) 1000 – 5000 ppm xanthan gum in the absence of SNPs (b) 1000 ppm xanthan gum and 0.1 – 0.5 wt% SNPs (c) 3000 ppm xanthan gum and 0.1 – 0.5 wt% SNPs (d) 5000 ppm xanthan gum and 0.1 – 0.5 wt% SNPs.

The emulsion quality can also be ensured by examining the microscopic images of the emulsions in terms of average size and droplet size distributions at various XG and SNPs concentrations. Fig. 7.7 demonstrates that with increase in concentration of SNPs, the oil droplet size distributions reduced. The droplet diameter varied from 0 to 22 µm (large droplets) in the absence of SNPs and reduced to 0 to 13 µm (small-moderate droplet) for 0.5 wt% SNPs concentration. The average diameter values of the droplets for 0, 0.1, 0.3 and 0.5 wt% SNPs solutions were found to be 7.52, 6.78, 5.97 and 5.12 µm respectively. Kumar et al. [106] also observed an average droplet size of 4.8 µm for carboxy methyl cellulose polymer (5000 ppm) with SiO_2 (0.3 wt%). The reduction in average droplet diameter or increase in the formation of small droplets prevents the aggregation of the droplets in which cohesive forces between droplets reduce due to the presence of silica nanoparticles [78, 106]. Binks and Whitby [179] also detected similar behaviour where the emulsion droplet decreased from 50 µm to ≤ 10 µm with increase in nanoparticle concentration. They reported that initially the phase breaks into drop fragments of similar extent irrespective of nanoparticles concentration. However, the retention of reduced droplet size depends upon the rate of coalesce of the oil droplets which is greatly controlled by the adsorption of nanoparticles on the drop surface. To observe the presence of SNPs on the oil-polymer-SNPs emulsion, a microscopic (Fig. 7.8a) and FESEM (Fig. 7.8b) analyses were performed at optimum concentrations. Microscopic image of the emulsion showed that SNPs adsorbed on the surface of the oil droplet. The detail structure of SNPs both in clusters and segregated state were found in FESEM analysis.

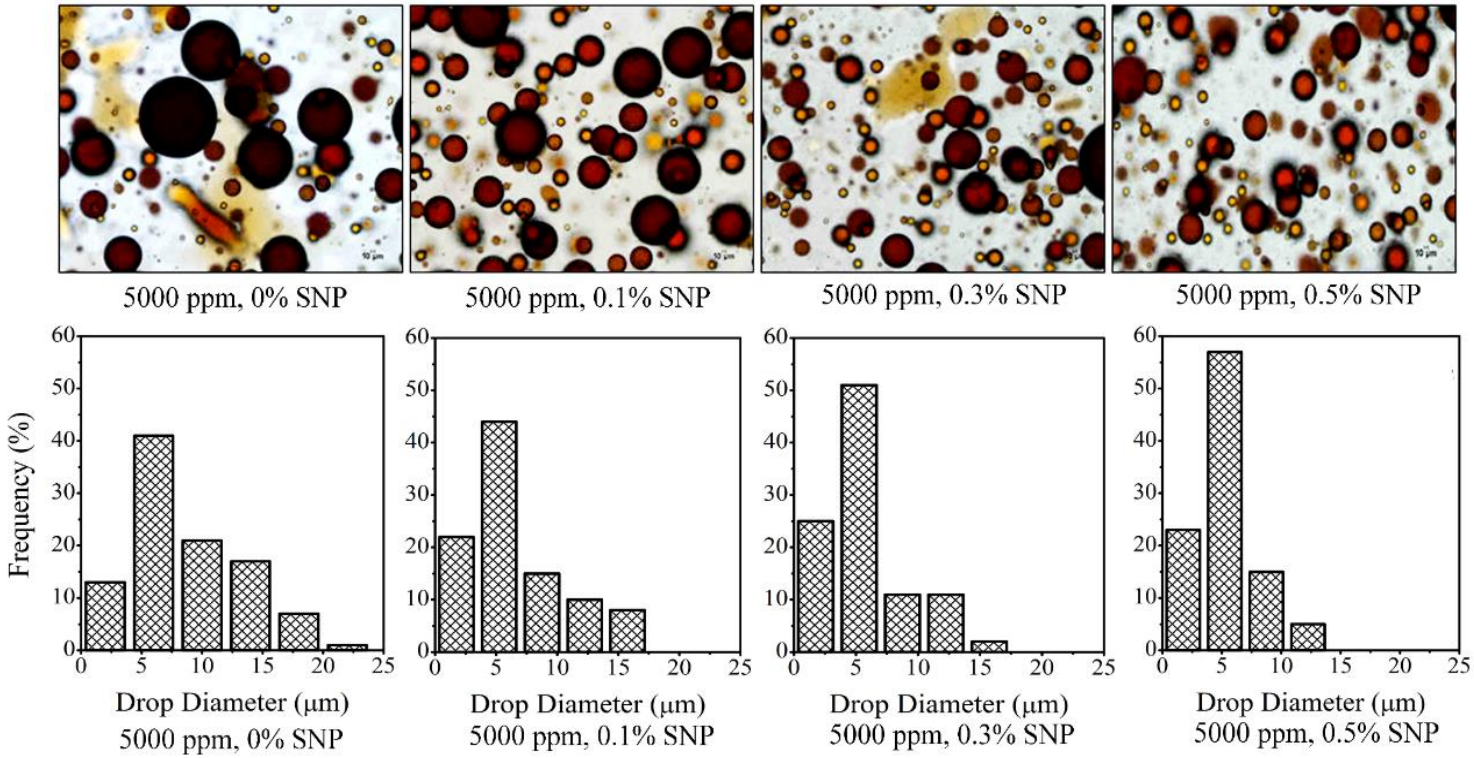

Fig. 7.7: Effect of SNPs concentration on emulsions quality and droplet size distributions at 30°C.

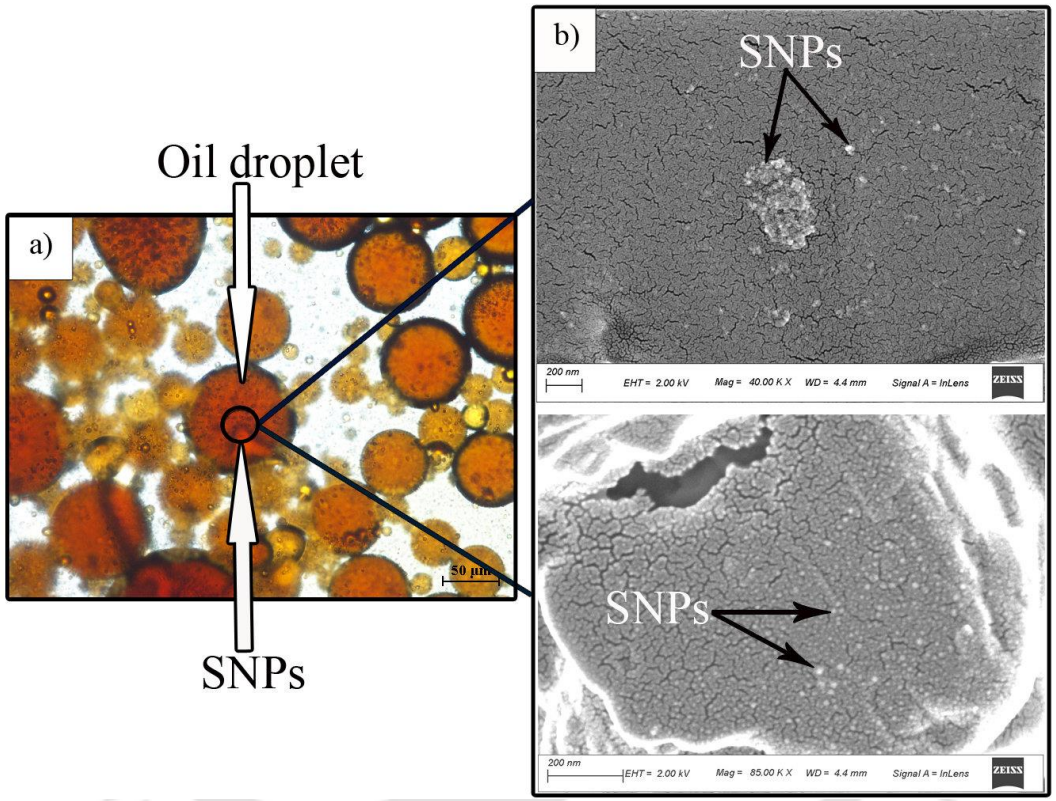

Fig. 7.8: Images of the oil-polymer-SNPs emulsion at optimum concentration (5000 ppm XG - 0.3% SNPs) denoting deposition of SNPs on the oil droplets a) Microscope analysis and b) FESEM analysis.

7.5 Effect of SNPs on Crude Oil - Xanthan Gum Emulsion (Creaming Index)

Creaming index (CI) analysis was carried out to have a better understanding of the emulsion stability process. CI values were calculated for 0.1 – 0.5 wt% SNPs concentrations (Fig. 7.9). The CI studies involved initial shaking of the crude oil - XG - SNPs system followed by undisturbed conditions for a said time period to evaluate creaming (separation) out of the aqueous and oil layers. Initially (day 0), the XG-SNPs solutions were found effective in emulsifying the crude oil. The rate of creaming was observed at 30°C (Fig. 7.9a) and 80°C (Fig. 7.9b). At lower temperature (30°C), the rate of creaming was found slow (day 1) with CI values as 88.6% and 92.9% for 0 wt% and 0.1 wt% SNPs respectively (Fig. 7.9a). After a duration of 10 days for the same samples, CI reduced to 78.6 for 0% SNPs and 85.7% for 0.1 wt% SNPs. However, no signs of creaming were observed at higher SNPs concentrations (0.3 and 0.5 wt%) at 30°C and duration of 10 days. At 80°C, the creaming rate increased enormously on day 1 with CI as 7.1% for 0% SNPs and 35.7% for 0.1 wt% SNPs (Fig. 7.9b). After 10 days, the CI of the sample reduced drastically to 0% and 14.2% for 0 and 0.1 wt% SNPs respectively. For 0.3 wt% SNPs sample (at 80°C), the CI reached to 57.1 % on day 1 and 14.2% on day 10. The CI values remained constant with further increasing SNPs concentration to 0.5 wt%. The data obtained suggest that emulsions formed are unstable at higher temperature and low SNPs concentration (≤ 0.1 wt%) due to high creaming rate. However, a higher amount of SNPs (0.3 - 0.5 wt%) at elevated temperature exhibited better performance with enhanced stability of the emulsion to some extent. The creaming rate decreases with increase in nanoparticle concentration which reduces the average droplet diameter of the emulsion. The stability of such emulsion depends on the

droplet stability which can be enhanced by continuous dense packing of the adsorbed nanoparticles at the oil-water interface [179].

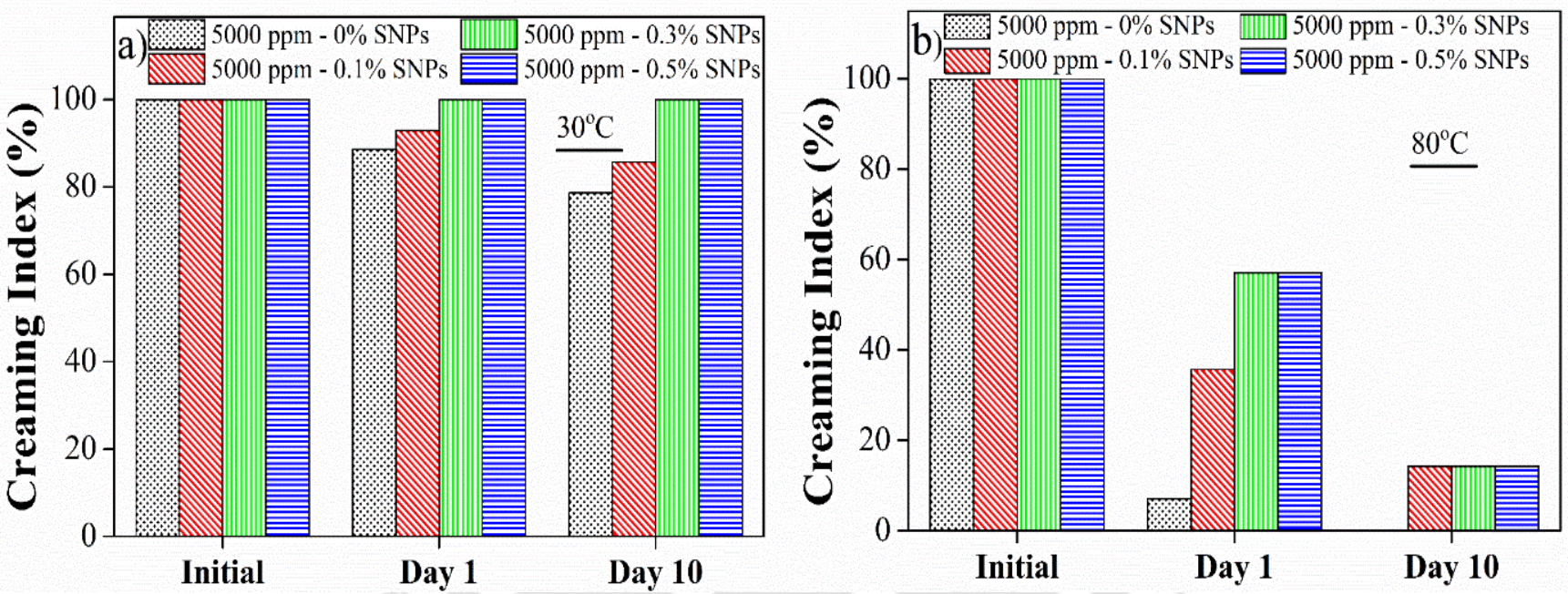

Fig. 7.9: Creaming index values of crude oil-xanthan gum-SNPs system at a) 30°C and b) 80°C.

7.6 Effect of Temperature on Emulsion Viscosity

Viscosity enhancement improves sweep efficiency or favourable mobility which facilitates injected aqueous phase to reach unswept regions of the reservoir rock to enhance capillary number and oil recovery [180, 181]. The viscosity is a function of temperature of the system and such parameter can severely affect the oil recovery. Hence the behaviour of viscosity at elevated temperature was observed (Table 7.2). The viscosity of polymer-oil emulsion improved with the addition of nanoparticles. The data at different shear rates (appendix C, Fig. C7.1) showed similar behaviour as for polymer-SNPs-aqueous solution (Fig. 7.3a and 7.3b). The viscosity of XG-SNPs-oil emulsion reduced at higher temperature, however, the values were found good enough to improve sweep efficiency (Section 7.8 and Table 7.3). The viscosity of emulsion is always greater than that of crude oil which is helpful to spread the chemical into the unswept region [123]. To validate the role of stability (creaming index), droplet size and viscous nature of the emulsion, flooding experiments were conducted at two different temperatures (30°C and 80°C) and residual oil recovery was calculated (Table 7.3).

Table 7.2: Viscosity of the emulsions formed for crude oil-xanthan gum-SNPs systems at shear rate of 1 s^{-1}.

Polymer concentration (ppm)	**5000**	**5000**	**5000**	**5000**
SNPs (wt%)	0	0.1	0.3	0.5
Viscosity at 30°C (mPa. s)	3256	4473	4770	4919
Viscosity at 80°C (mPa. s)	1894	1965	2177	2524

7.7 Effect of SNPs on Wettability Alteration

Contact angle measurements were conducted to visualize the effect of nanoparticles on wettability alteration for the chosen crude oil-polymer (5000 ppm) system (Fig. 7.10). The initial contact angle values decreased with increase in SNPs concentration; 86.2°, 72.7°, 66.5° and 50.4° for 0%, 0.1%, 0.3% and 0.5% SNPs respectively (Fig. 7.10b) [182]. The variation in the contact angle with time (till 10 min) for polymer solution (0 wt% SNPs) was not significant (86.2° to 51.2°) to alter the wettability (remains intermediate oil wet). However, after inducing 0.1 wt% SNPs, the contact angle decreased from 72.7° to 22.8°. The rate of change of contact angle was observed to be dominant with increasing the SNPs concentration and the lowest value of contact angle (18.84°) was achieved at 0.5 wt% SNPs. At higher concentration, the electrostatic repulsion force within the nanoparticles is large which causes the particles to spread along the solid surface decreasing contact angle [182]. It was also observed that the time required to reach stagnant value decreased as the concentration of SNPs increases (approximately 6-7 min, 5-6 min and 4-5 min for 0.1%, 0.3% and 0.5% SNPs respectively). Thus, the inclusion of SNPs in the system alter the system wettability from intermediate oil wet to strongly water wet. This enables release of the trapped residual oil from the pores of the reservoir rock by increasing the capillary number and hence promotes oil recovery. The wettability alteration mechanism in the present study is very likely due to the adsorption of SNPs on the oil-wet surface which replaces the carboxylate group from oil-wet Berea core [183-185]. Maghzi et al. [185] investigated the mechanism responsible for wettability alteration using silica nanoparticles in a five spot model. The analysis exposed a formation of strong hydrogen bonding between silica

nanoparticles and water which increases the surface free energy and changes the wettability from oil-wet to water-wet.

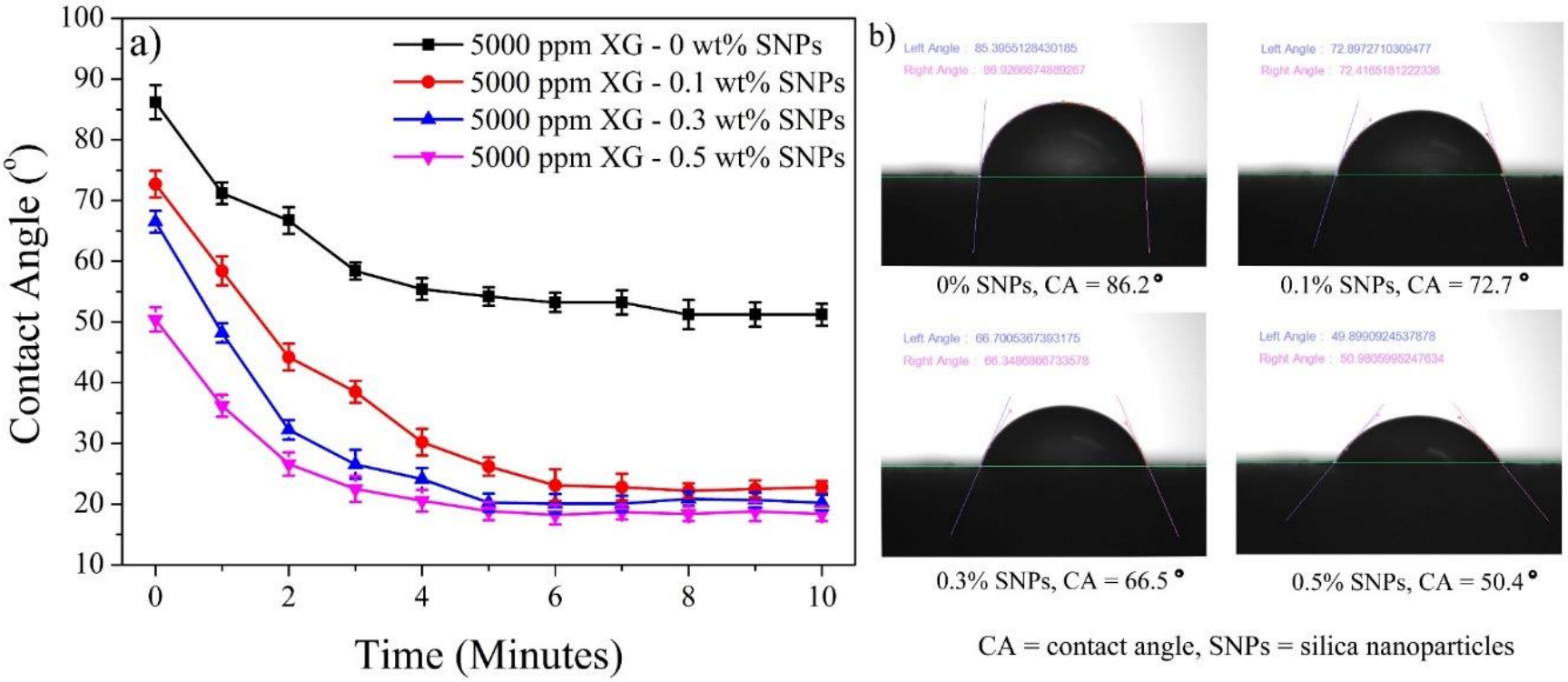

Fig. 7.10: (a) Variation of contact angle with time for XG (5000 ppm)-SNPs system (b) images at initial time = 0.

7.8 Oil Recovery by Core Flooding Experiments

Laboratory scale flooding experiments were performed using Berea core (Idaho Gray) sample at various nanoparticles concentrations. The data obtained from the flooding experiments are summarized in Fig. 7.11 and Table 7.3. Initially, a recovery factor of 14.5% oil in place (OIP) was obtained with only XG (5000 ppm) at 30°C. The oil recovery increased from 16.3% to 20.8% (OIP) with increasing concentration of SNPs from 0.1 to 0.3 wt%. At 0.5 wt% of SNPs the oil recovery factor reduced to 18.51 % of OIP. Oil recovery improves due to reduction in IFT, better emulsion stability, higher viscosity and wettability alteration. However, SNPs adversely affects the oil recovery factor due to the reduction in porosity and permeability [55, 102, 186]. The oil recovery trend can be further validated by the pressure drop curves as shown in Fig. 7.11b. For polymer flooding, lower pressure drop (24.5 psi) was measured which increases with increasing SNPs concentration due to higher viscosity effect [55]. The pressure drop was maximum (46.6 psi) at 0.3 wt% SNPs (optimum concentration) and decreased with further increase in SNPs concentration (0.5 wt%). Greater pressure drop signifies large formation of oil bank which eventually results in higher oil recovery [20, 36, 43].

At optimal concentration of SNPs (0.3wt %), the oil recovery reduced marginally with increase in temperature; 20.8% (at 30^{o}C) to 18.4% (at 80^{o}C). The pressure drop curve also revealed that at 80^{o}C, the oil bank formation is sufficient enough to increase recovery factor. Chen et al. [187] inferred that a direct correlation exists with respect to pressure drop and oil recovery i.e., higher oil recovery can be obtained at higher pressure drop. The emulsion so formed under this condition improves sweep efficiency by reducing viscous fingering/water channelling. The marginal reduction in oil recovery at higher temperature is probably due to higher creaming rate (confirmed through Fig. 7.9). FESEM images of Berea core before and

after flooding experiments (Fig. 7.12) clearly depict that SNPs do get adsorbed on Berea rock surface to form clusters. This is also in agreement with DLS characterization (Fig. 7.2).

Table 7.4 presents a summary of the results obtained in this work along with the literature findings for nanoparticles assisted chemical EOR systems. It can be observed that nanoparticles are effective in enhancing residual oil recovery. Sharma et al.[55] could increase the residual oil recovery using SNPs and the recovery was not affected with temperature (till 90°C). They also confirmed the combined role of IFT reduction and wettability alteration to recover residual oil. However, detail investigation of the emulsion formed, its stability and flow properties have not been considered. Yousefvand and Jafari [100] found that TiO_2 nanoparticles could enhance the oil recovery up to 43.3% IOIP. Cheraghian [188] and Maghzi et al. [101] also inferred similar behaviour of residual oil recovery enhancement with SNPs. However, additional investigations with respect to contact angle, IFT studies, emulsion formation and its stability were not considered in the context of their roles in polymer based EOR. Ehsan et al. [189] achieved 26.95 % OIP with surfactant-nanoparticles compared to sodium-dodecyl-sulfate surfactant alone (19.74%). Nanoparticles (SiO_2) stimulate IFT reduction and lessen contact angle to achieve strong water-wet reservoir. Detail investigation considering other mechanism such as emulsion stability, creaming rate, rheology, etc have not been reported. To understand such behaviour, this work attempts to provide a greater insight into the role of these complex interactions and phenomena for enhanced oil recovery of crude oil-polymer-SNPs systems.

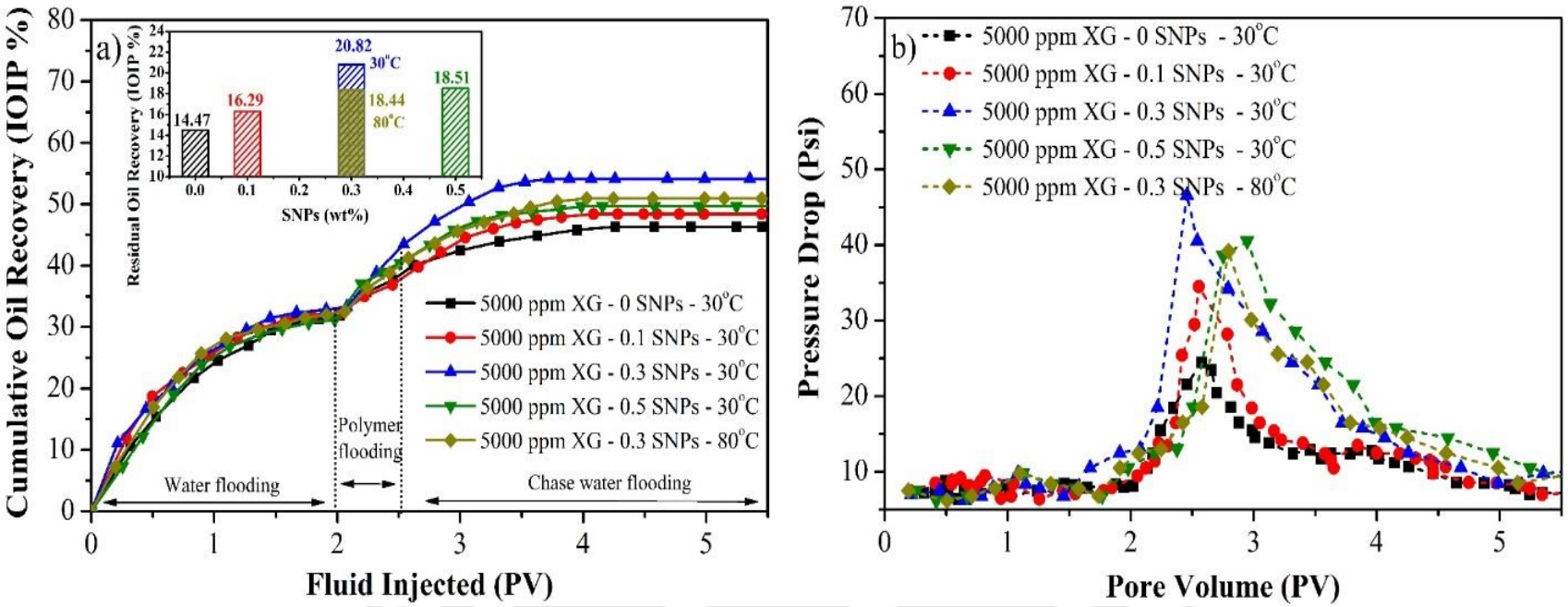

Fig. 7.11: Core flooding studies conducted with polymer (5000 ppm xanthan gum) concentration and 0.1 – 0.5 wt% SNPs concentration a) Cumulative oil recovery and b) Pressure drop profile.

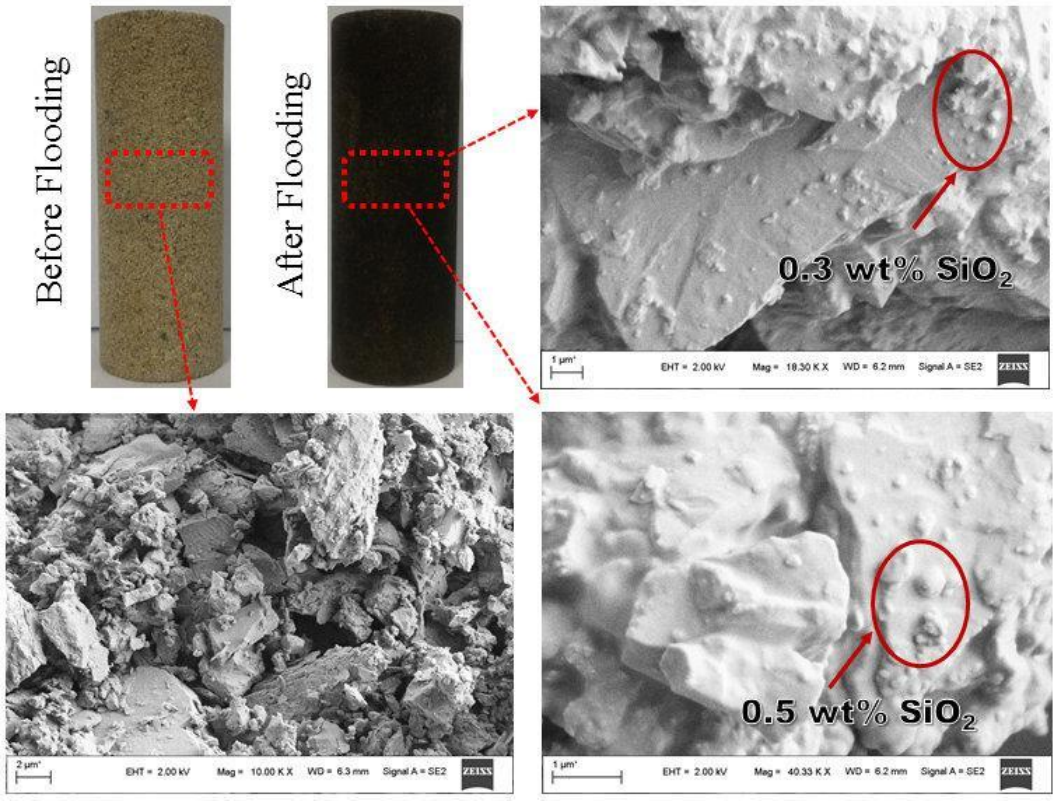

Fig. 7.12: FESEM images of Berea core (Idaho gray) before and after core flooding experiments (chemical composition - 5000 ppm xanthan gum and 0.3 wt% SNPs).

Table 7.3: Cumulative oil recovery data obtained for core flooding experiments conducted with xanthan gum-SNPs solutions.

Sr No.	Porosity (%)	Brine permeability (mD)	Xanthan Gum concentration (ppm)	Nanoparticles concentration (wt%)	Slug size (PV)	Initial oil saturation (%)	Temperature (°C)	Water flooding recovery (% OOIP)	Polymer flooding recovery (% OOIP)	Cumulative total recovery (%OOIP)
1	26.0	927	5000	0	0.5	78.3	30	31.84	14.47	46.32
2	25.8	834	5000	0.1	0.5	79.6	30	32.12	16.29	48.41
3	26.5	1002	5000	0.3	0.5	80.1	30	33.31	20.82	54.13
4	25.1	746	5000	0.5	0.5	80.5	30	31.17	18.51	49.68
5	25.3	772	5000	0.3	0.5	80.2	80	32.50	18.44	50.94

Table 7.4: Data summary of the best results obtained in this work and those reported in the literature for nanoparticle induced polymer enhanced oil recovery.

Reference	Rock	Polymer	Concentration (ppm)	Nanoparticles	Concentration (wt%)	Tertiary recovery (%)	Cumulative recovery (%)	Wettability alteration	IFT reduction
Sharma et al. [55]	Sandpack	Polyacrylamide (PAM)	1000	Silica dioxide	1.5	17.53	63.12	Yes	Yes
Yousefvand and Jafari [100]	Sandstone	Hydrolyzed polyacrylamide (HPAM)	3150	Titanium dioxide	2.3	43.3	52.8	-	-
Cheraghian [188]	Micromodel	HPAM	800	Silica dioxide	0.5	18.37	35.0	-	-
Maghzi et al. [101]	Micromodel	PAM	3000	Silica dioxide	0.1	-	68.0	-	-
Ehsan et al. [189]	Sandstone Core	SDS	2150	-	-	19.74	72.55	Yes	Yes
Ehsan et al. [189]	Sandstone Core	SDS	2150	Silica dioxide	0.1	26.95	79.76	Yes	Yes
Present Work	Berea Core	Xanthan Gum	5000	Silica dioxide	0.3	20.82	54.13	Yes	Yes

7.9 Conclusions

The present work provides several additional insights with respect to nanoparticles assisted polymer flooding of heavy crude oil systems. An optimal combination of polymer (5000 ppm) and SNPs (0.3 wt%) was achieved based on SNPs stability, rheology behaviour, IFT reduction, emulsification, creaming rate, wettability alteration and core flooding experiments. Stability analysis by DLS revealed stable nature of SNPs in polymer solution but not in aqueous phase (formation water). The viscosity of the polymer solution improved when SNPs was introduced in the system and such behaviour retained even at elevated temperature. Similar favourable behaviour was observed for IFT reduction phenomena too. The reduction in IFT promoted stable oil-water emulsions by reducing the droplet sizes and size distributions (7.52 - 5.12 µm). Creaming index values exposed the role of SNPs in effectively improving the emulsion stability. SNPs also altered the wettability of the chosen system from intermediate oil-wet to completely water-wet state. Pressure drop data indicated the formation of oil bank which resulted additional oil recovery of 20.82% at 30°C and 18.44% at 80°C during SNPs assisted polymer flooding. Overall, SNPs-polymer solution was found highly effective for EOR applications in moderate to higher temperature reservoirs. Further insights with respect to SNPs induced polymer EOR can be obtained by investigating variations in oil to chemical ratio, detailed rheological studies, salinity/pH effect on zeta potential, techno-economic analysis and cost analysis.

Chapter 8

Overall Summary and Future work

This chapter summarizes the overall conclusion drawn from the research work conducted in this dissertation. Furthermore, this chapter also emphasis on the scope for future research in the relevant area.

8.1 Overall Summary

The content of the thesis dealt with chemical enhanced oil recovery method to enhance oil production in Assam reservoir. The physiochemical properties of Assam crude oil (light to moderate and heavy crude) such as acid value, naphthenic content, API gravity and viscosity were examined to execute successful chemical EOR applications in Assam oil field. The detail investigation of different mechanism such as interfacial tension reduction, emulsification, sweep efficiency and wettability alteration which activate the residual oil flow towards higher oil recovery were scrutinized for both sandstone and carbonate reservoirs. In addition, the importance of nanoparticles in chemical EOR (polymer flooding) for improving the mechanisms responsible for higher residual oil recovery were explored. Nanoparticles also has the potential to produce higher residual oil recovery for reservoirs at higher temperature and saline system. Thereby, the major conclusions drawn from each part of the study are summarized as follows:

The effect of alkali flooding on residual oil recovery for light to moderate Assam crude oil was evaluated. Neutralization and extent of saponification of the acid group present in the crude oil were examined in detail and their role on residual oil recovery were estimated. The synergism effect of different mechanisms such interfacial tension, wettability alteration,

emulsification and displacement efficiency during alkali flooding were explored. The change in the contact between oil saturated rock surface and drop of alkali solution indicated the change in wettability of the system from intermediate wet to favourable water wet. Further, flooding parameters such as slug size and injection pattern were screened and optimized. Final residual oil recovery of 25.48% initial oil in place (IOIP) was obtained at 1 wt% NaOH with an alkali slug size of 0.5 PV using continuous injection pattern.

The potential of alkali and alkali-surfactant synergy to reduce the IFT, emulsify the crude oil and achieve higher residual oil recovery for moderate Assam crude oil were analysed. Alkali NaOH was found more effective in reducing the IFT to a minimum value of 5.15×10^{-2} mN/m and showed better emulsification properties with respect to Na_2CO_3. For alkali flooding experiments, NaOH showed higher residual oil recovery of 15.54% IOIP (24.25% residual oil in place) compared to Na_2CO_3 which could recover only 11.85% IOIP (18.75% residual oil in place). The synergism interaction of alkali-surfactant reduces the IFT to a value of 10^{-2} mN/m (similar to alkali) but the emulsification extent was increased greatly. Hence, considering the IFT reduction behaviour and emulsification extent, alkali-surfactant combination (0.1 wt% NaOH+0.1 wt% SDS) has been evaluated best with a maximum oil residual of 24.02% IOIP (38.79 % residual oil in place).

Surfactant has the efficacy to recover residual oil but shows adsorption characteristics on the reservoir rock surface which severely affects the optimum chemical formulation and economy of the process. Therefore, considering such limitation a detail investigation on the surfactant screening criteria and effect of several rock properties were scrutinized. The rock nature, mineral composition and surface properties were evaluated by EDX, XRD and BET analysis. Based on the IFT reduction values, surfactants were screened and it was observed that Triton X - 100 has greater potential in reducing the IFT compared to other six surfactants.

The stability of Triton X -100 was examined by aging the surfactant at 90°C for 10 days and no significant change in the surfactant structure were detected by NMR and FTIR. The IFT value for the aged and non-aged samples were almost same and no variation were observed. Additionally TGA data revealed that Triton X -100 can withstand temperature up to 305°C without any degradation. Adsorption studies showed that Langmuir isotherm model (R^2 = 0.99 and 2.58% error) and pseudo-second order model kinetics (R^2 = 0.99 and 3.64% error) are the best models obtained after fitting the experimental data. Thermodynamic studies showed that the adsorption behaviour was feasibility, spontaneity and exothermic in nature. The adsorption quantity was a function of rock minerology in the order of illite > feldspar > montmorillonite > kaolinite with R^2 value of 0.95, 0.92, 0.91 and 0.81 respectively.

Enhanced oil recovery with alkali-surfactant combination for heavy Assam crude oil in carbonate reservoirs was investigated and the role of various mechanism were explored. Chemical such as two alkali and eight different surfactants were systematically screened and optimum formulation was achieved. Alkali NaOH, surfactants CTAB and Triton X-100 and surfactant mixture of CTAB and Triton X-100 are the chemical combination which results in improved IFT reduction behaviour. Alkali reduces IFT to 10^{-1} mN/m, surfactant and surfactant mixture to 10^{-2} mN/m and alkali-surfactant mixture to 10^{-3} mN/m. The emulsification was negligible for alkali but increases with alkali-surfactant synergism and achieved better emulsion stability with surfactant mixture system. An oil layer break and fastest dynamic IFT reduction was observed with CTAB and CTAB-TX-100 which assist the emulsification extent. The variation in the contact angle between oil saturated rock surface and drop of chemical combination indicates the change in the wettability of the system from intermediate wet to water wet. Therefore, based on the combined effects of IFT reduction behaviour, extent of emulsification, wettability alteration and core flooding

experiments an optimum chemical combination and composition were formulated. Alkali of 0.6% NaOH , surfactant of 0.05% CTAB, surfactant mixture of 0.05% CTAB + 0.05% TX-100 and alkali-surfactant mixture of 0.6% NaOH + 0.05% CTAB + 0.05% TX-100 was obtained as the optimum concentration. Oil recovery estimated by flooding experiments are as 12.79% for alkali, 22-23% for surfactant, 24.58% for surfactant mixture and 14.46% for alkali-surfactant mixture. The residual oil recovery was affected when the concentration of surfactant mixture was increased beyond 0.1%. At such concentration, the formation of emulsion was strong which severely affected the displacement efficiency. Hence it was observed that the combination of IFT reduction, extent of emulsification, emulsion stability period and wettability alteration together were held responsible for higher tertiary oil recovery.

The influence of polymer and silica nanoparticles (SNPs) to improve essential properties for higher residual oil recovery were scrutinized. The properties such as IFT reduction, emulsification and its stability, rheological behaviour and wettability alteration were evaluated and based on which the optimal combination of 5000 ppm XG polymer and 0.3 wt% SNPs was achieved. The nanoparticles were effective in lowering the IFT at different temperature and promotes stable O/W (oi in water) emulsions by reducing the average droplet size from 7.52 to 5.12 µm. The creaming rate was also monitored with nanoparticles and better creaming index was achieved in the presence of nanoparticles even at elevated temperature. The wettability alteration was modified from intermediate wet to water wet by the adsorption of nanoparticles on the rock surface which helps in releasing the residual oil from the pores of the reservoir rock. SNPs polymer flooding resulted in higher pressure drop which indicates the formulation of oil bank and results in higher oil recovery of 20.82% at

30°C and 18.44% at 80°C. The flooding and pressure drop curves revealed that SNPs was effective in achieving higher oil recovery at elevated temperature. This clearly indicates the potential of nanoparticles for EOR applications in moderate to high temperature reservoirs.

8.2 Future Work

A detail investigation on chemical EOR (Alkali, Surfactant and Polymer) for Assam reservoirs were studied in the current project. The studies reveal successful chemical EOR applications with estimated percentage of oil recovered at laboratory scale. However considering the vast area of the field following are the scope which can be focused for future studies

- Alkali-surfactant-polymer flooding using natural or synthetic surfactant to obtain optimum chemical combination and to evaluate their adsorption characteristics.
- Detail investigation of chemical-nanoparticles solution for harsh reservoir conditions to formulate optimum chemical slug based on such scenario.
- Developing chemical EOR models and simulate to validate experimental data considering all reservoir complexities and to further predict real field oil recovery.
- Cost analysis of chemical EOR for real field applications.

References

[1] L. Siggel, M. Radloff, S. Reimann, M. Hansch, M. Nowak, M. Ranft, H. Weiss, E. Schreiner, F. Brand, Tpm's: A new class of viscoelastic solutions for enhanced oil recovery, in: SPE EOR Conference at Oil and Gas West Asia, Society of Petroleum Engineers, Muscat, 31 March – 2 April, 2014, pp. 1-11.

[2] A.O. Al-Amodi, U.A. Al-Mubaiyedh, A.S. Sultan, M.S. Kamal, I.A. Hussein, Novel fluorinated surfactants for enhanced oil recovery in carbonate reservoirs, Can. J. Chem. Eng. 94 (2016) 454-460.

[3] M.A. Ahmadi, M. Galedarzadeh, S.R. Shadizadeh, Wettability alteration in carbonate rocks by implementing new derived natural surfactant: Enhanced oil recovery applications, Transp. Porous Med. 106 (2015) 645–667.

[4] M.A. Ahmadi, Y. Arabsahebi, S.R. Shadizadeh, S.S. Behbahani, Preliminary evaluation of mulberry leaf-derived surfactant on interfacial tension in an oil-aqueous system: Eor application, Fuel 117 (2014) 749–755.

[5] S. Kumar, A. Mandal, Studies on interfacial behavior and wettability change phenomena by ionic and nonionic surfactants in presence of alkalis and salt for enhanced oil recovery, Appl. Surf. Sci. 372 (2016) 42–51.

[6] J. Raicar, R.M. Procter, Economic considerations and potential of heavy oil supply from lloydminster – alberta, canada, in: Meyer, R.F., Wynn, J.C., Olson, J. C. (Eds.), The Second UNITAR International Conference on Heavy Crude and Tar Sands, Caracas. McGraw-Hill, New York, February 7–17, 1984, pp. 212–219.

[7] A. Hemmati-Sarapardeh, H. Hashemi Kiasari, N. Alizadeh, S. Mighani, A. Kamari, Application of fast-sagd in naturally fractured heavy oil reservoirs: A case study, in: The 18th Middle East Oil & Gas Show and Conference, Manama, Bahrain, March 10-13, 2013.

[8] A. Hemmati-Sarapardeh, M. Khishvand, A. Naseri, A.H. Mohammadi, Toward reservoir oil viscosity correlation, J. Chem. Eng. Sci. 90 (2013) 53-68.

[9] J.J. Taber, F.D. Martin, R.S. Seright, Eor screening criteria revisited - part1: Introduction to screening criteria and enhanced recovery field projects, SPE Res. Eng. 12 (1997) 189-198.

[10] S.A.O.G.P. Limited, An introduction to enhanced oil recovery techniques, in, Australia, 2013.

[11] L. Lake, Enhanced oil recovery, in: E. Cliffs (Ed.), Prentice Hall, New Jersey, 1989.

[12] D.W. Green, G.P. Willhite, Enhanced oil recovery Richardson, Texas: SPE, SPE Textbook Series, 1998.

[13] C.E. Johnson, Status of caustic and emulsion methods, J. Pet. Technol. 28 (1976) 85-92.

[14] C.E. Cooke, R.E. Williams, P.A. Kolodzie, Oil recovery by alkaline waterflooding, J. Pet. Technol. 26 (1974) 1365-1374.

[15] H.A. Nasr-El-Din, K.C. Taylor, Dynamic interfacial tension of crude oil/alkali/surfactant systems, Colloids Surf. 66 (1992) 23-37.

[16] D.J. Pye, Improved secondary recovery by control of water mobility, J. Pet. Technol. 16 (1964) 911-916.

[17] H.L. Chang, Polymer flooding technology yesterday, today, and tomorrow, J. Pet. Technol. 30 (1978) 1-16.

[18] J.J. Sheng, Investigation of alkaline-crude oil reaction, Petrol. 1 (2015) 31-39.

[19] C.D. Yuan, W.F. Pu, X.C. Wang, L. Sun, Y.C. Zhang, S. Cheng, Effects of interfacial tension, emulsification, and surfactant concentration on oil recovery in surfactant flooding process for high temperature and high salinity reservoirs, Energy Fuels 29 (2015) 6165-6176.

[20] H. Pei, G. Zhang, J. Ge, L. Zhang, H. Wang, Effect of polymer on the interaction of alkali with heavy oil and its use in improving oil recovery, Colloids Surf. A 446 (2014) 57-64.

[21] S.M.F. Ali, S. Thomas, A realistic look at enhanced oil recovery, Scientia Iranica 1 (1994) 219 - 230.

[22] M. Tang, G. Zhang, J. Ge, P. Jiang, Q. Liu, H. Pei, L. Chen, Investigation into the mechanisms of heavy oil recovery by novel alkaline flooding, Colloids Surf. A 421 (2013) 91-100.

[23] J. Wang, M. Dong, M. Arhuoma, Experimental and numerical study of improving heavy oil recovery by alkaline flooding in sandpacks, J. Can. Pet. Technol. 49 (2010) 51-57.

[24] M.S. Almalik, A.M. Attia, L.K. Jang, Effects of alkaline flooding on the recovery of safaniya crude oil of saudi arabia, J. Pet. Sci. Eng. 17 (1997) 367-372.

[25] D. Xie, J. Hou, F. Zhao, A. Doda, J. Trivedi, The comparison study of ift and consumption behaviors between organic alkali and inorganic alkali, J. Pet. Sci. Eng. 147 (2016) 528–535.

[26] H. Gong, Y. Li, M. Dong, S. Ma, W. Liu, Effect of wettability alteration on enhanced heavy oil recovery by alkaline flooding, Colloids Surf. A 488 (2016) 28–35.

[27] R. Ehrlich, H.H. Hasiba, P. Raimondi, Alkaline waterflooding for wettability alteration - evaluating a potential field application, J. Pet. Technol. 26 (1974) 1335-1343.

[28] H. Pei, G. Zhang, J. Ge, M. Tang, Y. Zheng, Comparative effectiveness of alkaline flooding and alkaline–surfactant flooding for improved heavy-oil recovery, Energy Fuels 26 (2012) 2911-2919.

[29] H.Y. Jennings, C.E. Johnson, C.D. McAuliffe, A caustic waterflooding process for heavy oils, J. Pet. Technol. 26 (1974) 1344-1352.

[30] H. Atkinson, Recovery of petroleum from oil-bearing sands, US1651311 (1927).

[31] H.Y. Jennings, A study of caustic solution-crude oil interfacial tensions, Soc. Pet. Eng. J. 15 (1975) 197-202.

[32] P.G. Nutting, Chemical problems in the water driving of petroleum from oil sands, Ind. Eng. Chem. 10 (1925) 1035-1036.

[33] E.F. DeZabala, J.M. Vislocky, E. Rubin, C.J. Radke, A chemical theory for linear alkaline flooding, Soc. Petrol. Eng. 22 (1982) 245-258.

[34] J. Rudin, D.T. Wasan, Mechanisms for lowering of interfacial tension in alkali/acidic oil systems 2. Theoretical studies Colloids Surf. 68 (1992) 81-94.

[35] J. Ge, A. Feng, G. Zhang, P. Jiang, H. Pei, R. Li, X. Fu, Study of the factors influencing alkaline flooding in heavy-oil reservoirs, Energy Fuels 26 (2012) 2875-2882.

[36] H. Pei, G. Zhang, J. Ge, L. Jin, C. Ma, Potential of alkaline flooding to enhance heavy oil recovery through water-in-oil emulsification, Fuel 104 (2013) 284-293.

[37] H. Pei, G. Zhang, J. Ge, L. Jin, X. Liu, Analysis of microscopic displacement mechanisms of alkaline flooding for enhanced heavy-oil recovery, Energy Fuels 25 (2011) 4423-4429.

[38] M. Dong, Q. Liu, A. Li, Displacement mechanisms of enhanced heavy oil recovery by alkaline flooding in a micromodel, Particuology 10 (2012) 298-305.

[39] R. Ehrlich, R.J. Wygal, Interrelation of crude oil and rock properties with the recovery of oil by caustic waterflooding, in: SPE-AIME Fourth Symposium on Improved- Oil Recovery, Society of Petroleum Engineers, Tulsa, 22-24 March, 1976, pp. 263-270.

[40] G. Jerauld, J. Rathmell, Wettability and relative permeability of prudhoe bay: A case study in mixed-wet reservoirs, , SPE Reservoir Eng. 12 (1997) 58–65.

[41] N.R. Morrow, Wettability and its effect on oil recovery, J. Petrol. Technol. 42 (1990) 1476–1484.

[42] T. Austad, B. Matre, J. Milter, A. Saevareid, L. Oyno, Chemical flooding of oil reservoirs 8. Spontaneous oil expulsion from oil- and water-wet low permeable chalk material by imbibition of aqueous surfactant solutions, Colloids Surf. A 137 (1998) 117-129.

[43] L. Chen, G. Zhang, J. Ge, P. Jiang, J. Tang, Y. Liu, Research of the heavy oil displacement mechanism by using alkaline/surfactant flooding system, Colloids Surf. A 434 (2013) 63– 71.

[44] M. Budhathoki, T.-P. Hsu, P. Lohateeraparp, B.L. Roberts, B.-J. Shiau, J.H. Harwell, Design of an optimal middle phase microemulsion for ultra high saline brine using hydrophilic lipophilic deviation (hld) method, Colloids Surf. A 488 (2016) 36–45.

[45] Q. Liu, M. Dong, S. Ma, Y. Tu, Surfactant enhanced alkaline flooding for western canadian heavy oil recovery, Colloids Surf. A 293 (2007) 63-71.

[46] S.A. Pursley, H.L. Graham, Borregos field surfactant pilot test, J. Pet. Technol. 27 (1975) 695−700.

[47] J.M. Maerker, W.W. Gale, Surfactant flood process design for loudon, SPE Reservoir Eng. 7 (1992) 36-44.

[48] W.W. Gale, E.I. Sandvik, Tertiary surfactant flooding: Petroleum sulfonate composition-efficacy studies, Soc. Pet. Eng. J. 13 (1973) 191-199.

[49] D.C. Standnes, T. Austad, Wettability alteration in chalk 2. Mechanism for wettability alteration from oil-wet to water-wet using surfactants, J. Pet. Sci. Eng. 28 (2000) 123–143.

[50] K. Jarrahian, O. Seiedi, M.S. Sheykhan, M. V, S. Ayatollahi, Wettability alteration of carbonate rocks by surfactants: A mechanistic study, Colloids Surf. A 410 (2012) 1-10.

[51] L. Fu, G. Zhang, J. Ge, K. Liao, H. Pei, P. Jiang, X. Li, Study on organic alkali-surfactant-polymer flooding for enhanced ordinary heavy oil recovery, Colloids Surf. A 508 (2016) 230–239.

[52] W. Pu, C. Yuan, W. Hu, T. Tan, J. Hui, S. Zhao, S. Wang, Y. Tang, Effects of interfacial tension and emulsification on displacement efficiency in dilute surfactant flooding, RSC Adv. 6 (2016) 50640-50649.

[53] A.A. Al-Yousef, M. Han, S.H. Al-Saleh, Oil recovery process for carbonate reservoirs, U.S. Patent No. 8,550,164 (2013).

[54] M. Zargartalebi, R. Kharrat, N. Barati, Enhancement of surfactant flooding performance by the use of silica nanoparticles, Fuel 143 (2015) 21-27.

[55] T. Sharma, S. Iglauer, J.S. Sangwai, Silica nanofluids in an oilfield polymer polyacrylamide: Interfacial properties, wettability alteration, and applications for chemical enhanced oil recovery, Ind. Eng. Chem. Res. 55 (2016) 12387-12397.

[56] A. Bera, A. Mandal, B.B. Guha, Synergistic effect of surfactant and salt mixture on interfacial tension reduction between crude oil and water in enhanced oil recovery, J. Chem. Eng. Data 59 (2014) 89−96.

[57] S. Zendehboudi, M.A. Ahmadi, A.R. Rajabzadeh, N. Mahinpey, I. Chatzis, Experimental study on adsorption of a new surfactant onto carbonate reservoir samples-application to eor, Can. J. Chem. Eng. 91 (2013) 1439-1449.

[58] S. Kumar, P. Panigrahi, R.K. Saw, A. Manda, Interfacial interaction of cationic surfactants and its effect on wettability alteration of oil-wet carbonate rock, Energy Fuels 30 (2016) 2846−2857.

[59] M.S. Kamal, A.S. Sultan, I.A. Hussein, Screening of amphoteric and anionic surfactants for ceor applications using a novel approach, Colloids Surf. A 476 (2015) 17-23.

[60] S. Park, E.S. Lee, W.R.W. Sulaiman, Adsorption behaviors of surfactants for chemical flooding in enhanced oil recovery, J. Ind. Eng. Chem. 21 (2015) 1239-1245.

[61] T. Amirianshoja, R. Junin, A.K. Idris, O. Rahmani, A comparative study of surfactant adsorption by clay minerals, J. Pet. Sci. Eng. 101 (2013) 21-27.

[62] M.A. Ahmadi, S. Zendehboudi, A. Shafiei, L. James, Nonionic surfactant for enhanced oil recovery from carbonates: Adsorption kinetics and equilibrium, Ind. Eng. Chem. Res. 51 (2012) 9894−9905.

[63] B.B. Sandiford, Laboratory and field studies of water floods using polymer solutions to increase oil recoveries, J. Pet. Technol. 16 (1964) 917-922.

[64] E. Akiyama, A. Kashimoto, K. Fukuda, H. Hotta, T. Suzuki, T. Kitsuki, Thickening properties and emulsification mechanisms of new derivatives of polysaccharides in aqueous solution, J. Colloid Interface Sci. 282 (2005) 448–457.

[65] E. Akiyama, T. Yamamoto, Y. Yago, H. Hotta, t. Ihara, T. Kitsuki, Thickening properties and emulsification mechanisms of new derivatives of polysaccharide in aqueous solution 2. The effect of the substitution ratio of hydrophobic/hydrophilic moieties, J. Colloid Interface Sci. 311 (2007) 438–446.

[66] R.S. Seright, T.G. Fan, K. Wavrik, H. Wan, N. Gaillard, C. Favero, Rheology of a new sulfonic associative polymer in porous media, SPE Reservoir Eval. Eng. 14 (2011) 726–734.

[67] Y. Lu, W. Kang, J. Jiang, J. Chen, D. Xu, P. Zhang, L. Zhang, H. Feng, H. Wu, Study on the stabilization mechanism of crude oil emulsion with an amphiphilic polymer using the b-cyclodextrin inclusion method, RSC Adv. 7 (2017) 8156–8166.

[68] R.L. Jewett, G.F. Schurz, Polymer flooding-a current appraisal, J. Pet. Technol. 22 (1970) 675-684.

[69] W. Demin, Z. Zhang, L. Chun, J. Cheng, X. Du, Q. Li, A pilot for polymer flooding of saertu formation s ii 10-16 in the north of daqing oil field, in: SPE Asia Pacific Oil and Gas Conference, 28-31 October, Adelaide, Australia, Society of Petroleum Engineers, 1996, pp. 431-441.

[70] H. Saboorian-Jooybari, M. Dejam, Z. Chen, Heavy oil polymer flooding from laboratory core floods to pilot tests and field applications: Half-century studies, J. Pet. Sci. Eng. 142 (2016) 85–100.

[71] D.C. Standnes, I. Skjevrak, Literature review of implemented polymer field projects, J. Pet. Sci. Eng. 122 (2014) 761–775.

[72] W.M. Leung, D.E. Axelson, Thermal degradation of polyacrylamide and poly (acrylamide-coacrylate), J. Polym. Sci. A 25 (1987) 1852–1864.

[73] M.H. Yang, Rheological behavior of polyacrylamide solution, J. Polym. Eng. 19 (1999) 371-381.

[74] H. Kheradmand, J. Francois, V. Plazanet, Hydrolysis of polyacrylamide and acrylic acid-acrylamide copolymers at neutral ph and high temperature, Polymer 29 (1988) 860-870.

[75] Q. Chen, Y. Wang, Z. Lu, Y. Feng, Thermoviscosifying polymer used for enhanced oil recovery: Rheological behaviors and core flooding test, Polym. Bull. 70 (2013) 391–401.

[76] G. Muller, Thermal stability of high molecular weight polyacrylamide aqueous solution, Polym. Bull. 5 (1981) 31-37.

[77] B.F. Abu-Sharkh, G.O. Yahaya, S.A. Ali, E.Z. Hamad, I.M. Abu-Reesh, Viscosity behavior and surface and interfacial activities of hydrophobically modified water-soluble acrylamide/n-phenyl acrylamide block copolymers, J.Appl. Polym. Sci. 89 (2002) 2290–2300.

[78] T. Sharma, G.S. Kumar, B.H. Chon, J.S. Sangwai, Thermal stability of oil-in-water pickering emulsion in the presence of nanoparticle, surfactant, and polymer, J. Ind. Eng. Chem. 22 (2015) 324–334.

[79] B.P. Binks, A. Rocher, Effects of temperature on water-in-oil emulsions stabilised solely by wax microparticles, J. Colloid Interface Sci. 335 (2009) 94–104.

[80] A.E. Bayat, R. Junin, A. Samsuri, A. Piroozian, M. Hokmabadi, Impact of metal oxide nanoparticles on enhanced oil recovery from limestone media at several temperatures, Energy Fuels 28, (2014) 6255−6266.

[81] H. Sharma, S. Dufour, G.W.P.P. Arachchilage, U. Weerasooriya, G.A. Pope, K. Mohanty, Alternative alkalis for asp flooding in anhydrite containing oil reservoirs, Fuel 140 (2015) 407-420.

[82] A.A. Olajire, Review of asp eor (alkaline surfactant polymer enhanced oil recovery) technology in the petroleum industry: Prospects and challenges, Energy 77 (2014) 963-982.

[83] I.A. Malik, U.A. Al-Mubaiyedh, A.S. Sultan, M.S. Kamal, I.A. Hussein, Rheological and thermal properties of novel surfactant-polymer systems for eor applications, The Can. J. Chem. Eng. 94 (2016) 1693–1699.

[84] S.R. Clark, M.J. Pitts, S.M. Smith, Design and application of an alkaline-surfactant-polymer recovery system to the west kiehl field. , SPE Adv Technol Ser 1 (1993) 172-179.

[85] H. Pei, G. Zhang, J. Ge, Study on the variation of dynamic interfacial tension in the process of alkaline flooding for heavy oil, Fuel 104 (2013) 372–378.

[86] O. Mohammadzadeh, I. Chatzis, J.P. Giesy, A novel chemical additive for in-situ recovery of heavy oil using waterflooding process, J. Petrol. Sci. Eng. 135 (2015) 484–497.

[87] Y. Wu, M. Dong, S. Ezeddin, Study of alkaline/polymer flooding for heavy-oil recovery using channeled sandpacks, in: Canadian Unconventional Resources and International Petroleum Conference, SPE 137460-MS, Calgary, 2010.

[88] M.J. Pitts, P. Dowling, K. Wyatt, H. Surkalo, C. Adams, Alkaline-surfactante-polymer flood of the tanner field, in: SPE/DOE Symposium on Improved Oil Recovery, , SPE 100004, Tulsa, Oklahoma, USA, 22-26 April, 2006, pp. 1-5.

[89] H.S. Hadi, M. Degam, Z.X. Chen, Heavy oil polymer flooding from laboratory core floods to pilot tests and field applications: Half-century studies, J. Petrol. Sci. Eng. 142 (2016) 85–100.

[90] B. Ding, G. Zhang, J. Ge, X. Liu, Research on mechanisms of alkaline flooding for heavy oil, Energy Fuels 24 (2010) 6346-6352.

[91] Z. Youyi, Z. Yi, N. Jialing, L. Weidong, H. Qingfeng, The research progress in the alkali-free surfactant-polymer combination flooding technique Petrol. Explor. Dev. 39 (2012) 371-376.

[92] M. Aoudia, R.S. Al-Maamari, M. Nabipour, A.S. Al-Bemani, S. Ayatollahi, Laboratory study of alkyl ether sulfonates for improved oil recovery in high-salinity carbonate reservoirs: A case study, Energy Fuels 24 (2010) 3655-3660.

[93] D.M. Wang, C.D. Liu, W.X. Wu, G. Wang, Development of an ultra-low interfacial tension surfactant in a system with no-alkali for chemical flooding, in: SPE/DOE Improved Oil Recovery Symposium, Society of Petroleum Engineering, Tulsa, Oklahoma, USA, 2008, pp. 1-9.

[94] J.J. Sheng, Review of surfactant enhanced oil recovery in carbonate reservoirs, Adv. Pet. Explor. Dev. 6 (2013) 1-10.

[95] F.D.S. Curbelo, V.C. Santanna, E.L.B. Neto, T.V. Dutra, T.N.C. Dantas, A.A.D. Neto, A.I.C. Garnica, Adsorption of nonionic surfactants in sandstones, Colloids Surf. A 293 (2007) 1-4.

[96] M.A. Ahmadi, S.R. Shadizadeh, Adsorption of a nonionic surfactant onto a silica surface, Energy Sources Part A 38 (2016) 1455–1460.

[97] M.A. Ahmadi, S.R. Shadizadeh, Experimental investigation of adsorption of a new nonionic surfactant on carbonate minerals, Fuel 104 (2013) 462–467.

[98] S.B. Gogoi, Adsorption of non-petroleum base surfactant on reservoir rock, Curr. Sci. 97 (2009) 1059-1063.

[99] L. Hendraningrat, S. Li, O. Torsaeter, A coreflood investigation of nanofluid enhanced oil recovery, J. Pet. Sci. Eng. 111 (2013) 128–138.

[100] H. Yousefvand, A. Jafari, Enhanced oil recovery using polymer/nanosilica, Procedia Mater. Sci. 11 (2015) 565-570.

[101] A. Maghzi, R. Kharrat, A. Mohebbi, M.H. Ghazanfari, The impact of silica nanoparticles on the performance of polymer solution in presence of salts in polymer flooding for heavy oil recovery, Fuel 123 (2014) 123–132.

[102] M.I. Youssif, R.M. El-Maghraby, S.M. Saleh, A. Elgibaly, Silica nanofluid flooding for enhanced oil recovery in sandstone rocks, Egypt. J. Pet. xxx (2017) xxx-xxx.

[103] G. Costantinides, G. Arich, Fundamental aspects of petroleum geochemistry., In: Bartholomew, N., Colombo, Elsevier, Amsterdam (1967) 109.

[104] S. Hoeiland, T. Barth, A.M. Blokhus, A. Skauge, The effect of crude oil acid fractions on wettability as studied by interfacial tension and contact angles, J. Pet. Sci. Eng. 30 (2001) 91-103.

[105] Standard methods for the examination of water and wastewater, American Public Health Association, American Water Works Association, Water Environment Federation (1999).

[106] N. Kumar, T. Gaur, A. Mandal, Characterization of spn pickering emulsions for application in enhanced oil recovery, J. Ind. Eng. Chem. 54 (2017) 304–315.

[107] A. Kapoor, R.T. Yang, Correlation of equilibrium adsorption data of condensible vapours on porous adsorbents, Gas Sep. Purif. 3 (1989) 187-192.

[108] K.Y. Foo, B.H. Hameed, Insights into the modeling of adsorption isotherm systems, Chem. Eng. J. 156 (2010) 2-10.

[109] M.A. Ahmadi, S.R. Shadizadeh, Induced effect of adding nano silica on adsorption of a natural surfactant onto sandstone rock: Experimental and theoretical study, J. Pet. Sci. Eng. 112 (2013) 239–247.

[110] M. Schmitta, C.P. Fernandesa, F.G. Wolf, G.A.B.C. Netoa, C.P. Rahnera, V.S.S. Santos, Characterization of brazilian tight gas sandstones relatingpermeability and angstrom- to micron-scale pore structures, J. Nat. Gas Sci. Eng. 27 (2015) 785-807.

[111] K.S.W. Sing, D.H. Everett, R.A.W. Haul, L. Moscou, R.A. Pierotti, J. Rouquerol, T. Siemieniewska, Reporting physisorption data for gas/solid systems special reference to the determination of surface area and porosity, Pure Appl. Chem. 57 (1985) 603-619.

[112] L.M. Anovitz, D.R. Cole, Characterization and analysis of porosity and pore structures, Rev. Mineral. Geochem. 80 (2015) 61-164.

[113] H.-R. Li, Z.-Q. Li, X.-W. Song, C.-B. Li, L.-L. Guo, L. Zhang, L. Zhang, S. Zhao, Effect of organic alkalis on interfacial tensions of surfactant/polymer solutions against hydrocarbons, Energy Fuels 29 (2015) 459-466.

[114] L. Zhang, L. Luo, S. Zhao, J.Y. Yu, Ultra low interfacial tension and interfacial dilational properties related to enhanced oil recovery, Nova Science Publishers, New York, 2008.

[115] J.R. Kanicky, J.-C. Lopez-Montilla, S. Pandey, D.O. Shah, Surface chemistry in the petroleum industry, in: K. Holmberg (Ed.), John Wiley & Sons, Ltd, University of Florida, Gainesville, Florida, USA, 2001, pp. 251-267.

[116] J. Rudin, D.T. Wasan, Mechanisms for lowering of interfacial tension in alkali/acidic oil systems: Effect of added surfactant, Ind. Eng. Chem. Res. 31 (1992) 1899-1906.

[117] V. Pauchard, J. Sjoblom, S. Kokal, P. Bouriat, C. Dicharry, M. H, A. Al-Hajji, Role of naphthenic acids in emulsion tightness for a low-total-acid-number (tan)/high-asphaltenes oil, Energy Fuels 23 (2009) 1269–1279.

[118] A. Samanta, K. Ojha, A. Mandal, Interactions between acidic crude oil and alkali and their effects on enhanced oil recovery, Energy Fuels 25 (2011) 1642–1649.

[119] L. Davarpanah, F. Vahabzadeh, A. Dermanaki, Structural study of asphaltenes from iranian heavy crude oil, Oil & Gas Science and Technology – Revue d'IFP Energies nouvelles (2013).

[120] R.P. Borwankar, D.T. Wasan, Dynamic interfacial tensions in acidic crude oil/caustic systems part i: A chemical diffusion-kinetic model, AIChE Journal 1986; 32: 32 (1986) 455-466.

[121] J. Rudin, D.T. Wasan, Mechanisms for lowering of interfacial tension in alkali acidic oil system 1. Experimental studies, Colloids Surf. 68 (1992) 67-79.

[122] M. Dong, S. Ma, Q. Liu, Enhanced heavy oil recovery through interfacial instability: A study of chemical flooding for brintnell heavy oil, Fuel 88 (2009) 1049-1056.

[123] M. Arhuoma, M. Dong, D. Yang, R. Idem, Determination of water-in-oil emulsion viscosity in porous media, Ind. Eng. Chem. Res. 48 (2009) 7092–7102.

[124] H. Pei, G. Zhang, J. Ge, M. Ma, L. Zhang, Y. Liu, Improvement of sweep efficiency by alkaline flooding for heavy oil reservoirs, J. Disper. Sci. Technol. 34 (2013) 1548–1556.

[125] J. Sheng, Modern chemical enhanced oil recovery: Theory and practice, in: s. Edition (Ed.), Gulf Professional Publishing, 2010, pp. 648.

[126] S. Liu, Alkaline surfactant polymer enhanced oil recovery process, Rice University, PhD Thesis (2007).

[127] H. Yu, Y. Wang, Y. Zhang, P. Zhang, W. Chen, Effects of displacement efficiency of surfactant flooding in high salinity reservoir: Interfacial tension, emulsification, adsorption, Adv. Pet. Explor. Dev. 1 (2011) 32-39.

[128] Q.Z. Jiang, Surfactant science and application, in, China Petrochemical Press (in Chinese), Beijing, 2006.

[129] J. Zhao, C. Dai, Q. Ding, M. Du, H. Feng, Z. Wei, A. Chen, M. Zhao, The structure effect on the surface and interfacial properties of zwitterionic sulfobetaine surfactants for enhanced oil recovery, RSC Adv. 5 (2015) 13993-14001.

[130] A. Samanta, K. Ojha, A. Sarkar, A. Mandal, Surfactant and surfactant-polymer flooding for enhanced oil recovery, Adv. Pet. Explor. Dev. 2 (2011) 13-18.

[131] B. Bennett, S.R. Larter, Partition behaviour of alkylphenols in crude oils-brine systems under subsurface conditions, Geochim. Cosmochim. Acta 61 (1997) 4393-4402.

[132] J. Rudin, C. Bernard, D.T. Wasan, Effect of added surfactant on interfacial-tension and spontaneous emulsification in alkali/ acidic oil systems, Ind. Eng. Chem. Res. 33 (1994) 1150−1158.

[133] J.E. Puig, M.T. Mares, W.G. Miller, E.I. Franses, Mechanism of ultralow interfacial tensions in dilute surfactant-oil-brine systems, Colloids Surf. A 16 (1985) 139−152.

[134] L. Zhang, L. Luo, S. Zhao, Z. Xu, J. An, J. Yu, Effect of different acidic fractions in crude oil on dynamic interfacial tensions in surfactant/alkali/model oil systems, J. Pet. Sci. Eng. 41 (2004) 189−198.

[135] Z. Zhao, C. Bi, Z. Li, W. Qiao, L. Cheng, Interfacial tension between crude oil and decylmethylnaphthalene sulfonate surfactant alkali-free flooding systems, Colloids Surf. A 276 (2006) 186−191.

[136] L. Zhang, L. Luo, S. Zhao, J. Yu, Studies of synergism/ antagonism for lowering dynamic interfacial tensions in surfactant/ alkali/acidic oil systems, part 2: Synergism/antagonism in binary surfactant mixtures, J. Colloid Interface Sci. 251 (2002) 166−171.

[137] T.C.G. Kibbey, L. Chen, Phase volume effects in the sub- and super-cmc partitioning of nonionic surfactant mixtures between water and immiscible organic liquids, Colloids Surf. A 326 (2008) 73−82.

[138] Z. Zhao, Z. Li, W. Qiao, L. Cheng, Dynamic interfacial tension between crude oiland dodecylmethylnaphthalene sulfonatesurfactant flooding systems, Energy Sources, Part A 29 (2007) 207–215.

[139] C.A. Miller, K.H. Raney, Solubilization-emulsification mechanisms of detergency, Colloids Surf. A 74 (1993) 169-175.

[140] A. Barati, A. Najafi, A. Daryasafar, P. Nadali, H. Moslehi, Adsorption of a new nonionic surfactant on carbonate minerals in enhanced oil recovery: Experimental and modeling study, Chem. Eng. Res. Des. 105 (2016) 55-63.

[141] A. Bera, T. Kumar, K. Ojha, A. Mandal, Adsorption of surfactants on sand surface in enhanced oil recovery: Isotherms, kinetics and thermodynamic studies, Appl. Surf. Sci. 284 (2013) 87-99.

[142] A.V. Pethkar, K.M. Paknikar, Recovery of gold from solutions using cladosporium cladosporioides biomass beads, J. Biotechnol. 63 (1998) 121-136.

[143] M.A. Muherei, R. Junin, A.B.B. Merdhah, Adsorption of sodium dodecyl sulfate, triton x100 and their mixtures to shale and sandstone: A comparative study, J. Pet. Sci. Eng. 67 (2009) 149–154.

[144] E.C. Donaldson, R.F. Kendall, B.A. Baker, F.S. Manning, Surface-area measurement of geologic materials, Soc. Pet. Eng. J. (1975) 111-116

[145] P.L. Ghurcher, P.R. French, J.G. Shaw, L.L. Schramm, Rock properties of berea sandstone, baker dolomite, and indiana limestone, Soc. Pet. Eng. J. (1991) 431-446.

[146] A.J. Prosser, E.I. Franses, Adsorption and surface tension of ionic surfactants at the air–water interface: Review and evaluation of equilibrium models, Colloids Surf. A 178 (2001) 1-40.

[147] J. Jiravivitpanya, K. Maneeintr, T. Boonpramote, Experiment on measurement of interfacial tension for subsurface conditions of light oil from thailand, in: MATEC Web of Conferences, ICCME, 2016.

[148] D.L. Flock, T.H. Le, J.P. Gibeau, The effect of temperature on the interfacial tension of heavy crude oils using the pendent drop apparatus, J. Can. Pelrol. Technol. (1986) 72-76.

[149] O.S. Hjelmeland, L.E. Larrondo, Experimental investigation of the effects of temperature, pressure, and crude oil composition on interfacial properties, SPE Reservoir Eng. (1986) 321-328.

[150] L. Sun, W.F. Pu, Y.L. Wu, J. Xin, Study on the emulsification property of surfactant in high-temperature condition, Oilfield Chem. 28 (2011) 275−279.

[151] Z. Zhao, C. Bi, W. Qiao, Z. Li, L. Cheng, Dynamic interfacial tension behavior of the novel surfactant solutions and daqing crude oil, Colloids Surf. A 294 (2007) 191-202.

[152] L.X. Xia, Chinese Academy of Sciences Doctoral Dissertation (2003).

[153] A. Bera, K. Ojha, A. Mandal, T. Kumar, Interfacial tension and phase behavior of surfactant-brine–oil system, Colloids Surf. A 383 (2011) 114-119.

[154] P.S. Piispanen, M. Persson, P. Claesson, T. Norin, Surface properties of surfactants derived from natural products. Part 1: Syntheses and structure/property relationships-solubility and emulsification, J. Surfact. Deterg. 7 (2004) 147-159.

[155] M.A. Ahmadi, S.R. Shadizadeh, Experimental investigation of a natural surfactant adsorption on shale-sandstone reservoir rocks: Static and dynamic conditions, Fuel 159 (2015) 15-26.

[156] P. Kathel, K.K. Mohanty, Wettability alteration in a tight oil reservoir, Energy Fuels 27 (2013) 6460−6468.

[157] C.S. Vijapurapu, D.N. Rao, Compositional effects of fluids on spreading, adhesion and wettability in porous media, Colloids Surf. A 241 (2004) 335-342.

[158] O.R. Wagner, R.O. Leach, Improving oil displacement efficiency by wettability adjustment, Soc. Petrol. Eng. 216 (1959) 65-72.

[159] Q. Liu, M.Z. Dong, K. Asghari, Y. Tu, Wettability alteration by magnesium ion binding in heavy oil/brine/chemical/sand systems—analysis of hydration forces, Nat. Sci. 2 (2010) 450-456.

[160] S. Cobos, M.S. Carvalho, V. Alvarado, Flow of oil−water emulsions through a constricted capillary, Int. J. Multiphase Flow 35 (2009) 507-515.

[161] J. Ge, Y. Wang, Surfactant enhanced oil recovery in a high temperature and high salinity carbonate reservoir, J. Surfact. Deterg. 18 (2015) 1043–1050.

[162] J. Lu, A. Goudarzi, P. Chen, D.H. Kim, M. Delshad, K.K. Mohanty, K. Sepehrnoori, U.P. Weerasooriya, G.A. Pope, Enhanced oil recovery from high-temperature, high-salinity naturally fractured carbonate reservoirs by surfactant flood, J. Pet. Sci. Eng. 124 (2014) 122-131.

[163] B. Ghosh, D. Obassi, Eco-friendly surfactant for eor in high temperature, high salinity carbonate reservoir, in: SPE Enhanced Oil Recovery Conference, Society of Petroleum Engineering, Kuala Lumpur, Malaysia, 2013.

[164] R. Saha, R.V.S. Uppaluri, P. Tiwari, Influence of emulsification, interfacial tension, wettability alteration and saponification on residual oil recovery by alkali flooding, J. Ind. Eng. Chem. 59 (2018) 286-296.

[165] M.A. Mahmoud, K.Z. Abdelgawad, A new chemical eor for sandstone and carbonate reservoirs, in: Saudi Arabia Section Annual Technical Symposium and Exhibition, Society of Petroleum Engineering, Al-Khobar, Saudi Arabia, 2014.

[166] U. Farooq, M.T. Tweheyo, J. Sjöblom, G. Øye, Surface characterization of model, outcrop, and reservoir samples in low salinity aqueous solutions, J. Dispersion Sci. Technol. 32 (2011) 519-531.

[167] H.A. Son, K.Y. Yoon, G.J. Lee, J.W. Cho, S.K. Choi, J.W. Kim, K.C. Im, H.T. Kim, K.S. Lee, W.M. Sung, The potential applications in oil recovery with silica nanoparticle and polyvinyl alcohol stabilized emulsion, J. Pet. Sci. Eng. 126 (2015) 152–161.

[168] N.K. Maurya, A. Mandal, Studies on behavior of suspension of silica nanoparticle in aqueous polyacrylamide solution for application in enhanced oil recovery, Pet. Sci. Technol. 34 (2016) 429-436.

[169] M. Wisniewska, The temperature effect on the adsorption mechanism of polyacrylamide on the silica surface and its stability, Appl. Surf. Sci. 258 (2012) 3094-3101.

[170] K. Almdal, J. Dyre, S. Hvidt, O. Kramer, Towards a phenomenological definition of the term 'gel', Polym. Gels Networks 1 (1993) 5-17.

[171] W. Kang, B. Xu, Y. Wang, Y. Li, X. Shana, F. An, J. Liu, Stability mechanism of w/o crude oil emulsion stabilized by polymer and surfactant, Colloids Surf. A 384 (2011) 555–560.

[172] J.R.M. Kennedy, K.E. Kent, J.R. Brown, Rheology of dispersions of xanthan gum, locust bean gum and mixed biopolymer gel with silicon dioxide nanoparticles, Mater. Sci. Eng., C 48 (2015) 347–353.

[173] Y. Kazemzadeh, E.S. Eshraghi, K. Kazemi, S. Sourani, M. Mehrabi, Y. Ahmadi, Behavior of asphaltene adsorption onto the metal oxide nanoparticle surface and its effect on heavy oil recovery, Ind. Eng. Chem. Res. 54 (2015) 233−239.

[174] A. Roustaei, S. Saffarzadeh, M. Mohammadi, An evaluation of modified silica nanoparticles' efficiency in enhancing oil recovery of light and intermediate oil reservoirs, Egypt. J. Pet. 22 (2013) 427-433.

[175] E.C. Donaldson, G.V. Chilingarian, T.F. Yen, Enhanced oil recovery ii, processes and operations, in, Elsevier Science Publ. Co., New York, 1989.

[176] Y.H. Cao, E. Dickinson, D.J. Wedlock, Creaming and flocculation in emulsions containing polysaccharide, Food Hydrocolloids 4 (1990) 185-195.

[177] E. Dickinson, J.G. Ma, M.J.W. Povey, Creaming of concentrated oil in-water emulsions containing xanthan, Food Hydrocolloids 8 (1994) 481-497.

[178] A.K. Ghosh, P. Bandyopadhyay, Polysaccharide-protein interactions and their relevance in food colloids, in: The complex world of polysaccharide, Intech open science open minds, 2012, pp. 395-408.

[179] B.P. Binks, C.p. Whitby, Silica particle-stabilized emulsions of silicone oil and water: Aspects of emulsification, Langmuir 20 (2004) 1130-1137.

[180] L.W. Lake, Enhanced oil recovery, in: Soc. Petrol. Eng., 2010, pp. 550.

[181] S. Iglauer, M. Sarmadivaleh, C. Geng, M. Lebedev, In-situ residual oil saturation and cluster size distribution in sandstones after surfactant and polymer flooding imaged with x-ray micro-computed tomography, in: In International Petroleum Technology Conference, IPTC-17312-MS., Doha, Qatar, January 19−22, 2014.

[182] S. Li, L. Hendraningrat, O. Torsaeter, Improved oil recovery by hydrophilic silica nanoparticles suspension: 2 phase flow experimental studies, in: International Petroleum Technology Conference, IPTC - 16707, 2013, pp. 1-15.

[183] A.D. Monfared, M.H. Ghazanfari, M. Jamialahmadi, A. Helalizadeh, Potential application of silica nanoparticles for wettability alteration of oil−wet calcite: A mechanistic study, Energy Fuels 30 (2016) 3947−3961.

[184] A.D. Monfared, M.H. Ghazanfari, M. Jamialahmadi, A. Helalizadeh, Adsorption of silica nanoparticles onto calcite: Equilibrium, kinetic, thermodynamic and dlvo analysis., Chem. Eng. J. 281 (2015) 334−344.

[185] A. Maghzi, S. Mohammadi, M.H. Ghazanfari, R. Kharrat, M. Masihi, Monitoring wettability alteration by silica nanoparticles during water flooding to heavy oils in five-spot systems: A pore-level investigation, Exp. Therm Fluid Sci. 40 (2012) 168-176.

[186] H. Ehtesabi, M.M. Ahadian, V. Taghikhani, M.H. Ghazanfari, Enhanced heavy oil recovery in sandstone cores using tio2 nanofluids, Energy Fuels 28 (2014) 423−430.

[187] L. Chen, G. Zhang, J. Ge, P. Jiang, J. Tang, Y. Liu, Research of the heavy oil displacement mechanism by using alkaline/surfactant flooding system, Colloids Surf. A 434 (2013) 63-71.

[188] G. Cheraghian, Effect of nano titanium dioxide on heavy oil recovery during polymer flooding, Pet. Sci. Technol. 34 (2016) 633-641.

[189] E.S. Ehsan, Y. Kazemzadeh, M. Qahramanpour, A. Kazemi, Investigating effect of sio_2 nanoparticle and sodium-dodecyl-sulfate surfactant on surface properties: Wettability alteration and ift reduction, J Pet Environ Biotechnol 8 (2017) 1-5.

Appendix A

A.1 Material Matrix and Chemical EOR Schemes

The materials and different chemical enhanced oil recovery (EOR) schemes used in this thesis is listed in Table A1.1. Alkali and alkali-surfactant flooding were carried out for light to moderate crude oil in sandstone reservoirs as described in chapter 3 and 4 respectively. Adsorption characteristics of surfactant on reservoir rocks were investigated in chapter 5. Alkali-surfactant flooding for heavy crude in carbonate reservoirs are addressed in chapter 6. Polymer flooding and nanoparticles assisted polymer flooding is described in chapter 7.

Table A1.1: Overall materials and different chemical EOR schemes considered in this work

Materials							EOR schemes
Crude oil	**Reservoir rock**	**Rock nature**	**Alkalis**	**Surfactants**	**Surfactant types**	**Polymer**	**Chemical EOR**
Light to moderate Assam crude	Sandpack	Sandstone	NaOH	CTAB	Cationic	Xanthan Gum	Alkali
Heavy Assam crude	Hapjan		Na_2CO_3	SDS	Anionic		Alkali-surfactant
	Jorajan			SDBS		**Nanoparticle**	Surfactant
Aqueous phase	Carbon Tan			Na-Lignosulfate		Silicon dioxide	Polymer and Nanoparticle-polymer
Assam reservoir formation water	Idaho Gray			Span 80	Non-ionic		
Millipore water	Gray Berea Sandstone			Tween 80			
				Brij 30			
	Silurian Dolomite	Carbonate		Triton X-100			

Appendix B

B.1. Block Diagram for Core Flooding Procedure

The core flooding experiments procedure is describes in schematic diagram as shown below. The experimental method is described in detail in the materials and methods section chapter 2.

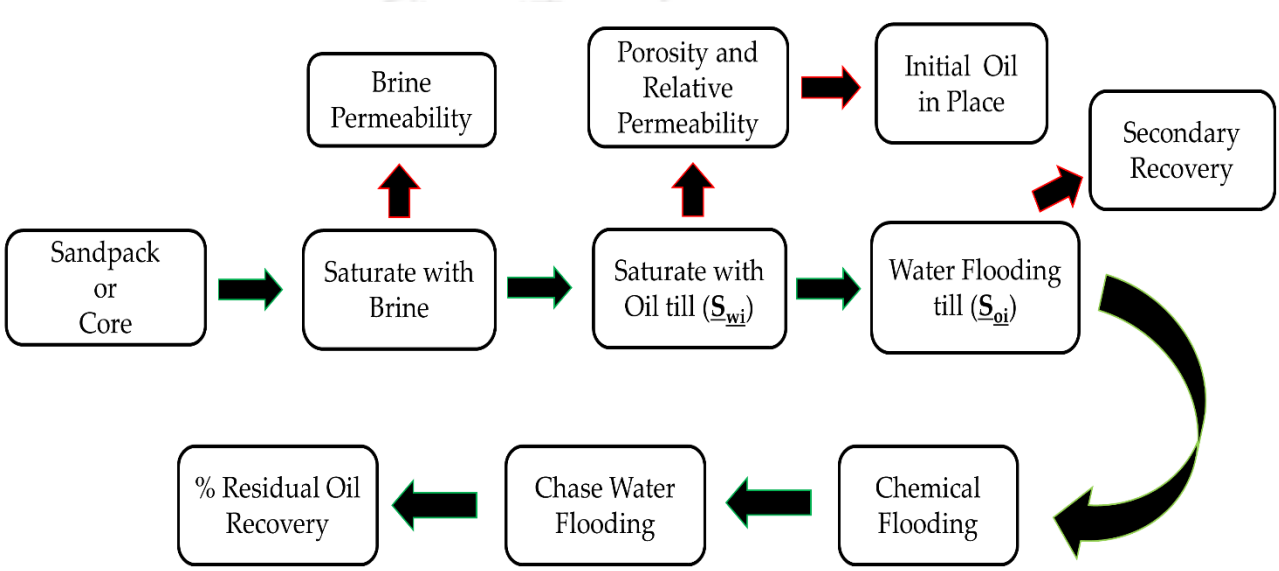

Fig. B2.1: Schematic diagram for core flooding procedure.

Appendix C

C.1 Supplementary Data

The supplementary information on core flooding experiments (pressure drop, water cut and oil recovery), calibration curve, CMC, XRD (minerology analysis) and viscosity data are given below

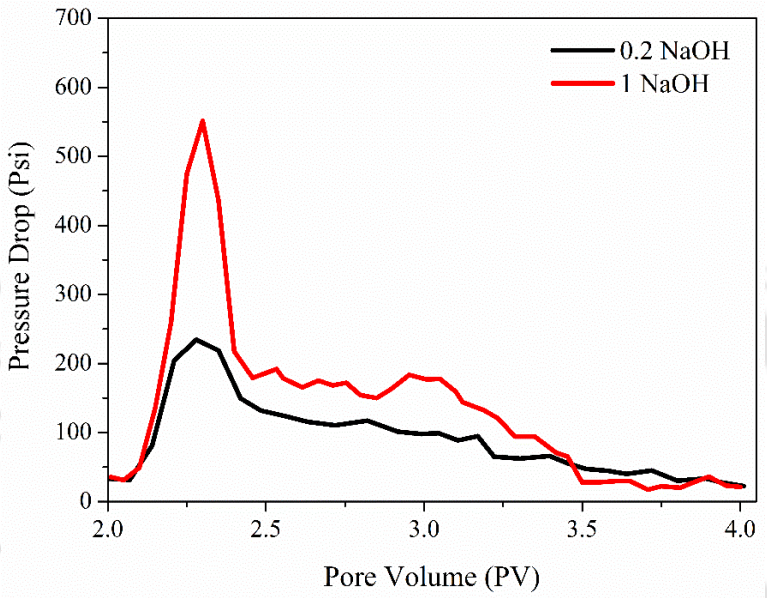

Fig. C3.1: Pressure drop data during the alkali flooding (0.2 wt% and 1 wt% NaOH)

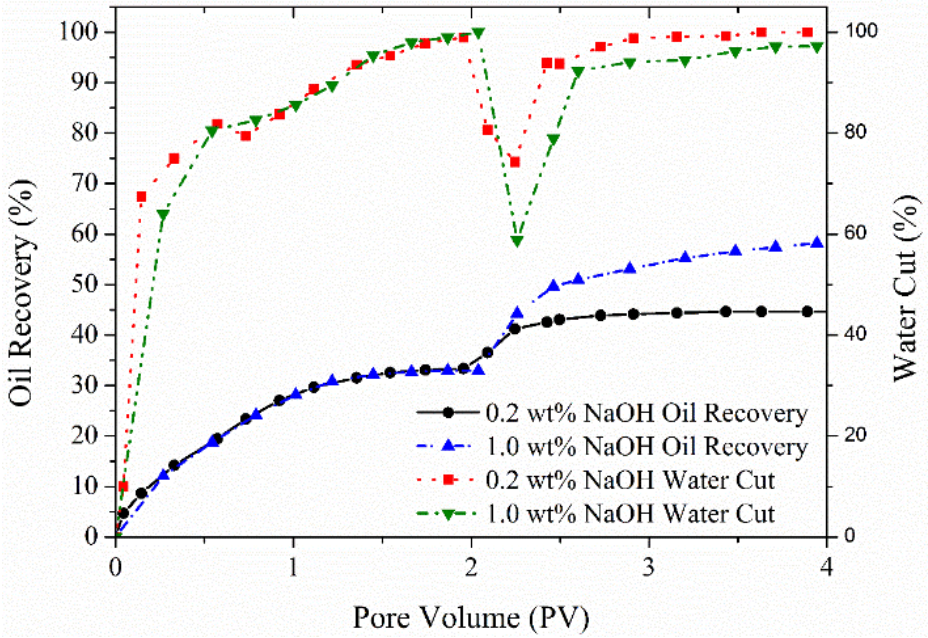

Fig. C3.2: Oil recovery with water cut during alkali flooding (0.2 wt% and 1 wt% NaOH).

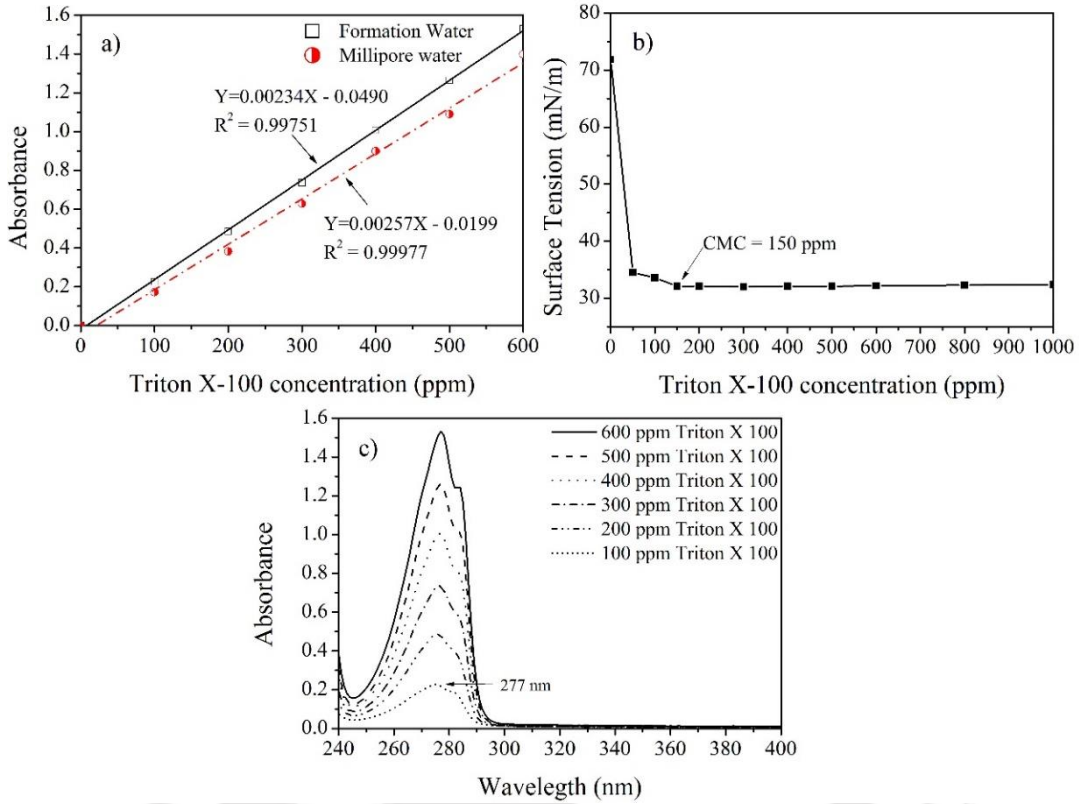

Fig. C5.1: Behaviour of Triton X-100 in order to obtained (a) Wavelength at maximum absorbance (λ_{max}) (b) Calibration curve with formation water and millipore water and (C) Critical micelle concentration (CMC) value with millipore water.

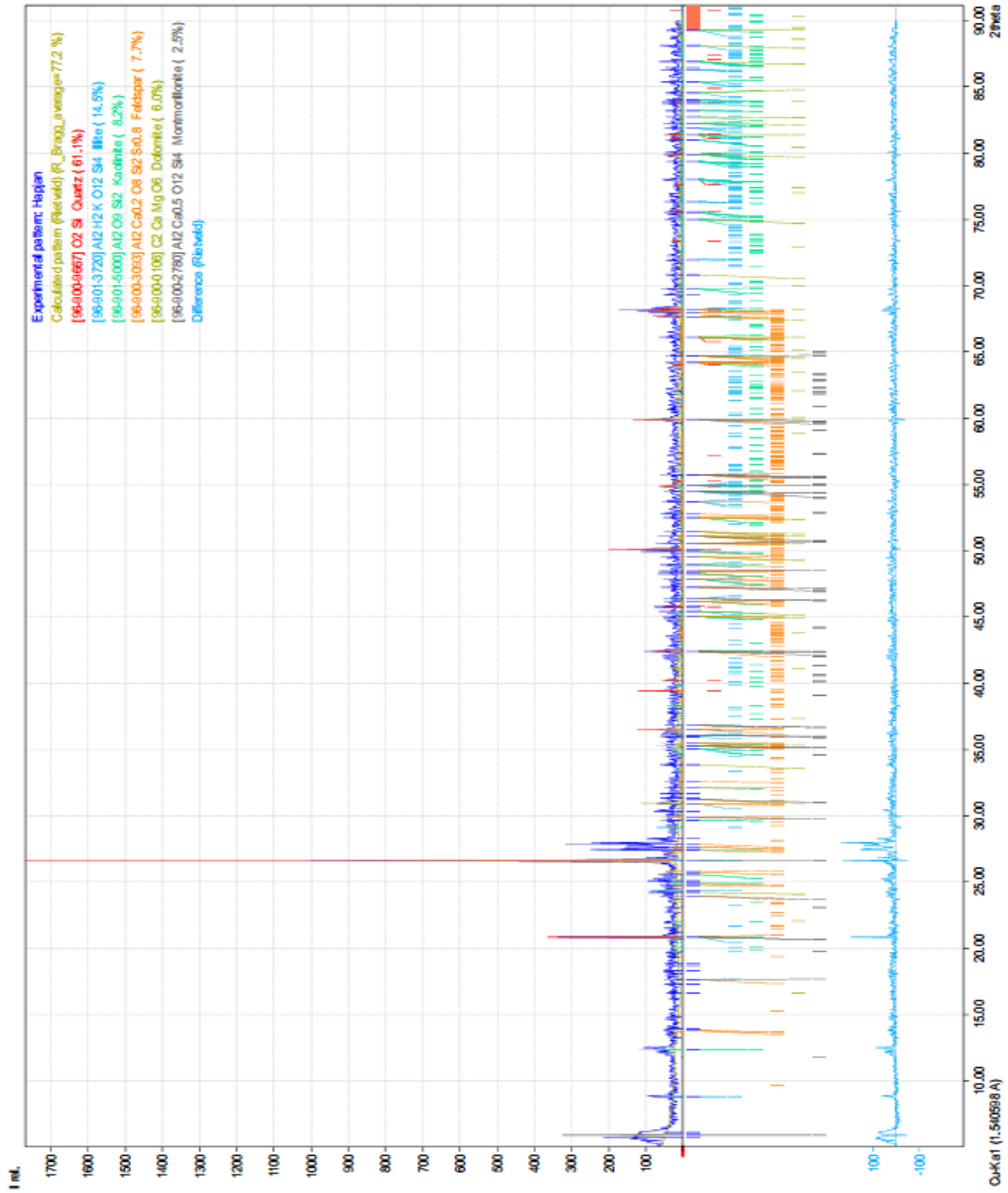

Fig. C5.2: XRD of Hapjan rock with its minerology content.

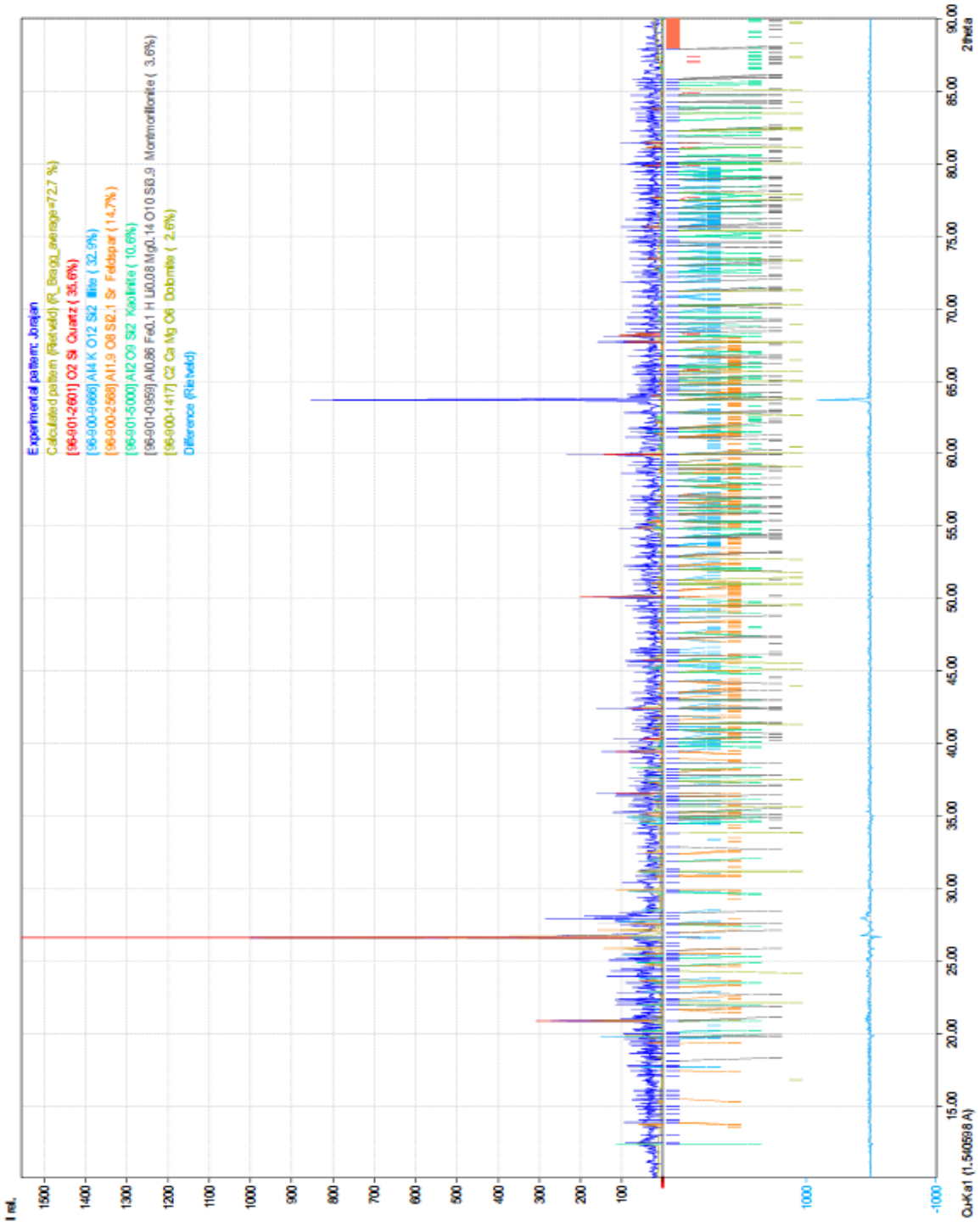

Fig. C5.3: XRD of Jorajan Rock along with its minerology content.

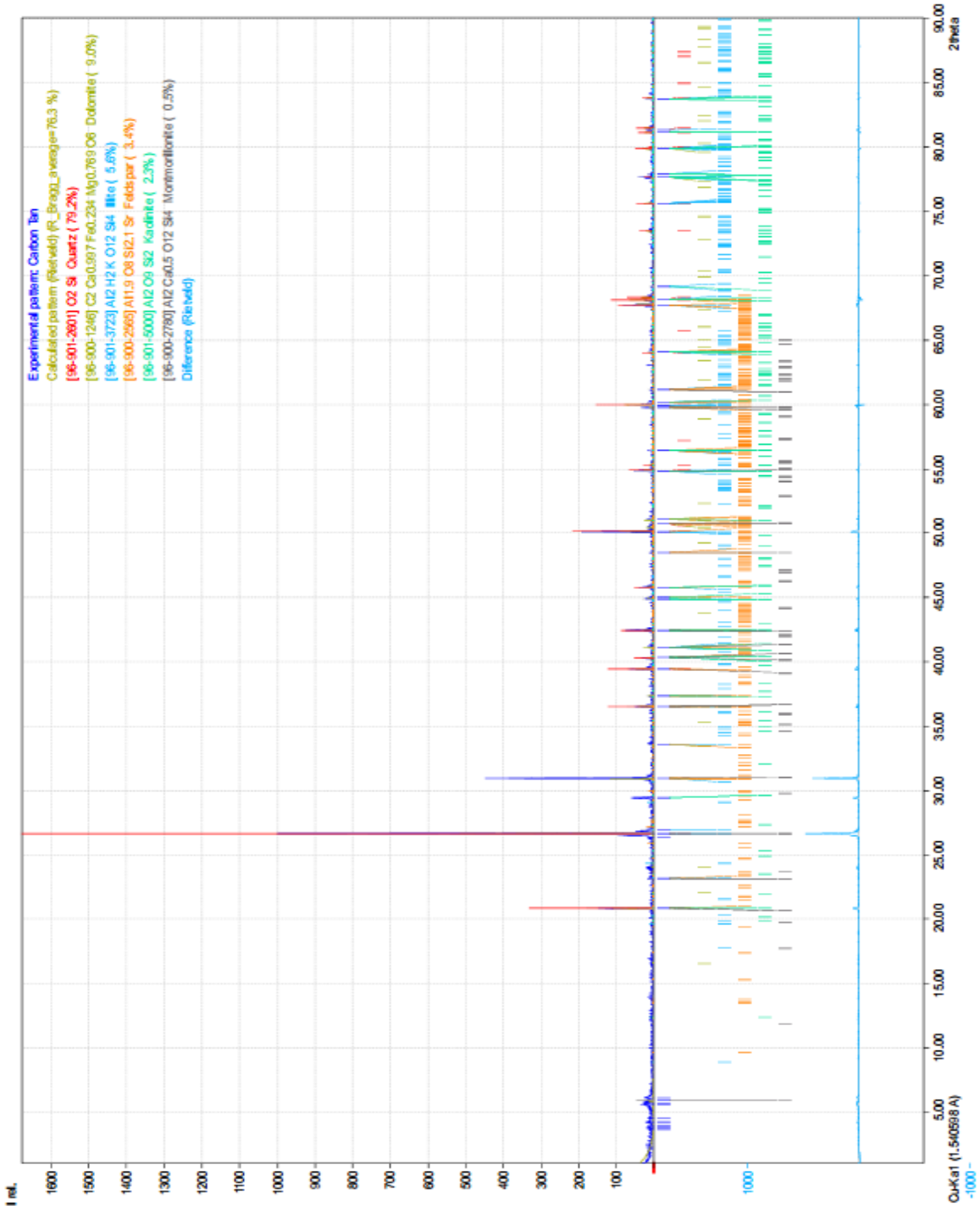

Fig. C5.4: XRD of Carbon Tan with its minerology composition.

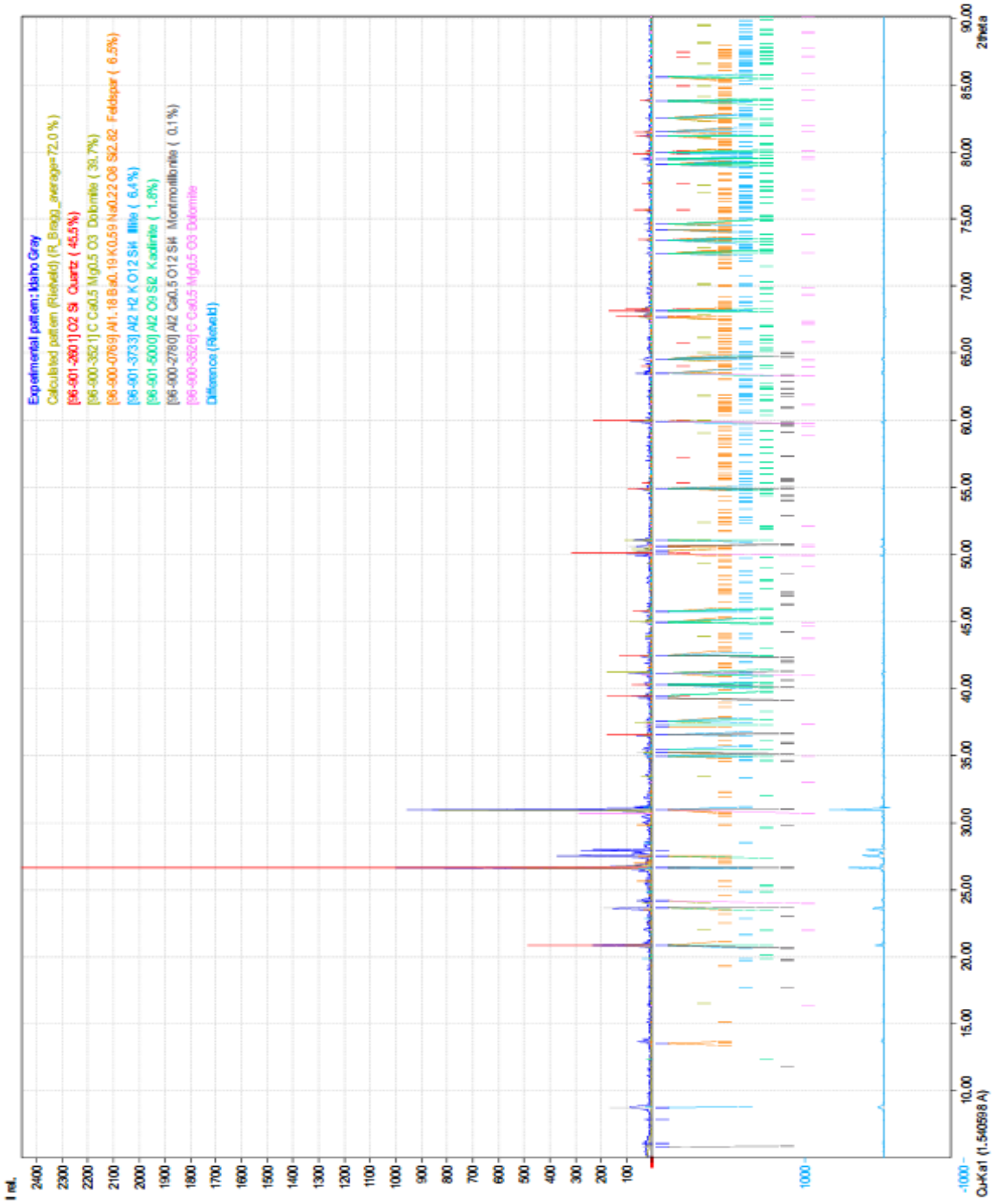

Fig C5.5: XRD of Idaho Gray indicating its minerology composition.

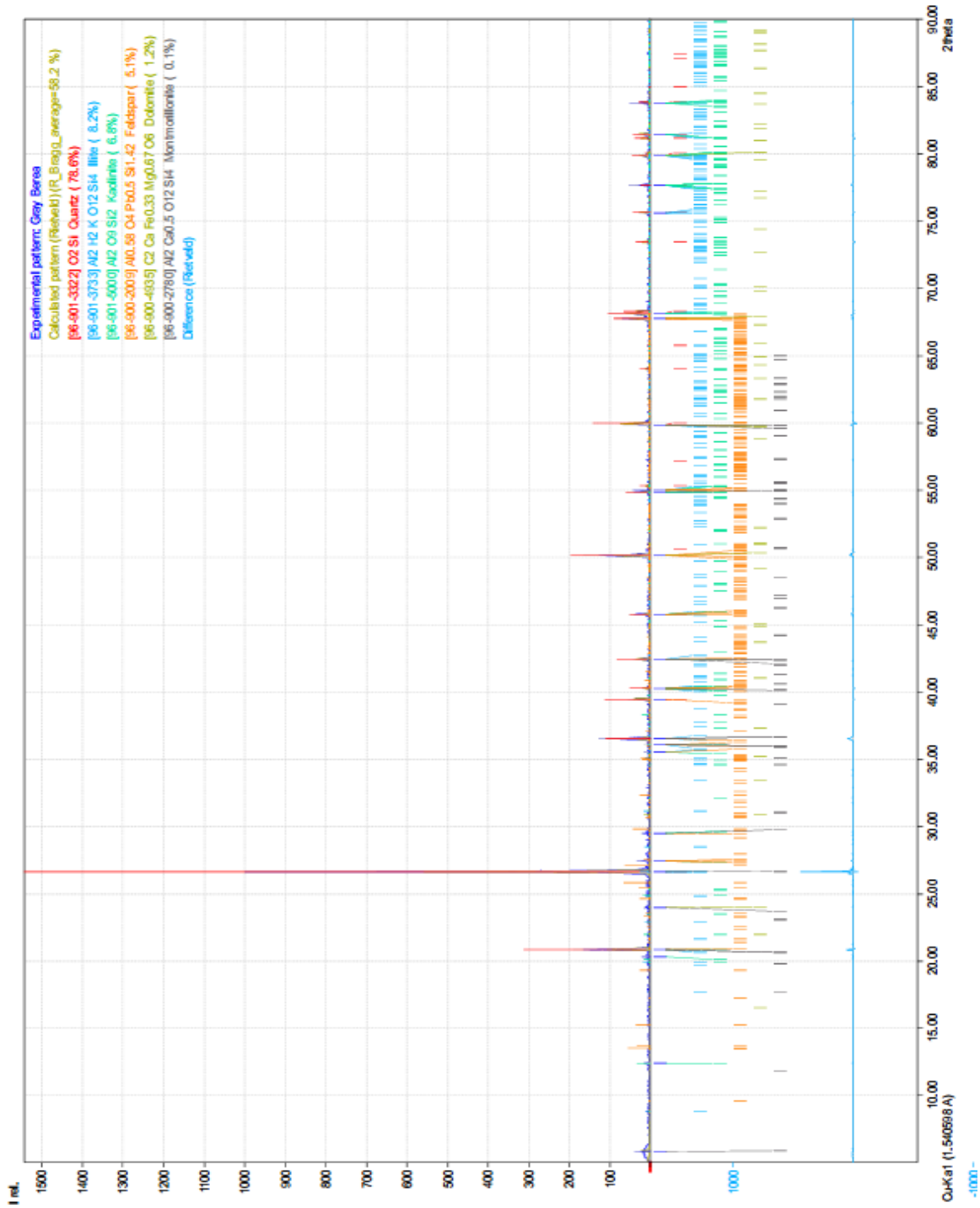

Fig C5.6: XRD of Gray Berea representing minerology composition.

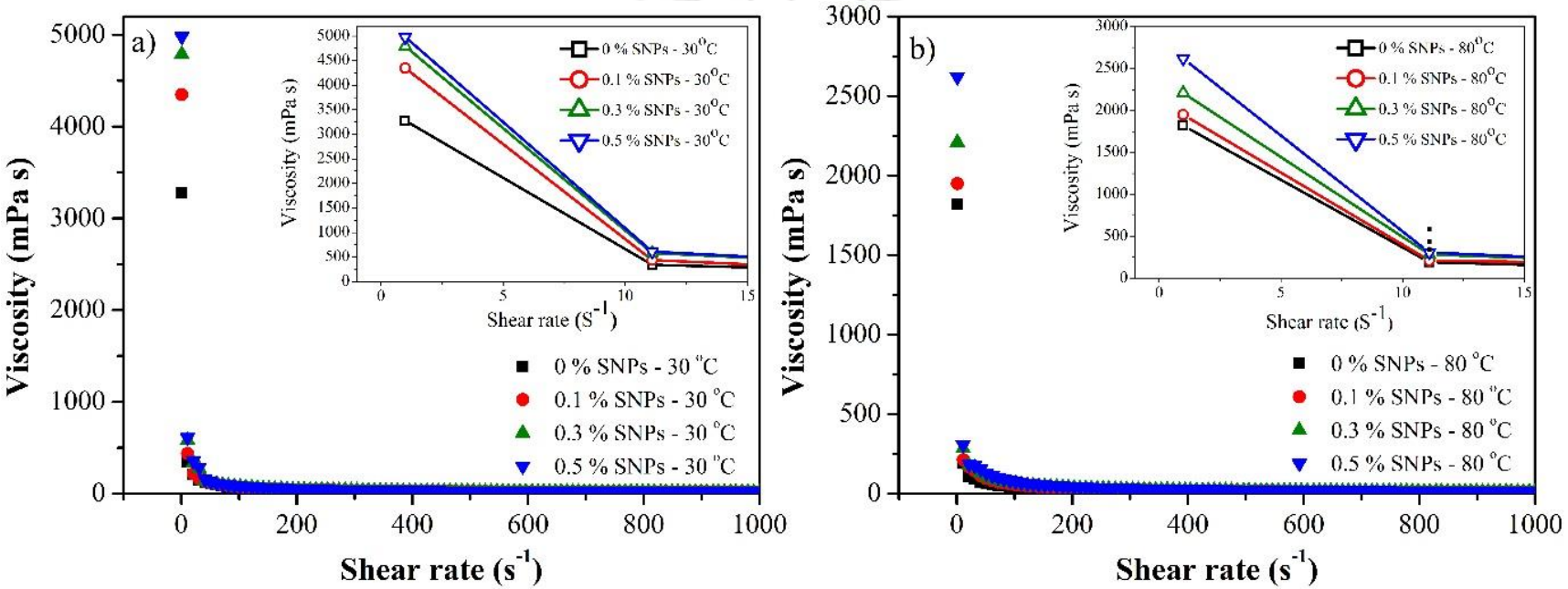

Fig. C7.1: Viscosity vs shear rate curves of O/W emulsions produced with varying concentration of SNPs at (a) 30°C and (b) 80°C.

Journal Publications

1. **R. Saha,** R.V.S. Uppaluri and P. Tiwari, Effect of Mineralogy on the Adsorption Characteristics of Surfactant − Reservoir Rock System, **Colloids Surf. A**, 2017, 531, 121-132.
2. **R. Saha,** R.V.S. Uppaluri and P. Tiwari, Influence of emulsification, interfacial tension, wettability alteration and saponification on residual oil recovery by alkali flooding, **J. Ind. Eng. Chem.**, 2018, 59, 286-296.
3. **R. Saha,** A. Sharma, R. V.S. Uppaluri and P. Tiwari, Interfacial interaction and emulsification of crude oil to enhance oil recovery, **Int. J. Oil, Gas and Coal Technology**, 2018, DOI: 10.1504/IJOGCT.2018.10011553
4. **R. Saha,** R.V.S. Uppaluri, and P. Tiwari, Silica nanoparticle assisted polymer flooding of heavy crude oil: Emulsification, rheology and wettability alteration characteristics, **Ind. Eng. Chem. Res.,** 2018, 57, 6364–6637.

Manuscript communicated and to be communicated:

5. **R. Saha,** V. S. R. Uppaluri, and P. Tiwari, Optimum formulation of chemical slug for carbonate reservoir: Effects of interfacial tension, oil layer break time, emulsification and wettability alteration (under review).
6. **R. Saha,** V. S. R. Uppaluri, and P. Tiwari, "Potential of natural surfactant (Reetha), polymer (Xanthan Gum) and silica nanoparticles to enhance residual oil recovery" (to be submitted).

Conferences Presentation (National and International):

1. **Rahul Saha,** Ramgopal Uppaluri and Pankaj Tiwari, *Alkali and surfactant interaction with Assam crude to recover residual oil.* International conference on advances in petroleum, chemical, and energy challenges APCEC, 24th - 25th March 2017, Amethi, India. (Oral)
2. **Rahul Saha,** Kartik Anem, Ramgopal Uppaluri and Pankaj Tiwari, *Experimental and simulation studies for recovery of residual Assam crude oil: Characterization of rock-fluid and screening of chemicals*. 22nd International congress of chemical and process engineering CHISA, 27th - 31st August 2016, Prague, Czech Republic. (Poster)
3. **Rahul Saha,** Ramgopal Uppaluri and Pankaj Tiwari, *Chemical induced enhanced oil recovery for Assam crude oil*, MRSI, 18th - 21st February 2016, Jorhat, India. (Poster)
4. **Rahul Saha,** Ramgopal Uppaluri and Pankaj Tiwari, *Chemical induced enhanced oil recovery for Assam crude oil*, Chemcon, 27th - 30th December 2015, Indian Institute of Technology Guwahati, India (Oral)
5. **Rahul Saha,** Ramgopal Uppaluri and Pankaj Tiwari, *Experimental and simulation studies of chemical based enhanced oil recovery*, Reflux, 29th - 30th March 2015, Indian Institute of Technology Guwahati, India. (Poster)
6. **Rahul Saha,** Aditi Sharma, Subrata Gogoi, Ramgopal Uppaluri and Pankaj Tiwari, *Experimental and simulation studies of chemical based enhanced oil recovery*, IITG-ABB workshop, 19th Feb 2015, Institute of Technology Guwahati, India. (Poster)

7. **Rahul Saha,** Ramgopal Uppaluri and Pankaj Tiwari, *Role of rock minerology on adsorption characteristics of potential surfactant for chemical enhanced oil recovery*, ISCRE, 20th - 23rd May 2018, Florence, Italy. (Poster)